Investigation into metabolic profile changes in environmental hypoxia and the potential for dietary nitrate to alleviate hypoxic stress.

O'Brien, Katie Alice

Awarding institution:
King's College London

Investigation into metabolic profile changes in environmental hypoxia and the potential for dietary nitrate to alleviate hypoxic stress.

A thesis submitted for the degree of Doctor of Philosophy at King's College London.

2017

Katie Alice O'Brien

Centre of Human and Aerospace Physiological Sciences

Faculty of Life Sciences and Medicine

King's College London

Acknowledgements

First and foremost, I would like to thank my supervisors Professor Stephen Harridge and Dr Lindsay Edwards. They have provided first class supervision throughout the course of my PhD and have always given their full support and invaluable advice towards all aspects of my studies.

My PhD work has been highly collaborative and I feel exceptionally fortunate to have worked with some outstanding researchers and research teams. This includes the Xtreme Everest group, both for providing the blood samples from the Caudwell Xtreme Everest (CXE) expedition and for allowing me to be an investigator on the Xtreme Everest 2 expedition, which was an incredible field work experience. The expertise of the Human Nutrition Research group led by Professor Jules Griffin was paramount to the analysis of the CXE samples. I am very grateful for the guidance from Professor Griffin and the technical support provided from Drs Larissa Richardson and Albert Koulman. I am thankful to the White Mars expedition team for providing blood samples along with a multitude of other physiological measures, to which the work of Dr Ross Pollock and Lindsey Marjoram were crucial. I feel extremely privileged to have worked with Drs Nicholas Hopkinson and Katrina Curtis (The Royal Brompton) and be included in the day to day running of the clinical study, as well as in the taking and analysis of blood samples. Central to the nitrate/nitrite analysis of these samples was the involvement of Professor Martin Feelisch at the University of Southampton. A common thread in each of these human studies was the use of nuclear magnetic resonance spectroscopy. This could not have happened without the technical expertise of Dr Andrew Atkinson (Centre for Biomolecular Spectroscopy, KCL), for which I am extremely grateful.

The animal work presented in this thesis was conducted in the laboratory of Dr Andrew Murray (University of Cambridge). I am hugely appreciative to Dr Murray for including me in this study, for sparking my fascination with mitochondria and for inspiring me for the next step in my research career. Essential to the success of this study was the laboratory team, led by Dr Horscroft and including Jules Deveux, Alice Strang-Steele, Ross Lindsay and Anna Clark. In addition to the technical support, the good humour of this team made for an exceptionally enjoyable lab experience. Additionally, I would like to thank Dr Andy Philp for allowing me to run the Western Blots in his laboratory at University of Birmingham and Dr Sophie Joanisse for her guidance in preparing the muscle samples for

these. I would also like to thank those at my lab in King's including Michaeljohn Kalakoutis for teaching me the SDS-PAGE technique and helping to troubleshoot and Drs Julien Ochala and Anthea Rowlerson for their assistance with this also. I would also like to thank Dr Georgina Ellison for allowing me to use equipment and freezer space in her laboratory.

Throughout my PhD, I have always been given tremendous support from my department at King's and am very grateful to past and present members of CHAPS for making my time extremely enjoyable. Included in this is the former Head of Physiology, Professor Jeremy Ward. Professor Ward has been hugely supportive, both during my undergraduate and PhD studies, and has been an exceptional mentor for my teaching work. His encouragement has been invaluable.

Obtaining a PhD is a long and often rocky road. There is no way that I could have achieved the success and pursued through the failures of my research without the unwavering love and support of my family and friends. They never fail to make me laugh, to take interest in my work and to inspire me. For this, I am forever thankful.

Finally, thank you to KCL Dance Society for being my outlet. Creating pieces and sharing a stage with such a talented, wonderful bunch of people has been an incredible privilege. Thank you for keeping me sane. When in doubt, dance it out.

Abstract

Oxygen (O_2) insufficiency (hypoxia), either in response to environmental exposure or pathological states is a driver of metabolic remodelling, the details of which are ill- defined. This work aimed to further understanding of metabolic responses to environmental hypoxia. In the first study, plasma metabolite changes were measured in 198 human subjects upon ascent to Everest Base Camp (5300m) using metabolomic and lipidomic techniques. Results were indicative of a shift towards anaerobic glycolysis, a mobilisation of fat stores and alterations to fat lipoprotein transport with ascent. In the second study, a pilot study, subjects (n=5) were examined pre and post an attempted winter crossing of Antarctica, including a 24 week stay above 2,500m. Metabolomics analysis of serum samples alongside whole body physiological and exercise measurements were indicative of a shift in metabolic signature, including an increased reliance upon carbohydrate metabolism during exercise.

Developing a means of attenuating the metabolic stress of hypoxia would be highly beneficial for aiding human adaptation and ameliorating the effects of disease states where hypoxia is a comorbidity. An additional aim was to explore the potential of dietary nitrate for this purpose. In the third study, the potential for nitrate supplementation to aid hypoxic acclimatisation of skeletal muscle mitochondria and the role of PPARα (a master regulator of fat oxidation) were assessed using a mouse model of wild type (n=42) and PPARα$^{-/-}$ strains (n=42). Nitrate supplementation (0.7mM) recovered hypoxic induced decreases in fatty acid and carbohydrate oxidation in response to prolonged, severe hypoxic exposure (10% O_2, 28 days) and did so independently of PPARα. In the fourth study, the effects of acute dietary nitrate supplementation (12mM nitrate vs. placebo ingested 3 hours pre-exercise) upon exercise endurance and related metabolite changes were investigated in chronic obstructive pulmonary disease (COPD) patients (n=21, age 68$\pm$7 years). Whilst neither median endurance time nor targeted plasma metabolites differed between treatments, O_2 consumption was significantly lower following nitrate treatment vs. placebo. The absence of plasma lactate changes between treatments indicates this effect was not mediated through increased reliance upon anaerobic metabolism.

In conclusion, this work highlighted several potential biomarkers of interest in healthy humans exposed to environmental hypoxia, including alterations to carbohydrate and lipid metabolism. Dietary nitrate demonstrated potential for recovering metabolic function *in vitro*, yet failed to illicit beneficial effects in a clinical population *in vivo.*

Declaration of study conduct

The studies presented in this thesis were highly collaborative, involving numerous different institutions across the UK. The role of each of these collaborators along with a clear outline of the work I performed are detailed below. For each study utilising nuclear magnetic resonance spectroscopy, technical support was provided by Dr Andrew Atkinson (KCL).

Chapter 2 (Study 1):

The Caudwell Xtreme Everest (CXE) medical research expedition was designed and led by Professor Mike Grocott, University of Southampton, with input from numerous members of the CXE team. Presented in this thesis is the analysis of plasma samples taken from subjects upon their ascent to EBC by CXE investigators. The preparation of blood samples for nuclear magnetic resonance (NMR) spectroscopy and mass spectrometry (MS) was performed by myself, with guidance provided by Professor Jules Griffin. Manual alignment and phasing of resulting spectra was performed by myself and subsequent pre-processing (including scaling and normalisation) was performed by Dr Edwards.

MS analysis was performed in the laboratory of Professor Jules Griffin at the MRC Human Nutrition Research Unit, Cambridge. Preparation of pooled quality controls and plate loading was conducted by myself, with guidance from Dr Larissa Richardson whom additionally provided technical expertise for the MS runs. Initial pre-processing stages, including data conversion and running of the peak picking algorithm (devised by Professor Griffins' laboratory), was performed by myself at the MRC, with subsequent data refinement conducted by Dr Albert Koulman. Bayesian modelling of results was conducted by Dr Edwards.

Data regarding physiological variables (SpO_2, body weight) were obtained from subjects by CXE investigators. Statistical analysis of this data was performed by myself as was correlation/linear regression analysis.

Chapter 3 (Study 2):

The White Mars project is the scientific investigation conducted upon subjects undertaking the first attempted winter crossing of Antarctica, otherwise termed The Coldest Journey. The organisation of this project was a collaborative effort between Drs Mike Stroud and Alexander Kumar. Data collection during the expedition was conducted by Dr Rob Lambert. This data is presented in this thesis, alongside a comprehensive range of measures taken pre and post expedition at the Centre of Human and Aerospace Physiological Sciences (CHAPS), KCL. Preparation of serum samples was performed by myself. Processing and analysis of NMR spectra was a joint effort between myself and Dr Edwards. Whole body physiological measurements, including cardiopulmonary exercise testing and maximal voluntary contraction, were led by Dr Ross Pollock with assistance from Lindsey Marjoram and myself. Analysis of this data set alongside that obtained during the expedition was a joint effort between myself and Dr Pollock.

Chapter 4 (Study 3):

This study was undertaken at Dr Andrew Murray's lab at the Department of Physiology, Development and Neuroscience, University of Cambridge. The respirometry protocols were developed as a joint effort between myself and Dr James Horscroft, with guidance from Dr Andrew Murray. Animal husbandry and dissection was a combined effort between Dr Horscroft, Alice Strang-Steele, Jules Devreux and myself. Soleus respirometry and citrate synthase activity experiments were performed by myself. Western blot experiments for metabolic targets were performed by myself at the laboratory of Dr Andy Philp, University of Birmingham. Myosin heavy chain isoform identification was performed by myself at KCL, with help in protocol development from Michaeljohn Kalakoutis. Data analysis was conducted by myself, with guidance from Dr Horscroft.

Chapter 5 (Study 4):

This study was conducted by the NIHR Respiratory Biomedical Research Unit at Royal Brompton and Harefield and NHS Foundation Trust and Imperial College London in collaboration with Drs Nicholas Hopkinson and Katrina Curtis. Patient recruitment, screening and testing of baseline characteristics were undertaken by Dr Curtis. The exercise testing days required a collaborative input between Dr Curtis, myself, Rebecca Tanner and clinical physiologists at the NIHR Respiratory Biomedical Research Unit. Analysis of the raw cardiopulmonary exercise data and derivatisation of isotime values were conducted by Dr Curtis.

Preparation of plasma samples for NMR spectroscopy was performed by myself. Pre-processing of NMR data was a joint effort between myself and Dr Edwards. Initial principal component analysis was conducted by Dr Edwards, and subsequent targeted analysis of specific analysis by myself.

Plasma nitrate/nitrite analysis was performed in collaboration with Professor Martin Feelisch and Dr Magdalena Minnion at the Faculty of Medicine, Clinical and Experimental Sciences, University of Southampton and Southampton NIHR Respiratory Biomedical Research Unit, Southampton General Hospital. Preparation of plasma samples was performed by myself and Dr Curtis and subsequent analysis undertaken by Dr Minnion and Professor Feelisch.

Contents

Contents of Figures

Contents of Tables

Contents of Equations

Common abbreviations

ADP	Adenosine diphosphate
ANOVA	Analysis of variance
ATP	Adenosine triphosphate
Ca_2^+	Calcium
CoA	Coenzyme A
cGMP	Cyclic guanosine monophosphate
sGC	Soluble guanylate cyclase
COPD	Chronic obstructive pulmonary disease
COX	Cytochrome c oxidase (ETS complex IV)
CPMG	Carr-Purcell-Meiboom-Gill pulse sequence
CPT	Carnitine palmitoyl transferase
CS	Citrate synthase
Cr	Creatine
CXE	Caudwell Xtreme Everest
$\Delta\mu H^+$	Proton motive force
δ	Chemical shift
DIHRMS	Direct infusion high resolution mass spectrometry
DIMS	Direct infusion mass spectrometry
DNL	de novo lipogenesis
D_2O	Deuterium oxide
DSS	3-trimethylsilyl-1-propanesulfonic acid sodium salt
DXA	Dual energy X-ray absorptiometry
EBC	Everest Base Camp

EDTA	Ethylenediamine-tetra-acetic acid
ETS	Mitochondrial electron transport system
FADH	Flavin adenine dinucleotide
FEV_1	Forced expired volume in 1 second
FVC	Forced vital capacity
GLUT	Glucose transporter
Hb	Haemoglobin
HDL	High density lipoprotein
HIF	Hypoxic inducible factor
^{1}H-NMR	Proton nuclear magnetic resonance
HOAD	3-hydroxyacyl-CoA dehydrogenase
HRE	Hypoxic response element
iCa^{2+}	Intracellular calcium
KTM	Kathmandu
LCAD	Long chain acyl CoA
LC-MS	Liquid chromatography-mass spectrometry
LPC	Lyso-phosphatidylcholine
LDN	London
LDL	Low density lipoprotein
LEAK	Leak state respiration
LPL	Lipoprotein lipase
MFN2	Mitofusin 2
MiR	Mitochondrial respiration medium
MS	Mass spectrometry
MyHC	Myosin heavy chain
m/ z	Mass to charge ratio

NAD^+	Nicotinamide adenine dinucleotide
NADH	Reduced nicotinamide adenine dinucleotide
NAM	Namche
NO	Nitric oxide
NO_3^-	Inorganic nitrate
NO_2^-	Nitrite
NOS	Nitric oxide synthase
O_2	Oxygen
OAA	Oxaloacetate
OCE	Oxidative phosphorylation coupling efficiency
OXPHOS	Oxidative phosphorylation
P_B	Barometric pressure
PCA	Principal component analysis
PC	Phosphatidylcholine
PCr	Phosphocreatine
PDK	Pyruvate dehydrogenase kinase
PHE	Pheriche
Pi	Inorganic phosphate
P_IO_2	Partial pressure of inspired oxygen
PKG	Protein kinase G
^{31}P-MRS	31-phosphorus magnetic resonance spectroscopy
^{31}P-NMR	31-Phosphorus nuclear magnetic resonance
PO_2	Partial pressure of oxygen
PGC1α	Proliferator-activated receptor gamma coactivator 1-alpha
PPARα	Peroxisome proliferator-activated receptor alpha
PS	Phosphatidylserine

QC	Quality control
ROS	Reactive oxygen species
SERCA	Sarcoplasmic reticulum Ca^{2+} ATPase
SCD1	Stearoyl-CoA desaturase 1
SD	Standard deviation
SM	Sphingomyelin
SpO_2	Arterial O_2 saturation
sGC	Soluble guanylyl cyclase
TCA	Tricarboxylic acid
Tfam	Mitochondrial transcriptional factor A
TG	Triglyceride
UCP	Uncoupling protein
V_E	Minute ventilation
VEGF	Vascular endothelial growth factor
VLDL	Very low density lipoprotein
VO_2	Pulmonary oxygen uptake
VO_2 max	Maximal oxygen uptake

Relevant research publications

O'BRIEN, K. A., HORSCROFT, J. A., EDWARDS, L. M., HARRIDGE, S. D. & MURRAY, A. J. 2016. Nitrate supplementation and peroxisome proliferator-activated receptor alpha knockout in hypoxia: Effects on skeletal muscle mitochodnrial function. . *Proc Physiol Soc*.

O'BRIEN, K. A., POLLOCK, R., STROUD, M., KUMAR, A., LAMBERT, R. J., GREEN, D. A., EDWARDS, L. M. & HARRIDGE, S.D.R. 2015. Physiological and metabolic responses to prolonged hypoxia and extreme cold: Preliminary data from the White Mars Antarctica winter expedition. *Extreme Physiology & Medicine,* 4**,** 1-2.

CURTIS, K. J., O'BRIEN, K. A., TANNER, R. J., POLKEY, J. I., MINNION, M., FEELISCH, M., POLKEY, M. I., EDWARDS, L. M. & HOPKINSON, N. S. 2015. Acute Dietary Nitrate Supplementation and Exercise Performance in COPD: A Double-Blind, Placebo-Controlled, Randomised Controlled Pilot Study. *PloS one,* 10**,** e0144504.

O'BRIEN, K. A., GRIFFIN, J. L., MURRAY, A. J. & EDWARDS, L. M. 2015. Mitochondrial responses to extreme environments: insights from metabolomics. *Extreme physiology & medicine,* 4**,** 7.

1 **Chapter 1:** Introduction and literature review

1.1 Introduction

The entire macro and micro-anatomy of large animals is constrained by the need for an adequate provision of O_2 (Koch et al., 2008). The constant O_2 requirement has necessitated the evolution of an extensive cardiovascular and respiratory system in higher animals to ensure adequate oxygenation of all tissues. The transferral of O_2 from the atmosphere, across the alveoli and to the tissues, ending at the mitochondria occurs via a process termed the O_2 cascade. In this cascade, O_2 moves from areas of high O_2 pressure (air) to regions of low O_2 pressure (mitochondria). The partial pressure of O_2 (PO_2) falls in a stepwise fashion down this cascade. Within mitochondria, O_2 is essential for the generation of adenosine triphosphate (ATP) via oxidative phosphorylation (OXPHOS). A sufficient supply of O_2 to the tissue is thus required to maintain oxidative metabolism, and so both energetic and redox homeostasis, within complex organisms.

Disruption of any part of the O_2 cascade can result in an insufficient supply of O_2 to the tissues, termed hypoxia. This occurs in healthy humans upon exposure to high altitudes, whereby the fall in barometric pressure (P_B), or the downwards force exerted by the atmosphere, leads to a decrease in inspired partial pressure of O_2 (P_IO_2). This compromises the transfer of O_2 down the O_2 cascade resulting in hypobaric hypoxia.

A plethora of disease states are also associated with disruptions to the O_2 cascade. This includes chronic obstructive pulmonary disease (COPD), a leading cause of death worldwide that is associated with progressive airflow limitation (Lozano et al., 2013). The resultant hypoxic state is a key component of disease pathology (Pauwels et al., 2012).

In these hypoxic states, oxidative metabolism and so ATP production, becomes compromised in turn impairing cellular function. Metabolic remodelling is therefore required to enable the maintenance of order and homeostasis. However, the details of remodelling processes remain ill-defined.

In the instance of hypobaric hypoxia in healthy humans, current evidence suggests that acclimatisation involves a shift towards anaerobic ATP generation alongside alterations

to mitochondrial oxidative processes including tricarboxylic acid (TCA) cycle function and electron transfer chain/system (ETS) activities, as well as suppression of β-oxidation (Horscroft et al., 2014). However, a significant lack of consensus exists between studies, making this a highly contentious field. This is likely a result of discrepancies in study design, with large degrees of variation in the duration and degree of hypoxic exposure apparent in both human and rodent models. Particularly in the case of investigations into human physiology, this is further confounded by low subject numbers as the majority of high altitude studies are performed on fewer than 20 subjects. In addition, many previous studies focus on specific aspects of complex metabolic pathways such as activities of select enzymes, as opposed to metabolic profiles, which have the potential to provide far greater insight and may highlight biomarkers for hypoxic exposure (Sreekumar et al., 2009, Nicholson et al., 2008).

Despite the utmost importance of metabolic remodeling in enabling acclimatisation to hypoxic states, the details of this process thus remain ill-defined. Furthering our understanding of these changes has implications clinically for those disease states in which hypoxia plays an integral part and also for the growing numbers of healthy humans sojourning to, or residing at, high altitudes (Woolcott et al., 2015). By gaining a more complete picture of the healthy human metabolic remodelling response, it thus becomes feasible to further the development of potential strategies that lessen the impact of pathological hypoxia. There is a clear need for studies that better define responses across differing durations and severities of hypoxia using more sophisticated techniques and, where possible, larger subject numbers.

Developing a means of attenuating the metabolic stress of hypoxia would be highly beneficial for aiding human adaptation either in response to environmental exposure or pathological states. A candidate for such an intervention is dietary nitrate supplementation. At the level of the mitochondria, this intervention has been associated with enhancing mitochondrial efficiency (Larsen et al., 2011) and β-oxidation capacity, the latter of which was an effect shown to be reliant upon the master regulator of β-oxidation, peroxisome proliferator activated receptor α (PPARα) (Ashmore et al., 2015b). At the whole-body level, this intervention has been associated with decreasing the O_2 cost of submaximal exercise in both normoxic and hypoxic conditions (Larsen et al., 2007, Bailey et al., 2009, Larsen et al., 2010, Vanhatalo et al., 2010, Lansley et al., 2011). Evidence thus suggests that dietary nitrate is a prime candidate for alleviating hypoxic induced metabolic stress. However, this

potential is yet to be greatly explored in a hypoxic context. Particularly, mechanisms of nitrate action in hypoxia are yet to be sufficiently investigated. In addition, little is known about the potential for nitrate supplementation to act as a therapeutic intervention in disease states associated with hypoxia.

In this thesis, two key aims are addressed. The first overarching aim was to better define the metabolic responses of healthy humans to hypobaric hypoxia. This involved examination of the metabolic and lipid profiles of a large cohort of subjects in response to acute, progressive high altitude exposure to 5,300m. In addition, the examination of a small cohort in response to chronic exposure to 2,500m was conducted. The second overarching aim was to investigate the potential of dietary nitrate supplementation to alleviate metabolic stresses of hypoxia. This involved exploration into the mechanisms of nitrate action at the level of the mitochondria in an animal model, as well as translation to a disease population, whereby the effects of dietary nitrate on metabolism and exercise performance of COPD patients were investigated.

A common theme that persists through each study presented in this thesis is examination of metabolic responses to hypoxic perturbation. This is with and without dietary nitrate intervention, explored at the level of the blood in healthy humans and COPD patients and at the level of skeletal muscle mitochondria in an animal model. As a prelude to the detailed report of these investigations, it is therefore appropriate to firstly delve into the intricacies of mammalian metabolic systems. The literature review begins with an overview of cellular respiration. The effects of hypoxia upon this complex process is then considered and the current consensus on adaptive remodelling explored. Following this, detail upon dietary nitrate supplementation is presented, along with proposed mechanisms of action and effects upon O_2 delivery and utilisation.

1.2 Literature review

1.2.1 Cellular respiration

Life is a complex phenomenon that is dependent upon a high degree of activity and order among constitutent components of an organism. In terms of thermodynamics, the entropy of the universe, being a measure of disorder, must increase over time. Maintenance of the ordered structures composing an organism thus relies upon a positive entropy change. This requires reactions with a negative entropy to be coupled to those with a positive entropy change. A total positive entropy change in turn provides energy, being the ability of

a system to do work. In other words, neither activity nor order can be maintained without a continuous input of energy and this energy results from a positive entropy change (Nicholls et al., 2013).

For the majority of protozoa and metazoa alike, this energy is derived from combustion of organic macromolecules including carbohydrates, fats and proteins. The energy released from this process is transferred into the phosphoanhydride bonds of adenosine triphosphate (ATP), a process termed phosphorylation. Hydrolysis of these bonds results in the production of adenosine diphosphate (ADP) as follows in **Equation 1.1.**

$$\boldsymbol{ATP \leftrightarrow ADP + Pi}$$

Equation 1.1. ATP synthesis and breakdown.

This reaction is catalysed by ATP synthase. ATP synthesis or hydrolysis takes place on the F_1 sector of this enzyme, being the catalytic domain, located at the matrix side of the inner mitochondrial membrane (Stock et al., 2000).

The breakdown of ATP in this manner is almost solely responsible for providing the free energy required for thermodynamically unfavourable reactions, and so maintenance of order, within mammalian cells. ATP thus acts as the energy currency of the cell (Weibel, 1984, Nicholls et al., 2013). However, ATP itself is not a high energy compound. The reason it is part of the energy system is because the ATP hydrolysis reaction, and so the ratio of ATP:ADP, lies very far from equilibrium (Nicholls et al., 2013). In essence, this reaction can be depicted as a highly compressed spring, with the degree of compression being relative to the distance from equilibrium.

The main site of ATP production is within the ‘furnaces’ of the cell, the mitochondria. Here, organic compounds are broken down via a series of oxidation and reduction reactions involving the passage of electrons through coenzymes and proteins associated with mitochondrial membranes, otherwise termed the ETS. Energy released in this process is required for the generation of ATP from its precursor ADP through the action of the final complex of the ETS, ATP synthase. This rotary motor enzyme utilises the proton motive force, generated from movement of electrons into the inter membrane space, to drive ATP synthesis (Stock et al., 2000).

The close relationship between the components and the mechanisms of both oxidation and phosphorylation allow these processes to be studied together. The enzymatic dependent breakdown of organic compounds and subsequent capture of the energy released into phosphate bonds is therefore termed OXPHOS. Briefly, this process is initiated by the generation of acetyl coenzyme A (CoA) from the catabolism of substrates including carbohydrates, fatty acids, amino acids and ketone bodies. Within the mitochondrial matrix, acetyl CoA enters the TCA cycle through a reaction catalysed by citrate synthase (CS), involving the condensation of the acetyl group with oxaloacetate forming citrate. The TCA cycle proceeds through a series of enzymatically driven oxidation reactions, crucially producing hydrogen ions/protons (H^+) and electrons that are accepted by the redox coenzymes nicotinamide adenine dinucleotide (NAD^+) and flavin adenine dinucleotide (FAD). The reduced forms of these enzymes, NADH and $FADH_2$, transfer these reducing equivalents to the ETS, thus becoming oxidised. The ETS complexes contain both electron exchangers and proton pumps. Transferral of electrons through these complexes via a series of redox reactions thus transduces the energy required to pump H^+ into the intermembrane space. The rate of electron transport in this manner in turn determines the rate of proton pumping, with the transfer of two electrons stimulating the transport of ten protons (Nicholls et al., 2013).

Accumulation of H^+ in the intermembrane space generates an electrochemical proton gradient, also termed the proton motive force ($\Delta\mu H^+$), which drives flux of H^+ back across the inner mitochondrial membrane. In other words, the mitochondrial complexes can be envisaged as batteries creating a voltage, being $\Delta\mu H^+$, which when connected to the circuit generates a proton current. Passage of protons back across the membrane, driven by $\Delta\mu H^+$, occurs by the pathway of least resistance, being ATP synthase. Transferral of eight protons through this motor protein is required to drive the synthesis of three molecules of ATP (Nicholls et al., 2013). Coupling of phosphorylation to electron and hydrogen transfer in this manner is termed chemiosmosis (Mitchell, 1961).

Oxygen (O_2) has a central role in driving this series of reactions by being the final acceptor of electrons in the ETS. The rate of mitochondrial O_2 consumption is equivalent to the current of electrons and so the rate of proton pumping. The end result of mitochondrial OXPHOS is a highly efficient generation of ATP. O_2 is thus among those elements whose reduction provides the largest energy release per electron transfer.

Dissipation of the H^+ electrochemical potential proton gradient can also occur through the movement of H^+ back across the inner mitochondrial membrane through routes other than ATP synthase. In doing so, the proton circuit becomes short-circuited, meaning the coupling of respiration to ADP phosphorylation is partially loose or uncoupled (Nicholls et al., 2013). This can occur via endogenous leak, which is thought to result from H^+ movement across the junction between the adenine nucleotide translocator protein and lipid bilayer, contributing to a high proportion of basal metabolic rate in some tissues (Nicholls et al., 2013). In addition, the proton gradient can be dissipated by the action of uncoupling proteins (UCPs).

UCPs belong to the family of anion carriers, or solute exchangers, present in the inner mitochondrial membrane. The action of UCPs that has been best described is that specific to brown adipose specific UCP1, which is known to dissipate the energy of substrate oxidation as heat, making it essential to non-shivering thermogenesis (being the production of heat from cellular respiration) (Rousset et al., 2004). Homologues of UCP1 have been identified: UCP2 and 3, with UCP2 expressed ubiquitously and UCP3 predominantly in skeletal muscle (Rousset et al., 2004). This naming is perhaps misleading, given that both have roles that differ quite considerably from UCP1 as neither is thought to contribute towards adaptive thermogenesis. Instead, both UCP2 and 3 have links to regulation of metabolism, specifically to fatty acid metabolism. It has been suggested that UCP2/3 regulate free fatty acid levels by exporting fatty acid anions out of the mitochondrial matrix when they are in excess (Schrauwen et al., 2002, Garlid et al., 1998, Harper et al., 2002). Indeed, fatty acids are thought to be essential cofactors for UCP proton transport (Rousset et al., 2004). The lateral binding of fatty acids to the UCP2 peripheral site is thought to be essential for the UCP2-catalyzed fatty acid flipping action required for proton translocation across the membrane (Berardi et al., 2014). Fatty acids are also known to upregulate UCP3 (Schrauwen et al., 2002). Beyond relations to fatty acid metabolism, UCP2 has also been linked to decreasing insulin secretion in pancreatic β-cells and restoring glucose sensing (Zhang et al., 2001). In addition, both UCP2/3 are thought contribute towards the resting metabolic rate.

Basal proton leak, whether endogenous or UCP mediated, is linked to restricting oxidative damage. O_2 is capable of accepting an additional electron to create the superoxide ion, a more reactive form of O_2. Respiration is thus associated with production of reactive O_2 species (ROS). Modest increases in proton leak cause reductions in superoxide

generation via a lowering of membrane potential, thus acting as a key defence mechanism (Nicholls et al., 2013).

Second to OXPHOS is the synthesis of ATP from the cytosolic breakdown of glucose into two molecules of pyruvate via glycolysis. ATP is produced in the phosphoglycerate kinase and pyruvate kinase reactions by direct phosphorylation from ADP. This process, termed substrate level phosphorylation, can occur independently of O_2, so anaerobically, and produces a far lower yield of ATP in comparison to OXPHOS. Despite this, the capacity of glycolysis in providing ATP is seemingly great in certain conditions. Most cancerous cells, for instance, 'ferment' glucose into lactate even in the presence of an ample supply of O_2, a phenomenon termed the Warburg effect (Vander Heiden et al., 2009). Additionally, human lung fibroblast populations have been shown to demonstrate normal functioning without the presence of a mitochondrial network, with reliance on ATP generation shifting to glycolysis (Correia-Melo et al., 2016). Dependence upon glycolytic mechanisms may therefore be a feature apparent in proliferating cell types, particularly those cultured in high glucose media. However, the capacity of glycolysis to support life at the whole organism level over long periods of time is inconceivable. A sufficient level of mitochondrial oxidative metabolism is a vital requirement for metazoans. Indeed, impairments in the OXPHOS system as demonstrated through mitochondrial defects markedly impair physiological function and can be fatal. For instance, knockouts of proteins essential for fundamental dynamic processes such as mitochondrial fusion are shown to cause death in early gestation (Youle et al., 2012).

As already stated, the role of O_2 as a terminal electron acceptor is crucial for driving the series of reactions that constitute mitochondrial OXPHOS. A sufficient O_2 supply is thus required to maintain both energetic and redox homeostasis and so normal physiological functioning. For O_2 dependent lifeforms, the ability to adapt to changing O_2 availability through adjustment and remodelling of metabolic processes offers a crucial advantage to survival. A summary of ATP production via glycolysis and mitochondrial oxidative metabolism is provided in **Figure 1.1**.

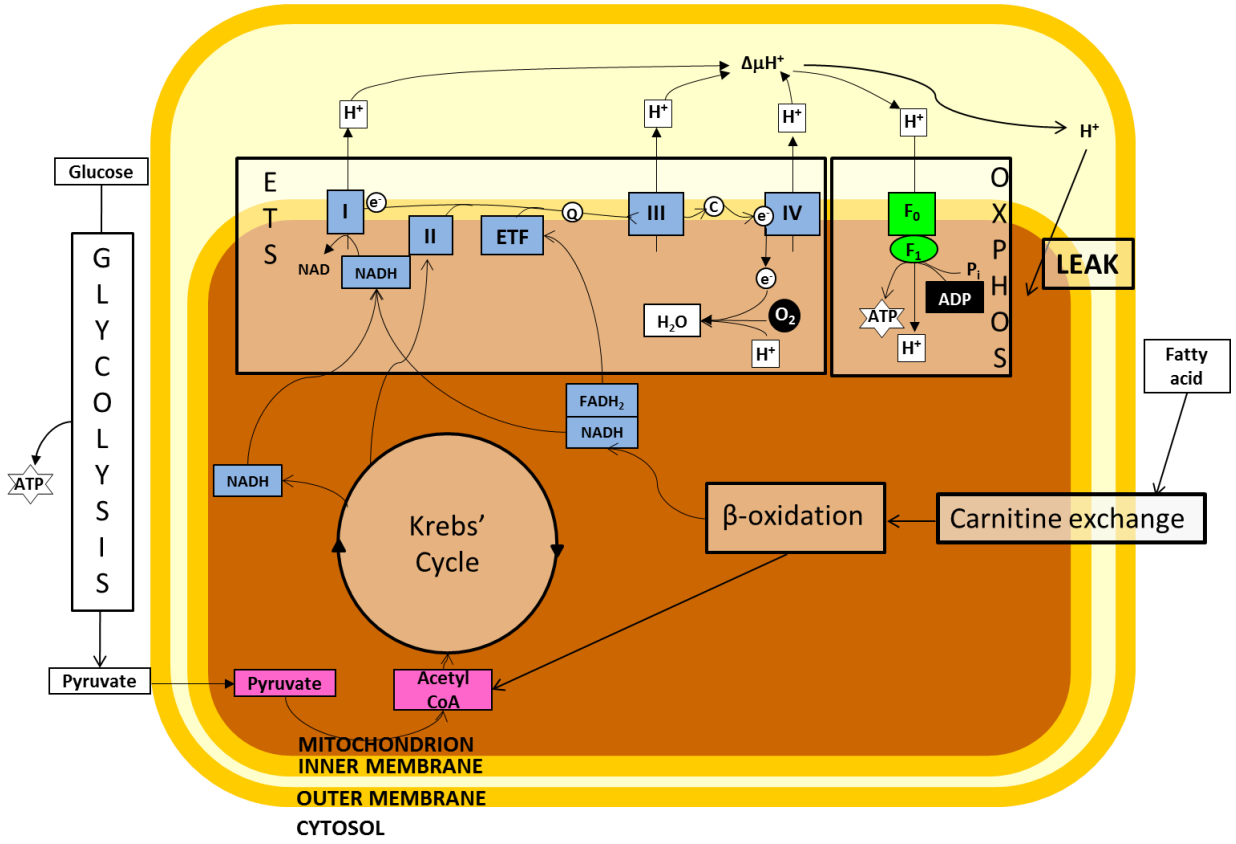

Figure 1.1. A diagrammatic representation of ATP production via glycolysis and mitochondrial oxidative metabolism.

Where: ATP = adenosine triphosphate, ADP = adenosine diphosphate, CoA = coenzyme A; Pi = inorganic phosphate, F_0/F_1 = ATP synthase; NADH = nicotinamide adenine dinucleotide; $FADH_2$ = flavin adenine dinucleotide; ETS = electron transfer system; I,II,III,IV = ETS complexes; ETF = electron transfer flavoprotein, e^- = electrons, Q = ubiquinol, c = cytochrome c; $\Delta\mu H^+$ = proton motive force, OXPHOS = oxidative phosphorylation, LEAK = leak state respiration/basal proton leak.

1.2.2 Hypoxia

As already stated, hypoxia can be experienced in healthy humans in response to high altitude exposure. At high altitudes, the atmospheric pressure falls as atmospheric mass is reduced. This causes the P_B to also decrease and it continues to fall as the altitude increases. The air at high altitudes is therefore less compressed and so thinner. At sea level, the atmospheric pressure is at 760mmHg compared to 253mmHg at the top of Mount Everest, which is 8848m (29,029 ft) (Grocott et al., 2007b) . This means that, although the fraction of O_2 remains the same at 0.21, the partial pressure of O_2 is reduced.

A fall in P_IO_2 generates a smaller diffusion gradient in the lungs, which in turn impairs alveolar gas exchange. PO_2 is decreased further as inspired O_2 is mixed with the contents of the lung and as gases cross the alveolar blood barrier due to the effects of ventilation-perfusion mismatch. A reduced P_IO_2 therefore interferes with the O_2 cascade **Figure 1.2.** leading to impaired oxygenation and a decrease in arterial O_2 tension. O_2 content of the capillaries in turn falls, meaning an inadequate O_2 supply reaches the tissues. This fall in P_IO_2 resulting from a low atmospheric pressure is termed hypobaric hypoxia (Rainford, 2006). The changes in P_B and P_IO_2 with increasing altitude are displayed in context of a climb to the summit of Mount Everest in **Figure 1.3.**

Hypoxia can also result from a plethora of clinically important conditions, both acute and chronic that can affect those of all ages. This encompasses any clinical condition where either convective or diffusive O_2 transport is impaired. Examples include lung disease, heart failure, anaemia and regional vascular diseases (Tuder et al., 2007, Giordano, 2005, Semenza, 2001, Forristal et al., 2013, Pe'er et al., 1995). A pathological consequence of the airway limitation in COPD, for instance, is alveolar hypoxia. This leads to an abnormally low level of O_2 in arterial blood, termed hypoxaemia, so in turn tissue hypoxia. This becomes particularly prominent in the more progressed stages of the disease and after exercise in patients with the milder form. A state of chronic hypoxia is thus common for COPD sufferers, the degree of which depends upon disease severity (Raguso et al., 2004).

Understanding the mechanisms that underpin mammalian adaptation to O_2 insufficiency and ways that may aid adaptation are areas of intense investigation worldwide. This is both in relation to high altitude exposure, which is becoming more common as travel to high altitude destinations becomes more accessible, also in clinical settings where physiological adaptations to low O_2 play a key role in disease pathology.

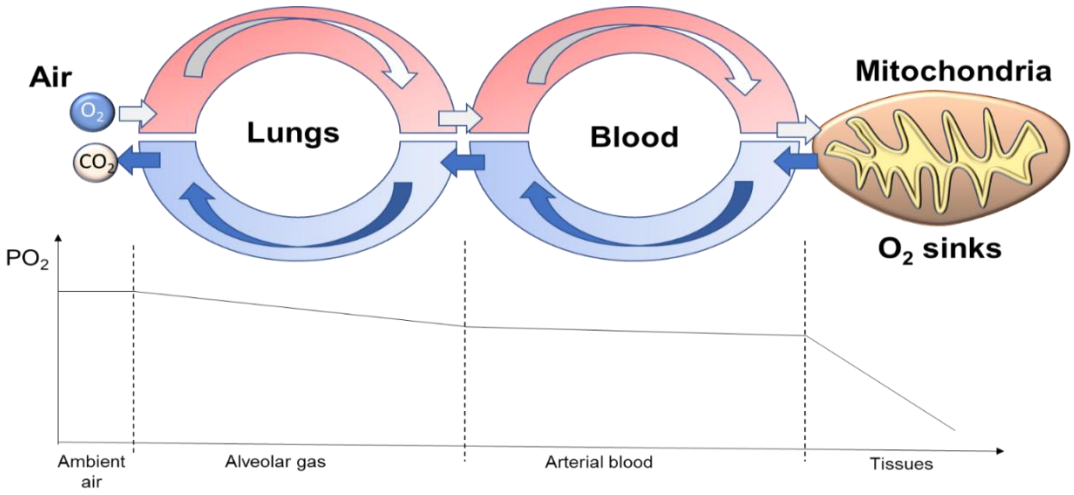

Figure 1.2. A model of the O_2 cascade.

Describing the flow of oxygen (O_2) from ambient air through arterial blood to tissues. At the cellular level, O_2 is consumed by mitochondria, which are thus referred to as the O_2 'sinks'. The partial pressure of O_2 (PO_2) falls progressively from environmental values to close to zero at the sink. The O_2 flow is driven by this gradual reduction in PO_2 and, in particular, O_2 consumption at the mitochondria. Waste products from cellular respiration, including CO_2 are transferred via the venous system to be expired.

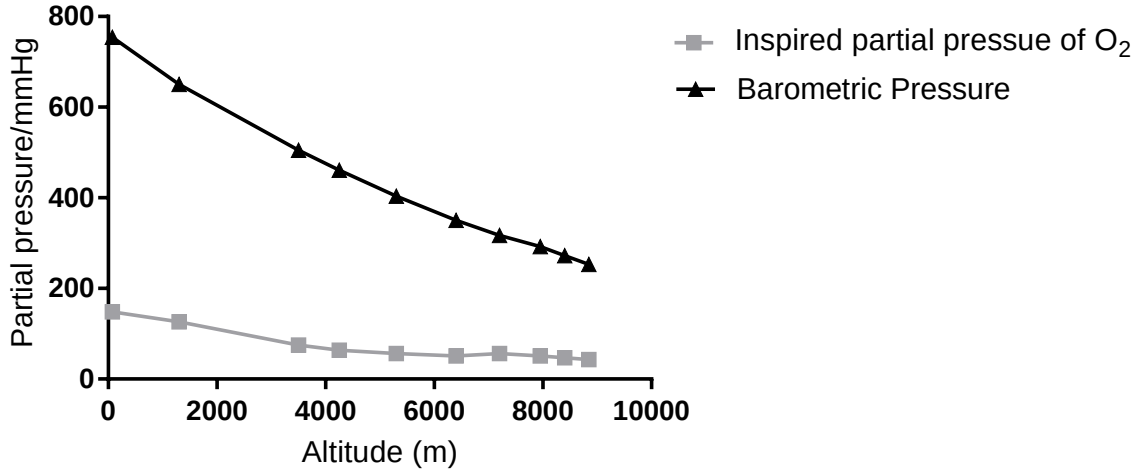

Figure 1.3. Alterations in barometric pressure and the corresponding changes in inspired partial pressure of oxygen (O_2) upon ascent to the summit of Mount Everest.

Values begin at sea level, followed by key checkpoints upon ascent, being: Kathmandu, Namche, Pheriche, Everest Base Camp, Camp 2, Camp 3, Camp 4, the balcony and the summit.

1.2.3 Physiological adjustments to hypoxia in healthy humans

Physiological adjustments need to occur upon hypoxic exposure to enable ATP production to continue without compromising the redox balance of the cell. This ensures cell survival and enables the body to undergo additional stresses such as exercise in hypoxic conditions.

Oxygen (O_2) delivery

Certain aspects of these adjustments are well understood, including: increased ventilation, heart rate, erythropoiesis and a possible enhanced vascularisation of tissues (Sutton et al., 1988, Rainford et al., 2006, Martin et al., 2010). These changes are geared at improving O_2 delivery and enabling maintenance of arterial O_2 saturation and O_2 content. In the context of high altitude exposure, these adjustments can be sufficient to maintain arterial O_2 saturation at values comparable to those taken at sea level up to an altitude of ~7100m (Grocott et al., 2007b). Following acclimatisation to high altitude, cardiac output also remains unchanged from sea level values for a given work load during submaximal exercise, implying the O_2 delivery system is maintained (Pugh, 1964, Sutton et al., 1988).

In spite of these observations, exercise capacity is severely limited at altitude, a phenomenon that appears to be worsened in elite athletes (Grover et al., 1985, Gore et al., 1996). There is also a considerable degree of inter-individual variation to hypoxic adaptation (Thompson et al., 2007). Changes at the tissue level, so at the level of O_2 utilisation, must therefore play a pivotal role in the adaptive process (Martin et al., 2010). Central to tissue adaptations is alteration in protein levels mediated by changes to gene expression.

Hypoxic inducible factor (HIF)

An array of gene expression changes are induced by prolonged hypoxic exposure. Master regulators of the adaptive responses at both cellular and tissue levels are hypoxic inducible factors (HIFs). HIFs are heterodimeric basic helix-loop-helix transcription factors that are members of the PAS family (Wang et al., 1995).

HIFs consist of an O_2 sensitive α subunit (HIF-α) and a constitutively expressed β subunit (HIF-β); interaction of both subunits is required for activation (Ratcliffe et al., 1998, López-Barneo et al., 2001). In normoxic conditions, HIF-α subunits are tagged for proteasomal degradation through von Hippau Lindau protein dependent polyubiquitination.

This constant degradation of HIF-α is a process reliant on O_2 dependent hydroxylation of proline residues by prolyl hydroxylase 2, which utilises O_2 and α-ketoglutarate as co-substrates (Ivan et al., 2001, Kaelin et al., 2008). It thus follows that the rate of HIF hydroxylation is suppressed in hypoxia, so HIF-α is stabilised and accumulates spontaneously in the hypoxic cell. It enters the nucleus, where it binds the stable subunit HIF-β. The resulting complex binds hypoxia response elements in the regulatory regions of hundreds of genes (~200 in the case of HIF-1α), the levels of which are precisely controlled in response to cellular O_2 levels (López-Barneo et al., 2001, Kaelin et al., 2008).

Three isoforms of the HIF-α subunit have been identified: HIF-1α, HIF-2α and HIF-3α. The HIF-1α and HIF-2α responses are well defined, both acting to regulate a unique set of target genes to improve O_2 delivery through angiogenesis (e.g. vascular endothelial growth factor) and erythropoiesis (via erythropoietin), as well as cell proliferation (Suzuki et al., 2014, Semenza et al., 1992, Forsythe et al., 1996). In addition, HIF-1α regulates a host of genes that influence cellular metabolism including glycolytic enzymes, whereas HIF-2α is an inducer of antioxidant genes (e.g. superoxide dismutase 2) (Suzuki et al., 2014).

Far less certainty surrounds the roles of HIF-3α. The HIF-3α gene gives rise to multiple variants of HIF-3α, which are differentially expressed across different tissues and have varying responses to hypoxic exposure (Duan, 2016). Whilst HIF-3α lacks a transactivation domain, and so is considered to be transcriptionally inactive, its actions appear to regulate HIF-1/2α, with some variants inducing inhibitory effects (Duan, 2016, Suzuki et al., 2003)

Although much controversy exists with regards to the effects of changing HIF expression, for instance upon fatty acid oxidation (Cole et al., 2016), it is clear that the HIF pathway plays a central role in regulating the transcriptional response to changing O_2 availability, including mediation of metabolic responses (Kaelin et al., 2008).

1.2.4 Metabolic remodelling

The metabolic response of healthy humans to hypoxia is complex and remains incompletely resolved. As previously described, in a rested state in normoxia, the majority of ATP is produced from mitochondrial OXPHOS. Few cells are able to rely solely upon anaerobic means of ATP generation (Weibel, 1984). Survival in the face of reduced O_2 availability thus requires a profound shift in metabolic processes including changes in O_2 dependent processes. This is crucial in those oxidative tissues critically dependent upon a sufficient supply of O_2 to maintain oxidative and redox homeostasis, such as skeletal muscle.

A range of techniques can be utilised to assess metabolic changes within an organism. In this thesis, frequently utilised measures were metabolomic and lipidomic techniques. Specifically, both techniques were adopted in Chapter 2, whilst only metabolomic methods employed in Chapters 3 and 5. In addition, in depth examination of mitochondrial function was assessed through respirometry in Chapter 4.

A brief introduction to metabolomic and lipidomic techniques is given below, with further detail provided in Chapter 2. As mitochondrial respirometry measures are restricted to Chapter 4, detail on this approach is provided in the relevant chapter.

Metabolomics

Recent technological advances have allowed for the unbiased detection, identification and semi-quantification of many low molecular weight (<1500 Da) compounds in cells, tissues, biofluids or organisms, in a single experiment. These compounds are metabolites, being the reactants, intermediates or products of enzymatic reactions in the body. They represent the final products of key cellular processes including mRNA and protein activity, and are key components of oxidative mitochondrial processes such as the tricarboxylic acid (TCA) cycle and β-oxidation. Investigation into the metabolic phenotype, or metabolome, in response to a physiological stimulus or genetic modification is termed metabolomics. It is a functional level of systems biology (Sauer et al., 2007).

The metabolome is highly dynamic and subject to fluxes over a period of seconds or less. This thus sets it apart from proteome or transcriptome changes, which are usually measured over minutes to hours. The metabolome is therefore an extremely sensitive measure of biological phenotype and can unmask seemingly silent phenotypic changes that have no frank physiological or characteristic behaviour (Dunn et al., 2011b, Griffin, 2006), particularly when used alongside other -omics approaches (Gulston et al., 2008, Mukherjee et al., 2014, Waterman et al., 2010).

Lipidomics

An extension of metabolomics is the specific measurement of the lipid complement of a cell, tissue or organism termed the lipidome. This focused approach, termed either lipidomics or lipid profiling with both terms being used interchangeably, has become necessary due to the complex nature of lipid classes and their variable yet distinct chemical properties (Roberts et al., 2008). Lipids are functionally and structurally a highly diverse group of compounds. This is partly due to the many possible variations of lipid building

blocks, mainly originating from combinations of fatty acids with variable chain lengths and possible head groups. This is coupled with possible non-covalent linkages both with variable fatty acid and non-lipid moieties such as carbohydrates (Yetukuri et al., 2008).

The extensive role lipid species play within the cell is fast becoming apparent. Previously, the majority of lipids were considered either as components of a homogenous, fluid membrane or an energy store. Whilst their function as structural compounds and energy stores are essential, the diversity of their roles, for instance in signalling processes and as biomarkers, is also becoming clear. It is now understood that lipid domains within cellular membranes, termed lipid rafts, partake in a variety of dynamic cellular processes including trafficking, signal transduction and regulation of the activity of membrane proteins (Niemelä et al., 2007). Maintenance of membrane composition is thus paramount to the preservation of normal cellular physiology. Even minor changes in lipid composition have been demonstrated to affect elastic and dynamic properties of membranes, whilst also likely having effects upon the regulation of membrane proteins (Niemelä et al., 2007). In addition, lipids have roles in mediation of cell-cell interactions as well as transcriptional and translational processes (Roberts et al., 2008).

Recognition of the diverse functioning of lipids has thus driven interest towards defining changes in lipid profile, which has in turn become a powerful means for investigating the role of lipids in pathophysiological states such as diabetes (Kraegen et al., 2001). Examination of the lipid profile can act as an indication of change within a cell or organism over time in response to environmental alterations (Roberts et al., 2008).

An outline of metabolomic and lipidomic approaches is provided in **Figure 1.4.**

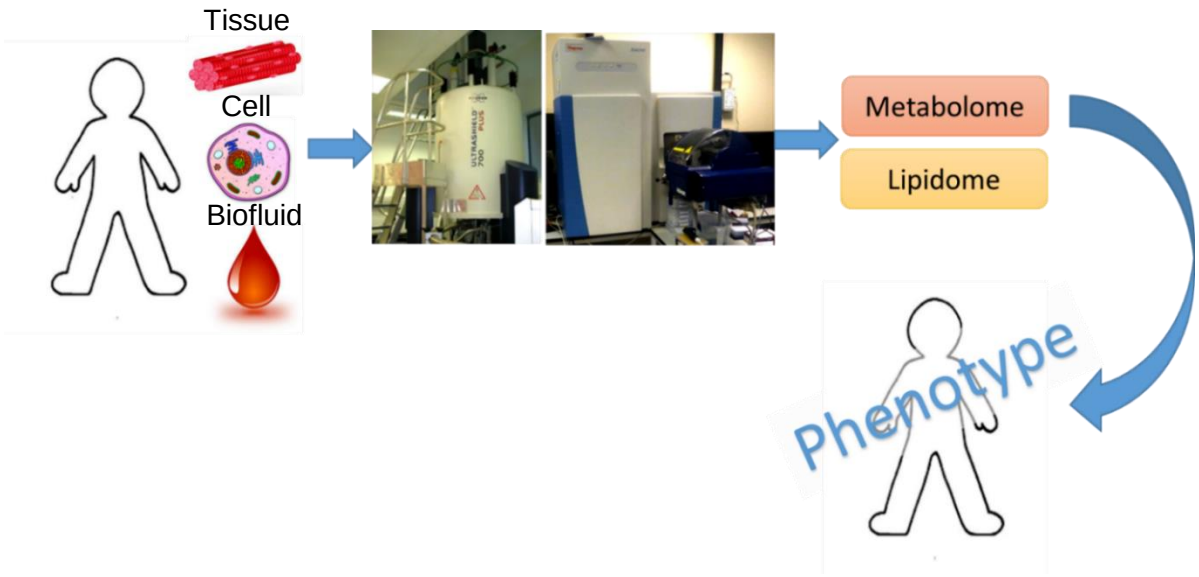

Figure 1.4. An outline of metabolomic and lipidomic techniques on human subjects.

This can include assessment of tissue, cells or a biofluid, such as blood, using a combination of nuclear magnetic resonance spectroscopy and mass spectrometry. These analytical platforms give a readout of the metabolome and lipidome, which provide detailed insight into the biological phenotype of the subject.

In line with the focus of this thesis, the following summary of metabolic remodelling in hypoxia includes those studies using metabolomic techniques and on those assessing specific markers of skeletal muscle metabolic processes alongside the wider field. The latter of these measurements is covered far more extensively in the literature than the former. The extant metabolomics experiments investigating the physiology of high altitude have focused on profiling plasma, serum or urine from hypoxia-exposed individuals. To the author's knowledge, lipidomic assessment has not been explored in this context. For the studies discussed below, both the degree and duration of hypoxic exposure is highly variable.

Glycolysis

A switch in cellular metabolite usage from the predominant breakdown of fatty acids, as occurs at rest in normoxia, to an increase in carbohydrate metabolism appears to be a logical adaptive process when considering the O_2 requirement of these essential metabolic processes. In comparison to fats, carbohydrates require less O_2 to breakdown (Opie, 2004). In theory, metabolism of free fatty acids requires ~13% more O_2 to generate the same amount of ATP in comparison to glucose (Opie, 2004). Shifting towards an increasing carbohydrate metabolism thus has the potential to maximise the yield of ATP per molecule of O_2, allowing cells to utilise metabolites more efficiently in low O_2 conditions.

Indeed, this concept is supported by a number of studies demonstrating that glycolytic capacity is enhanced in response to hypoxic exposure through HIF-1α mediated up-regulation of glucose transporters and degradation enzymes (López-Barneo et al., 2001, Roberts et al., 1996).

Glucose transport is a key rate-controlling step in glucose metabolism and hypoxia is a well-established stimulator of glucose uptake (Behrooz et al., 1999). This is a complex process involving an array of transporters, including a highly homologous group of facilitative Na^+ independent transmembrane sugar transporters, the GLUT family (Wood et al., 2003). This family is thought to consist of three subclasses (I-III), with class I containing GLUT1-4. Particularly of interest in hypoxia is the stimulation of GLUT-1 and 4 (Behrooz et al., 1999). The former is expressed ubiquitously and mediates non-insulin dependent transport of glucose in mammals, whereas the latter is insulin responsive and is found primarily in adipose tissue and striated (cardiac and skeletal) muscle. Translocation of GLUT1 and 4 from intracellular vesicles to the plasma membrane in response to hypoxic exposure has been demonstrated in mammalian striated muscle and numerous cell lines (e.g. L6 myotubes and 3T3-L1 adipocytes) (Behrooz et al., 1999). The protein levels of both

transporters were demonstrated to rise in rat skeletal muscle in reaction to hypoxic exposure, a response regulated by HIF-1α (Xia et al., 1997, Semenza, 1999).

HIF-1α has also been shown to up-regulate RNA expression for a host of glycolytic enzymes in human skeletal muscle and hepatocyte cell lines, including: aldolase A, phosphoglycerate kinase 1 and pyruvate kinase (Semenza et al., 1994, Green et al., 1989). This appears to occur alongside a shunting of pyruvate away from entry into the TCA cycle towards lactate production, as HIF-1α induces pyruvate dehydrogenase kinase (PDK) in mouse embryo fibroblasts, which blocks the activity of pyruvate dehydrogenase and so inhibits conversion of pyruvate to acetyl CoA (Kim et al., 2006). This is coupled with a reported up-regulation of lactate dehydrogenase by HIF-1α in human skeletal muscle and HeLa cells, which enhances the anaerobic conversion of pyruvate to lactate (Firth et al., 1995, Green et al., 1989). These gene expression changes induced by HIF-1α activation thus appear both to enhance the capacity for glycolysis and actively suppress the catabolism of pyruvate within the mitochondria. This hypoxic induced shift from fatty acid metabolism towards a more O_2 efficient metabolism of carbohydrates is an effect demonstrated to preserve cardiac function (Essop, 2007, Cole et al., 2016).

However, the evidence assessing glycolytic changes upon hypoxic exposure is far from conclusive and there are numerous human skeletal muscle studies that demonstrate a decrease in markers of glycolysis. This includes decreases both in protein levels and activity of glycolytic enzymes, such as α-enolase, phosphofructokinase and hexokinase (Viganò et al., 2008, Green et al., 1989, Green et al., 1992). Other studies demonstrate glycolytic markers to be unchanged (Levett et al., 2012, Young et al., 1984).

This lack of consensus extends to rodent skeletal muscle, with some studies demonstrating unchanged activity levels of glycolytic enzymes, such as lactate dehydrogenase and hexokinase (Abdelmalki et al., 1996, Ou et al., 2004). However, this is coupled with reported increases in phosphofructokinase and hexokinase activity as well as increasing levels of pyruvate kinase (Abdelmalki et al., 1996, De Palma et al., 2007, Daneshrad et al., 2000). In addition, decreases have been reported in the membrane proteins that facilitate the transport of lactate, monocarboxylate transporters, and in levels of β-enolase, phosphoglycercomutase 2 and triose phosphate isomerase (McClelland et al., 2002, De Palma et al., 2007).

The literature thus suggests that there is more to the acclimatisation story than a simple shift towards glycolysis. It may be that specific steps within glycolysis are altered, or that

the changes vary depending on the severity and duration of hypoxia. However, currently no clear patterns have emerged. To complicate matters further, metabolic plasticity during acclimatisation appears to vary depending upon tissue type. For instance, the heart and plantaris have been suggested to have a greater metabolic plasticity compared to the liver, gastrocnemius and soleus (McClelland et al., 2002).

The seemingly discordant data presented in the literature may be partly explained, or further complicated, by the 'lactate paradox' (Hochachka et al., 2002). This phenomenon is defined as a lower-than-expected accumulation of blood lactate in VO_2 max tests in native highlanders compared to lowlanders and also in acclimatised lowlanders compared to unacclimatised (Hochachka et al., 2002). It was first recorded in high altitude acclimatised lowland native subjects displaying lower peak and post exercise blood lactate concentrations with increasing altitude (West, 1986). The observation that less lactate production occurs under more O_2 limiting conditions may initially appear perplexing. However, numerous functional advantages for this have been recognised including: maintenance of metabolite homeostasis at fatigue, quicker recovery periods and avoidance of ATP generation through metabolically inefficient anaerobic pathways. The mechanisms behind this so called 'paradox' may result from tighter coupling between muscle ATP demand and supply pathways (Hochachka et al., 2002), a concept that has been demonstrated in Andean high altitude natives and lowlanders through the use of *in vivo* 31-phosphorus magnetic resonance spectroscopy (^{31}P-MRS) (Matheson et al., 1991). Measurements of phosphocreatine (PCr), free phosphate (Pi) and muscle pH in response to a maximal calf strength test indicated a closer coupling between ATP supply and demand in the working muscle (Matheson et al., 1991).

TCA cycle

Biomarkers of TCA cycle function include the activity and expression levels of its constituent enzymes. Amongst those enzymes studied include: CS, succinate dehydrogenase, aconitase, malate dehydrogenase, pyruvate dehydrogenase and α-ketoglutarate. Studies examining these factors in human skeletal muscle in response to high altitude exposure demonstrate either a decrease in enzyme activity and expression (Levett et al., 2012, Viganò et al., 2008, Green et al., 1989), or report no change (Levett et al., 2012, Jacobs et al., 2012, Green et al., 1992, Green et al., 2000) , with none demonstrating an increase (Horscroft et al., 2014). This appears to be true both for human and rodent studies alike, with some rodent studies demonstrating decreases in TCA cycle enzyme activities

and levels (Abdelmalki et al., 1996, De Palma et al., 2007, Pastoris et al., 1995) and some demonstrating no change (Abdelmalki et al., 1996, Morash et al., 2013, Pastoris et al., 1995, Daneshrad et al., 2000).

Unlike glycolytic changes, the loss of TCA activity in skeletal muscle appears to depend upon the severity of hypoxic exposure, with a greater degree of hypoxia being in turn associated with a greater loss in TCA function (Horscroft et al., 2014). This effect appears to be unrelated to the particular type of enzyme assay used (Horscroft et al., 2014).

Insight into TCA cycle functioning can also be gained from metabolic profiling, as demonstrated by Tissot van Patot and colleagues (Tissot van Patot et al., 2009). In this study, metabolomic profiling was performed on samples taken from human subjects following 8hrs exposure to 12% O_2 (equivalent to ~4300m) in a hypobaric chamber. Assessment of plasma using proton nuclear magnetic resonance (^{1}H-NMR) spectroscopy revealed an increase in L-lactic acid (HMDB00190) and succinic acid (HMDB00254) concentrations, by 29% and 158% respectively in response to hypoxia (Tissot van Patot et al., 2009). These findings thus align with those studies suggesting that hypoxia prompts a shift towards anaerobic means of ATP generation through an active shunting of pyruvate away from entry into the TCA cycle towards lactate production as well as inhibition of TCA cycle activity (Firth et al., 1995, Hoppeler et al., 2001, Kim et al., 2006). The consequences of increasing succinic acid concentrations are discussed below in relation to mitochondrial OXPHOS and the ETS.

Oxidative phosphorylation (OXPHOS)

OXPHOS rate is determined by flux of electrons through the complexes that constitute the ETS. Investigation in both humans and rodents into protein levels, gene expression and activity of these complexes, the latter being indicative of OXPHOS capacity, present a confusing picture. The majority of evidence appears to point towards a decrease in these parameter (Viganò et al., 2008, Levett et al., 2012, Pastoris et al., 1995, McClelland et al., 2002, De Palma et al., 2007, Gamboa et al., 2010) although some studies also present no change (Pastoris et al., 1995, Morash et al., 2013, Levett et al., 2012). An increase in complex V (ATP synthase) activity was demonstrated in mice, although this occurred alongside a decrease in levels of cytochrome c oxidase (complex IV, COX) (Gamboa et al., 2012).

Investigation into mitochondrial O_2 consumption in response to the addition of various substrates, termed mitochondrial respirometry, reveal little change in complex I and II function in human skeletal muscle in response to an altitude (4,559m) exposure for between 9-11 days (Jacobs et al., 2013). However, a significant decrease in these measures was recorded in human skeletal muscle following 28days exposure to 3,454m (Jacobs et al., 2012) and specifically in complex I dependent OXPHOS in rodents (Gamboa et al., 2012).

Given that the succinate dehydrogenase is also complex II of the ETS, insight into OXPHOS capacity can also be gained from assessment of the levels of the substrate of this enzyme, succinate. The accumulation of succinate in response to 8 hrs exposure to 12% O_2, as reported by Tissot Van Patot and colleagues, may be indicative of a concerted downregulation of both TCA cycle and ETS activity (Tissot van Patot et al., 2009). Interestingly, succinate is also suggested to have a toxic effect in the heart in response to ischemia, as its accumulation has been directly linked to mitochondrial ROS production from complex I (Chouchani et al., 2014).

Alongside repression of OXPHOS are reports of an increasing efficiency of complex IV of the ETS under hypoxic conditions through a switch in the composition of this complex. Complex IV, or cytochrome c oxidase (COX), belongs to a superfamily of multi-subunit terminal oxidases that catalyse the reduction of O_2, the final electron acceptor in the ETS, to H_2O. It comprises of 13 polypeptide COX subunits, some of which are subject to regulation. In mammalian cells, hypoxia has been shown to induce a shift from COX 4-1 subunit isoform utilisation to the more efficient COX 4-2 isoform, an effect coordinated by HIF (Fukuda et al., 2007).

β-oxidation

The literature examining fatty acid catabolism, otherwise termed β-oxidation, indicates a suppression in skeletal muscle in response to hypoxic exposure (Horscroft et al., 2014). Biomarkers include activity of enzymes, such as 3-hydroxyacyl-CoA dehydrogenase (HOAD), which is shown to be decreased (Galbès et al., 2008, Abdelmalki et al., 1996, Levett et al., 2012), with some studies demonstrating no change (Green et al., 1992, Morash et al., 2013, Daneshrad et al., 2000, Sterne et al., 1997, Green et al., 1989, Abdelmalki et al., 1996). Levels and activity of transport proteins that control fatty acid import are another commonly assessed parameter. This includes carnitine palmitoyltransferase and, to a lesser extent, carnitine-acylcarnitine translocase. Again, these parameters appear to be decreased

in response to hypoxic exposure in rat and human skeletal muscle (Galbès et al., 2008, Morash et al., 2013, Viganò et al., 2008).

Alongside examination of expression or activity of components of the β-oxidation pathway are functional mitochondrial respirometry measurements that assess OXPHOS of β-oxidation substrates. Hypoxic induced downregulation of β-oxidation is supported through evidence of suppressed palmitoyl carnitine OXPHOS in rodents (Morash et al., 2013, Galbès et al., 2008). Conversely, octanoyl carnitine measurements were unaffected by hypoxic exposure in human studies (Jacobs et al., 2012, Jacobs et al., 2013). This thus indicates that species specific responses may exist.

Peroxisome proliferator activator receptor alpha (PPARα)

The mechanisms behind the reported hypoxic induced suppression of β-oxidation remain to be fully elucidated, but evidence suggests it involves the ligand activated transcription factor peroxisome proliferator activator receptor alpha (PPARα) (Willson et al., 2000). This is a member of a family of nuclear hormone receptors discovered in the 1990's, first named by virtue of their activation by peroxisome proliferators in rodents (Issemann et al., 1990). Since then, the most prominent ligands of these receptors have been identified as natural fatty acids, preferably of a chain length above 10 carbons, fatty acid derivatives including eicosanoids such as leukotriene B4, as well as synthetic compounds such as the fibrate class of hypolipidaemic drugs (e.g. clofibrate) (Wahli et al., 1995, Barbier et al., 2002, Willson et al., 2000). The PPARs thus enable nutrient derivatives to act upon gene regulation in a similar way as steroid or thyroid hormones act on their nuclear receptors.

Ligand binding facilitates the heterodimerisation of PPARs with the retinoic acid receptor. The resulting heterodimer complex binds to the peroxisome response element in the promoter region of target genes, which consists of a specific direct repeat element, DR-1 (Wahli et al., 1995, Gearing et al., 1993). This process is aided by ligand mediated recruitment of cofactors alongside histone acetylase activity (Kota et al., 2005) and results in a change in the mRNA expression level of these target genes. This includes regulation of several genes encoding for proteins that control fatty acid metabolism, such as medium-chain acyl-coenzyme A dehydrogenase (MCAD), and glucose metabolism, including pyruvate dehydrogenase kinase 4 (PDK4) and glucose transporter 4 (GLUT4) (Gulick et al., 1994, Finck et al., 2002).

Three distinct subtypes of PPAR have been identified: PPARα, PPARγ and PPARδ. Each demonstrates a particular tissue distribution and ligand specificity. Distinction between the biological function of the subtypes is thought to result from variation in the N-terminal region of the receptor (Willson et al., 2000). The importance of PPARα in hypoxic adaptation has become evident in high altitude native populations (Simonson et al., 2010) and through various links between the HIF system regulating PPARα (Huss et al., 2001, Aragonés et al., 2008, Ferguson et al., 2015). Much debate exists in the literature regarding the links between HIF and PPARα expression and activity and also tissue specific responses of PPARα in hypoxia.

The role of PPARα in hypoxia has been explored in the most depth in the heart. Cole and colleagues (Cole et al., 2016) observed a decrease in cardiac PPARα expression in response to hypoxic exposure in mice (11% O_2 for ~3 weeks), coupled with suppression of β-oxidation and UCP3 levels. These responses were linked to a preservation of cardiac function, reflected in the maintenance of normoxic [ATP] and contractile function. They occurred alongside upregulated carbohydrate metabolism, shown through increased expression of PDK4 and GLUT4. This suggests that in the heart, PPARα plays a key role in regulating the balance between fatty acid and glucose metabolism. This conclusion was further supported through the effects of PPARα genetic ablation, which was shown to induce a similar shift in metabolic preference. This adaptation was lost in high fat feeding conditions that provoked PPARα upregulation (Cole et al., 2016). Along with this, a prior study reported PPARα activity to be deactivated in hypoxic rat cardiomyocytes through a reduction in its co-factor, retinoid x receptor; a process suggested to be regulated by HIF-1α (Huss et al., 2001).

Contrary to these findings, an earlier study by Morash and colleagues demonstrated an increase in PPARα protein levels in the mouse heart by 30% in response to 7 days hypoxic exposure (13% O_2), occurring alongside a 30% decrease within mouse skeletal muscle. Interestingly, these seemingly opposing responses were accompanied by decreases in levels and activity of the PPARα target CPT1 in both tissues (Morash et al., 2013).

However, other studies support an increase in skeletal muscle PPARα activity in response to hypoxia. For instance, findings in human skeletal muscle demonstrate an increase in PPARα protein levels in subjects returning from the summit of Mount Everest (Levett et al., 2012). Indeed, dependence upon PPARα activity for inducing hypoxia

tolerance has been demonstrated in mouse skeletal muscle myofibres. The loss of O_2 sensing HIF prolyl hydroxylase (Phd1) in mouse skeletal muscle induced a reduction in O_2 consumption and a reprogramming of the metabolic pathway from oxidative to anaerobic ATP production through activation of PPARα. The increase in PPARα activity was thus related to HIF accumulation, the resultant effects mediated specifically though HIF-2α., (Aragonés et al., 2008). Whilst this mechanism impaired oxidative performance in normoxic conditions, it reduced oxidative stress, conferring protection against ischemic injury (Aragonés et al., 2008).

Links between PPARα and HIF-2α have extended to the liver. Through constitutive activation of HIF-2α, Rankin and colleagues demonstrated a HIF-2α dependent onset of severe hepatic steatosis. This was associated with impaired β-oxidation, including downregulated expression of PPARα target genes and downstream mRNA levels, suggesting impairment in PPARα signalling. This occurred alongside substantial decreases in OXPHOS of fatty acid substrates that was recovered with the addition of glutamate and succinate, suggesting a β-oxidation specific defect (Rankin et al., 2009).

Fat storage and synthesis

Key to the breakdown of fatty acids via β-oxidation is the control of fat store mobilisation. Triglycerides (TGs), made up of free fatty acids esterified to the 3-carbinol O_2 atoms of glycerol, act as a benign form of fatty acid storage. Although cells of most tissues are capable of TG synthesis, few are capable of high levels of TG storage. Those that are include skeletal and cardiac muscle, with the most prominent store in mammals being the liver and adipose tissue. Prior to their usage as an energy source, TGs are mobilised via lipolysis. This process can be initiated by catecholamine stimulated phosphorylation of hormone sensitive lipase (Nilsson, Strålfors et al. 1980), the activity of which stimulates lipolysis and so the mobilisation of adipose tissue TG stores (Gibbons, Islam et al. 2000). Given that hypoxic exposure has been linked to increasing release of catecholamines, particularly noradrenaline (Young et al., 1989, Siervo et al., 2014), it likely acts as a stimulator for mobilising adipose TG stores. Indeed, changes in circulating TGs have been reported in numerous altitude studies, with some demonstrating moderate increases and some decreases (Wee et al., 2015, Wagner, 2010).

Systemic transport of TGs is mediated by soluble lipoproteins. Fatty acids released from the adipose tissue act as the predominant substrate for the production of hepatic very low density lipoproteins (VLDL), to be transported systemically (Gibbons, Islam et al. 2000).

In turn, the fatty acids carried by VLDL can be returned to adipose tissue via the action of lipoprotein lipase. The action of lipoprotein lipase has been shown to be strongly inhibited by acute hypoxia in differentiated adipocytes (Mahat et al., 2016a). This may result from a hypoxic induced increase in activity of a major post-translational regulator of lipoprotein lipase, ANGPT4, causing inactivation at the plasma membrane of adipocytes (Wood et al., 2011). Together, this suggests that hypoxia may impair the uptake of lipids in adipose tissue.

Another lipoprotein generated during TG transport is high density lipoprotein (HDL). This acts both as a site for cholesterol esterification and as a transporter of cholesterol from peripheral tissues to the liver (Eisenberg, 1984). HDL levels were reported to undergo a 23% increase in response to hypobaric hypoxic exposure (Young et al., 1989), however, this is not the case across all high altitude studies with some showing decreases in HDL and others no change (Wee et al., 2015).

Beyond the transport of lipids is import from serum and regulation of the balance in availability of saturated and unsaturated fatty acids. This latter point is partially mediated through the activity of stearoyl-CoA desaturase 1 (SCD1). This catalyses an oxidative reaction converting saturated fatty acids to unsaturated, a key step in lipogenesis from acetyl-CoA that is essential for cell growth (Hess et al., 2010). Given the dependence of SCD1 upon O_2, its activity is suppressed in hypoxic conditions (Kamphorst et al., 2013, Matschke et al., 2016). In an attempt to compensate for impaired SCD1 activity, it appears that fatty acid import from serum particularly that sourced from lysolipids is enhanced through serum and glucocorticoid-inducible kinase in hypoxic cancer cell lines (Matschke et al., 2016, Kamphorst et al., 2013). This thus decreases requirement for *de novo* fatty acid synthesis (Kamphorst et al., 2013).

At the transcriptional level, HIF-1/2α appear to play a key role in the hypoxic mediation of fatty acid homeostasis. HIF-1α signalling has been suggested to increase adiposity, serum TGs and free fatty acids as well as induce insulin resistance in high fat feeding mouse models (Sun et al., 2013, Jiang et al., 2013, Jiang et al., 2011). This is in addition to enhanced secretion of a suggested inhibitor of *de novo* lipogenesis adiponectin, a process mediated through HIF-1α via the SOC3-STAT3 pathway (Jiang et al., 2013, Suzuki et al., 2014). Alongside this is an upregulation of fatty acid synthase, a key enzyme in lipogenesis that catalyzes the condensation of acetyl CoA and malonyl Co-A to produce palmitic acids. This was upregulated in hypoxia via sterol regulatory-element binding protein

(SREBP) through activation of Akt and HIF-1α in hypoxic human breast cancer cells (Furuta et al., 2008).

The importance of HIF-2α activity has been highlighted through genome-wide scans of high altitude native Tibetan populations, whereby the HIF-2α subunit associated with the PPARα gene (Simonson et al., 2010). As aforementioned, the activity of HIF-2α has also been associated with enhanced lipid storage capacity, with constitutive expression of HIF-2α leading to hepatic steatosis (Rankin et al., 2009).

Together, these results suggest that hypoxic exposure affects transportation, uptake and utilisation of lipids. This inevitably disrupts the finely tuned regulation of this cycle, potentially exposing tissues to the toxic effects of high levels of circulating free fatty acids (Gibbons, Islam et al. 2000, Kennedy, Martinez et al. 2009, Mayer and Belsham 2010, Shen and McIntosh 2016). Particularly in the case of palmitate, prolonged exposure is associated with glucose intolerance, as well as inflammation and apoptosis (Mayer et al., 2010, Vazquez-Jimenez et al., 2016, Kennedy et al., 2009). Together with HIF induced effects, increases in circulating fatty acids may go to explaining why high altitude exposure has been associated with insulin resistance in humans (Siervo et al., 2014, Young et al., 1989).

Despite the progress made in the area of fat storage and synthesis in hypoxia, details of this response remain ill-defined, particularly in healthy subjects. Studies assessing changes in full lipid profile in response to hypobaric hypoxia are currently lacking, yet would provide extensive insight into systemic lipid changes.

Mitochondrial network dynamics

The O_2 dependent processes discussed above are intimately related to mitochondrial morphology. Mitochondria form part of a highly dynamic tubular network, the structure of which is highly responsive to changes in cellular energy state (Youle et al., 2012). In the face of stressful, energy demanding conditions, maintenance of energy output can be achieved through mitochondrial fusion. This process involves sharing of components between mitochondria, in effect enabling mitochondria to compensate for one another's defects. Alternatively, the most seriously damaged mitochondria can be segregated through a process termed fission. In instances where the degree of mitochondrial damage is beyond a certain threshold, a process of autophagy is initiated, whereby old and damaged mitochondria are removed. Fusion and fission are closely linked to autophagy. The end goal

of these interlinked processes is to maintain a healthy mitochondrial network in the face of metabolic or environmental stresses (Youle et al., 2012).

Given that modifications to the mitochondrial network are initiated in response to the changing metabolic state of the cell, it is not surprising that O_2 limiting conditions appear to have significant effects upon mitochondrial dynamics.

A number of studies have investigated alterations in mitochondrial density of skeletal muscle in response to hypoxic exposure using various biochemical measures of mitochondrial components as biomarkers. This includes cardiolipin content and the activities of CS and complex I, which show strong correlations with mitochondrial content as assessed by transmission electron microscopy in human skeletal muscle (Larsen et al., 2012).

The number of studies demonstrating a decrease in skeletal muscle mitochondrial biomarkers in comparison to baseline measurements increases with increasing severity of hypoxia, with 57% showing a decrease in extreme hypoxia ($PO_2 \leq 10$, ca. 6250m), compared to 31% at milder exposures ($11.7 < PO_2 \leq 15$kPa, ca. 3000-5000m) (Horscroft et al., 2014). It thus appears that a loss in mass specific mitochondrial function in the short term may be followed by a loss in mitochondrial density with longer term exposure (Horscroft et al., 2014).

The loss in mitochondrial density has been reported to total ~30% of the total mitochondrial mass in human skeletal muscle, with the greatest loss occurring in the subsarcolemmal population (Hoppeler et al., 2001). It is in this region of the muscle that accumulation of lipofuscin occurs. This is a product of lipid oxidation thought to originate from mitochondrial breakdown. Biopsies taken from the vastus lateralis of seven subjects following 8-10 week exposure to altitudes above 5000m showed close to a three-fold increase in levels of lipofuscin, predominantly around the subsarcolemmal region (Martinelli et al., 1990).

Numerous factors are associated with inducing such changes in the mitochondrial network, yet effects of hypoxia upon their regulatory effects remains uncertain. The main driver for a reduction in mitochondrial density is likely autophagy, driven in part by HIF-dependent up-regulation of the pro-apoptotic protein BCL2/adenovirus E1B 19kDa interacting protein ($BNIP_3$) (Zhang et al., 2008). $BNIP_3$ increased in response to hypoxic exposure in mice, an effect shown to be mediated by HIF-1α , alongside a decrease in mitochondrial mass and respiration (Zhang et al., 2008). On the one hand, this response has been shown to enable survival of mouse embryonic fibroblasts for long periods in

hypoxia (Zhang et al., 2008). Conversely, it has been associated with promoting mitochondrial defects and cell death of rat ventricular myocytes (Regula et al., 2002).

Alterations to mitochondrial morphology have also been shown in cardiac derived cells in response to ischemia. This was demonstrated to induce mitochondrial fragmentation, a process dependent upon the mitochondrial fission protein dynamin-related protein- 1 (Drp1). Inhibition of Drp1 reduced myocardial infarct size following coronary artery occlusion (Ong et al., 2010).

Mitochondrial biogenesis may be restricted by a downregulation of mitobiogenesis factors such as peroxisome proliferator activated receptor γ co-activator alpha or beta (PGC1α/β). This is in addition to downregulation of protein synthesis through inhibition of the cell growth regulator mTOR, an effect transduced by HIF via REDD proteins in *Drosophila* (Wullschleger et al., 2006). Along with PGC-1α, mTOR is a necessary component of the transcriptional complex controlling mitochondrial biogenesis (Cunningham et al., 2007).

The effect of O_2 insufficiency on morphology of the mitochondrial network, and the mechanisms inducing any observed changes remain unclear. This again is likely due to a lack of consensus between studies with relation to the severity and duration of hypoxic exposure.

Reactive Oxygen Species (ROS)

Aside from the requirements of energy production is the paradoxical increase in oxidative stress in hypoxia, caused by an enhanced generation of ROS, such as superoxide. The mechanisms of the ETS are such that single electrons can be lost at various points to O_2, in turn forming ROS. This leak, accounting for ~3% loss in electron flux through the ETS, predominantly occurs at complexes I and III (Ward, 2008). Production of ROS in transient low levels is recognised to be a key signalling mechanism. In hypoxia however, ROS production is reported to increase, with complex III acting as a major donator of electrons, resulting from a highly reduced respiratory chain (Ward, 2008, Murray, 2009). Whilst the release of ROS from complex III appears to be an essential step in HIF stabilisation in human derived cell lines (Guzy et al., 2005), this seemingly vital signalling function is coupled with the harmful capability of ROS to oxidise proteins, lipids and nucleic acids, causing cell dysfunction. Excessive production, as occurs in hypoxia, can be toxic and induce apoptosis.

Harmful effects of ROS production have been examined through the effects upon oxidative stress. Human plasma analysis by Tissot van Patot and colleagues, for instance, revealed a reduction in the levels of the antioxidant glutathione along with an increase in urinary prostane excretion (Tissot van Patot et al., 2009). In a study by Lundy et al (2003), two weeks of altitude exposure at 4100m resulted in an increase in DNA strand breaks. Together, this thus goes along with previous reports of hypoxia increasing oxidative stress (Magalhaes et al., 2005). However, this response may be ameliorated with longer term exposure. Lundby and colleagues found DNA strand breaks reduced back to sea level values after 8 weeks exposure, suggesting certain adaptations are occurring to reduce oxidative stress. As antioxidant levels weren't increased, this indicates changes elsewhere act to restore redox homeostasis (Lundby et al., 2003).

Further evidence that oxidative stress can be ameliorated following sufficient acclimatisation time is presented through metabolic analysis of human placentas taken following labour birth, from subjects either at altitude (3,100m) or sea level (van Patot et al., 2010). ^{1}H-NMR and ^{31}P-NMR spectroscopic analysis suggested that those placentas which had developed at altitude had adapted to hypoxia, demonstrating a blunted oxidative stress response during labour, with greater concentrations of taurine and inositol potentially indicating a greater antioxidant potential. This occurred alongside a maintenance of ATP:ADP ratios and higher PCr concentrations, indicating a preconditioning to energy storage (van Patot et al., 2010).

Anthropometric measures and nutritional intake/absorption

Metabolic remodelling processes occurring at the cellular level may be downstream of changes to nutritional uptake. It also follows that such changes may be reflected in alterations to anthropometry measures. The following refer specifically to responses reported in human subjects.

Weight loss is a commonly reported consequence of high altitude exposure, worsening with increasing degrees of high altitude severity (for example: (Rose et al., 1988, Guilland et al., 1985, Boyer et al., 1984). This effect has been attributed to loss of appetite, often referred to as 'high altitude anorexia', and has prompted investigation into the effects of hypoxic exposure on appetite regulating hormones. Levels of circulating plasma acylated ghrelin, the one known appetite stimulating hormone, have been shown to fall in response to acute hypoxia in healthy male subjects (Wasse et al., 2012, Bailey et al., 2015, Shukla et al., 2005). The response of appetite suppressing hormones are less clear, with evidence

suggesting higher levels of plasma leptin (Shukla et al., 2005) yet no significant changes to peptide YY (Wasse et al., 2012).

The effects of high altitude exposure upon nutrient intake appears to extend beyond appetite regulation. The degree of body weight loss with altitude exposure has been shown to exceed that expected from the reported reduction in energy intake. For instance, the 30-50% decrease in energy intake reported upon a 40 day simulated ascent of Mt Everest was estimated to induce a 1.7kg loss in weight, which was far below the 7.4kg reported (Rose et al., 1988). Whilst authors speculated that this loss was largely attributed to detraining, it highlights the possibility of additional factors coming into play beyond appetite regulation. Indeed, alongside hormone changes are reported changes occurring to intestinal nutrient absorption, which has been examined in subjects exposed to 6300m in comparison to sea level. Stool sampling revealing decreases in fat intake (sea level vs altitude, 128g/day vs. 79g/day) were accompanied by a 48.5 % decrease in fat absorption. This occurred alongside malabsorption of carbohydrates at the small intestine, as measured through decreases in urinary xylose excretion (Boyer et al., 1984).

A combination of appetite suppression along with impaired intestinal absorption would be expected in turn to alter body composition. However, no clear patterns in body composition changes emerge with previous studies, as some demonstrate an initial loss in fat mass at lower altitudes followed by lean mass at extreme altitudes (Boyer et al., 1984) and some vice versa (Guilland et al., 1985).

Alterations to anthropometric measures and nutritional uptake with hypoxic exposure remain unclear. The lack of clarity is likely a result of discrepancies in study design, as it is highly likely changes to these measures will depend upon duration and severity of hypoxic exposure. For instance, neither loss of body weight or changes in body composition are universal findings, with no changes being observed in response to moderate altitude (<3500m) exposure (Jacobs et al., 2012). Equally, duration of hypoxic exposure is likely a determining factor, as are genetic pre-determinants, given that highland natives are reported to maintain weight and body composition at 5,400m whilst their Caucasian counterparts incurred significant losses in weight and body fat (Boyer et al., 1984).

Muscle energetics

It is not clear whether these apparent adjustments in metabolic processes evoked by hypoxic exposure translate to an altered economy of exercising muscle. An indication of

energy status of the muscle can be gained through assessment of the creatine kinase energy shuttle system. In essence, this system operates to maintain constant ATP levels through the transfer of phosphate in the reaction outlined in **Equation 1.2.**

$$\boldsymbol{ATP + Cr \leftrightarrow PCr + ADP + H^{+}}$$

Equation 1.2. The creatine kinase shuttle

Where ATP = adenosine triphosphate, Cr = Creatine, PCr = Phosphocreatine, ADP = adenosine diphosphate, H^{+} = free hydrogen ion.

Examination of this system was performed by Edwards and colleagues both in subjects trekking to 5300m and climbers ascending above 7950m. Through the use of ^{31}P-MRS, levels of exercise metabolites ADP, Pi and PCr were found to remain at sea level values. This was indicative of a retained balance between ATP: ADP production, and so skeletal muscle mitochondrial function, was maintained. This occurred despite a reduction in muscle cross sectional area (CSA) and aerobic capacity. It suggests that metabolic changes occurring in healthy humans at high altitude may preserve *in vivo* function in the face of profound structural changes (Edwards et al., 2010). This conclusion aligns with findings in high altitude native populations that demonstrate minimal perturbation to parameters associated with phosphorylation potential in the working muscle (discussed previously relating to the lactate paradox) (Matheson et al., 1991). However, the manner in which muscle function is maintained remains poorly understood. Additionally, both aforementioned studies were conducted at sea level, thus meaning the translation to functioning during hypoxic exposure is limited.

Interestingly, the reported atrophy of muscle is usually coupled with preservation of the capillary bed, meaning an increase in capillary density is a common occurrence. This would increase the O_2 delivery to remaining muscle fibres (Hoppeler et al., 2001). In humans, there appears to be no preferential loss of fibre type and the significant atrophy tends to coincide with preservation of muscle function (Hoppeler et al., 2001, Edwards et al., 2010). Thus, the reported atrophy of muscle may be an adaptive response to enhance O_2 delivery to the working muscle.

The causes of this hypoxic-induced muscle atrophy are unclear. Vigano and colleagues reported a decrease in mTOR protein levels in human skeletal muscle upon hypobaric

hypoxic exposure, which is thus evidence of a decreased stimulus for muscle hypertrophy (Viganò et al., 2008). However, this decrease is not a consistent finding, as de Palma and colleagues observed no changes in mTOR expression in rat muscle in response to the same duration of hypoxic exposure (2 weeks), suggesting it is not controlled by PO_2 changes (De Palma et al., 2007). It may simply be that the loss in muscle mass is secondary to the common reports of a loss in appetite or even activity upon hypoxic exposure (Abdelmalki et al., 1996).

The maintenance of tissue energetics in the face of a decreased O_2 availability, as has been reported in skeletal muscle, does not appear to be true for all tissues. Human cardiac PCr/ATP levels, for instance, become impaired both in lowlanders (Holloway et al., 2011, Holloway et al., 2014) and highland native Sherpa populations (Hochachka et al., 1996). It may suggest that the heart, which has a greater mitochondrial density and metabolic rate than skeletal muscle, is incapable of preserving sufficient levels of OXPHOS.

The apparent maintenance of skeletal muscle energetics also does not appear to translate to maintenance of exercise performance in hypoxic conditions.

Hypoxia and exercise

The work required to perform exercise requires an input of energy to drive cross bridge cycling in skeletal muscle. To maintain a specific steady work rate, ATP must be supplied to the working muscle at the same rate at which it is used. As the duration of high intensity work rises, so the reliance on OXPHOS for ATP generation is also increased. The ability to perform maximal exercise is limited primarily by the ability of the cardiovascular system to deliver O_2 to the working muscle (Bassett et al., 2000). Maximum oxygen uptake (VO_2 max), defined as the highest rate at which O_2 can be taken up and utilised by the body, is thus decreased in hypoxic conditions leading to impairment of exercise tolerance (Bassett et al., 2000, Grover et al., 1985). The strain experienced by the cardiovascular system to meet O_2 requirements is reflected in the cardiac output and heart rate values in response to submaximal exercise. At a P_B equivalent to 4572m, both measurements exceeded sea level values at any submaximal exercise level, a response worsened with prolonged (40 day) exposure to lower P_B (Wagner, 2000). Whilst it is clear exercise capacity and cardiac output are reduced, the mechanisms involved remain to be fully elucidated (Wagner, 2000) and likely involves a combination of the complex physiological responses to hypoxia discussed above.

Despite the restriction in exercise capacity, training in hypoxic conditions has gained much interest in the sports science field. Much interest exists around the question of whether potential beneficial effects of hypoxia, such as enhanced O_2 carrying capacity and glycolytic capacity evoked by HIF signalling, can be elicited without the detrimental effects upon muscle wasting and limited training capacity through intermittent hypoxic training (Faiss et al., 2013).

1.2.5 Conclusion

Hypoxia thus appears to act as a driver of metabolic re-programming, a process that is summarized in **Figure 1.5**. Exposure to hypoxic conditions imposes stresses upon mitochondria that result in a decreased oxidative capacity and an increased ROS production. Successful adaptation therefore needs to encompass both the restrictions on energy production and limit the potential toxicity of ROS. Current evidence suggests that despite remaining restrictions upon exercise performance, these requirements can be largely met in healthy humans after a period of acclimatisation. This is mediated through the following changes: a shift towards anaerobic ATP generation, alterations to TCA cycle and ETS activities and changes to oxidative stress markers. In the short term (≤14days) it appears that hypoxic-induced decreases in skeletal muscle mitochondrial function, as shown through decreases in β-oxidation, TCA function and OXPHOS, are occurring alongside maintenance of mitochondrial density. This is followed by a loss of mitochondrial density in response to longer term exposures (≥42days) (Horscroft et al., 2014). Evidence suggests that skeletal muscle energetics, particularly energy storage capability, can be maintained in healthy humans following acclimatisation.

However, it is clear to see that metabolic remodelling processes induced by hypoxia remain controversial. Much is left unanswered and there is a significant lack of consensus between studies. Perhaps the most prominent of these discrepancies is the duration and degree of hypoxic exposure, both in human and rodent models. Particularly in the case of investigations into human physiology, this is further confounded by low subject numbers as the majority of high altitude studies are performed on fewer than 20 subjects. In addition, many previous studies focus on particular aspects of complex metabolic pathways, including the activities of specific enzymes, such as mitochondrial complexes. Although useful, these measurements are inaccurate indicators of mitochondrial function, or dysfunction (Kuznetsov et al., 2008). A far more rigorous measure is the functional analysis of intact mitochondrial O_2 consumption through respirometry. Beyond the specificities of

mitochondrial function are techniques that encompass a full metabolic profile of a tissue or biofluid, which have the potential to present a far greater insight.

There is a clear need for these issues to be addressed and for more sophisticated measures to be included in the continued investigation into mammalian physiology and molecular biology in response to hypoxic exposure. Such work has the potential to further our understanding of diseases that result from, or are akin to, physiology in this extreme environment.

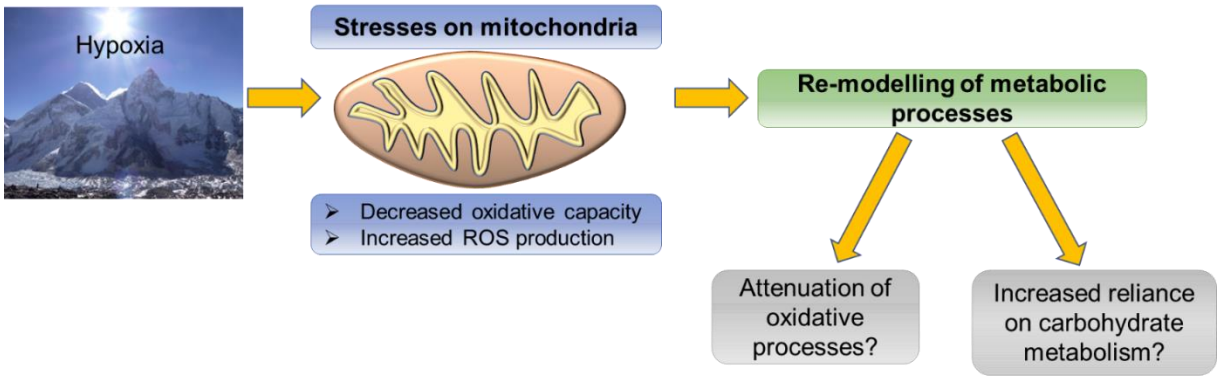

Figure 1.5. A summary of the metabolic stresses of hypoxia

Hypoxia induces metabolic re-modelling, the details of which are unclear.

1.2.6 Hypoxia in disease: chronic obstructive pulmonary disease (COPD)

As aforementioned, hypoxia plays a key role in the pathology of numerous disease states. An aspect of this thesis focuses upon hypoxic effects in chronic obstructive pulmonary disease (COPD), particularly the exercise limiting component of this disease.

COPD is a leading cause of morbidity and mortality worldwide, affecting 10-15% of the adult population aged ≥40 yrs (Lozano et al., 2013, Buist et al., 2007). The burden of COPD is set to increase in the coming decades due to the continued exposure to risk factors (predominantly smoking) and aging of the population, as prevalence increases with age (Buist et al., 2007). COPD is characterised by persistent and progressive airflow limitation, caused by a mixture of small airways disease (obstructive bronchitis) and parenchymal destruction (emphysema). This is associated with an enhanced chronic inflammatory response to noxious particles in the airways and lung, causing structural changes and narrowing of the small airways. Diagnosis and characterisation of COPD has thus far relied upon measurement of airflow limitation, assessed by forced expiratory volume in 1 second (FEV_1) (Pauwels et al., 2012). However, it is now widely recognised that COPD is a heterogeneous disease with features that are not captured by FEV_1, including muscle dysfunction, systemic inflammation and cardiovascular disease (Pauwels et al., 2012).

Exercise limitation is a common symptom in COPD patients and one that severely affects quality of life. Improving exercise tolerance is considered a key goal of effective COPD management (Pauwels et al., 2012). The causes behind the reduction in exercise capacity are complex. Initially, it was believed respiratory limitation and dyspnoea were the main contributors. However, it has been frequently demonstrated that patients with similar values for airflow obstruction have variable exercise capacities. Indeed, peripheral muscle fatigue has been defined as a key determinant of exercise capacity, which has been shown to precede the sense of breathlessness (Killian et al., 1992b). This muscular limitation is likely affected by atrophy and dysfunction of skeletal muscle, with a reported decrease in skeletal muscle cross sectional area and shift towards glycolytic type II fibre makeup (Swallow et al., 2007, Jobin et al., 1998) with a preferential loss in oxidative type I and IIa fibres (Jobin et al., 1998, Gosker et al., 2002).

A factor likely contributing to exercise limitation is hypoxia. In COPD sufferers, increasing perfusion of a poorly ventilated lung leads to a ventilation-perfusion mismatch,

resulting in hypoxaemia (Pauwels et al., 2012). Delivery of O_2 is further confounded at the level of microcirculation, as both capillary number and capillary/fibre ratio are decreased in vastus lateralis muscle in COPD patients relative to healthy controls (Jobin et al., 1998). Various aspects of COPD pathophysiology are likely linked to hypoxia, including alterations in skeletal muscle function. This is reflected in the findings of Koechlin, which demonstrate a greater reduction in quadriceps endurance and worsening of muscle oxidative stress at rest and post exercise in chronic hypoxemic COPD patients compared to non-hypoxemic patients (Koechlin et al., 2005).

The hypoxic effect is likely driving changes observed in metabolic state. This includes a depletion of skeletal muscle energy stores, with positive correlations being shown between arterial O_2 concentrations (PaO_2) and both muscle glycogen and phosphocreatine (PCr) concentrations (Jakobsson et al., 1990). Hypoxia may also have a role in inducing the shift towards anaerobic means of ATP generation through glycolysis, with increased lactate levels found in lower limb muscles (Jakobsson et al., 1990, Shields et al., 2015). This occurs alongside a reduction in oxidative capacity, with a loss of oxidative enzymes (Swallow et al., 2007) and a decline in mitochondrial oxidative capacity (Rabinovich et al., 2007).

Interestingly, the hypoxic responses observed in COPD patients appear to differ in some aspects compared to healthy subjects. Although healthy subjects exposed to hypobaric hypoxia via high altitude also experience significant muscle atrophy, they appear to retain muscle function (Edwards et al., 2010) and capillary density (Hoppeler, 2001) neither of which are maintained in COPD patients. A number of cellular responses also support the idea that COPD sufferers do not respond as healthy humans do to hypoxia. An example of this is a blunting of the fundamental HIF-α response. This has been attributed to a reduction in levels of the enzyme histone deacetylase (HDAC), specifically to HDAC 7 (To et al., 2012, Ito et al., 2005). A lack of HIF-1α induction was demonstrated through a suppressed expression of the HIF target gene VEGF, as levels increased to just a quarter of that of healthy controls (To et al., 2012).

Taken together, these findings suggest that tissue O_2 delivery, intramuscular O_2 transport and mitochondrial dysfunction may all contribute to exercise limitation in COPD. Approaches that reduce the O_2 cost of exercise may thus be of therapeutic benefit.

1.2.7 Aiding hypoxic acclimation

Given the common occurrence of hypoxia, both environmentally and clinically, and its potential tragic consequences, it would be of considerable benefit to develop pharmacological strategies to aid human adaptation/hypoxic survival. Ability to do this could potentially benefit subjects suffering from hypoxia as a comorbidity of diseases such as COPD, as well as healthy humans that are exposed to hypoxic environments. Little is known about how to reduce O_2 utilisation at the tissue or cellular level in humans.

There are several ways to lessen the O_2 requirements of a cell. The first is to reduce cell work, an approach used by sea turtle hepatocytes (Hochachka et al., 2001). The second is to improve the biophysical economy of the cell processes by, for instance, decreasing the ATP consumed by an active transporter. The third is to improve mitochondrial efficiency through improved the energy coupling. This is measured as the amount of O_2 consumed per ATP produced, and is termed the P/O ratio. Nitrate have been proposed to decrease the O_2/ATP at the level of the respiratory chain, as well as having whole body physiological effects such as improving exercise performance (discussed below). A major component of this thesis is to examine the potential of dietary nitrate to alleviate hypoxic induced metabolic stress.

Dietary nitrate supplementation

Inorganic nitrate (NO_3^-) can be consumed as part of a normal, healthy diet with high levels present in green leafy vegetables and beetroot (Hord et al., 2009). Dietary exposures to NO_3^- in the general population is estimated to be 52mg/day, with vegetables contributing ~70% to this (Ysart et al., 1999). Once consumed, NO_3^- is reduced in a stepwise fashion firstly to nitrite (NO_2^-) and then nitric oxide (NO). NO is a diatomic free radical gas that serves as a ubiquitous, multi-functioning signalling molecule.

As mammalian cells are not capable of converting NO_3^- to NO_2^-, this process is reliant on the nitrate reductase activity of commensal bacteria present within the oral cavity, which generate NO_2^- from NO_3^- rich saliva (Spiegelhalder et al., 1976, Duncan et al., 1995). This stepwise reduction is potentiated in low O_2 tension and low pH conditions (Castello et al., 2006, Modin et al., 2001). The subsequent reduction of NO_2^- to NO can occur in a number of ways, including: enzymatic reduction by xanthine oxidoreductase requiring hypoxic conditions and the presence of NADH (Millar et al., 1998), acidic reduction in areas of low pH such as the stomach (Benjamin et al., 1994) and reduction by deoxyhemoglobin (Cosby

et al., 2003). NO_2^- is thus a major vascular storage pool for NO, existing in far larger concentrations than the protein carriers of NO S-Nitrosothiols (Cosby et al., 2003). The NO_2^- pool is a relatively stable source that enables NO to reach distal areas to exert its biological effects. Supplementation of inorganic dietary nitrate thus increases plasma NO_2^- concentration, in turn enhancing NO availability (Lundberg et al., 2004).

In addition, NO can be derived endogenously through the O_2 dependent catabolism of L-arginine, a reaction catalysed by one of three isoforms of nitric oxide synthase (NOS) (Stamler et al., 2001). The generation of NO via these two mechanisms is summarised in **Figure 1.6.**

NO is regarded to be the chief mediator of the responses observed with nitrate supplementation (Jones, 2014). The following summary of the effects of nitrate supplementation are therefore focused upon the signalling responses of NO. In these studies, nitrate is either given through consumption of high nitrate containing beetroot juice (human study) or by ingesting nitrate salt (e.g. sodium nitrate, $NaNO_3^-$).

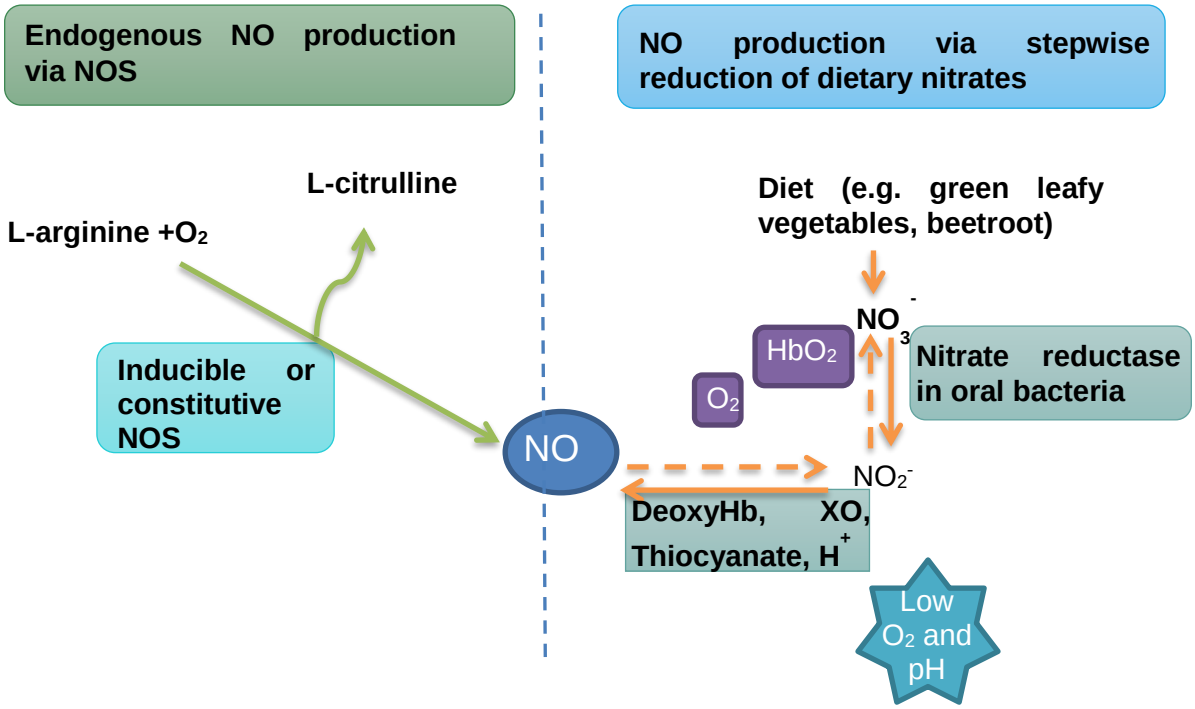

Figure 1.6. The mechanisms of nitric oxide (NO) production via endogenous or dietary pathways

The following abbreviations are used: NOS = nitric oxide synthase, DeoxyHb = deoxygenated haemoglobin, HbO_2 = oxygenated haemoglobin, XO = xanthine oxidase.

Nitric oxide (NO) action

The signalling responses of NO are complex and are mediated through numerous mechanisms, including S-nitrosylation of cysteine redox centres within proteins, which involves incorporation of the NO moiety to a sulfur atom. Motifs for S-nitrosylation have been identified on various ion channels, receptors, enzymes, transcription factors and small G proteins (Stamler et al., 2001). In addition, NO can interact with haeme-containing proteins, such as cytochrome-c oxidase (COX, or complex IV), thus enabling interaction with cellular respiration (Stamler et al., 2001). NO binds with high affinity to the haeme cofactor present on the soluble guanylate cyclase (sGC) sensory domain. This binding activates the catalytic site, in turn increasing levels of cyclic guanosine monophosphate (cGMP) generated from guanosine triphosphate (Underbakke et al., 2014, McDonald et al., 1996). sGC is considered the primary cellular receptor of NO. The importance of the NO/sGC/cGMP signalling pathway is reflected through responses to defects in this system, which have been linked to the following: heart disease, stroke, hypertension, neurodegeneration and erectile dysfunction (Bredt, 1999). However, the specific mechanisms involved in the downstream responses of this second messenger system, along with defects resulting from these pathologies, are less clear.

Perhaps the best defined downstream signalling pathway of NO derived cGMP is that involved with vascular homeostasis. NO is released from endothelial cells (also termed endothelial derived relaxing factor) (Palmer et al., 1987) in response to a range of stimuli. cGMP-dependent protein kinase G (PKG) is subsequently activated via the sGC mediated mechanism. This induces smooth muscle relaxation and so vasodilation likely via changes in levels of, and sensitivity to, intracellular calcium (i[Ca^{2+}]), although exact mechanisms remain unclear (Taylor et al., 1989, Surks, 2007, Carvajal et al., 2000). The resulting drop in blood pressure is a well-defined response to short term nitrate supplementation (Lansley et al., 2011, Vanhatalo et al., 2010, Bailey et al., 2010, Bailey et al., 2009, Hobbs et al., 2012).

In rat skeletal muscle, NO derived cGMP signalling has been demonstrated to enhance fatty acid oxidation capacity through the master regulator of fatty acid oxidation, PPARα (Ashmore et al., 2015b), as outlined in **Equation 1.3**

$$NO \rightarrow sGC \rightarrow \uparrow cGMP \rightarrow PKG \rightarrow PPAR\alpha$$

Equation 1.3. Proposed mechanism for dietary nitrate action upon skeletal muscle metabolism

The pathway of action for nitrate dependent enhancement of β-oxidation (Ashmore et al., 2015b). Where sGC = soluble guanylate cyclase, cGMP= cyclic guanosine monophosphate, PKG = protein kinase G and PPARα = peroxisome proliferator activated receptor.

This mechanism demonstrated direct effects upon PPARα expression and transcriptional activity**,** resulting in turn in the upregulation of intra-mitochondrial pathways of fatty acid oxidation alongside released inhibition of mitochondrial fatty acid import via the carnitine palmitoyl transferase (CPT) system (Ashmore et al., 2015b). These expression changes were demonstrated to have functional effects, by enhancing OXPHOS rates in response to the addition of the long chain fatty acid palmitoyl carnitine. This is discussed in further depth in Chapter 4.

In mouse cardiac muscle, the PKG second messenger system has been linked to endogenous hydrogen sulphide (H_2S) production and in turn to cardio protection in ischemic conditions (Salloum et al., 2009, Salloum et al., 2015). Upregulation of this system has been associated with dietary nitrate consumption, although mechanisms of H_2S function remain ambiguous (Salloum et al., 2015).

Whilst questions undoubtedly remain on the specific details of NO signalling mechanisms, it is distinctly evident that NO signalling plays a key part in regulating the delivery of O_2 and nutrients along with mitochondrial O_2 consumption, with direct effects upon cellular respiration.

Implications for O_2 delivery and utilisation

NO production, either via endogenous NOS action or NO_3^--NO_2^- pathway reduction, has been reported to regulate numerous biological effects that influence the transport and utilisation of O_2 in the tissues as well as production of ROS. Perhaps the best characterised of these effects is the previously mentioned mediation of vasodilation and so basal vascular tone. Vasodilation increases blood flow, and so O_2 delivery, to the tissues. This is particularly pertinent in conditions where O_2 demand is increased, as occurs in the working muscles during exercise, thereby inducing hypoxia-dependent vasodilation. The effects upon tissue oxygenation are uncertain and may vary depending on exercise intensity.

Interactions between NO and mitochondria

Beyond vasodilation, NO has been demonstrated to implicate O_2 consumption at the mitochondria through direct interactions with mitochondrial components. For instance, complex I, a major site for ROS production (Lambert et al., 2004), appears to be a key NO target. S-nitrosylation of thiols, the functional groups of cysteine residues, leads to inhibition of this complex. This response is well documented in rodent models (Shiva et al., 2007, Clementi et al., 1998) and is reported to have particular relevance in both hypoxic and ischemic conditions, as discussed below.

Links between NO and the respiratory chain extend to COX/complex IV. In addition to its O_2 reducing ability, this enzyme appears to have significant links to NO function. NO has been shown to compete with O_2 for the bimetallic binding site of COX , resulting in inhibition of respiration (Brown et al., 1994, Brudvig et al., 1980). It has been proposed that this inhibition of O_2 consumption allows for diffusion of O_2 deep into the tissue thereby enhancing tissue oxygenation and improving the O_2 status of fibres situated further away from capillaries (Hagen et al., 2003, Thomas et al., 2001, Victor et al., 2009).

The effects of NO upon COX function are thought to be regulated endogenously through mitochondrial NO production, mediated in part through endothelial NOS (eNOS). This enzyme is located on the cytoplasmic face of the outer mitochondrial membrane, within close proximity to COX (Gao et al., 2004). Deletion of the pentabasic sequence domain that anchors eNOS to the mitochondrial outer membrane causes an increase in O_2 consumption, thus confirming the role of NO as a physiological regulator of COX (Gao et al., 2004). Evidence also suggests COX itself is a mediator of mitochondrial NO synthesis in mammals independently of eNOS; a process induced in hypoxia that is dependent upon the presence of NO_2^- (Castello et al., 2008, Castello et al., 2006).

The close relationship between COX and NO is hardly surprising given the evolutionary history of COX. It is thought that COX originated within a common ancestor of archaea and bacteria from denitrification enzymes at a time prior to oxygenic photosynthesis. The site of O_2 reduction at the binuclear copper centre of COX is thought to have originated from an exchange of genes between the nitric/nitrous oxide reductase and primitive oxidases (Castresana et al., 1994, Saraste, 1994).

Links have also been made between NO and mitochondrial biogenesis. NO production by eNOS has been related to an upregulation of key factors involved in mitochondrial

biogenesis in calorie restriction, including PGC-1α, nuclear respiratory factor (NRF) 1 and mitochondrial transcription factor A (Tfam) (Nisoli et al., 2005). In addition, dietary nitrate supplementation has been shown to counteract the hypoxic induced suppression of PGC-1α in rat skeletal muscle (Ashmore et al., 2015b). However, the link between NO and regulation of mitochondrial function is not a consistent finding, as nitrite supplementation has been shown to have no effect on mRNA levels of PGC-1α or NRF-2 in rodents (Shiva et al., 2007, Nisoli et al., 2005).

It is therefore clear that NO signalling has implications upon the delivery and usage of O_2. This thus leads to the question: what are the ramifications of this signalling response upon tissue work? Can supplementation of dietary nitrate enhance ability to perform work? This has been explored through human exercise studies.

Effects of nitrate supplementation during exercise

Investigations into the effects of nitrate supplementation on exercise demonstrate a reduced O_2 cost of low intensity/submaximal (Larsen et al., 2007, Vanhatalo et al., 2010, Bailey et al., 2009, Lansley et al., 2011) and high intensity/maximal exercise alongside an improved tolerance to maximal exercise (Bailey et al., 2009, Larsen et al., 2010, Cermak et al., 2012). These effects occurred in the absence of a rise in circulating lactate concentrations, indicating the fall in O_2 requirement was not compromised for through an increase in substrate level phosphorylation via glycolysis, and maintenance of exercise work performance (Larsen et al., 2007, Bailey et al., 2009, Vanhatalo et al., 2010, Larsen et al., 2010). These prior results suggest that efficiency of both mechanical processes and oxidative ATP production were improved with nitrate supplementation. Indeed, the ATP turnover rate was reported to be lowered with nitrate supplementation, alongside a fall in muscle [PCr] degradation, [Pi] and [ADP], following exercise (Bailey et al., 2010). The authors thus linked the observed reduction in O_2 cost to a fall in ATP cost of muscle force production.

Effects upon skeletal muscle contraction extend to interactions with contractile processes within the muscle that are heavily reliant on ATP hydrolysis. This includes a slowing of cross-bridge cycling kinetics, as nitrate supplementation induced a higher force generation at the expense of a reduced velocity (Evangelista et al., 2010), and a decreased Ca^{2+} uptake into the sarcoplasmic reticulum due to an NO induced inhibition of sarcoplasmic reticulum Ca^{2+} ATPase (SERCA) activity (Ishii et al., 1998). This SERCA inhibition occurred

independently of the cGMP-PKG system, instead being linked to direct interaction with NO (Ishii et al., 1998).

This effect upon the contractile processes in skeletal muscle appears to be most prominent in type II, fast twitch fibres (Hernández et al., 2012). Nitrate supplementation has been linked to increasing myoplasmic free [Ca^{2+}], which was associated both with an increased contractile force and faster rate of force development in mice. This occurred alongside a rise in expression of the Ca^{2+} handling proteins, calsequestrin 1 and dihydropyridine receptor, a response that was absent in slow twitch fibres (Hernández et al., 2012). The beneficial effects of NO signalling upon fast twitch fibres may be aided by the lower PO_2 present in this fibre type, which is thought to facilitate the reduction of NO_3^- to NO (Ferguson et al., 2015).

In addition to the mechanics involved in muscle contraction, interplay has also been demonstrated between NO and processes directly linked to the generation of muscle fatigue specifically the phosphocreatine (PCr) system. Fatigue development during exercise is partially linked to the decrease in muscle [PCr] and this decrease is reported to be attenuated in subjects undertaking repeated maximal voluntary contractions following nitrate rich beetroot juice supplementation (Fulford et al., 2013).

Despite these seemingly beneficial effects of nitrate supplementation, the ergogenic effects are debatable and significant inconsistencies exist between studies. Indeed, some studies demonstrate no change in performance with nitrate supplementation in submaximal exercise (e.g.(Kelly et al., 2014)) and others a decline in high intensity intermittent exercise performance (e.g.(Martin et al., 2014)). There are likely numerous reasons for such discrepancies. Firstly, it may relate to exercise duration. The ergogenic effect of nitrate supplementation has been reported for short intermittent maximal intensity exercise (Wylie et al., 2016, Thompson et al., 2015, Aucouturier et al., 2015), whereby increasing perfusion aids oxygenation of type II muscle fibres (Aucouturier et al., 2015, Wylie et al., 2016, Ferguson et al., 2015), which are preferentially recruited during high intensity intermittent exercise (Essén, 1978). In contrast, minimal evidence exists to support its benefit for longer durations (Jones, 2014).

The discrepancy may also be due to the choice of subject cohort. nitrate supplementation has been shown to have the greatest effects in subjects of lower fitness in comparison to athletes (Porcelli et al., 2014). Whilst it has also been demonstrated to improve the performance of well-trained athletes, it appears to have little effect in the elite

athlete cohort (Jonvik et al., 2015). The reasoning behind the lack of response in the elite cohort is unclear, but may be linked to the higher baseline production of NO via NOS, or higher dietary intake as a secondary to greater daily energy intake, alongside a higher proportion of type I fibres present in these highly trained subjects (Hultström et al., 2015, Jonvik et al., 2015). This signifies that perhaps increasing NO bioavailability is better targeted to populations of advanced age, particularly with pathologies, whose baseline NO production may be compromised (Hultström et al., 2015).

A factor that is often overlooked is the potential for inter-individual differences in the handling of dietary nitrate within similar subject cohorts. For instance, even within the elite athlete cohort, 'responders' to nitrate treatment still exist. The source of such differences may include variability in nitrate reductase activity within the oral cavity to convert nitrate to nitrite as some subjects do not show the characteristic increase in plasma nitrite (Hultström et al., 2015). It may also stem from differences in intrinsic nitrite reductase capabilities of mitochondrial aldehyde dehydrogenase (ALDH2). Those subjects exhibiting a common polymorphism termed the ALDH2*2 allele demonstrated differences in nitrite handling and sGC activity compared to subjects exhibiting the wild type allele following inorganic nitrite administration (Ormerod et al., 2017).

Lastly, the discrepancies may reflect issues in protocols, with the use of inadequate dosing levels and time allowed for the increase in plasma nitrite levels to occur, which takes 2-3hrs and corresponds to a decrease in blood pressure (Jones, 2014). Mechanistic studies also demonstrate that longer supplementation periods (3-7 days) are required for changes to occur in contractile and mitochondrial proteins (Jones, 2014).

Together, evidence thus suggests there is close relationship between NO regulation of O_2 delivery and usage and that nitrate supplementation has the potential to aid human performance. These processes are summarised in **Figure 1.7.** A legitimate question from this is what is the role of NO signalling in conditions where O_2 supply becomes limited through hypoxic exposure, resulting either from high altitude exposure or a disease state? Can dietary nitrate supplementation aid human adaptation to these conditions?

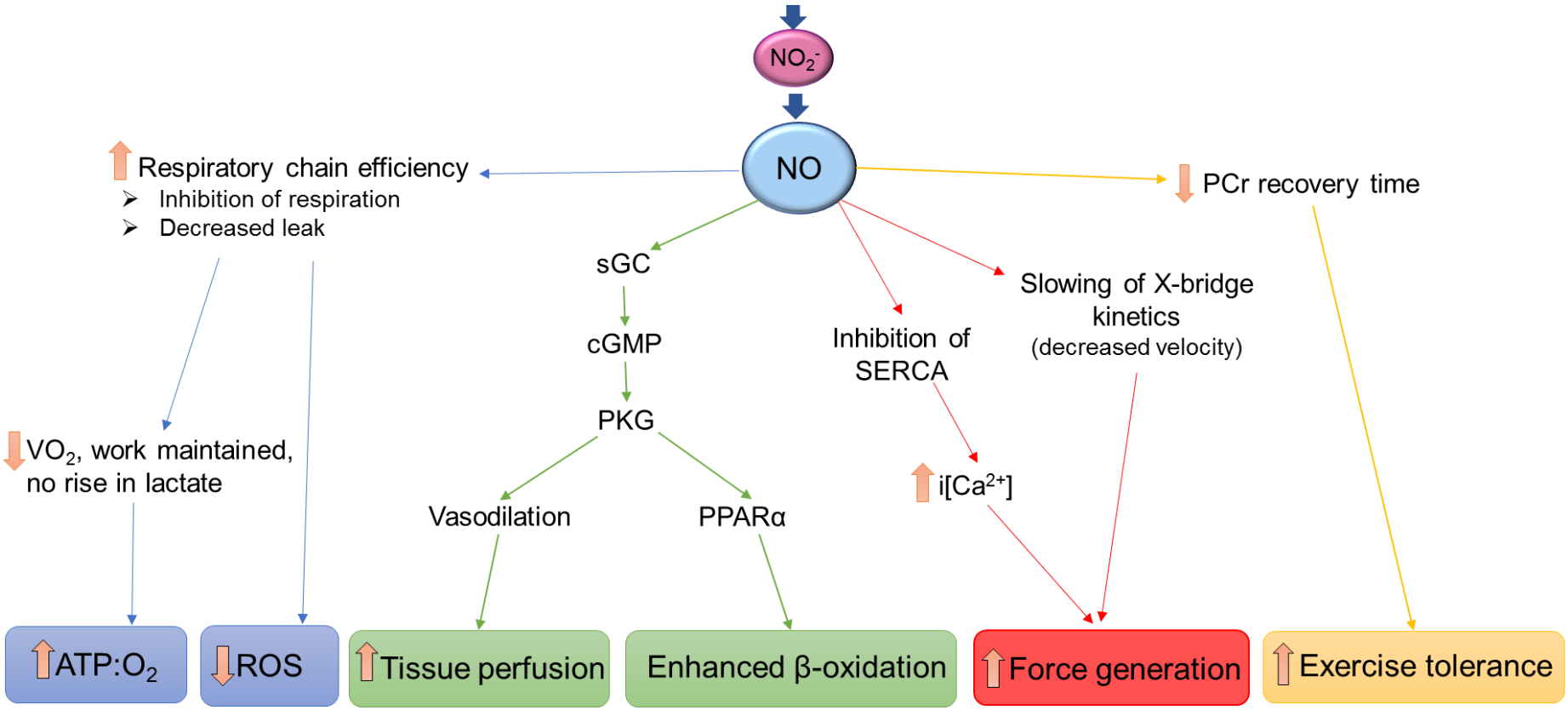

Figure 1.7. Reported effects of dietary inorganic nitrate (NO_3^-) supplementation and proposed mechanisms elicited by nitric oxide (NO) action.

Where: NO_2^- nitrite, VO_2 – pulmonary O_2 uptake, ATP-adenosine triphosphate, O_2-oxygen, ROS-reactive oxygen species, sGC-soluble guanylate cyclase, cGMP-cyclic guanosine monophosphate, PKG - protein kinase G, PPARα –peroxisome proliferator activated receptor alpha, SERCA – sarco/endoplasmic reticulum Ca^{2+} ATPase, $i[Ca^{2+}]$-intracellular calcium concentration, PCr – phosphocreatine.

The role of NO in hypoxia

The importance of NO signalling in hypoxia has already been eluded too, with the reliance upon low O_2 tension for the reduction of NO_2^- to NO. The hypoxic induced increase in NO production has also been observed at a whole-body level in high altitude studies, with biomarkers of NO production, being plasma nitrate and nitrite, increasing in healthy subjects with ascent to 5300m along with an increase in a marker of NO activity cGMP. S-nitrosothiol production was also increased, suggesting multiple pathways contribute to enhancing NO availability (Levett et al., 2011). Circulating levels of bioactive NO products have been found to be greater in high altitude native Tibetan populations compared to lowland natives. This was associated with a greater forearm blood flow, and so increased O_2 delivery (Erzurum et al., 2007).

Thus, the high levels of circulating NO influence the delivery of O_2 and nutrients through its vasodilatory effects. Beyond this is the utilisation of O_2 in mitochondrial oxidation. Indeed, mitochondrial production of NO is reported to be increased in hypoxia (Valdez et al., 2004, Schild et al., 2003), with some of this synthesis occurring independently of NOS, for instance through COX mediated NO production (Castello et al., 2006). The potential for NO to increase efficiency of O_2 usage in this process has inevitably sparked significant interest into the effects of NO upon mitochondrial functioning in conditions where O_2 supply is compromised.

NO protecting against low O_2 conditions

Evidence suggests that nitrate supplementation improves the ratio of O_2 consumed: ATP produced (P/O ratio). Such a process may involve a decrease in proton leak meaning a larger portion of the mitochondrial inner membrane becomes geared towards ATP synthesis rather than uncoupling actions (Larsen et al., 2011, Clerc et al., 2007). This is thus suggestive of enhanced respiratory chain efficiency, an effect that is particularly important in conditions where O_2 availability is limited and which is supported through investigations into interactions with specific complexes, particularly complex I.

Complex I is understood to be the primary site of injury and mitochondrial ROS production following ischemia/reperfusion (IR) and so is a key contributor to IR injury (Lesnefsky et al., 2001). Ischemia initially induces low levels of complex I activity. The rapid reversal of this upon reperfusion leads to production of hydrogen peroxide and so oxidative damage. This damage was attenuated in murine cardiac cells in the presence of NO donors,

with a reduction in protein carbonylation (a marker of oxidative damage), necrotic and apoptotic cell death (Chouchani et al., 2013). The s-nitrosation of Cys 39, which is exposed on complex I during the low activity condition, was thought to lock complex I in the low active state likely by disrupting its interaction with ubiquinone. Reactivation of complex I was initiated upon reperfusion through reduction of the S-nitrosothiol by glutathione and thioredoxin, but this reactivation is gradual, meaning ROS production became attenuated (Chouchani et al., 2013).

This cardio protective effect has similarly been demonstrated in the rat heart with nitrate supplementation during hypoxic conditions (13% O_2 for 14 days) (Ashmore et al., 2014). Hypoxic induced suppression of complex I supported state 3 respiration (in the presence of ADP) was shown to be recovered with nitrate supplementation. This occurred alongside an increase in both complex I enzyme activity and protein levels. In addition, nitrate supplementation restored cardiac ATP and ADP levels and alleviated the rise in protein carbonyls in response to hypoxic exposure (Ashmore et al., 2014).

The interaction between nitrate and complex I has also been demonstrated in skeletal muscle, as expression of the complex I subunit *Ndufs1* was shown to increase in cultured myocytes (C2C12) in response to supplementation with nitrate both 50 and 500μM (Ashmore et al., 2015b). Effects upon skeletal muscle function have also been demonstrated through mitochondrial respirometry, with nitrate supplementation enhancing fatty acid OXPHOS in both hypoxic and normoxic conditions and also recovering rat skeletal muscle energetics in hypoxia (Ashmore et al., 2015b).

It may seem logical to assume that recovery of cellular respiratory capacity in hypoxic conditions may be solely due to enhanced O_2 delivery resulting from NO induced vasodilation. However, nitrate dependent enhancement of oxidative capacity occurred in normoxic conditions, whereby O_2 delivery is plentiful, in addition to hypoxia. Furthermore, evidence clearly indicates direct interactions with mitochondrial machinery. It is therefore plausible to conclude that nitrate supplementation has direct effects upon metabolic regulation.

Does dietary nitrate supplementation enhance performance in hypoxia?

Supplementation of nitrate has been attributed to decreasing VO_2 at rest and during submaximal exercise in hypoxia, an effect associated with an improved tissue oxygenation index, which was independent of an increased muscle blood flow (Masschelein et al., 2012).

Similar results have been shown when O_2 carrying capacity is reduced following blood donation, whereby nitrate supplementation recovered decrements in submaximal performance in addition to decreasing O_2 uptake (McDonagh et al., 2016). This improvement in VO_2 kinetics has also been demonstrated during high intensity exercise, an effect associated with improved hypoxic exercise tolerance (Kelly et al., 2014, Vanhatalo et al., 2011). These results thus go to support the concept that NO improves efficiency of mitochondrial O_2 consumption in hypoxia.

However, the increase in endogenous NO production and activity at high altitude, as reported by Levett and colleagues, was not associated with any change in O_2 cost of exercise or mechanical efficiency. It in fact correlated inversely with microvascular blood flow, which was impaired at altitude (Levett et al., 2011). This is in contrast to previous findings in response to dietary nitrate supplementation at high altitudes, which was related to enhanced flow mediated dilation, indicative of improved endothelial function (Bakker et al., 2015).

In addition to the whole body effects, NO has been shown to play a key role in cellular hypoxic signalling. It has been linked to both induction of nuclear hypoxic genes (Castello et al., 2006) and HIF-1α signalling, although effects upon the latter are not clear. Endogenous production of NO by COX has been linked to HIF-1α stabilisation in mammalian cells (Ball et al., 2012). However, addition of NO along with other respiratory chain inhibitors to HEK293 cells grown in 1% O_2 caused prolyl hydroxylase dependent inhibition of HIF-1α, resulting in its impaired accumulation and transcriptional activity (Hagen et al., 2003).

The literature thus suggests that NO plays an integral part of the hypoxic response. However, details on the mechanisms of actions remain unclear.

Detrimental effects of nitrate supplementation

The above summary of the effects of nitrate supplementation focus on the potential for improving metabolic efficiency. However, an important consideration is the capacity of nitrate to cause a harmful effect. Indeed, many of the studies that show beneficial effects do so with doses that exceed the recommended daily nitrate intake (Kapil et al., 2014, WHO, 2003). Interestingly, commercially available beetroot juice also exceeds this limit. The potential detrimental effects include the formation of carcinogenic N-nitrosamines, the onset of intolerance and endothelial dysfunction. However, there is currently no evidence that nitrate is carcinogenic to humans and has in fact been linked to decreasing risks of many

cancers (Kapil et al., 2014). In fact, the detrimental effects appear to be more closely associated with synthetically synthesised inorganic nitrate and exposure to high levels of NO_2^-. This is reflected, for instance, in reported cases of methaemoglobinaemia in children. This condition occurs due to interaction of NO_2^- with haemoglobin in the ferrous state, in turn impairing the O_2 carrying capacity of haemoglobin. In these cases, onset was associated with improper storage of cooked or salted vegetables that accumulated NO_2^- resulting from bacterial contamination. No reports of vegetable induced methaemoglobinaemia have been reported in adults (Kapil et al., 2014).

1.2.8 Conclusion

In conclusion, there appears to be two key responses occurring with nitrate supplementation and subsequent NO signalling that directly relate to the use and delivery of O_2:

1. **Vasodilation.** This mediation of vascular tone will result in an increased delivery of more O_2 to the working muscle. This is observed within 2-3 hours of supplementation and corresponds to an increase in plasma nitrite (Jones, 2014).
2. **Actions upon mitochondrial function**, resulting in a decrease in VO_2, and an improvement in energy coupling. This is associated with changes in mitochondrial proteins occurring with longer term supplementation (Jones, 2014).

At the outset, these two factors may appear contradictory. Why should O_2 delivery be increased when O_2 use is being restricted? However, when considered in the context of hypoxic exposure, both factors would likely work together to ensure O_2 supply is matched to usage. It may also be the case that a decreased VO_2 in the mitochondrial population located close to the capillary will allow for O_2 to reach more distal regions.

There is still a large degree of controversy in the field of nitrate supplementation, with some studies showing supplementation of dietary nitrate has no effect upon function or performance. This may be due to poor study design and a lack of consensus between studies regarding dosage, duration of supplementation and exercise protocols. It may also be the case that nitrate supplementation in a healthy population, whom have an optimal production of endogenous NO, has less of an effect in comparison to a patient population, where NO production may be compromised. This may be particularly relevant in populations where hypoxia is a key factor in disease pathology. Indeed, the potential for nitrate

supplementation to act as a therapeutic measure in disease states associated with hypoxia remains to be determined.

Equally, many questions remain regarding mechanisms of nitrate action. The signalling mechanisms and specificities of NO action upon mitochondrial function, particularly in the context of hypoxia, remain largely unexplored.

1.3 Summary

A sufficient supply of O_2 to the tissue is required to maintain oxidative metabolism, in doing so preserving ATP production. This is in turn required to fuel energy consuming processes within the cell and so is central to the maintenance of order and homeostasis within complex organisms. In hypoxia, the lack of O_2 causes this fundamental process to be compromised and metabolic stress ensues. Metabolic remodelling is therefore required to maintain energetic and redox homeostasis. However, it is clear to see that the details of hypoxic induced metabolic changes remain ill defined. Furthering our understanding of these changes has implications both for healthy humans sojourning to high altitudes and also for the plethora of disease states in which hypoxia plays an integral part. By understanding mechanisms of healthy hypoxic adaptation, this may provide insight into the processes of pathological hypoxia and into developing potential strategies that lessen the impact of pathological hypoxia.

This thesis encompasses two themes. The first was to investigate the metabolic responses of healthy humans to hypobaric hypoxic exposure. The second was to investigate the potential of nitrate supplementation to alleviate metabolic stresses of hypoxia and to shed light upon the mode of nitrate action.

1.4 Thesis aims

The aims of this thesis were as follows:

1. To examine the metabolic responses of healthy humans to acute, progressive hypoxic exposure. This was achieved through employment of metabolomic and lipidomic techniques on plasma samples obtained from subjects ascending to EBC (5300m).
2. To examine the effects of chronic hypoxic exposure, along with extreme cold, on human physiology and metabolism. A small cohort of subjects was assessed before and after a Trans-Antarctic winter expedition, involving prolonged

exposure to moderate altitude (≤2500m). Metabolomics assessment of plasma was employed alongside anthropometric and exercise physiology measures.

3. To investigate the potential for dietary nitrate supplementation to ameliorate the metabolic stresses of hypoxia in skeletal muscle and the role of PPARα in this process. A mouse model of wild type and PPARα$^{-/-}$ was used and the focus of analysis was upon skeletal muscle mitochondrial function.
4. To assess the effects of acute dietary nitrate supplementation upon exercise duration and related metabolic changes in a clinical population of COPD sufferers. This was examined using a submaximal exercise test alongside metabolomic analysis of plasma samples.

A flow diagram outlining the goal of each of the 4 studies is presented in **Figure 1.8.**

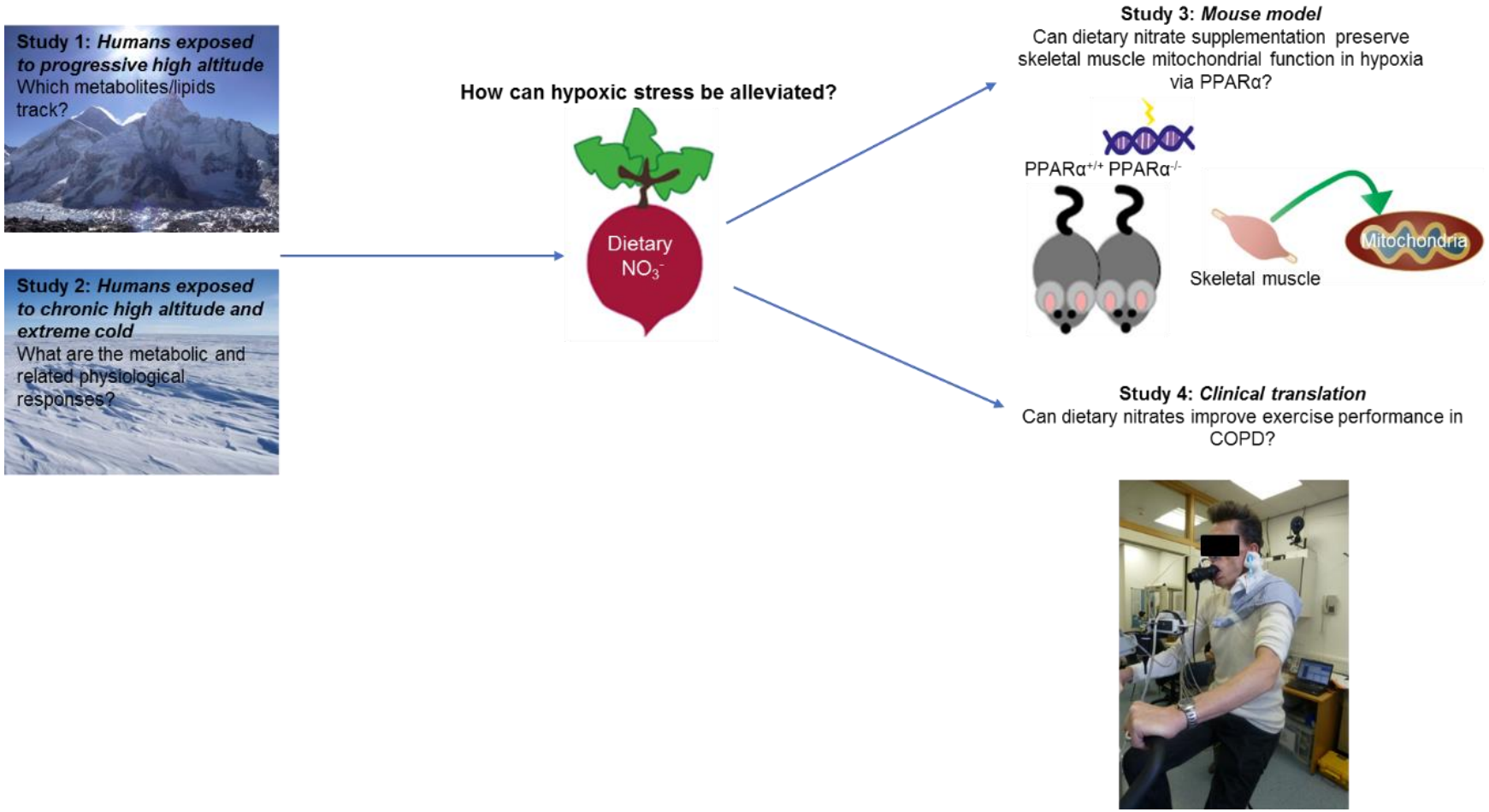

Figure 1.8. Outline of the goals behind the 4 studies presented in this thesis

2 **Chapter 2 (Study 1):** Metabolomic and lipidomic profile changes in healthy subjects exposed to progressive hypobaric hypoxia upon ascent to Everest Base Camp

2.1 Introduction

Ascent to high altitudes is associated with changes in a number of environmental factors, including: PO_2, ambient temperature, relative humidity and solar radiation. It is generally accepted that the majority of physiological changes that occur in response to high altitude exposure are elicited by a decrease in PO_2 (Woolcott et al., 2015), a consequence of a fall in P_B. This leads to a decreased P_IO_2 and impaired O_2 transfer down the O_2 cascade, resulting in impaired tissue oxygenation and hypobaric hypoxia.

As described in the literature review, an inadequate O_2 supply to the tissues can severely compromise oxidative metabolism and elicit a stress response resulting in increased ROS production. Acclimatisation to hypoxic conditions thus requires a robust physiological response allied with metabolic remodelling to ensure that ATP demand is met in the face of restricted O_2 availability. The remodelling process is complex and currently ill defined. Furthering current understanding of this response is of high importance in relation to the increasing numbers of lowlanders sojourning to high altitude destinations, as well as the growing proportion of the world's population (currently 7%, ~440million (Woolcott et al., 2015)) residing above 1500m.

Given that hypoxia is prevalent amongst a range of diseased populations, investigation into hypoxic adaptation is also highly clinically relevant. Indeed, much of the work conducted on metabolic adaptations to hypoxic exposure has been in the context of cancer, obesity and respiratory disease (Danhier et al., 2017, Hosogai et al., 2007). However, the pathways involved in adaptation to hypoxia remain unclear and are particularly difficult to study in pathological states, given the plethora of confounding factors and complications prevalent in a diseased population (Grocott et al., 2007a). It therefore makes

sense to better define the adaptive response in healthy humans before translating this to a clinical population. A method of assessing hypoxic exposure in healthy humans is through exposure to environmental hypobaric hypoxia, as is experienced at high altitudes.

The Caudwell Xtreme Everest (CXE) expedition was a large scale field study that assessed the healthy human response to progressive environmental hypoxia during an ascent to EBC (Levett et al., 2010, Grocott et al., 2007b). Field studies prior to CXE that aimed to investigate hypoxic adaptation tended to use highly selected small groups of subjects (n = 12-36) (Cerretelli, 1976, Pugh et al., 1964, West et al., 1983, Johnson et al., 2005). Studies using larger cohorts of volunteers failed to standardise hypoxic exposure and the ascent profiles varied between subjects (Pollard et al., 1996, Pollard et al., 1997, Woods et al., 2002). Discrepancies between duration and degree of hypoxic exposure that exist in previous studies undoubtedly contribute to the current controversies that exist in the literature with regards to metabolic adaptations (Horscroft et al., 2014). CXE was thus the first high altitude field study to use a large subject group with strictly controlled ascent profiles (Levett et al., 2010, Grocott et al., 2007b).

The aspect of CXE described in this chapter is the analysis of metabolomic and lipidomic profiles of subjects. These 'omics' techniques measure a large number of variables of interest within the metabolic, and lipid, systems. They form a fundamental part of the system-level understanding of the body and are highly informative techniques for assessing responses to a perturbation, such as hypoxic exposure. Indeed, systems biology and the study of humans in extreme environments are argued to be natural symbionts (Edwards et al., 2013). Combining these approaches may help to explain the discrepancies and paradoxes that have evolved in high altitude physiology studies (e.g. the Lactate paradox, in which an apparent blunting of glycolysis occurs upon chronic adaptation to high altitude) (Murray, 2009).

2.2 Aims and objectives

The aim of this chapter was to examine the effects of acute, progressive hypoxic exposure on human metabolism. This was achieved using metabolomic and lipidomic analysis of plasma obtained from healthy humans. The objectives of analysis were to answer the following questions:

- What is the normal, healthy human metabolic response to progressive hypoxia?
- How do individuals vary in their response?

This study is the first to investigate metabolic profile changes in a large study cohort undertaking a strictly controlled ascent to 5300m. An untargeted approach was employed for analysis, meaning no *a priori* hypothesis was considered. Instead, it presents as a hypothesis generating study.

Given the complexity of the metabolomic and lipidomic techniques, a detailed background precedes the study methods section.

2.3 Metabolomics and Lipidomics Overview

A large body of work in this thesis assesses potential metabolite changes in response to a perturbation, being hypoxia or dietary nitrate supplementation, by use of 'omics' techniques. This includes metabolomics and lipidomics. A detailed explanation of analytical tools and data handling and analysis strategies are discussed below.

2.3.1 Analytical tools

The human metabolome is estimated to comprise many tens of thousands of individual metabolites. This includes both those confirmed and predicted, endogenous and xenobiotic (Psychogios et al., 2011, Wishart et al., 2012, Thiele et al., 2013). The human metabolome database (available at www.hmdb.ca) for instance, contains 41,992 metabolite entries. An example of a similar publicly free database but that is specific for lipids, LIPID BANK (http://lipidbank.jp), contains spectral information on 7009 naturally occurring lipid structures.

As already indicated, metabolites have both a highly diverse atomic arrangement and an enourmous variation of chemical properties. They range from hydrophilic, polar metabolites with a low molecular weight (e.g. amino acids) to hydrophobic, non-polar higher molecular weight metabolites (e.g. lipids) (Dunn et al., 2011b). This sets metabolome analysis apart from that of the transcriptome or proteome as information within DNA, RNA or peptides is encoded in patterns constructed from uniform constituent chemical subunits (i.e. polymerised nucleic acids and amino acids). Furthermore, the range of metabolite concentrations varies from mmol/L to pmol/L or less. Few good methods exist for amplification of metabolite levels as there exists for genomics and transcriptomics in the various forms of the polymerase chain reaction.

The extreme diversity amongst metabolite species makes unbiased detection exceptionally challenging. Indeed, detection and quantification of all metabolites in human

samples cannot currently be achieved using a singular analytical technique. However, the combination of nuclear magnetic resonance (NMR) spectroscopy and mass spectrometry (MS) are popular and increasingly used analytical approaches (Psychogios et al., 2011). The resulting signals are identified using data libraries, such as the human metabolome database (Wishart et al., 2007), or experimentally using analytical chemistry techniques for structure elucidation and with metabolite standards where available.

In this thesis, the method used for metabolomic analysis of human plasma or serum was proton (^{1}H)-NMR. In the present chapter, this was used alongside MS, which was employed for lipidomic assessment of the non-aqueous phase of plasma extract. The use of these spectrometric techniques in this instance was combined with Bayesian statistical modelling to confer a highly informative multidisciplinary approach.

Nuclear magnetic resonance (NMR) spectroscopy

NMR experiments are typically performed on samples in the liquid state. This includes biofluids, such as plasma or serum, as were used in the experiments in this thesis. NMR utilises the properties of atomic nuclei with a non-zero spin quantum number. This is a quantum property of the nucleus related to angular momentum and charge, and is often symbolized as a spinning magnetic field. Examples include ^{1}H, ^{13}C or ^{31}P. These nuclei possess a spin angular momentum quantum number ½ and can exist in two energy levels – often referred to as spin up or spin down. In the NMR experiments described in this thesis, ^{1}H-NMR was used.

In a large population of identical nuclei at equilibrium, the spin and related magnetic moments of individual nuclei have equal energy (i.e. they are degenerate), and both are randomly arranged. In an NMR experiment, nuclei are exposed to a powerful magnetic field which creates a population difference between the spin up and down nuclei as there is a slight excess of the lower energy state (this is often the spin down state). The energy difference is relatively small, comparable to the thermal energy in the system. Irradiation with a pulse radiofrequency wave of the right frequency will convert spins of the lower energy state to the higher one until the population difference is cancelled out. The irradiating radiofrequency waves are then turned off, allowing the nuclei to relax back to their equilibrium potential over a period of time by emitting a characteristic radiofrequency signal. This is called a free induction decay, and if the signal is transferred from time to frequency using a mathematical approach called a Fourier Transform then a spectrum arises. The area of the resonance is directly proportional to the concentration of nuclei that generate it,

making NMR innately quantitative. The chemical environment each nucleus is found within modulates the frequency, meaning that output extends beyond the mere ability to separate nuclei of different atoms. The spectrum produced by a metabolite will encode precise information about the structure, making it a powerful analytical approach. Another important advantage is that the sample itself has only to be exposed to a magnetic field and radiofrequency pulse, making NMR completely non-destructive enabling re-use of samples and avoiding the instrument being impaired by the accumulation of unwanted analyte (Rattle, 1995).

As mentioned, the properties of the chemical environment surrounding the nuclei cause a shift in the resulting resonances. This is mediated by a number of factors, including the shielding effects of the electron cloud surrounding the nucleus that alters the local field at the nucleus. The ^{1}H nuclear resonances will reflect the chemical group to which that particular nucleus belongs. Variation in this NMR frequency, or 'chemical shift', is small (most ^{1}H frequencies only vary within a range of 10 parts per million), but can be measured with great accuracy enabling a detailed identification of compounds (Bothwell et al., 2011, Rattle, 1995).

Chemical shift (δ) is also affected by the properties of surrounding nuclei. The energies of nuclei positioned close together interact, a phenomenon denoted spin-spin coupling, which causes the δ to be split into sub-peaks. Distinct molecules have a characteristic number and pattern of peaks and sub-peaks (Bothwell et al., 2011).

Analysis of NMR spectra gives precise information regarding chemical structure and abundance of the molecules of which the nuclei form a part, thus enabling metabolite identification (Rattle, 1995, Bothwell et al., 2011). The quantitative nature, high reproducibility and relatively simple sample preparation make NMR a highly desirable technique. It is also non-selective, as the sensitivity is independent of the hydrophobicity or acidity of the compounds being analysed (Dunn et al., 2011b). One large downside to the approach is its relatively poor sensitivity, which arises because the nuclear transitions that are measured in the NMR experiment are very close to the thermal energy of the system, meaning population differences between the low and high energy states are very small (Dunn et al., 2011b). Only those metabolites in high abundance (100nmol/l to 1µlmol/l or higher) can be detected, with usually less than 100 metabolites detectable per sample in a typical liquid-state metabolomics experiment (Dunn et al., 2005, Bothwell et al., 2011). Further, 1D spectroscopy (typically used for metabolomics experiments and the method

adopted in this thesis) results in spectral crowding whereby alterations in low abundance metabolites may be obscured by those species in higher abundance and with similar chemical shifts, which in turn limits biomarker discovery. An additional limitation is the lack of sensitivity towards compounds that form part of plasma lipoprotein complexes and aggregates. This includes resonances from abundant plasma lipids such as cholesterol, cholesterol esters and phosphatidylcholine. These present in relatively immobile micellular structures with partially constrained molecular motions (Nicholson et al., 1983, Nicholson et al., 1989). In the present chapter, the ^{1}H-NMR analysis was reserved for the aqueous phase of plasma.

NMR experiments are typically performed on samples in the liquid state. This includes biofluids, such as plasma or serum, as was used in the experiments in this thesis. Sample preparation is relatively minimal and requires addition of a small amount of deuterated solvent (e.g. deuterium oxide (D_2O)) to provide a frequency lock signal required to control for magnetic field drift. A δ reference compound may also be added (Dunn et al., 2011a). For the ^{1}H-NMR experiments presented in this thesis, a Carr-Purcell-Meiboom-Gill (CPMG) pulse sequence was applied in each experiment. Essentially, this approach enhances the sharp features in the spectrum by suppressing the broad features (Nicholson et al., 1989). In doing so, it enables better visualisation of low molecular weight metabolites. The extracted lipid fraction of plasma was assessed using MS.

Mass spectrometry (MS)

The other major technique currently applied for metabolite detection, which is used in the lipidomics section of the Everest project described here, is MS. This operates by the formation of positively or negatively charged species (ions) from analytes of interest (in this case metabolites). Ions, including molecular, fragment and adducts, are then separated according to their mass-to-charge ratio (*m/z*). Separation and detection are performed under high vacuum pressures to reduce the number of ion-ion or ion-molecule collisions, which can influence mass resolution, accuracy and instrument sensitivity. In metabolomics or lipidomics experiments, the vast majority of ions carry a single charge (i.e. $z = 1$), meaning that m/z usually = m.

Structural similarities within lipid classes (e.g. the eight broad classes outlined in the LIPID MAPS classification system (www.lipidmaps.org) (Fahy et al., 2009)) allow the measurement and (at least partial) classification of a large number of lipid species in a single MS run. However, the increased structural complexity and size of many lipids, including

differing isomers and fatty acid constituents, makes completely unambiguous identification particularly challenging and presents the most significant current analytical and experimental obstacle for investigators (Wishart, 2011). Positive identification of a metabolite requires several parameters including accurate mass, fragmentation pattern, isotope abundance pattern and retention time, to match with that of a purified metabolite under identical conditions. This definitive identification is not plausible for large numbers of metabolites. It is therefore broadly accepted for metabolites to be 'putatively annotated', a term defined by the Metabolomics Standards Initiative (Sumner et al., 2007). This method of identification uses a single measured parameter, such as accurate mass, and matches this to a metabolite present in a library or database. Although less time-consuming than definitive identification, the confidence in correct identification is lower (Dunn et al., 2011a), hence 'key' compounds still need to be annotated more rigorously. Indeed, some claim that unless metabolites are identified by two orthogonal techniques the assignment should still be labelled as tentative (Sumner et al., 2007). An option is use of targeted or semi-targeted experiments, the latter being used in the present chapter of this thesis as discussed below, which involved the addition of internal standards to the sample.

MS based metabolomics has been successfully applied as a biomarker tool in both epidemiology and stratified medicine (Sreekumar et al., 2009, Nicholson et al., 2008). By their very nature, these studies are large scale designs, thus requiring multiple MS batch runs. This, in turn, substantially increases experimental variation arising from the MS measurements. Of high interest in the metabolomics field, therefore, is the development of highly reproducible and robust MS measurements. Strength of experimental design is thus imperative to achieving such results. Good practice has been shown to involve the use of three sample types: biological, pooled quality controls (QC's) and blanks (Kirwan et al., 2014).

MS can be performed with or without a precedent chromatography separation step, and with it exist multiple advantages and disadvantages. The dominant MS platform for some years was gas-chromatography-MS, however technological improvements led to widespread adoption of liquid chromatography-MS as the tool of choice. This includes those technologies with enhanced sensitivity and separation resolution such as ultra-performance liquid chromatography (Dunn et al., 2011b). Chromatographic separation of molecular species within a sample prior to infusion into the MS simplifies the resultant spectra and improves the ionisation of individual analytes.

The application of a prior chromatography step is, however, vastly time consuming in comparison to direct infusion MS (DIMS) techniques, which enable rapid, high throughput analysis. In comparison to LC-MS, whereby metabolites are broken up into fragments, the metabolites detected in DIMS are whole. Whilst DIMS has been demonstrated to present comparable classification and prediction capabilities to LC-MS (Lin et al., 2010), it benefits from rapid analysis time consuming ~5% of the time required for analysis of LC-MS data (Lin et al., 2010). DIMS also demonstrates high technical reproducibility and requires minimal sample biomass (Kirwan et al., 2014). However, the absence of chromatography does come with some disadvantages, including ion suppression and co-elution of metabolites into the MS. In addition, the spectra produced from DIMS are more complex, yielding only m/z alongside intensity values. This means that without the addition of internal standards, identification of metabolites is limited to putative annotations at best (Sumner et al., 2007) .

The advantages outlined for the DIMS method make this the optimal choice for analysis of the lipidomics data presented in the current chapter. Here, a high resolution DIMS approach was adopted (DIHRMS). Given the sample number, multiple batches were run, with each batch containing the biological sample, quality control, blanks and internal standards. This thus ensured reproducibility between sample runs and enabled accurate metabolite identification.

2.3.2 Experimental design

Targeted or non-targeted?

Design of metabolomics experiments can either take a targeted or non-targeted approach. Both have their advantages and disadvantages and can be highly effective and complementary when used in conjunction.

Untargeted metabolomics, or metabolic profiling, attempts to measure all the analytes in a sample, including chemical unknowns. In this approach, the study begins with limited biological knowledge. Whilst there may be a general hypothesis available (e.g. there is a metabolic difference between two conditions), there is no specific *a priori* hypothesis stating which metabolites are related to the (patho-) physiological change. It aims to produce data on an extensive range of metabolites present in multiple metabolite classes or pathways that are dispersed across the metabolic network. The metabolome coverage is therefore intended to be unbiased and as comprehensive as possible. This method is not

quantitative and metabolite identification is a challenge. In order to reduce the resulting data sets into more manageable entities, dimension-reduction techniques such as principal components analysis (PCA) or multidimensional scalings (a method for visualising the level of similarity of individual cases of a dataset) can be employed. The results of such experiments can be inductive or hypothesis-generating and can provide insight into novel changes occurring to the metabolome as a result of the perturbed state (Roberts et al., 2013, Dunn et al., 2011b). The examination of metabolic profiles in this manner has led to numerous advances in biological understanding, including the role of sarcosine in prostate cancer progression (Sreekumar et al., 2009).

Targeted metabolomics involves the detection of a specific number of metabolites (typically in the order of tens to hundreds) that are related in function or class. This method is used in hypothesis testing or deduction studies whereby the metabolites (or at least, pathways) of interest are known (Dunn et al., 2011a).

A major development effort is required to establish a successful targeted technique. Absolute quantitative metabolite concentrations are determined with high specificity and accuracy by using the addition of internal standards. These are typically isotopically-labelled versions of the endogenous metabolites, usually containing ^{13}C or ^{2}H isotopes (Dunn et al., 2011b). As only those targeted metabolites are detected, this does mean that the number of discovery opportunities is reduced. However, one hybrid option is to use semi-quantitative/targeted methods where a number of ‘class specific’ standards are spiked into samples. This relies on the assumption that similar classes of compounds give comparable signals.

In Chapter 2 of this thesis, an untargeted profiling approach was adopted for the assessment of the aqueous phase of plasma using ^{1}H-NMR. A semi-targeted approach, with the addition of deuterated standards, was used for the assessment of the plasma lipid fraction using DIHRMS. The untargeted profiling approach was also applied to serum analysis in Chapter 3 of this thesis. In Chapter 5 of this thesis, a small scale targeted approach was employed.

2.3.3 Data processing

A single NMR or MS spectrum represents a vast amount of data. This is both in terms of data points per sample (typically 32k or 64 k for NMR (Dunn et al., 2011a)) and also the number of samples, and so resulting spectra, acquired to obtain meaningful results. Several

pre-processing steps are therefore required to transform the raw spectroscopic data in such a way that subsequent analysis is easier, more robust and accurate. Various advancements in these procedures strive to prevent loss of data and to eliminate unwanted variation. Given the difference in the output from the NMR and MS techniques, the intermediary pre-processing steps can differ for each method, as is the case for this thesis, although some overlap exists between the two.

NMR data pre-processing

NMR spectra produced from analysis of a complex set of biofluids can be influenced by variances including the following: incorrect phasing, varying baselines, varying biofluid concentrations and shifting peak locations. Pre-processing steps are thus required to ensure these variances do not interfere with subsequent data analysis. In this thesis, a variety of pre-processing methods were employed within each study, depending upon the study design and the quality of the spectra produced. For each study, specific detail on the pre-processing steps are outlined in the respective methods sections, but an overview and background of these processes is outlined as follows.

Accounting for the effects of shifting peaks

A biofluid matrix is highly complex. Variances can exist in the relative concentrations of specific ions, salts and metabolites as well as the overall dilution of samples. These parameters can influence the chemical shifts of peaks, affecting different peaks by varying extents, even if they belong to the same metabolite (Dieterle et al., 2006). Given that peak shifts are not desired for most applications, steps are usually taken to handle these variations.

A simple approach for this is alignment of peaks to a reference compound. In chapter 2 and 3, the compound 3-trimethylsilyl-1-propanesulfonic acid sodium salt (DSS) was added to the NMR buffer and was used to reference spectra (δ =0). Alternatively, the endogenous compound formate (δ = 8.44 ppm) can be used, as was the case in Chapter 5 (Kriat et al., 1992). This can be performed manually, using either Topsin (Chapters 2 and 5) or ACD labs (Chapter 3). However, human error can become problematic with the manual approach in large data sets, as was the case for Chapter 2, therefore further refinement was performed in Matlab using the *i*coshift program (Savorani et al., 2010). This algorithm enables fast alignment of all spectra simultaneously and at full resolution.

It is at this stage that phasing can be corrected (using either Topsin or ACD labs) and the over dominating water peak removed (De Meyer et al., 2008).

1. Normalisation

The pre-processing method of normalisation scales spectra to the same overall virtual concentration. This method takes into account variances such as differences in sample dilution, the range of which will depend upon the water intake of the subject. Dilution will influence all metabolite concentrations, meaning intensities of all peaks within a spectrum will be altered by the same factor. In addition, metabolomic fluxes may only affect select metabolites and so select peaks of the corresponding spectrum. Such specific changes are usually of interest, therefore normalisation is adopted to compensate for differences in overall concentration whilst avoiding obscuring specific metabolite changes. The end goal is for effective normalisation between spectra to ensure large peaks do not dominate subsequent analysis.

An approach that encompasses both changes in overall dilution and those of specific metabolites is probabilistic quotient (PQ) normalisation (Dieterle et al., 2006). This method assumes that changes in the concentration of single analytes only influence specific regions of the spectrum whereas changes in the overall concentration influence the spectrum in its entirety. It is an advancement upon the standard normalisation approach that uses integrals (De Meyer et al., 2010). This assumes integrals of a spectra are mainly a function of the overall sample concentration and so normalises the individual intensities of a specific spectrum by dividing them all by the summed intensity of that spectrum. Spectra are therefore scaled to the same total integral. PQ normalisation usually begins with spectra following integral normalisation and generates a reference spectrum from this, typically a median spectrum (De Meyer et al., 2010). The distribution of the quotients, derived from amplitudes of the spectrum, are then normalised with those of the reference spectrum. This approach has been demonstrated to be far more robust than integral normalisation (Dieterle et al., 2006).

2. Spectral binning

Statistical analysis of the complex data set produced can be aided by data reduction. This requires a reduction in the number of variables and so spectral resolution through binning methods, which can be employed either before or after the normalisation step.

Standard or equidistant binning involves division of the spectra into equally sized bins, usually between 0.02-0.04ppm (De Meyer et al., 2010). These discrete regions are then integrated and a list of integral values is produced for each spectrum, essentially reducing the spectrum to a bar chart. This reduces the resolution of the data and can lead to a loss of information, as for instance smaller peaks within a bin can be obscured, whereas other bins may only contain noise. In addition, peaks at the edge of bins may be scattered over several bins, leading to the presence of artefacts, the distribution of which may change between spectra depending upon variations in peak locations (De Meyer et al., 2008). This has been addressed through the development of more advanced binning algorithms such as adaptive intelligent binning. This is a non-equidistant approach that focuses upon better peak definition. It recursively identifies the edges of existing bins and avoids the use of arbitrary parameters or reference spectra (De Meyer et al., 2008). However, both methods remain in common usage, depending on the specifics of the data at hand.

3. Scaling

In principle, the integral values across an NMR spectrum are proportional to both the concentration and the number of resonances present. The variation in intensity within an NMR spectrum is therefore directly proportional to changes in concentration and proton density. However, in the absence of scaling, the largest resonances would in turn have the greatest influence upon subsequent data analysis, thus obscuring variations of interest in regions of low intensity. Whilst PQ normalisation addresses this issue between spectra, scaling is required to bring down the effects of the larger peaks within a spectrum. Appropriate scaling thus ensures the relative importance of each variable within the dataset is suitable.

A standard method of scaling to the unit variance uses the reciprocal of the standard deviation as the scaling weight, and so does not address this problem as it results in all variables having equal potential to influence the model (Keun et al., 2003). Instead, an effective method of 'bringing down' the larger peaks whilst ensuring they aren't lost into the noise of the data set is Pareto Scaling. This is an intermediary between the extremes of no scaling and unit variance and uses the scaling weight of $1/\sqrt{\sigma}$, where σ = standard deviation (Keun et al., 2003).

4. Controlling for bias.

Medium to large scale metabolomics experiments are constrained by the fact that it is not possible to run samples in one batch. This brings into light the issue of instrument reproducibility. In the case of NMR spectroscopy, this is not normally an issue as the sample does not physically interact with the operating parts of the instrument, so changes in the sensitivity from instrument contamination are normally not observed (Dunn et al., 2011b). Instead, this feature is usually reserved for LC-MS experiments.

Despite this, a batch effect was observed in the NMR data set produced from Chapter 2, as is discussed further in the results section of this chapter. Briefly, PCA clearly revealed separation of two groups that was entirely unrelated to experimental differences. In order to correct for this, a method was applied that has been shown previously to normalise the batch effects observed in LC-MS metabolomics data collection termed Eigen MS (Karpievitch et al., 2014, Karpievitch et al., 2012). This singular value decomposition based method applies the following steps, as described by Karpievitch and colleagues (Karpievitch et al., 2014):

- ANOVA is used to capture and preserve the variation due to treatment effects of the study. This is done by using the R function lm(), which estimates the treatment effects. The residuals (loosely meaning an error in the result) function () also accesses a matrix of residuals.
- Singular value decomposition is then applied to the matrix of residuals to find any systemic trends that can be attributable to bias.
- The number of bias trends is subsequently determined by a permutation (or randomisation) test.
- The effects of bias are then removed from the data. In the present study, a conservative approach to bias trend removal was adopted and only the most obvious bias trend removed.

MS data pre-processing

Controlling for Bias

In the case of mass spectrometry, where the sample inevitably interacts directly with the instrument, changes in the measured analyte response over time are inevitable (Dunn et al., 2011b). This can attenuate the signal detected, the degree and timing of which is inconsistent.

To assist controlling for this effect and to provide robust quality assurance for the chemical features detected, Quality Control (QC) samples can be periodically analysed throughout an analytical experiment. During the data pre-processing steps (see below), data conditioning algorithms can be applied using the QC sample responses as a bias to assess the quality of the data. This includes removal of peaks with poor repeatability, correction of any signal attenuation and integration of batch data (Dunn et al., 2011b).

For the MS experiments performed in Chapter 2 of this thesis, QC samples obtained from pooled samples were used alongside internal standard blank samples to correct for batch effects.

Following signal correction and batch integration using QC's, further quality assurance is required for each detected peak (Dunn et al., 2011b). For the MS experiments presented in Chapter 2, only peaks with deviations within $\pm$ 5ppm of the target mass defined by the internal standard with an intensity threshold >1000 were retained. Lipid molecules with >10% missing values were removed.

2.3.4 Statistical analysis

The output of any -omics experiment is production of a vast data set. In the instance of metabolomics, levels of thousands of metabolites can be measured in hundreds of samples. Such high dimensionality in a data set makes it difficult to visualise samples and to undergo simple exploration.

In addition, there are a number of technical features that can present challenges with data analysis. For instance, MS spectral data are known to be noisy and inherently contain various sources of uncertainty (Katajamaa et al., 2007). Whilst NMR is generally regarded as being highly quantitative and reproducible, there are a number of potential sources of experimental error akin to MS, including sample preparation, peak identification and summarisation (Katajamaa et al., 2007). A high level of noise in the data set can result in an excessive false discovery rate and can mask small, discrete metabolite changes (Broadhurst et al., 2006, Saccenti et al., 2014). Necessary precaution thus needs to be taken when considering analysis strategies.

Along with these potential problems are features of metabolomics data sets that can aid with data analysis and interpretation. For instance, metabolomic data are known to be highly collinear, meaning multiple things tend to change together or along the same line

(Suvitaival et al., 2014a). This property arises from the concurrent involvement of compounds in biological processes and lends itself to multivariate statistical methods that are able to distinguish patterns within a data set. The differing statistical approaches to analysis of such data sets and the benefits and hindrances of these are discussed below.

Univariate statistics

Univariate analysis involves measurement of 1 variable at a time and includes, for instance, t tests. In the context of metabolomics data sets, this would result in significance testing for tens of hundreds of metabolites. The very nature of univariate testing is that the more tests that are performed (so the more metabolites tested) the higher the chance of claiming a difference that is actually false (type I error). In other words, a null hypothesis of there being no difference between groups that is actually true is rejected. It is common practice to allow a 5% or one in 20 chance that a type I error is made. The criteria for defining a significant difference between two population means is therefore set at 5%, which is a parameter referred to as α of 0.05.

Correction is therefore required for multiple testing to prevent against the increasing probability of having false positives, or a type I error (Saccenti et al., 2014). However, these corrections (such as Bonferroni tests) are highly conservative and can incur the risk of introducing false negatives, or type II errors, whereby the null hypothesis is actually false yet the test fails to reject it (Saccenti et al., 2014). It follows that the probability of making a type II error is known as β. The power of a test, being the probability that a significant difference is found, is 1-β.

Alongside the number of tests, a p value is also affected by sample size. For a fixed α (so 0.05), the relationship between the number of samples measured and the difference in population means is critical. In turn, this means that the likelihood of distinguishing a significant difference is a function of sample size, so will increase with increasing sample number (Broadhurst et al., 2006). In addition, the dependence of the p value upon only one hypothesis is that a huge effect observed in a small trial can result in the same p value as a minute and uninteresting effect in a large trial. This therefore presents as an inadequate measure of the strength of evidence (Broadhurst et al., 2006, Cornfield, 1966).

Therefore, despite its common use, the p value does have significant limitations that in turn bring into question the degree of its usefulness. Caution must thus be taken when interpreting p values and particularly when employing such testing methods to a

metabolomics data set and should be restricted to examination of a few select metabolites, if at all.

Multivariate statistics

Adoption of multivariate methods enables for all variables to be used simultaneously, essentially acting as a pattern recognition process. Aside from the mean, such methods make use of co-variances or correlations that reflect the extent of the relationships among variables. This approach therefore contrasts to univariate methods that focus solely upon the mean and variance of a single variable (Saccenti et al., 2014). Using all variables together avoids loss of information and finds underlying trends in the data set.

One such multivariate method that is used routinely as a first step in the analysis of metabolomics data is principal components analysis (PCA). In essence, this approach attempts to find a small set of variables that explain the pattern of the original data set (Nicholson et al., 2008). This is achieved by reducing the dimensionality of the data and modelling underlying trends, or 'latent variables', whilst retaining most of the variation within the data set (Ringnér, 2008). This is accomplished by identifying directions, termed principal components, along which the variation in the data set is maximal.

A principal component (PC) is thus a weighted linear combination of each of the original variables. The original data matrix becomes compressed into a smaller number of latent variables, typically three to four PCs. Within these few components, each sample is represented by relatively few numbers instead of values for thousands of variables. The weight given to each variable within a PC describes how influential that variable is in relation to others. The first PC is the direction along which samples show the largest variation. The projection of each sample onto this first PC reduces the dimensionality from a two-dimensional to a singular dimension data set. Information that is not captured in the first PC forms the residuals through which the second PC is calculated. This second component is thus the direction uncorrelated to the first component along which the samples show the largest variation. The lack of correlation between PCs means they may represent different aspects of the dataset.

The output of PCA is a plot of samples. This makes it possible to visualise the data set and assess similarities and differences between samples. It may result in grouping of the samples, separating possible regularities or trends in the data set from noise, and also enables determination of outliers.

PCA is therefore designed to identify directions with the largest variation. As it is unsupervised, it does not separate classes of samples. It also does not capture repeated measures in a data set. In addition, it does not distinguish experimental artefacts that result from the high throughput technologies used in omics analysis, meaning dominant PCs may in fact correlate with these artefacts (Ringnér, 2008). This latter point was dealt with later in the present chapter, whereby the initial PCA plots of the NMR data revealed separation of samples based on experimental artefacts, which were subsequently corrected for using EigenMS. PCA results therefore critically depend upon the aforementioned data pre-processing steps (Ringnér, 2008).

Statistical Inference

Statistical inference is a process of drawing conclusions about populations or scientific truths from the underlying distribution of the data. These inferred properties include testing hypothesis and deriving estimates. The population is assumed to be sampled from a larger population, which sets it aside from the uni/multivariate descriptive statistics already described that are solely concerned with the properties of the observed data set.

Many models of inference exist and include broad theories such as Bayesian statistics.

Bayesian statistics

Obtaining data from an experiment, but not knowing either the mean (θ) or variance (σ^2), requires for inferences to be made about the values of θ and σ^2 based upon the data observations (y). In a Bayesian approach, a prior distribution (p) is introduced into the model. This either expresses a state of knowledge or ignorance about θ or σ^2 before the data were obtained. From here, it becomes possible to calculate the probability distribution of θ and σ^2, given the data y, using the following equation*:* $p(y|\theta, \sigma^2)$ (Box et al., 2011). Inferences can be made about the parameters derived from this distribution. This concept is the basis of Bayes theorem, which can be expressed as in **Equation 2.1** (Box et al., 2011).

$$p(\theta|y) = cp\,(y \mid \theta)\, p(\theta)$$

Equation 2.1. The basis of Bayes theorem

Where:

p(θ) = what is known about θ without knowledge of the data, aka the prior distribution of θ.

$p(\theta|y)$ = what is known about θ given the knowledge of the data, aka the posterior distribution. This can also be called the likelihood function and may be regarded as a function of y but not of θ. It contains all relevant information about the sample and is the function through which the data y modifies prior knowledge of θ.

c = normalising constant to ensure the $p(\theta|y)$ integrates or sums to one.

This theorem tells us that the posterior distribution is proportional to the product of prior distribution multiplied by the likelihood for *θ* given *y* (Box et al., 2011). In other words, Bayes theorem describes the probability of an event based upon prior knowledge of conditions that may be related to that event. Through the use of Bayes theorem, subjective degrees of belief obey the rules of probability. It allows sufficient flexibility to react to the complexity of biological systems that is free from technical limitation. As this system of inference can be readily applied to any probability model, it allows for greater emphasis to be placed upon scientific interest and less to mathematical convenience (Box et al., 2011). Importantly, the Bayesian approach focuses upon distributions as opposed to single numbers.

The general framework of Bayesian statistics thus codifies how to proceed in a rational way with analysis and inference of data taken from high dimensional biological systems where only a minute subset of relevant variables are measured (Baldi et al., 2001). A complete Bayesian treatment is highly computationally demanding, therefore shortcuts can be developed that strike a balance between rigor and computational efficiency (Baldi et al., 2001).

The use of Bayesian statistics for analysis of multi-dimensional data sets is not a new concept and indeed has been employed previously to -omics data to great effect. This includes the use of Bayesian integration to define functionally related genes and metabolites identified using transcriptomics and metabolomics respectively (Bradley et al., 2009). Here, the transcript-metabolite correlations were evaluated in light of the experimental context in which they occurred, as well as the class of metabolite involved. In this way, Bayesian integration was able to effectively predict known enzymatic and genetic regulatory

relationships, including those central to the glycolytic-gluconeogenic switch (Bradley et al., 2009).

Bayesian approaches have proven particularly useful in the assessment of metabolomics data obtained from MS analysis. For instance, application of a Bayesian alignment model to LC-MS data was demonstrated to integrate relevant information required to significantly improve the performance of the retention time alignment (Tsai et al., 2013). Bayesian approaches have also been adopted in the integration of spectral peaks in MS analysis originating from the same compound (Suvitaival et al., 2014a, Suvitaival et al., 2014b).

Posterior/Non-informative prior

As already stated, the formulation of models from Bayesian statistics requires prior distributions (or knowledge) for any known parameters. This prior distribution is supposed to represent what is known and unknown about the parameters before the data is available. Such a distribution thus represents either the degree of prior knowledge or relative ignorance (Box et al., 2011). This concept has faced controversy, with some viewing the use of prior knowledge in the analysis as interfering with the process of scientific inference by bringing a degree of prejudice. In other words, it is usually preferred to let the data 'speak for themselves' rather than distorting 'what the data are trying to say'. However, this is can be dealt with through a combination of careful model choice and the use of appropriate 'non-informative' prior distributions, which aim to obtain inference that is appropriate for an unprejudiced observer (Box et al., 2011). Essentially, this means that the prior is developed as the model progresses, ending with the construction of a posterior prior, or distribution. This approach was adopted in the analysis presented in the present chapter and it results in the construction of a fluid and sophisticated model.

Hierarchical modelling

In the experiment described in Chapter 2, the data are naturally hierarchical: there are multiple measurements of each metabolite in each subject, while we seek the trends in these metabolites across the entire study population. For this reason, we adopted a hierarchical approach to statistical modelling. This was achieved by fitting linear models to each binned ^{1}H-NMR region or lipid variable at the subject level and further fitting distributions to the parameters from these models. By adopting a Bayesian hierarchical method, we were able to build fully connected hierarchical models where the distributions of

the parameters (at the 'highest' level of the model) constrained the values of the parameters for an individual subject, a phenomenon known as 'shrinkage' (Kruschke et al., 2015, Kruschke, 2010). In other words, this allowed layers of the hierarchical model to communicate, in doing so ensuring the observations are treated in context of the data set as a whole as opposed to in isolation.

However, as alluded to above, Bayesian statistics are computationally expensive. Simple frequentist hierarchical models were therefore fitted initially to select variables of interest for further modelling. Mean slopes residing around 0 indicate little change with altitude, and so were considered uninteresting and were discarded. Selected were those mean slopes that were > ±1.96 SDs from the mean. Finally, Bayesian inference is somewhat different to frequentist approaches (e.g. there are no p-values). Hence we adopted the criterion that metabolites should not include 0 in the high-density (95%) interval of the posterior distribution of z-transformed slopes. Together, this means that two levels of filtering were employed to ensure that only those slopes undergoing large degrees of change were considered.

2.3.5 Reporting of methods

Effective communication of methodology, analytical approaches and methods of identification is key to avoiding misinterpretation of results in metabolomics studies. Attempts have been made to build a general consensus upon reporting strategies (Sumner et al., 2007). This is recognised to be an ongoing process within a field that is continuously developing and the need to reassess reporting standards for metabolite identification has been recognised (Creek et al., 2014, Salek et al., 2013). However, the guidelines for chemical analysis and metadata remain highly applicable and are an essential means of determining whether the distribution of claimed biomarkers in fact results from confounding factors (Sumner et al., 2007, Broadhurst et al., 2006). This includes detail regarding the experimental design, subjects, treatment, collection, sampled preparation and NMR/MS spectral acquisition. The methodology reported in this thesis therefore encompasses each of these factors.

2.4 Study Methods

The study design, risk management plan and individual protocols for Caudwell Xtreme Everest (CXE) were approved by the University College London (UCL) Research Ethics Committee (in accordance with the declaration of Helsinki). The study was designed

and conducted by the UCL Centre for Altitude Space and Environment Medicine (CASE). Both verbal and written informed consent was obtained from all subjects.

2.4.1 Study Participants

Subjects were members of the public and were recruited by word of mouth and via public advertising. Subjects, males and females aged over 18 with no upper age limit, were required to pass two separate health screening stages (Levett et al., 2010). Exclusion criteria were as follows:

- Diabetes mellitus: defined as the need to control blood glucose levels through diet, oral hypoglycaemics or insulin therapy
- Significant respiratory disease: defined as a disease that could deteriorate at altitude, rendering the subject at risk during the trek to EBC. For instance, severe chronic obstructive airways was an exclusion criteria whereas mild asthma was not.
- Significant cardiovascular disease: defined as disease that could deteriorate at altitude, rendering the subject at risk during the trek. For instance, ischemic heart disease with angina and symptomatic heart failure were excluded whereas controlled hypertension was not.
- Females were required to not be pregnant.

From this screening process, 198 healthy volunteers were selected to participate in the study.

2.4.2 Study design

Ascent profiles and logistical details have been reported previously (Levett et al., 2010). Baseline measurements were performed in London (LDN) in a laboratory at UCL (75 meters above sea level) between January 4th and February 26th 2007. Field studies were performed between 31st March and 6th June 2007 at laboratories set up at the following locations (altitudes expressed as meters, m): Kathmandu (KTM, 1,300m), Namche (NAM, 3,500m), Pheriche (PHE, 4,250m) and Everest Base Camp (EBC, 5,300m). Data collection, including plasma sample collection, was performed at each of these time points.

Trekkers were split into 13 smaller groups (16 subjects max in each) and two groups left the UK each week for the duration of the expedition. The ascent rate was chosen in order to minimise the incidence of high altitude illness during the trek and so maximise the number of participants able to participate in laboratory tests at EBC (Hackett et al., 1976). All subjects

underwent an identical ascent profile, arriving at EBC on day 11 (**Figure 2.1**). To maintain an identical pattern of hypoxic exposure, subjects were restricted to ascending no higher than 300 vertical meters above the laboratory altitude on rest days. Details on P_B, PiO_2 and temperature are displayed in **Table 2.1**

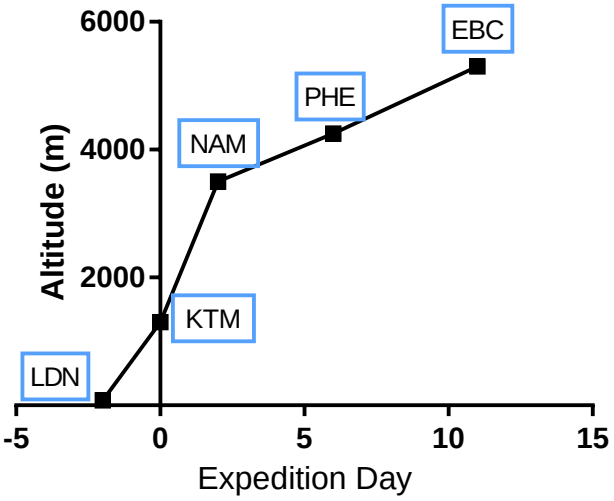

Figure 2.1. A depiction of the ascent and descent profiles of trekker subjects participating in the Caudwell Xtreme Everest study.

Abbreviations are as follows: LDN = London, KTM = Kathmandu, NAM = Namche, PHE = Pheriche, EBC = Everest Base Camp.

Table 2.1. Laboratory altitude, temperature and inspired partial pressure of O_2.

Laboratory	Altitude (m)	Ambient Temp (˚C)	P_B (mmHg)	PiO_2 (mmHg)	P_B (kPa)	PiO_2 (kPa)
LDN	75	24.1 (1)	754 (10)	148.0	100.5	19.7
KTM	1300	26.1 (1.5)	650 (3)	126.2	86.7	16.8
NAM	3500	19.6 (2.6)	505 (3)	95.4	67.3	12.8
PHE	4250	13.1 (1.7)	461 (2)	86.7	61.5	11.6
EBC	5300	21.5 (5.6)	404 (3)	74.7	53.8	9.9

***Notes**: Altitudes derived from map values to the nearest 50m; Barometric pressure (P_B) and temperatures are mean (SD) values recorded in the field laboratory during testing. PiO_2 = inspired partial pressure of O_2, derived from P_B (Levett et al., 2010).*

2.4.3 Plasma sample Analysis

Blood sampling

All blood samples were taken in a rested, fasting state from the antecubital vein and collected in 10ml BD ethylenediamine-tetra-acetic acid (EDTA) blood tubes (Southern Syringe Services LTD). Plasma was separated from blood cells by centrifugation of whole blood at 800G for 15 mins and immediately frozen in 1 ml aliquots in liquid nitrogen. Samples remained in liquid nitrogen for the duration of the expedition (including carriage back to Kathmandu) and were transported back to the UK on dry ice, where they were stored at -80°C in a commercial cryostorage facility until transport to King's College London on dry ice. Here, they were maintained at -80°C until analysis.

Plasma preparation

Plasma samples were defrosted at room temperature. A chloroform: methanol extraction was used to separate the plasma sample into aqueous and lipid fractions. A 1:1:1 extraction was performed (Beckonert et al., 2007), with 500µl of methanol (Hypergrade for LC-MS, Merck) and 500µl of chloroform (HiPerSolv Chromanorm for HPLC, VWR international), both ice cold, being added to 500µl of plasma in a 1.5ml Eppendorf. This was vortexed for 2 mins and then left in the freezer (-20°C) to stand for 30 mins. They were subsequently centrifuged for 3 mins at 9100G (Force 1624 Microcentrifuge) to separate the sample into the upper (methanol, and so aqueous, fraction) and lower phases (chloroform, and so lipid, fraction), as depicted in **Figure 2.2**. 700µl of the upper phase was pipetted into an Eppendorf ready for further preparation before NMR analysis. ~200µl of the lower phase was pipetted off into an Eppendorf and frozen at -80°C ready for mass spectrometry analysis. Key stages of sample preparation and data processing are presented in **Figure 2.2**.

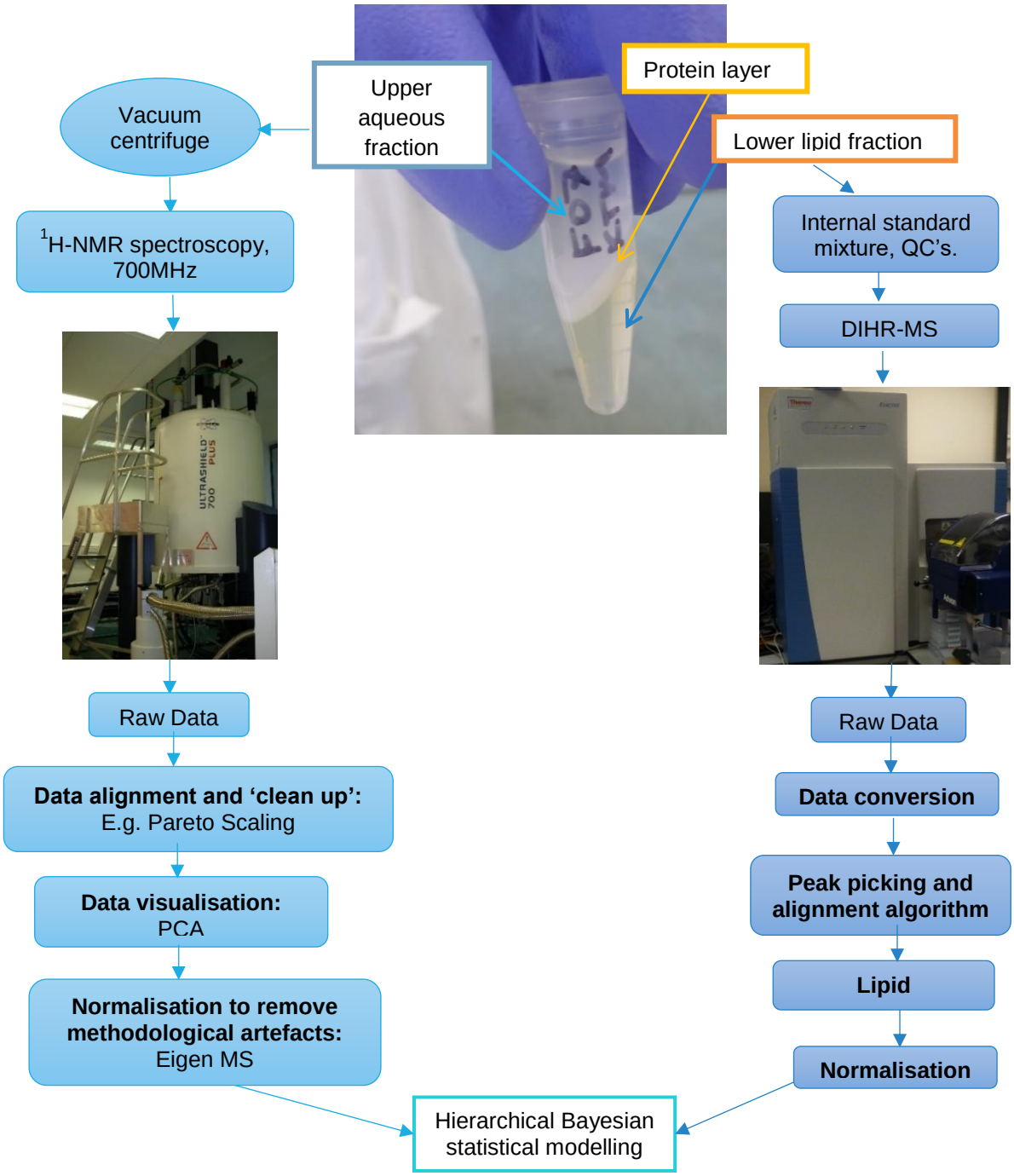

Figure 2.2. Outline of the preparation and analysis of plasma sample fractions, separated by methanol: chloroform extraction.

This includes the preparation of the upper aqueous fraction for ^{1}H-Nuclear Magnetic Resonance (NMR) spectroscopy and the lower lipid fraction for direct infusion high resolution mass spectrometry (DIHR), where samples were infused in the Exactive Orbitrap using a Triversa Nanomate. Data processing steps followed, after which hierarchical Bayesian statistical modelling was employed for analysis of both data sets.

Upper phase/methanol fraction preparation

The upper fraction was dried down at 30°C for 4 hours using a vacuum centrifuge (Eppendorf Concentrator 5301) and then re-suspended in 600µl of the following solution: double distilled H_2O containing 5% D_2O for NMR (Acros organics, CAS: 7789-20-0) and 1 mM DSS (Aldrich, 178837-5G). D_2O was required for the magnetic lock and DSS was used as a reference compound. The resulting solution was transferred to 5mm NMR tubes within a 96 tube rack.

^{1}H-NMR spectral acquisition

^{1}H-NMR spectra of plasma samples were obtained using a Bruker Avance III 700 MHz spectrometer (Bruker Biospin, Karlsruhe, Germany) at the operating ^{1}H frequency 700.2 MHz with a temperature of 298K. A Carr-Purcell-Meiboom-Gill (CPMG) pulse sequence (Bruker experiment: cpmgpr1d) was applied to better visualise low molecular weight metabolites. A spin relaxation delay of 76msec was used and a total of 32 scans acquired. An exponential window function was applied with a line broadening of 0.3Hz prior to Fourier transformation.

All samples were analysed on a subject by subject basis, meaning plasma taken from the same subject at all 5 time points was defrosted and treated at the same time and run within the same NMR experiment. This was to ensure any daily differences in experimental procedure were removed from analysis when data between time points were compared.

Data processing

Resulting spectra processed using Topsin (Bruker). Spectra were converted from time to frequency domain using serial processing. The phase was adjusted so all peaks within the spectra were positive. Spectra were aligned so that the DSS peak was at 0. This was initially performed manually, yet some spectra remained improperly aligned, therefore further refinement was performed in Matlab using the *i*coshift program (Savorani et al., 2010).

The spectra were then split into two regions using Matlab. The aromatic region (δ 6-10ppm; including resonances from polyphenols, compounds with single aromatic rings and carboxylic acids e.g. formic acid) was found to be particularly noisy, therefore was excluded from analysis. The second region, the aliphatic region, was taken forward for analysis following removal of the water peak. This region was normalised via PQ normalisation using R software. At this stage, spectra were not binned so remained at a full resolution. To ensure subsequent analysis was not dominated by the larger peaks, Pareto scaling was employed. An average spectra resulting from these normalisation steps is presented in **Figure 2.3**.

In order to visualise the spread of the data, PCA was performed on this spectral region. Plotted below is PC1 vs. PC2 (**Figure 2.4).** This plot revealed a clear separation of the data from region 1 into two distinct groups captured by PC1. As this data was coloured based on location, the spread into two groups is not due to variation dependent on the experiment i.e. a change with location (so altitude). Instead, it was likely due to sample processing differences, such as slight alterations in gain between NMR batch runs.

Further investigations were thus carried out to determine what factor was causing the change and this was subsequently excluded. The method employed for this was EigenMS (Karpievitch et al., 2014). Three bias trends were found to capture most of the variance in the data, the first of which was easily identified visually as it captured 77% of the variance (**Figure 2.5).** This essentially corresponds to the variance captured by PC1. This trend was then normalised using the EigenMS programme.

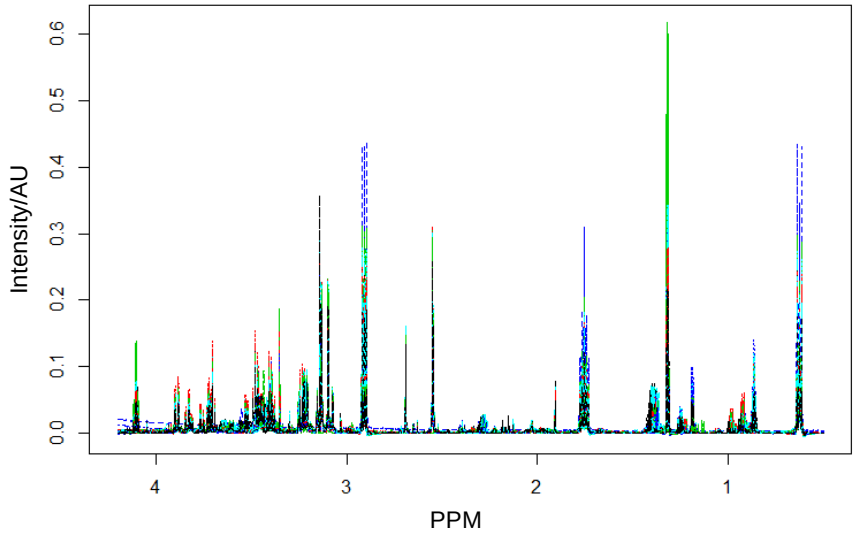

Figure 2.3. Aliphatic spectral region, overlaid.

An average of all spectra at all time points following alignment, PQ normalisation and scaling.

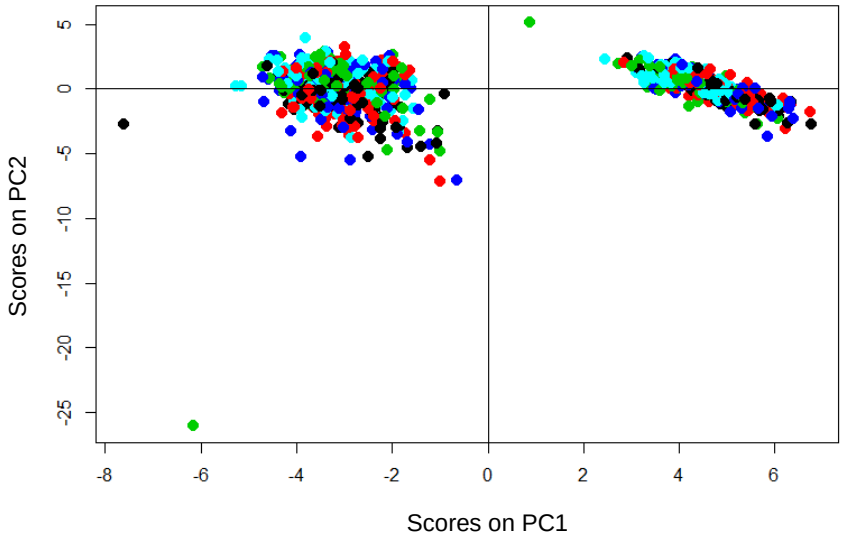

Figure 2.4. Principal component (PC) analysis scores plot

Coloured based on altitude location, demonstrating the separation of groups based on a methodological artefact as oppose to experimental intervention. A clear batch effect is captured by PC1.

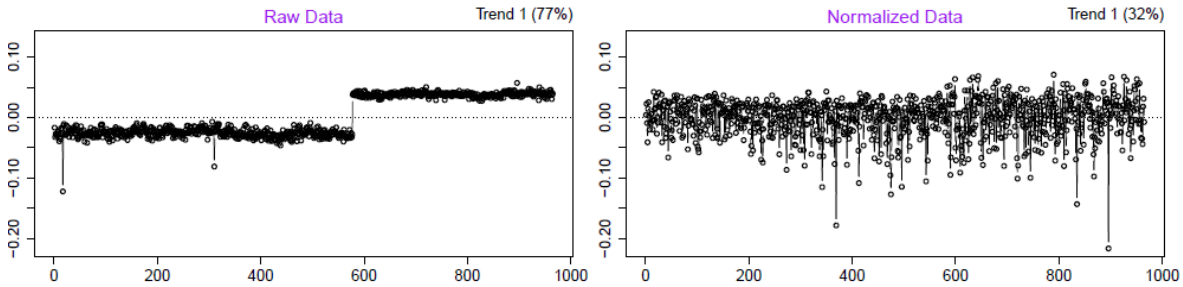

Figure 2.5. Identification of bias trend and correction using Eigen MS.

Bias trend 1 was found to capture 77% of the variance within the data (left panel), which was normalised using Eigen MS (right panel). Each dot is representative of a spectrum, plotted in time order. Units are arbitrary and correspond to the variance captured by the trend.

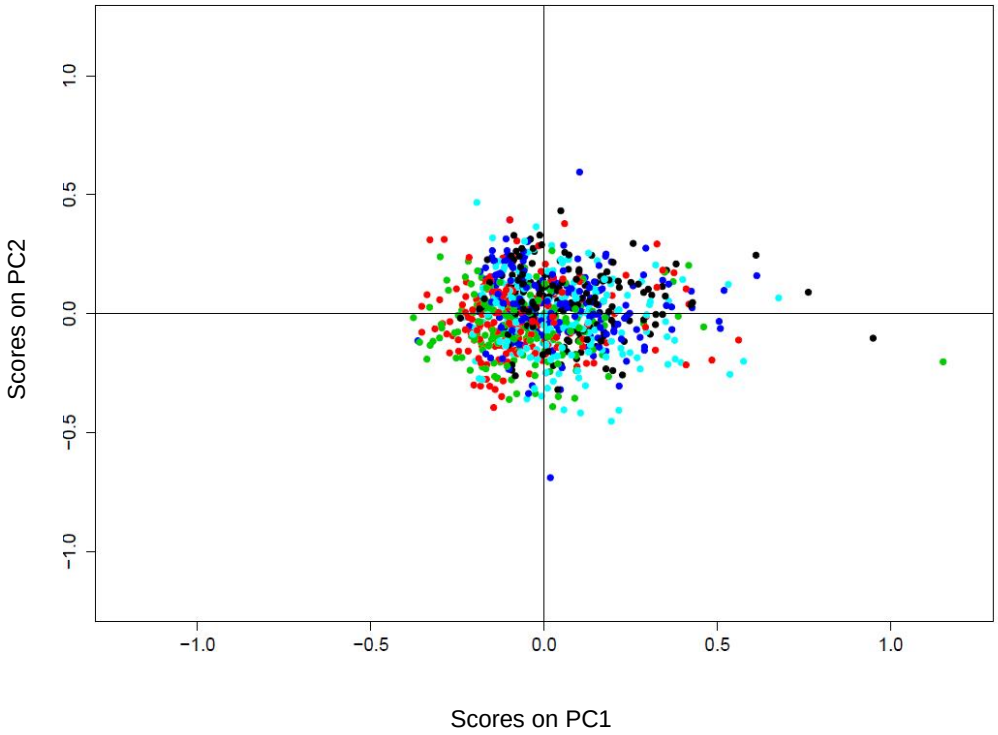

Figure 2.6. PCA scores plot following Eigen MS processing.

Coloured according to altitude location.

The above plot (**Figure 2.6**) depicts the data set colour coded based on altitude location. At this stage, both Dr Edwards and I remained blinded to which altitude was represented by each colour to ensure no preconceptions or bias were introduced to the subsequent analyses. Although discrete, a separation can be observed between groups in this figure. As this data set was treated using EigenMS, we can be confident that this separation is not due to technical processing differences, but due to the differences in experimental intervention, being altitude.

Spectral binning

Following EigenMS, the full resolution spectra were binned at a ratio of 10:1, meaning each bin consisted of 10 data points. This ratio was found to sufficiently reduce the size of the data set, whilst retaining maximal information.

Influence of EDTA and DSS on ^{1}H-NMR spectra

As mentioned, the tubes used to collect blood contained the anticoagulant EDTA. Both free EDTA and that which complexes with endogenous compounds including Ca^{2+}, magnesium (Mg) and Zinc (Zn), are known to produce sharp ^{1}H-NMR resonances that can mask metabolite peaks of interest and so can severely inhibit recovery of information from the resulting spectra (Barton et al., 2010). Whilst it is clear that a number of metabolites give rise to peaks obscured by EDTA, these also have other resonances that allow their identification and quantification meaning relevant biochemical information can still be recovered (Barton et al., 2010).

Another potential interference with the resulting spectra are resonances derived from DSS. The methyl peak from DSS gives rise to the reference peak at δ 0 ppm. In addition, peaks arise from methylenes 1,2, and 3 at 2.91, 1.76 and 0.63 ppm, respectively (Gottlieb et al., 1997).

The presence of EDTA and DSS derived spectral peaks were apparent upon the resulting spectra and also appeared in subsequent analysis steps. However, given that metabolites within these regions present additional peaks, this was not seen as a major hindrance upon data interpretation.

Lower phase/lipid fraction

The lower chloroform/lipid fraction was examined using DIHRMS. In preparation for this, samples were randomised and QC's prepared to run alongside samples. Where possible, samples were kept on dry ice and were transferred to the -80°C freezer in periods between protocol stages. All solvents were of LC-MS or HPLC grade (Sigma Aldrich, Gillingham, UK).

Randomisation

Randomisation was required to prevent against possible 'batch effects' occurring between multiple DIHRMS runs. Sample randomisation was generated using MATLAB and was based upon subject BMI and sex as well as the altitude/location of the sample collection.

Quality Controls (QC's)

These were required across a range of dilutions to define the linear range of the instrument, ensuring lipid species detected within the very low range could be excluded. QC's were prepared by pooling 20µl of each CXE sample and diluting to a range of concentrations with the addition of chloroform as follows:

- QC 100: 1ml pooled sample
- QC 50: 500µl pooled sample, 500µl chloroform
- QC 25: 250µL pooled, 750µl chloroform

In addition, QC samples were obtained from pooled human plasma samples used as a standard QC for MS experiments in the laboratory of Prof Griffin. These were diluted using the same ratios as above, but using PBS as opposed to chloroform.

Both sets of QC's were run with each plate alongside PBS and chloroform, which thus acted as blanks. Together, QC's and blanks were utilised to correct for batch effects in the data processing stages outlined below.

Plate loading

30µl of CXE sample, QC's and blanks were loaded onto a glass coated 96 well plate, with the loading of CXE samples following the randomised order defined previously. To the 96 well plate, 150µl of internal standard (IS) mix and 750µl methyl tert-butyl ether (MTBE) were added, with MTBE ensuring full extraction of lipids. The IS mix contained the following six internal standards: 1,2-di-o-octadecyl-sn-glycero-3-phosphocoline, 1,2-di-O-phytanyl-

sn-glycero-3-phosphoethanolamine, C8-ceramide, N-heptadecanoyl-D-erythro-sphingosylphosporylcholine, undecanoic acid, and trilaurin. The internal standards were used to correct for variations in m/z across the dataset acquired.

The first chloroform 'blank' sample for each plate was retained as such through the addition of 150µl chloroform instead of IS mix. The plate was subsequently shaken for 30s. Using a VIAFLO 96/384 electronic pipette (Integra), 25µl of the resulting sample mixture was transferred to a glass coated 384 well plate and 90µl Mass spectrometry (MS) mix [7.5 mM NH_4Ac IPA:MeOH (2:1)] added. The plates were then sealed using Corning aluminium micro-plate sealing tape (Sigma Aldrich Company, UK) and kept at -80°C until required for DIHRMS analysis.

Direct infusion high resolution mass spectrometry (DIHRMS)

The method used was akin to that presented previously (Koulman et al., 2014). Samples were infused into an Exactive Orbitrap (ThermoScientific, Hemel Hampstead, UK) using a Triversa Nanomate (Advion, Ithaca, US). Each well of the 364 well foil-sealed plate was pierced using the Nanomate infusion manual prior to analysis. Following this, a fresh tip was used to take up and aspirate 5µl of sample, followed by a 1.5µl air gap. The tip was pressed against a fresh nozzle and the sample dispensed using 0.2 psi nitrogen pressure. Ionization was achieved with a voltage of 1.2 kV, resulting in the production of both positive and negative ions, with an acquisition time of 72s and a mass acquisition window from 200 to 2000 m/z. Data acquisition by the Exactive in the positive mode began 20s following aspiration. After 72s, the Nanomate and Exactive switched to negative mode with a decrease in voltage to -1.5 kV. The spray was maintained for another 66 s, after which analysis stopped. The tip was discarded prior to analysis of the subsequent sample. Throughout analysis, the plate was maintained at 15°C. Samples were run in row order.

An example spectrum produced from this analysis, with both negative and positive modes, is presented in **Figure 2.7**.

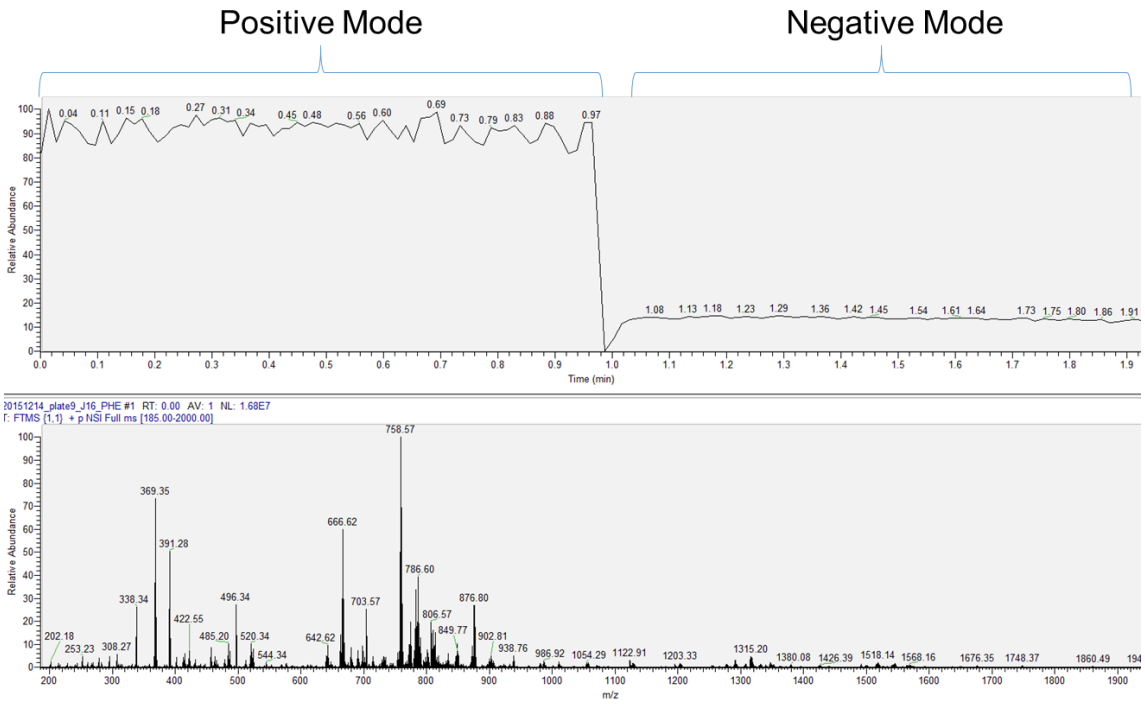

Figure 2.7. An example spectrum produced from direct infusion high resolution mass spectrometry.

This spectrum was produced from analysis of the lipid fraction of a plasma sample (subject J16, Pheriche) in negative and positive modes using direct infusion high resolution mass spectrometry.

Data processing

Initial processing of resulting MS data was performed using R studio. Raw data files were converted to .mzXML file format using MS convert (ProteoWizard). Any raw file formats below ~10,000 kb were discounted as this was indicative of a failed run, for instance due to problems with the direct spray. These samples were subsequently re-run.

The next stage was 'peak picking' of the data set, which essentially involved automatic assignment of each ion detected using an algorithm. To do this, an R script was run using the following programmes downloaded from http://www.bioconductor.org/: data.table, xcms, mzR and Rcpp. Using a script developed by Prof Griffins' laboratory, the data were processed in both positive and negative modes to produce .csv files containing m/z and m/z deviation information. During this process, only peaks with deviations within ±5 ppm of target mass and with intensity >1000 were retained and those with >10% missing spectral values removed. Also added to the R working directory, and essential for peak assignment, was a lipid library. This was based upon masses taken from the LIPID MAPS directory, from which appropriate masses were calculated for each potential lipid. Isobaric species have been identified and this library currently contains 3400 ions in positive mode and 1600 ions in negative mode. It was at this stage that QC and IS standard samples were used to correct for a batch effect.

Finally, each individual lipid peak was displayed in the .csv file as a ratio of what was detected. Lipids were identified based upon accurate mass in relation to the IS mix, thus enabling a semi-quantitave/targeted approach. From here, it was possible to proceed to statistical analysis.

2.4.4 Data modelling using Bayesian statistical methods

The overarching question in this study was as follows: which metabolites respond to changes in altitude? In light of this, we hoped to capture the consistent movement of metabolites in a specific direction with increasing altitude. Due to the nature of the study design, measurements of each metabolite were reported for each subject across 5 locations (with some exceptions in cases where sample collection was missed or spectra quality insufficient). The analytical approach aimed to capture the overall metabolite trend across these 5 locations occurring across all subjects, as opposed to individual changes at specific locations.

Metabolite trends across time points can be captured in the most basic sense utilising a linear model, whereby it becomes possible to assess whether the regression line for all subjects is above 0, thus, metabolites undergoing obvious changes can be visualised. Regression lines can be fitted for each subject and an average calculated. This thus presents two levels of hierarchy:

1. Slope derived from linear regression
2. Distribution of the data set, derived from the mean and SD values.

In this simple hierarchical model, no communication exists between these two entities, so the individually fitted regression lines are fixed and the average is calculated separately. By use of Bayesian hierarchical modelling, it becomes possible for both the individual and average regression lines to be influenced by one another. In doing so, this method of analysis captures the fact that both individual and average linear regressions should be changing together. This is thus the method adopted in the present study.

The first level of this model is the individually fitted regression, which were then used to inform the second level, being analysis of the average slope. This approach models at the level of the individual subject and this is then built on for an overall analysis of the group as a whole. Thus, both the individual and group regression can be assessed simultaneously and the individual regression lines are constrained by the average regression lines. This is in contrast to classical methods such as analysis of variance (ANOVA), whereby changes at each time-point are assessed through multiple comparisons of the entire dataset and the relationship between metabolite changes occurring within the same subject is ignored. Essentially, these classical approaches do not capture the 2 layers of analysis that it is possible to combine in the Bayesian model, being: the individual response and the group response.

The Bayesian approach enabled a highly sophisticated, fluid model to be built. Communication existed between the two layers of analysis, being the individual and group responses, enabling the full structure of the data to be captured. The first step in applying this model was to identify which spectral peaks and corresponding metabolites are undergoing changes distinct enough to warrant further investigation. Exclusion criteria for this were derived from an r^2 plot for all regression lines. R^2 was used because all values dealt with are positive (squaring of a negative number = positive). All signals from r^2 that were of a greater frequency than 0.1 (i.e. not residing around 0), so those appearing at the tail end of the adjusted R^2 vs. Frequency plot, represent spectral regions (from ^{1}H-NMR) or

identified metabolites (from DIHRMS) undergoing a large change. These were then taken forward for Bayesian hierarchical modelling.

Of crucial importance when interpreting the output of this modelling approach is the slope of the resulting credible regression lines. The slope is essentially the relationship of how one metabolites is transmitted across time points. This is representative of the effect size, therefore depicts metabolite changes per km change in altitude. It has numerous advantages over more traditional methods of significance testing as it places emphasis upon the size of the difference rather than confounding this measure with sample size as significance does (Broadhurst et al., 2006). This thus avoids a scenario where a large sample size, as is the case in this study, presents hugely significant changes in a small, and likely uninteresting, difference.

Identified metabolites are presented with corresponding identification codes from either the human metabolome database (HMDB), or in the case of certain lipids where HMDB identification was not available, chemical entities of biological interest (CHEBI) are included.

2.4.5 Calculation of absolute changes

From the Bayesian modelling output, the direction of metabolite change with progressive altitude exposure can be clearly observed. However, it is difficult to gauge from this output the degree of change and to compare this between observations. This was approached through the following assessments.

For the aqueous phase metabolites, the binned ^{1}H-NMR spectral regions corresponding to an identified metabolite that underwent the largest slope change from the Bayesian model output were assessed. The change in spectral intensity between LDN and EBC was calculated and from this the median % change derived. Given that this was a measure of spectral intensity, no absolute value such as concentration/ml plasma could be given for the change, instead arbitrary units were employed. The LDN and EBC values were also corrected to the LDN value, to give a normalised ratio of change. The same approaches were employed for assessment of the degree of change in lipid abundance, although this only included those definitively identified lipids.

The median value was chosen as in most instances, data within a variable (so comparison between individuals within a spectral region or lipid) did not follow a Gaussian

distribution, as assessed using the D'Agostino-Pearson (omnibus K2) normality test, therefore would likely skew the mean.

This absolute measure of change with ascent is presented alongside the relative measure, derived from the median of the slope (AU/km). In addition, this absolute change was normalised to the LDN value and plotted as LDN: EBC ratio to enable visualization of the changes.

2.4.6 Physiological variables

Physiological measurements were conducted shortly after waking, prior to any oral intake in the morning of the same day that blood samples were obtained. This includes arterial O_2 saturation and body weight.

Arterial O_2 saturation (SpO_2)

An estimation of arterial O_2 saturation (SpO_2) was measured from the right index finger using a pulse oximeter (Onyx 9500, Nonin, USA) following 10 minutes of rest. Measurements were taken by independent individuals, meaning the subject was blind to the oximeter to prevent feedback alterations to respiratory rate, thus SpO_2.

Statistical analysis

The LDN and EBC values for SpO_2 and body weight data were abnormally distributed, as assessed using the D'Agostino-Pearson (omnibus K2) normality test. Therefore, a Wilcoxon matched-pairs signed rank test was employed for analysis. This was performed and graphs constructed in Graphpad Prism 7. By focusing upon the differences between LDN and EBC, it provided insight into the extreme nature of the EBC environment in comparison to LDN.

Correlation/Linear regression Analysis

To assess whether a relationship exists between changes to metabolic/lipid profile and those of physiological variables (SpO_2, body weight), correlation analysis was performed. The Δ abundance of metabolites/lipids from LDN to EBC that were identified as undergoing large changes with ascent were plotted against the Δ SpO_2 or body weight from LDN to EBC. For the aqueous fraction metabolites, this specifically refers to the Δ of spectral region intensity undergoing the greatest change, and for lipids, the definitively identified lipid variables (as outlined in section 2.4.5). Data that followed a Gaussian distribution, as assessed using a D'Agostino-Pearson (omnibus K2) normality test, were tested using a

Pearson Correlation Coefficient to distinguish whether a relationship existed between these parameters. For data that did not follow a Gaussian distribution, a non-parametric Spearman rank correlation (two tailed) was applied to distinguish whether a relationship existed between these parameters. If a significant relationship was identified, linear regression analysis was subsequently performed to find the best line that predicts Y from X.

2.5 Results

2.5.1 Subject details

198 subjects (125 male, 73 female, 44 $\pm$ 14 years of age, BMI 25.07 $\pm$ 3.16 kg/m^2) participated in the expedition to EBC. Details on the subject recruitment process have been outlined previously by Levett and colleagues (Levett et al., 2010). All subjects arrived at KTM, 197 at NAM, 195 at PHE and 190 (96%) at EBC. Those not reaching the specific altitudes suffered either acute mountain sickness or non-altitude related medical conditions (Levett et al., 2010).

SpO_2 and body weight changes with ascent

The degree of hypoxic exposure experienced at this extreme altitude was reflected through progressive decreases in arterial O_2 saturations (SpO_2) with ascent (**Figure 2.8A**). A 20.4 % decrease (median, n=187, p<0.0001) from 98% observed at LDN to 73% at EBC (**Figure 2.8C**).

Body weight similarly underwent a progressive decrease (**Figure 2.8B**), with differences from LDN to EBC presenting an average (median) weight loss of 3.7% (3 kg) (median, p<0.0001, n=157) (**Figure 2.8D**).

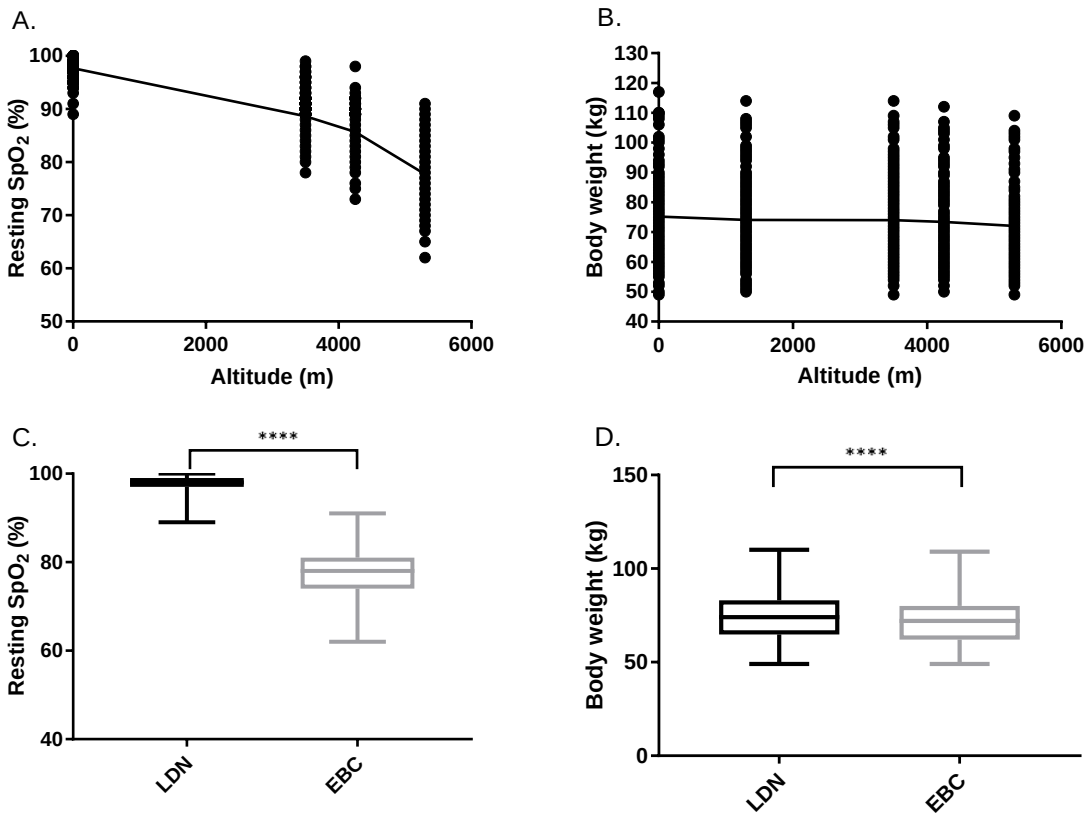

Figure 2.8. Changes in physiological variables with ascent to EBC.

*This includes recording of resting arterial O_2 saturation (SpO_2) **(A)** and body weight (kg) **(B)** across all altitudes. Differences in SpO_2 **(C)** and body weight **(D)** between LDN and EBC, presented as minimum to maximum box and whisker plots, with the middle line representing the median and the box the interquartile range (25^{th} to 75^{th} percentiles), tested using a Wilcoxon matched-pairs signed rank test, **** p<0.0001, n=146-188.*

2.5.2 Plasma metabolomics/lipidomic analysis

As a result of subjects failing to arrive at the laboratory or insufficient amounts of plasma being obtained for subsequent analysis, samples were not analysed for all 198 subjects at every altitude location. A total of 965 samples were obtained for metabolomics/lipidomics analysis, with exact numbers at each altitude specified in **Table 2.2**. The goal of this analysis was to examine which metabolites responded to changes in altitude and to detect an overall trend across the 5 altitude locations.

Table 2.2. Total plasma sample number analysed using metabolomics and lipidomics from each laboratory location.

Laboratory location	Sample number obtained on expedition	Sample number for NMR and MS
LDN	197	197
KTM	198	198
NAM	195	195
PHE	193	193
EBC	192	182

Plasma aqueous fraction analysis

The focus for Bayesian analysis was upon the big changes with altitude ascent. These were identified as the binned regions of the ^{1}H-NMR spectrum undergoing the largest degree of change and so residing at the tail ends of the distribution curve, situated ± 1.96SD away from the mean. A total of 50 bins were found to fit this criteria.

The spectral regions identified as undergoing the largest degree of change were correlated through a heatmap displayed in **Figure 2.9.** From this, it is clear to see that the spectral regions undergoing the largest changes display the strongest correlation with regions corresponding to the same metabolite, thus confirming that metabolite identification of 'big changers' was accurate. Here, the presence of peaks related to EDTA and DSS become clearly apparent. The changes in these particular spectral regions are likely indicative of alterations to plasma concentration with increasing altitude.

To derive changes with altitude, these binned spectral regions were taken forward for hierarchical Bayesian analysis. The results from the Bayesian model represent

alterations in the abundance of circulating levels of the metabolites relating to these specific spectral regions. These changes are visible through the slope, or simple regression, which depicts the effect size, therefore how much that particular metabolite changes per unit change with altitude. If the slope is positive, this indicates an increase in the respective metabolite, if negative, it is indicative of a decrease. The slope is expressed as arbitrary units per km change in altitude.

Aqueous metabolite changes

Changes in aqueous metabolites are summarised in **Table 2.3** and include alterations in the substrate and product of glycolysis as glucose (D-Glucose HMDB00122) decreased and lactate (L-lactic acid, HMDB00190) increased with ascent to EBC. A progressive decrease was observed in the isomer of the essential branched chain amino acid leucine, isoleucine (L-isoleucine HMDB00172). The spectral peaks corresponding to these metabolites that underwent the largest degree of change were identified as 1.31ppm for lactate (27.4% increase), 3.35ppm for glucose (52.4% decrease) and 0.92 ppm for isoleucine (60.5% decrease). An example of the Bayesian hierarchical model output is displayed in **Figure 2.10** below, whereby the responses of the individual are presented alongside the overall group response. Both relative and absolute changes for each of these peaks is presented in **Table 2.3.** The differences in peak intensity from LDN to EBC, corrected to the LDN value, are presented in **Figure 2.11**

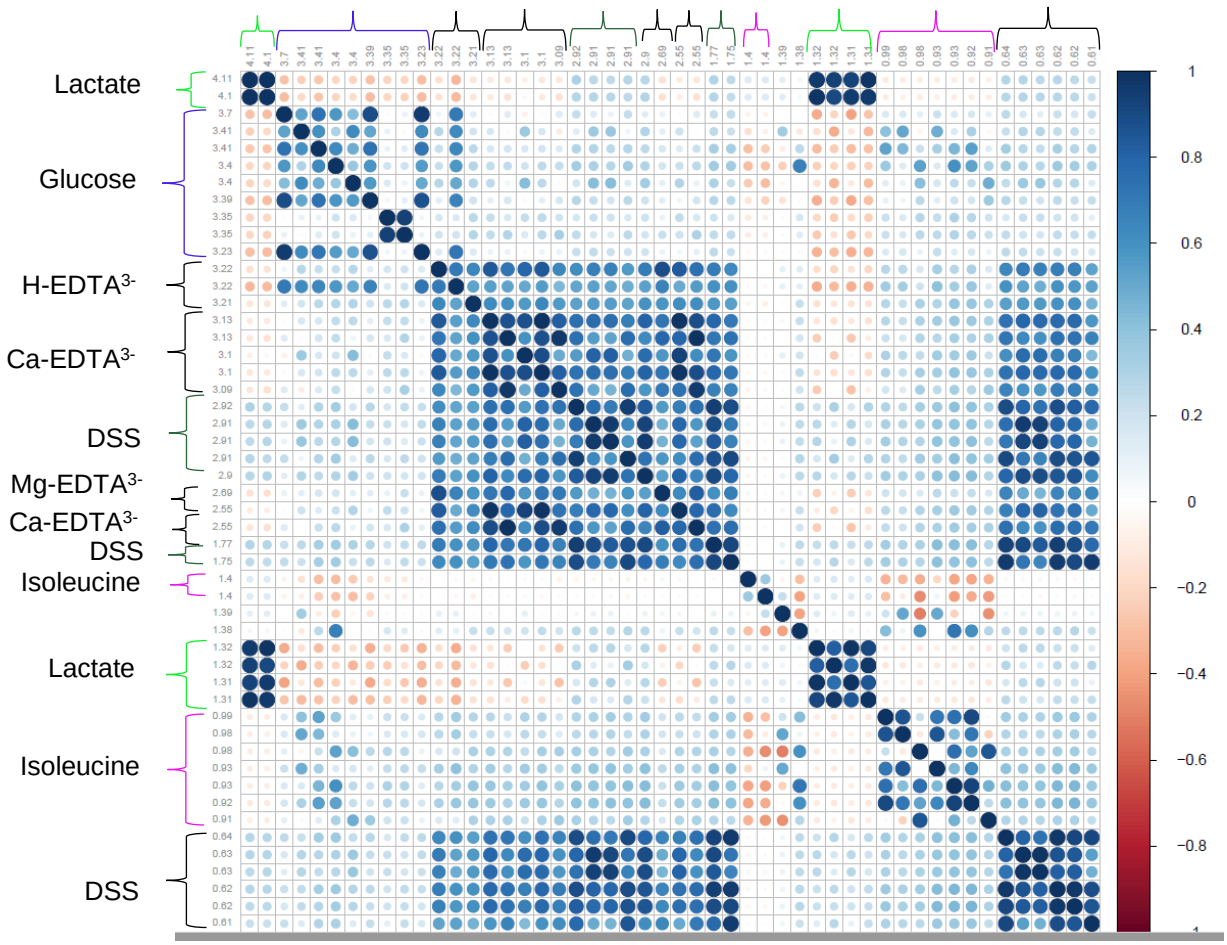

Figure 2.9. Heatmap correlation plot of spectral regions identified as undergoing large changes with increasing altitude.

Spectral regions are identified as parts per million (ppm) and metabolites corresponding to these regions are labelled. Those regions belonging to the same metabolite are shown to be strongly positively correlated, as represented by the dark blue, large dots. Orange regions represent negatively correlated regions, likely presenting a degree of noise in the data set.

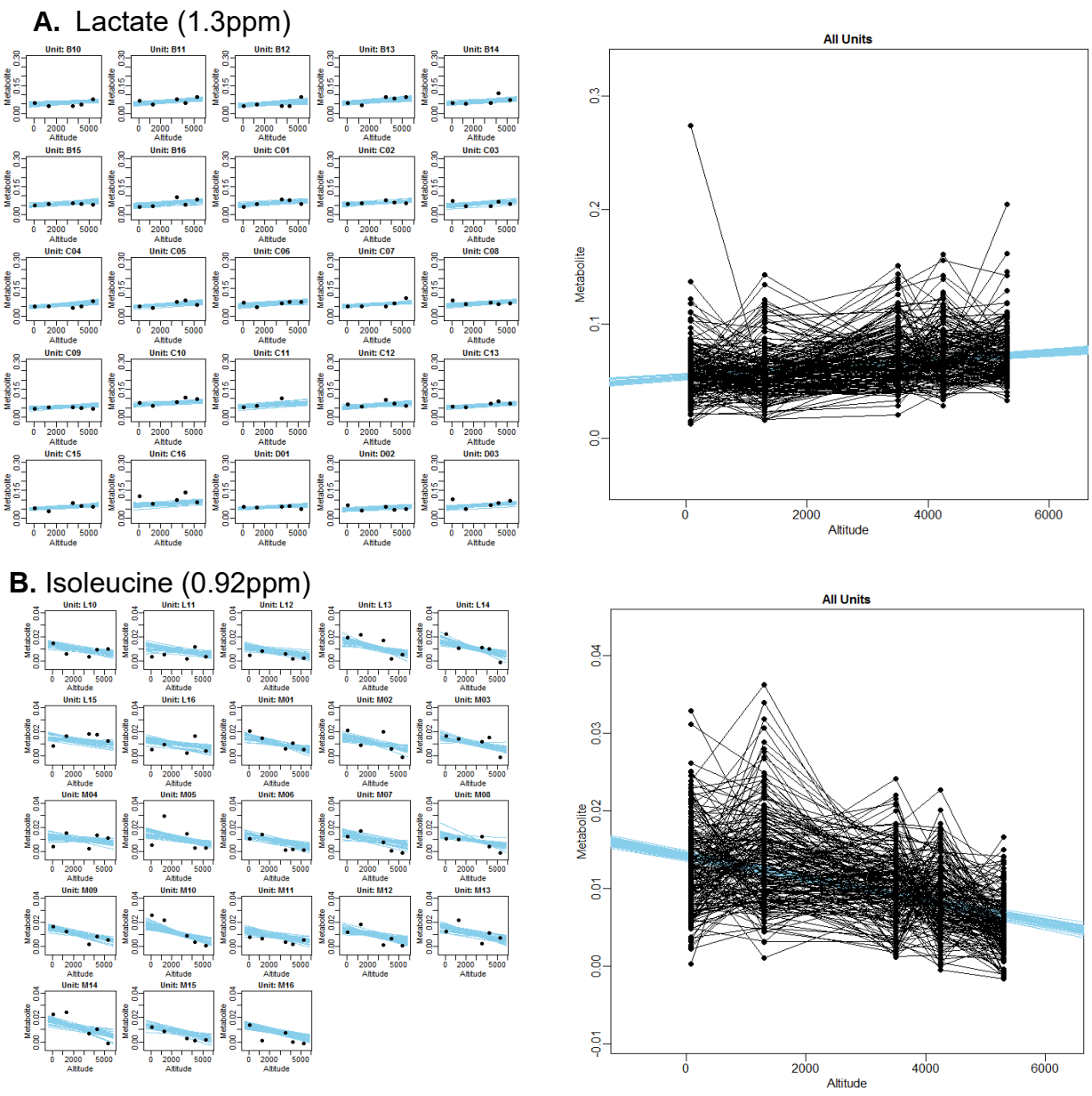

Figure 2.10. Spectral regions and related metabolites presenting a significant trend with increasing altitude, identified using Bayesian hierarchical modelling.

A *Lactate.* ***B.*** *Isoleucine. On the left hand side of each graph set is presented a select example of individual responses of the group (expressed as a 'Unit') at each altitude. The multiple blue lines are credible regression lines, representing the top (or most likely) underlying distribution. The most likely distribution from the individual response was then taken to inform the distribution of the group. The individual response is therefore constrained by the average response of the group, which is presented on the right hand side as 'All Units'. Here, the changes in each individual across each altitude are presented. Y axes metabolite units are arbitrary units, derived from the spectral intensity changing per km altitude.*

Table 2.3. Aqueous metabolites identified as undergoing large changes with increasing altitude.

.

Metabolite	Binned spectral region (ppm)	LDN intensity (AU)	EBC intensity (AU)	Δ% LDN to EBC	Slope (AU/km)	Increasing or decreasing with altitude
Isoleucine	0.92	0.012	0.0049	-60.5	-0.00142	Decreasing
Glucose	3.35	0.016	0.0081	-52.4	-0.0014	Decreasing
Lactate	1.31	0.057	0.0719	27.4	0.00361	Increasing

Note: *Displayed is the metabolite peak (ppm) undergoing the largest degree of change, with intensities at LDN and EBC, the median % change between these two locations and the slope.*

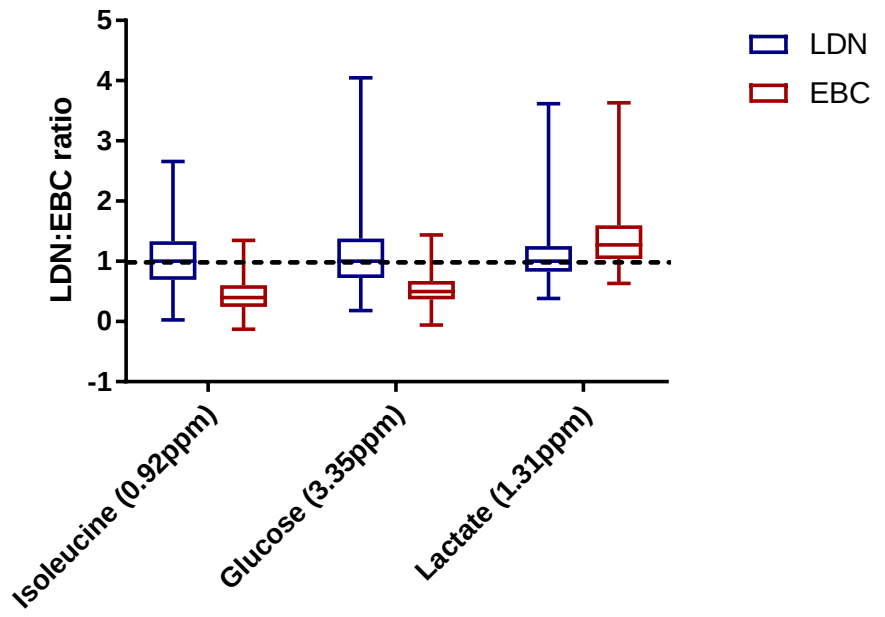

Figure 2.11. Alterations in aqueous metabolite intensities from LDN to EBC

^{1}H-NMR spectral regions (and corresponding metabolites) undergoing the largest degree of change with ascent to EBC, identified using Hierarchical Bayesian statistics. Values are corrected to LDN, and so are expressed as a ratio of LDN: EBC, with a value of 1 indicative of no change. Presented as minimum to maximum box and whisker plots, with the middle line representing the median and the box the interquartile range (25th to 75th percentiles).

Plasma lipid fraction analysis

Negative ion mode revealed 1012 observations from 322 variables (including QC's and blanks) and positive mode 1012 observations of 238 variables. To identify variables, being lipids, to be taken forward for subsequent data analysis, a median of observations derived from each subject in positive and negative modes were calculated. From the negative mode, 6 metabolites were identified with mean slopes greater than 1.96 SD away from the mean, and 11 metabolites from positive mode. These were taken forward for Bayesian modelling.

Two examples of the lipidomic Bayesian modelling output are presented in **Figure 2.12.** All lipid species identified as undergoing large increases with ascent are outlined in **Table 2.4** and those undergoing large decreases outline in **Table 2.5**. The largest lipid increase was identified as triglyceride (TG) 52:3, with a median increase from LDN to EBC of 53.9%. The largest decrease in a definitively identified lipid was that of TG 48:1, with a median decrease of 43.1%. Alterations in abundance of identified lipids is expressed as LDN: EBC ratio and presented in **Figure 2.13**.

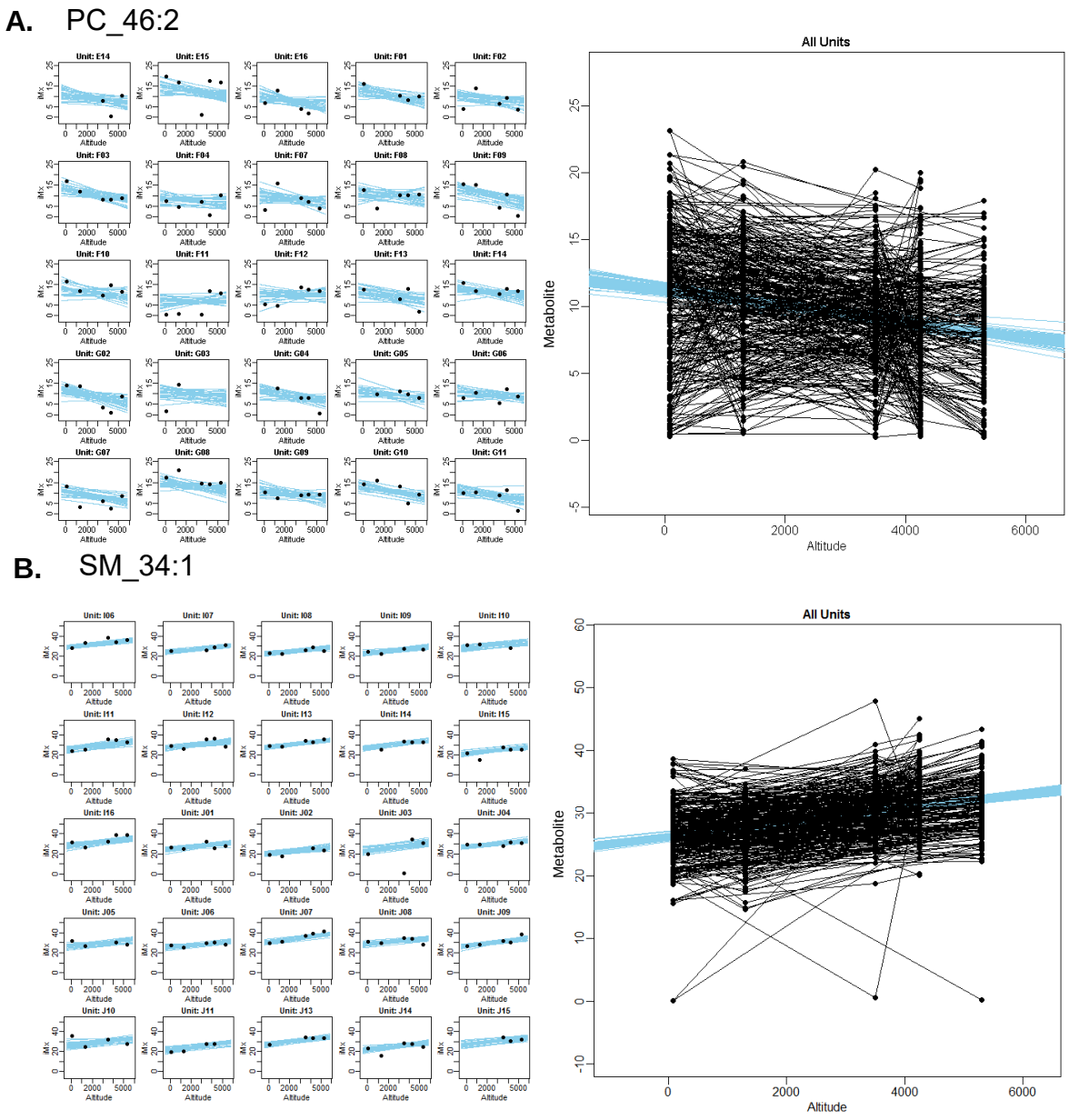

Figure 2.12. Example of hierarchical Bayesian analysis of plasma lipids undergoing significant changes with progressive altitude exposure, identified through DIHRMS.

A. *Phosphocholine (PC) 46 carbons: 2 double bonds (46:2), identified in negative ion mode.* ***B.*** *Sphingomyelin (SM) 34:1, identified in positive mode. An example of individual responses of the group (expressed as a 'Unit') at each altitude. This individual response is constrained by the average response of the group, which is presented on the right hand side as 'All Units'. Here, the changes in each individual across each altitude are presented. Y axes metabolite units are arbitrary units, derived from the spectral intensity changing per km altitude.*

Table 2.4. Lipids identified as undergoing increases with progressive altitude exposure

Lipid	Carbon chain length: double bond	Mode of ion detection	LDN abundance (AU)	EBC abundance (AU)	Δ% LDN to EBC	Δ Slope (AU/km)
Triglyceride	**52:3**	**Positive**	**30.1**	**45.0**	**53.9**	**1.59**
Triglyceride	**52:4**	**Positive**	**10.72**	**16.50**	**53.7**	**0.529**
Phosphatidylserine/ Phosphatidylglycerol	36:2 36:4	Positive	8.40	13.13	47.2	0.731
Oleic acid	**18:1**	**Negative**	**36.0**	**54.6**	**27.1**	**2.349**
Lyso-phosphatidylcholine/ Lyso-phosphoethanolamine	16:0 19:0	Positive	20.1	24.73	25.6	0.602
Linoleic acid	**18:2**	**Negative**	**17.83**	**23.39**	**23.7**	**0.828**
Sphingomyelin	**34:1**	**Positive**	**26.8**	**30.8**	**15.7**	**0.001**
Palmitic acid	**16:0**	**Negative**	**110.4**	**116.7**	**12.4**	**2.176**
Phosphatidylcholine/ Phosphoethanolamine/ Phosphatidic acid	34:1 37:1 39:2	Positive	52.24	53.70	11.4	0.725
Phosphatidylcholine/ Phosphoethanolamine/ Phosphatidic acid	34:2 37:2 39:3	Positive	104.0	110.0	4.1	1.584

***Note**: Displayed are the variables undergoing the largest degree of change, with intensities at LDN and EBC, the median % change between these two locations and the slope. Variables are listed in descending order of median % change from LDN to EBC. Text in non-bold indicates multiple possible lipid identifications at this m/z.*

Table 2.5. Lipids identified as undergoing decreases with progressive altitude exposure.

Lipid	Carbon chain length: double bond	Mode of ion detection	LDN abundance (AU)	EBC abundance (AU)	Δ% LDN to EBC	Δ Slope (AU/km)
Triglyceride	**48:1**	**Positive**	**4.25**	**2.42**	**-43.1**	**-0.334**
Phosphatidylcholine/ Phosphatidylserine	36:3 40:2	Negative	10.9	6.8	-31.2	-0.702
Phosphatidylcholine	**46:2**	**Negative**	**11.8**	**8.7**	**-25.0**	**-0.597**
Phosphatidylcholine/ Phosphatidylserine	36:2 40:1	Negative	24.9	17.9	-21.9	-1.05
Phosphatidylcholine/ Phosphoethanolamine/ Phosphatidic acid	36:3 39:3 41:4	Positive	24.73	19.24	-20.48	-1.155
Phosphatidylcholine/ Phosphoethanolamine/ Phosphatidic acid	36:2 39:2 41:3	Positive	52.25	46.55	-8.95	-1.187
Triglyceride	**50:1**	**Positive**	**10.95**	**9.69**	**-8.43**	**-0.524**

***Note**: Displayed are the variables undergoing the largest degree of change, with intensities at LDN and EBC, the median % change between these two locations and the slope. Variables are listed in descending order of median % change from LDN to EBC. Text in non-bold indicates multiple possible lipid identifications at this m/z.*

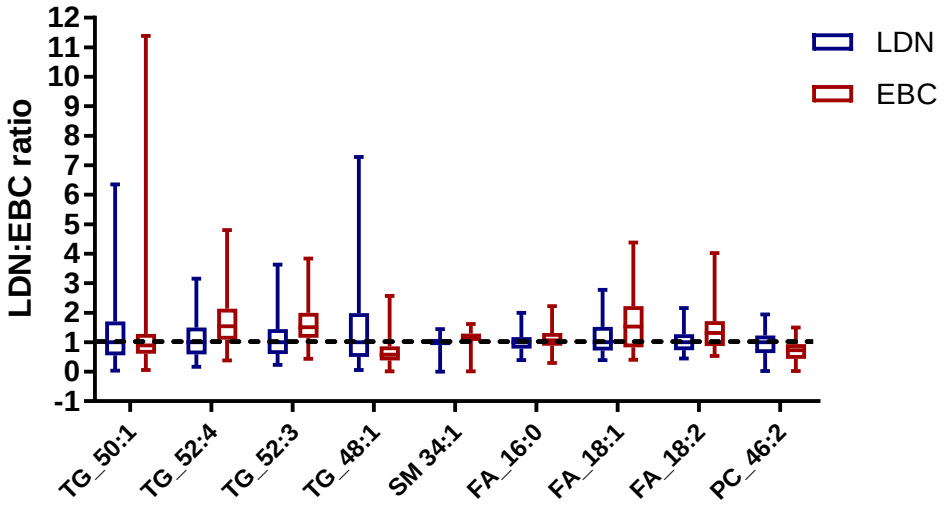

Figure 2.13. Alterations in lipid abundance from LDN to EBC.

Lipids (assessed using DIHRMS) undergoing the largest degree of change with ascent to EBC, identified using Hierarchical Bayesian statistics. Values are corrected to LDN, and so are expressed as a ratio of LDN: EBC, with a value of 1 indicative of no change. Presented as minimum to maximum box and whisker plots, with the middle line representing the median and the box the interquartile range (25th to 75th percentiles).

Triglyceride (TG) and free fatty acid changes

The abundance of triglycerides (TGs) with carbon chain: double bond ratios of 52:3 (CHEBI: 84661) and 52:4 (CHEBI: 84660) increased with ascent to EBC. Decreases with ascent were observed in TGs containing palmitate and oleate (50:1 (CHEBI: 84665), and 48:1 (CHEBI: 85726)). This occurred alongside increases in the most abundant fatty acids within adipose tissue, being the saturated palmitic acid (16:0) (HMDB00220) as well as unsaturated linoleic (18:2) (HMDB00673) and oleic (18:1) (HMDB00207) acids.

Phosphatidylcholine (PC)

Phosphatidylcholines (PC) 46:2 (CHEBI: 72430) decreased with ascent. In addition to their role as a key component of plasma membranes, PC's are the primary phospholipid required for lipoprotein synthesis (Eisenberg, 1984).

Sphingomyelin (SM)

Increases were observed in an essential cell membrane component, particularly within the membranous myelin sheath surrounding nerve cell axons, sphingomyelin (SM) 34:2 (CHEBI:64587).

Multiple lipid identifications

A number of variables identified as undergoing large degrees of change possessed an *m/z* value that corresponded to multiple possible lipids. These are presented in non-bold text in both **Table 2.4** and **Table 2.5.**

Amongst these changes are alterations to numerous PC's alongside phosphoethanolamines (PE's) and phosphatidic acids (PA's); increases in lyso-phosphatidylcholine (LPC) 18:0 (HMDB10382) alongside lyso-phosphoethanolamine (LPE) 19:0; and lastly increases in phosphatidylserine (PS) 36:2 (CHEBI:72066) alongside phosphatidylglycerol (PG) 36:4. Alterations in abundance of these lipids is of importance, given the degree of relative and absolute changes. Further investigation to establish a definitive identification is therefore warranted.

2.5.3 Correlation analysis

To assess whether a relationship existed between altitude dependent changes in metabolites/lipids from LDN to EBC and the specific physiological variables presented here, correlation plots were constructed.

Plots of changes in aqueous metabolites against body weight **Figure 2.14** revealed a significant correlation between changes in glucose and body weight (p=0.007), with decreases in body weight being associated with decreases in plasma glucose (**Figure 2.14B**). Linear regression analysis demonstrated a low p value (<0.05) coupled to a low r^2, thus indicating that although a significant degree of variance can be explained by the relationship between these variables, much remains unexplained. No significance was observed for either lactate or isoleucine. Equally, no significant correlations were observed between the changes in these aqueous metabolites and SpO_2 (**Figure 2.15**)**.**

Plots of the change in fatty acid vs. body weight from LDN to EBC revealed a significant correlation between the unsaturated oleic (18:1) (p=0.0127) and linoleic (18:2) (p=0.0062) FA's and body weight from LDN to EBC, with loss of body weight at altitude being associated with increasing levels of unsaturated FA's oleic and linoleic acids (**Figure 2.16B,C**). Linear regression analysis again demonstrated a low p value (<0.05) coupled to a low r^2. No correlation was found between these unsaturated FA's and SpO_2 (**Figure 2.17**) Equally, no correlation existed between changes in unsaturated FA's (**Figure 2.16, Figure 2.16**), TG's (**Figure 2.18**, **Figure 2.19**), PC or SM (**Figure 2.20)** and either body weight or SpO_2.

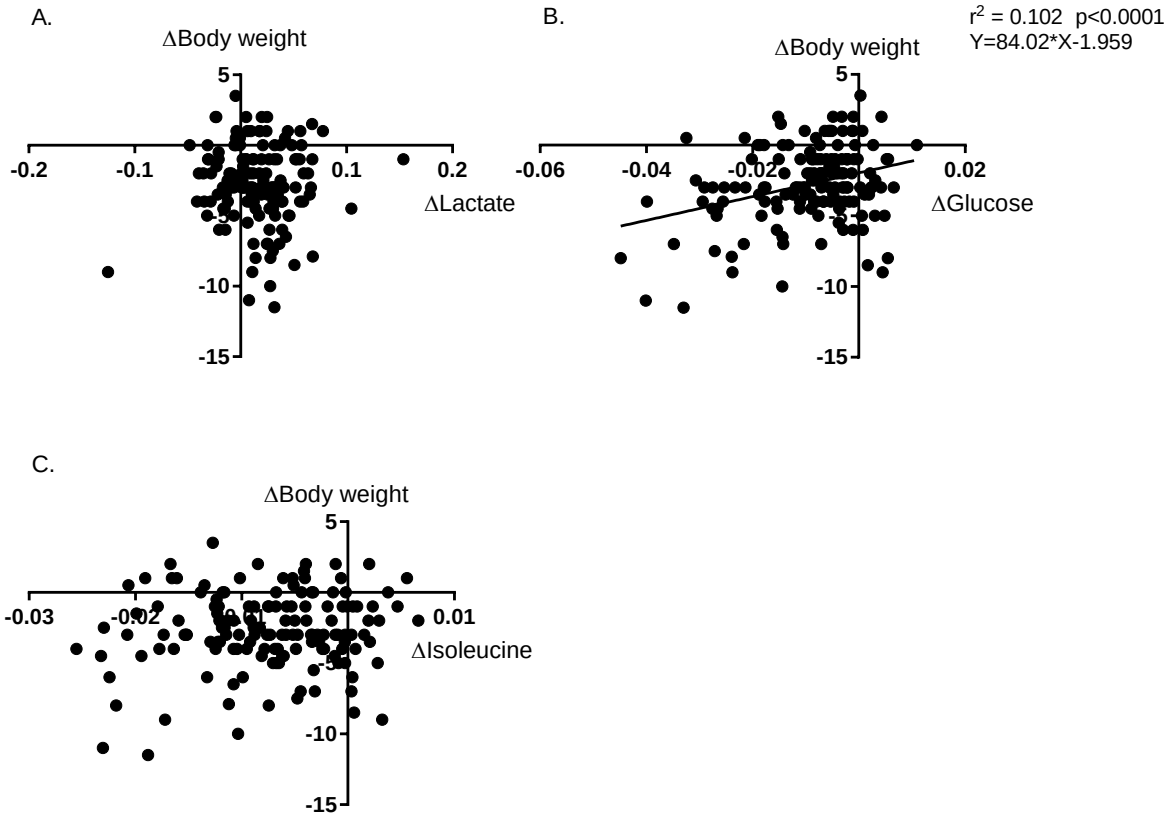

Figure 2.14.Correlation of Δ aqueous metabolites vs. Δ body weight.

A, *Lactate,* ***B,*** *Glucose****, C,*** *Isoleucine. These metabolites are those identified as undergoing large changes with progressive altitude exposure. Δ calculated as EBC-LDN. Correlation analysis performed using Pearson rank correlation coefficient as data was non-normally distributed. Significant (p<0.01) correlations were analysed further using linear regression.*

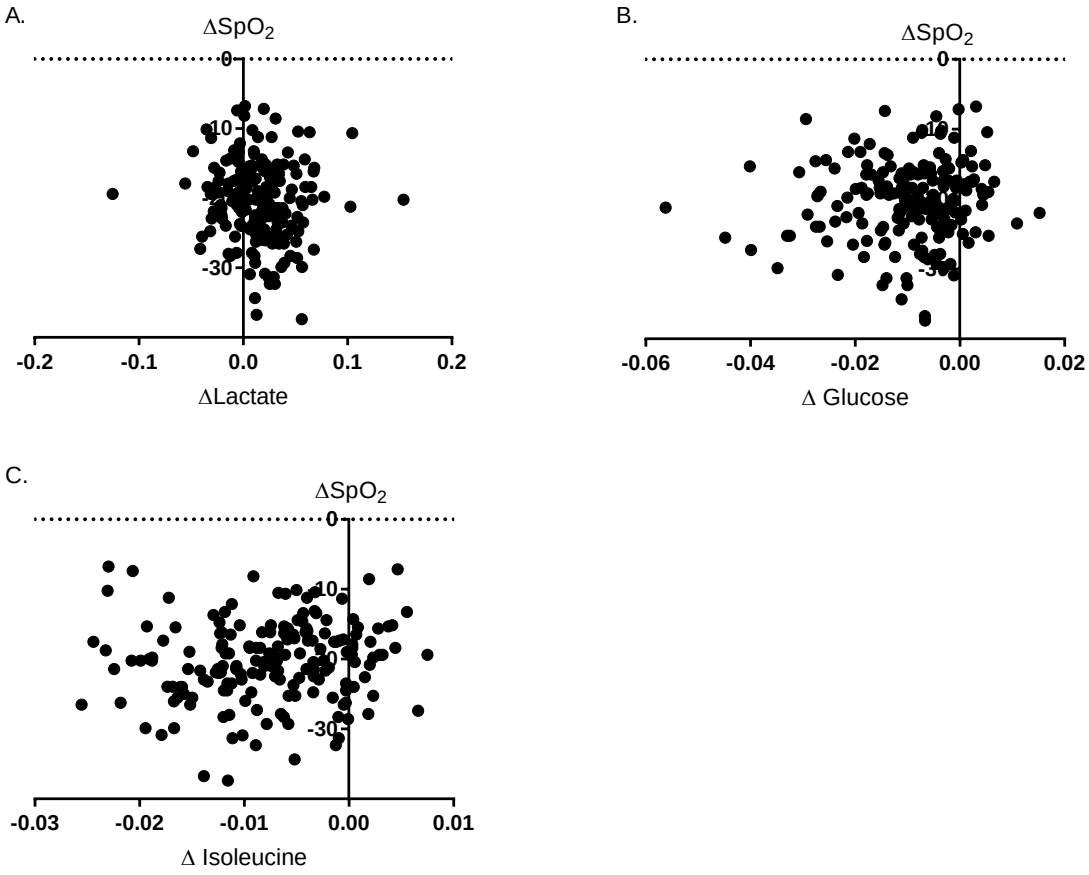

Figure 2.15. Correlation of Δ aqueous metabolites vs. Δ body weight.

A, *Lactate,* ***B,*** *Glucose****, C,*** *Isoleucine. These metabolites are those identified as undergoing large changes with progressive altitude exposure. Δ calculated as EBC-LDN. Correlation analysis performed using Pearson rank correlation coefficient as data was non-normally distributed. Significant (p<0.01) correlations were analysed further using linear regression.*

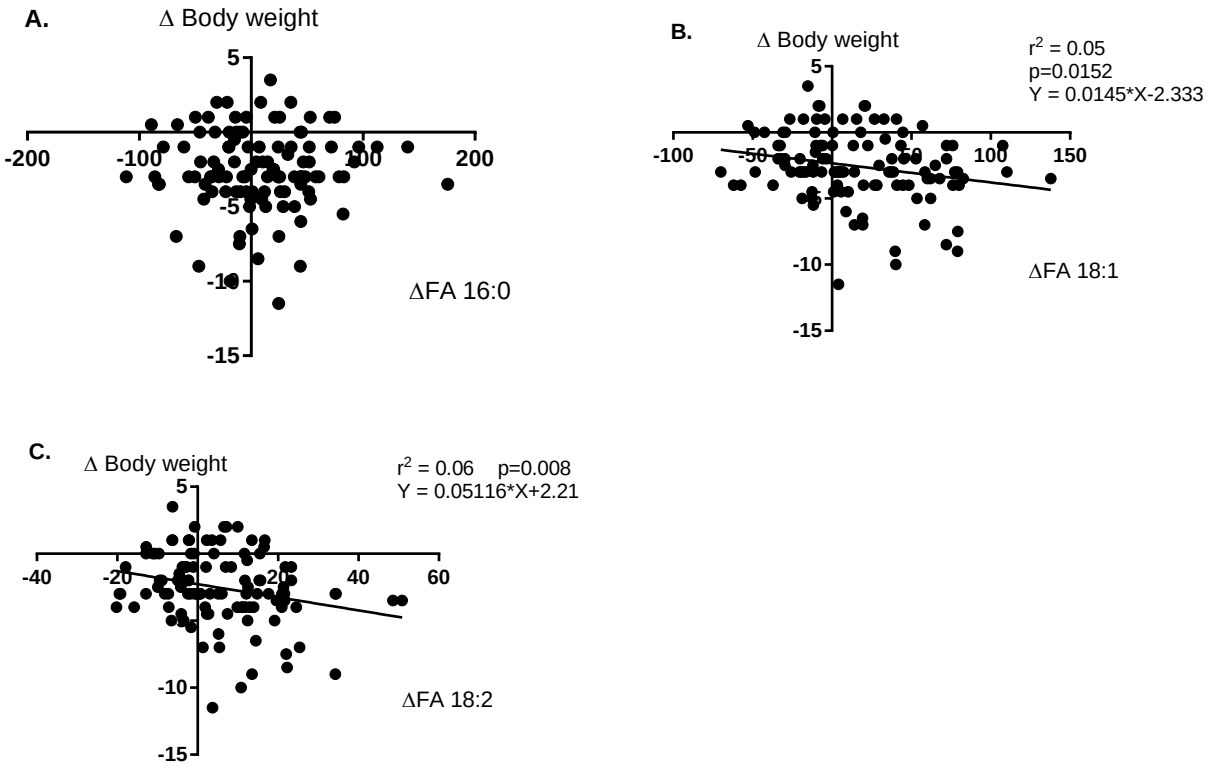

Figure 2.16. Correlation of Δ fatty acids (FA) vs. Δ body weight.

A, B: *Saturated FA's* ***C, D:*** *Unsaturated FA, shown as carbon: double bond ratio. These FA's are those identified as undergoing large changes with progressive altitude exposure. Δ calculated as EBC-LDN. Correlation analysis performed using Pearson rank correlation coefficient. Significant (p<0.01) correlations analysed further using linear regression.*

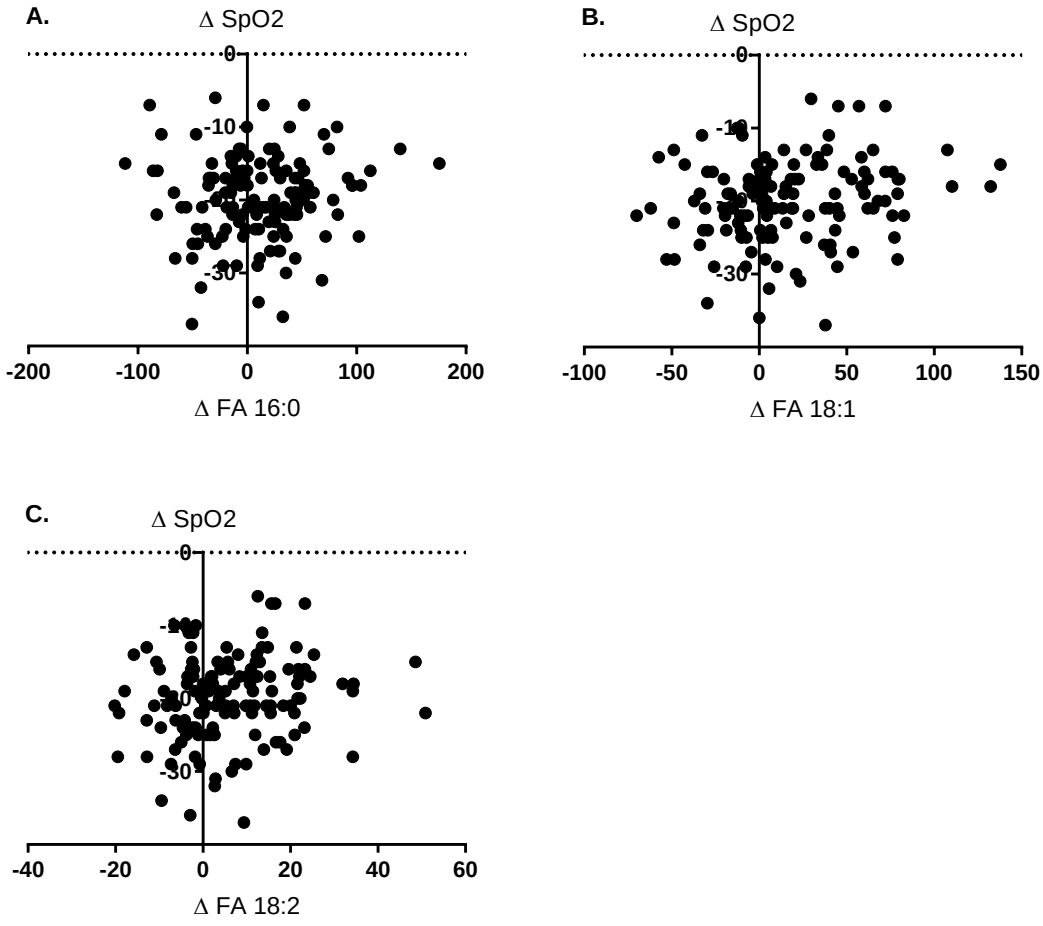

Figure 2.17. Correlation of Δ fatty acids (FA) vs. Δ SpO_2

A, B: *Saturated FA's* ***C, D:*** *Unsaturated FA, shown as carbon: double bond ratio. These FA's are those identified as undergoing large changes with progressive altitude exposure. Δ calculated as EBC-LDN. Correlation analysis performed using Spearman's rank correlation coefficient for normally distributed data or Pearson rank correlation coefficient on non-normally distributed data.*

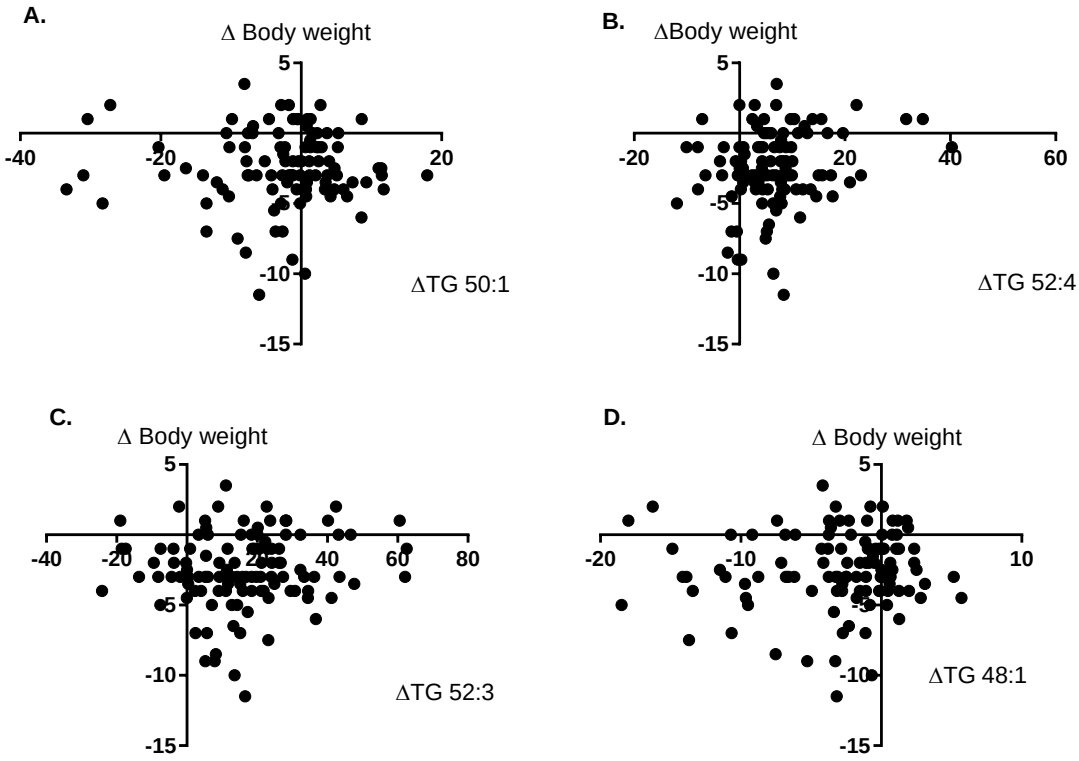

Figure 2.18. Correlation of Δ triglycerides (TG) vs. Δ body weight.

The TG's selected for this analysis were those identified as undergoing large changes with progressive altitude exposure, shown as carbon chain: double bond ratio. Δ calculated as EBC-LDN. Correlation analysis performed using Spearman's rank correlation coefficient for normally distributed data or Pearson Correlation coefficient on non-normally distributed data.

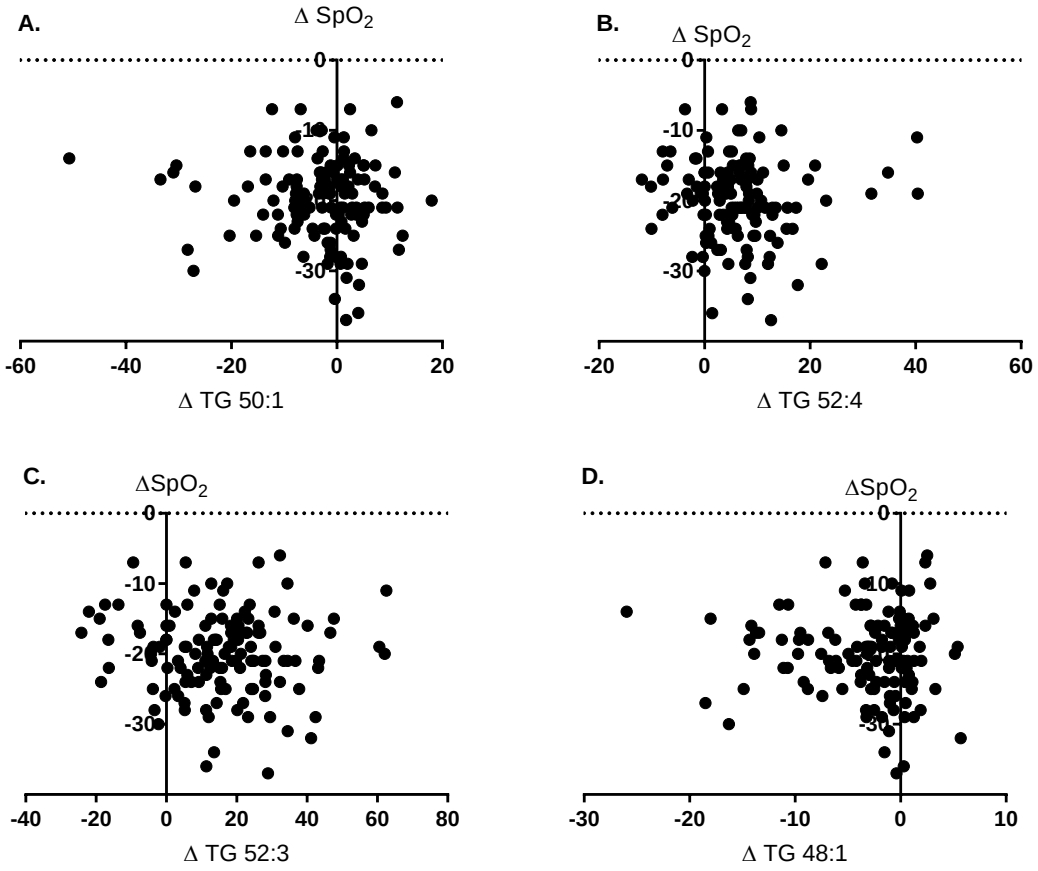

Figure 2.19. Correlation of Δ triglycerides (TG) vs. Δ SpO_2.

The TG's selected for this analysis were those identified as undergoing large changes with progressive altitude exposure, shown as carbon chain: double bond ratio. Δ calculated as EBC-LDN. Correlation analysis performed using Spearman's rank correlation coefficient for normally distributed data or Pearson Correlation coefficient on non-normally distributed data.

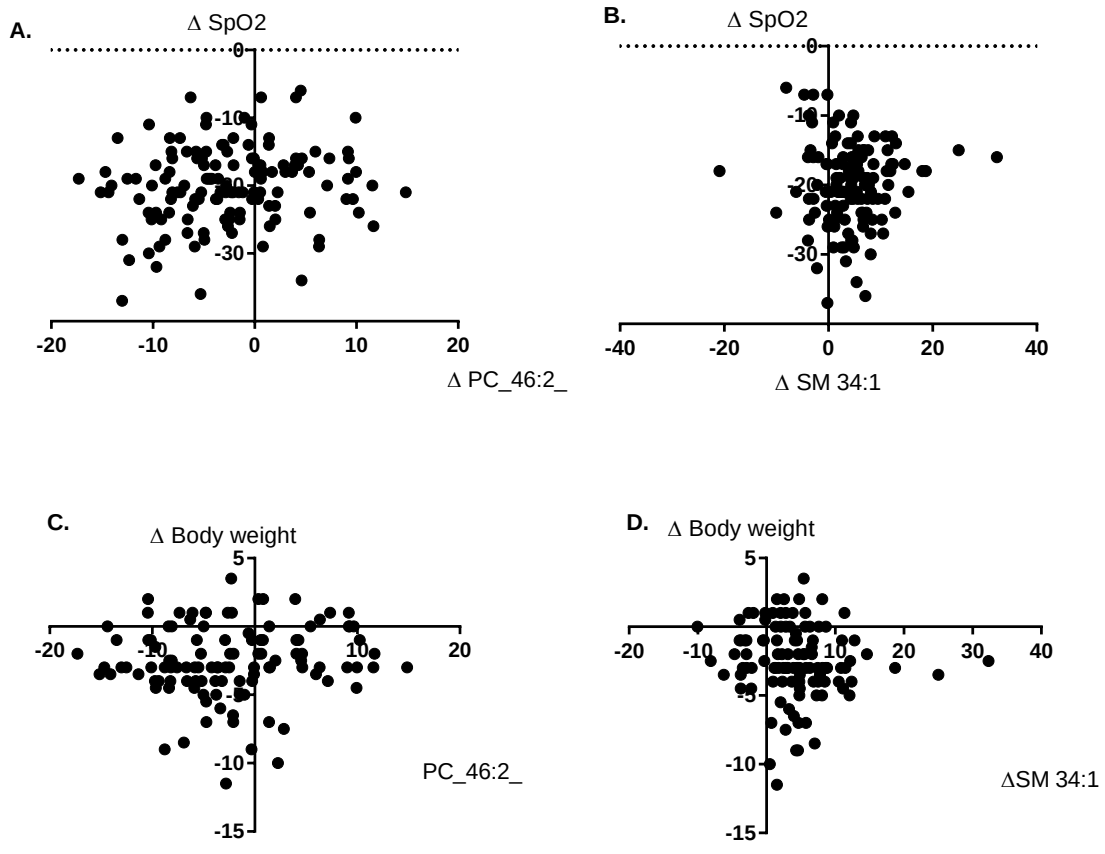

Figure 2.20. Correlation of Δ lipid vs. ΔSpO_2 or body weight.

A, B: *Phosphatidic choline (PC),* ***C, D:*** *Phosphatidylserine (PS). These lipids were identified as undergoing large changes with progressive altitude exposure, shown as carbon chain: double bond ratio. Δ calculated as EBC-LDN. Correlation analysis performed using Spearman's rank correlation coefficient for normally distributed data or Pearson rank correlation coefficient on non-normally distributed data. Significant ($p<0.01$) correlations analysed further using linear regression.*

2.6 Discussion

Hypoxia, either in response to environmental exposure or pathological states, induces metabolic stress and remodelling processes, the details of which are not well defined. In the first study of this thesis, metabolic adaptation to progressive hypoxia was examined using metabolomic and lipidomic analysis of the aqueous and lipid fractions of plasma, respectively, collected from 198 human subjects upon a strictly controlled ascent to EBC (5300m). The severity of hypoxic exposure could be observed through the ~20% decrease in SpO_2. This significant perturbation to the system was also reflected through decreasing body weight, which fell by ~3.7%, an effect that is in line with previous high altitude studies (Boyer et al., 1984, Guilland et al., 1985). Further investigation into downstream metabolic alterations was therefore warranted.

The aims of metabolomics and lipidomic assessment were twofold: 1) to identify commonalities in the healthy human response to progressive hypobaric hypoxia, 2) to distinguish how individuals vary in their response. To capture the altitude vs. metabolite relationship across these two layers in both metabolomics and lipidomics data sets, a hierarchical Bayesian model was employed.

In addition to the effects of altitude, subjects experienced a number of other perturbations upon their ascent to EBC that could potentially be reflected in their metabolic profiles. This includes the effects of the flight, both to KTM from LDN and from KTM to Lukla to begin their trek, as well potential dietary changes. A vital part of the analysis was therefore to distinguish the effects of increasing altitude from other perturbations to the system. The approach for identification of circulating metabolites undergoing the greatest perturbations with increasing altitude was to focus upon those located at the tail ends of the distribution curve (≤1.96 SD away from the mean). The Bayesian hierarchical modelling method was then adopted to assess the overall trend in metabolites. If an altitude effect was present, then this trend should be distinctive across all 5 locations.

An overview of the largest metabolite changes identified in both plasma fractions and possible consequences of these alterations are presented in **Figure 2.21.**

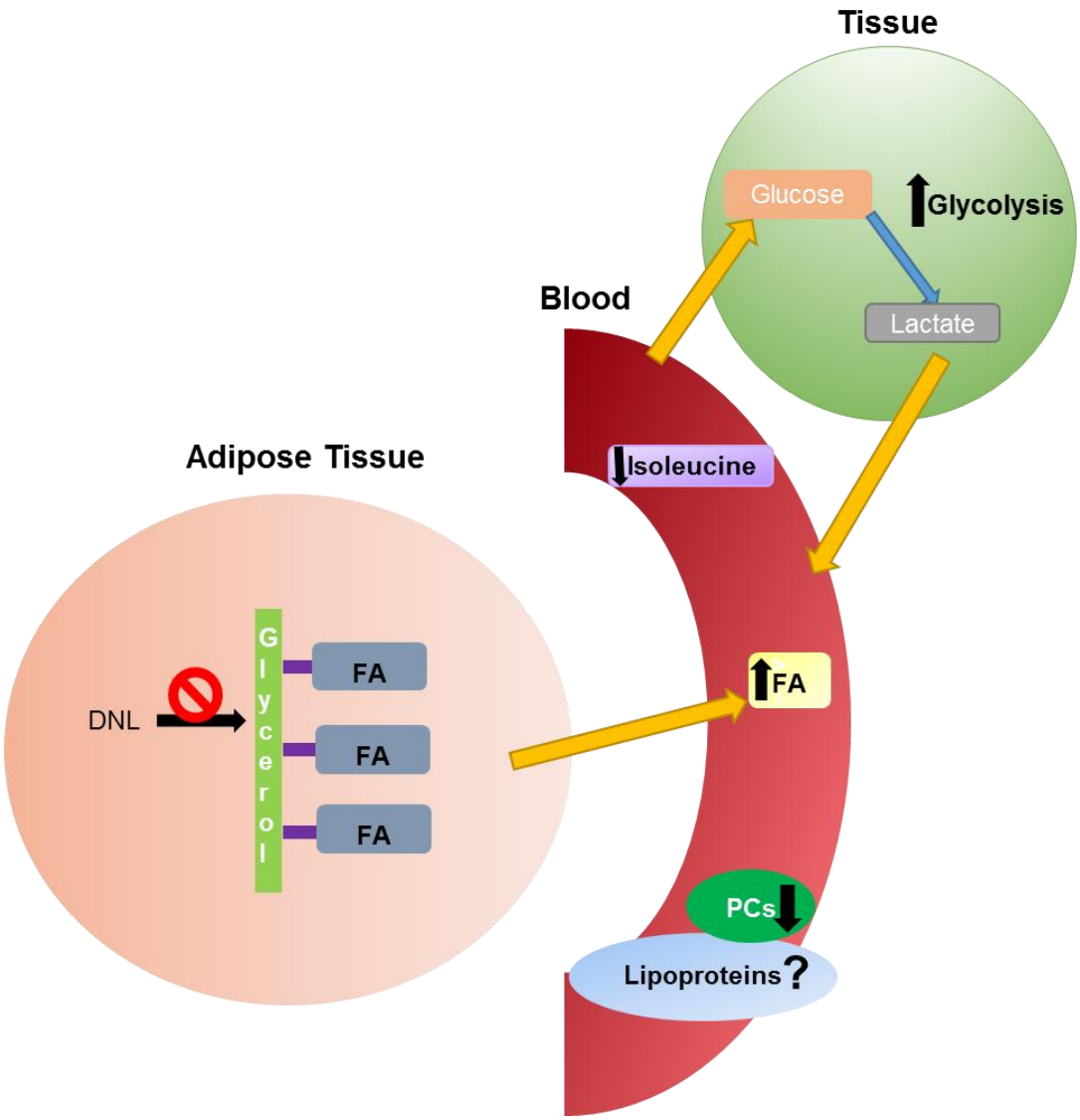

Figure 2.21. A summary of plasma metabolite changes and possible effects these changes indicate with ascent to Everest Base Camp.

*Derived from analysis of both lipid and aqueous phases, and the insight this provides into metabolic adaptation**. Aqueous fraction changes:** decrease in glucose, increase in lactate, indicative of increasing glycolysis; decrease in isoleucine. **Lipid fraction changes:** a decrease in triglycerides TGs containing palmitate and oleate along with increases in these free fatty acids (FA). This change is indicative of adipose tissue mobilisation and impaired de novo lipogenesis (DNL). Decreases in phosphatidylcholines (PCs), perhaps indicative of changes to lipoprotein protein synthesis.*

2.6.1 Aqueous metabolite changes

Specific changes in aqueous metabolites were indicative of increasing reliance upon anaerobic glycolysis, with a decrease in the substrate glucose occurring alongside an increase in the product lactate. A shift towards glycolytic metabolism is a key theme in numerous prior high altitude studies. For instance, a HIF-1α mediated increase in glucose transporters (GLUT-1 and GLUT-4) to the plasma membrane (Xia et al., 1997, Semenza, 1999) and upregulation of lactate dehydrogenase (Firth et al., 1995, Green et al., 1989) have been demonstrated in response to hypoxic exposure in both human and animal studies. This is alongside reports of a shunting of pyruvate away from entry to the TCA cycle and towards lactate formation, as shown through HIF-1α dependent inhibition of PDH through induction of PDK1, a response essential for hypoxic adaptation in mouse embryo fibroblasts (Kim et al., 2006). Indeed, the increase in lactate is supported by prior studies related to the CXE expedition, where the use of colorimetric enzyme assay kits demonstrated progressive increases in plasma lactate upon ascent, peaking at EBC (Siervo et al., 2014).

However, much discordance exists in relation to the lactate response, culminating in the 'lactate paradox' (Hochachka et al., 2002). This phenomenon presents as a lower lactate production under O_2 limiting conditions. It is a response reported post exercise (West, 1986) that may be explained through tighter coupling between ATP demand and supply (Hochachka et al., 2002). It has been recognised to occur in hypoxic-acclimatised individuals and highland native populations, becoming particularly prominent following exercise (Hochachka et al., 2002, Matheson et al., 1991). On this presumption, the present results would suggest that subjects remained unacclimatised following the 11 day ascent. Proteomic analysis of muscle biopsies acquired from subjects (CXE lab staff) exposed to 5300m for 6 days following the same ascent prolife as the subjects in the present study, revealed a decline in the abundance of enzymes required for glycolytic metabolism (Levett et al., 2015). This thus indicates that a longer stay at altitude may be required for acclimatisation to occur in lowland native subjects.

A seemingly novel response outlined in the aqueous plasma fraction was a decrease in isoleucine. This has not been highlighted in previous environmental hypoxia studies and is, to the author's knowledge, a novel finding. The consequences of this are not clear.

Isoleucine is an essential branched chain amino acid (BCAA), therefore cannot be endogenously synthesised, but rather needs to be provided by the diet. The fact that this change may be related to a dietary shift therefore cannot be ruled out. However, if the

decrease was due to a reduction in protein consumption, this would likely be reflected in changes to other BCAA's, being leucine and valine and this was not the case. The specificity of the change thus indicates the fall in isoleucine levels is due to increased utilisation as opposed to a decreased supply, either from dietary sources or protein turnover.

Prior studies examining responses to very acute hypoxia (5-18hrs) in rats (9.5% O_2) (Muratsubaki et al., 2011) and HeLa cells (1% O_2) (Troy et al., 2005) have been associated with increasing isoleucine levels. The disparity with the results of chapter 2 may be reflective of the differences in duration and severity of hypoxic exposure.

It may seem logical to associate the apparent increasing isoleucine utilisation observed in the present study with rising energy demand. An instance whereby rising energy demand is not met is fatigue. This is in turn associated with impaired mitochondrial function, as demonstrated through falling ATP production (Kume et al., 2015). In rats, fatigue has been associated with mobilisation of BCAA metabolites leading to an increased plasma isoleucine level, detected via metabolic profiling and related to proteolysis of skeletal muscle in rats (Kume et al., 2015). In this scenario, O_2 supply is ample, meaning the metabolic stresses are not akin to what is experienced in hypoxia. It suggests the BCAA metabolic pathway response is complex and may differ depending upon the specific form of metabolic stress and levels of O_2 availability.

There are a number of possible functional consequences of decreasing plasma isoleucine content. This includes structural effects within skeletal muscle. An optimal ratio of BCAA's (leucine:isoleucine:valine) has been shown to be crucial in development of intramuscular fat (Duan et al., 2016a) and protein synthesis, for instance through upregulation of mTOR signalling (Duan et al., 2016b). These results, whereby isoleucine is decreasing independently of leucine or valine thus suggests a disruption of this ratio, which may have downstream implications both for fat and protein metabolism. In relation to this, mTOR is downregulated in hypoxia (Wullschleger et al.) and levels decreased in response to 7-9 days exposure to 4559m in human vastus lateralis (Viganò et al., 2008). Again, associations between changes in muscle protein synthesis and decreasing plasma isoleucine are speculative, requiring further investigation.

Interestingly, lower BCAA levels have been associated with improving metabolic health. Dietary restriction of BCAA intake has been shown to improve glucose tolerance in both mice and humans (Fontana et al., 2016). In rats, a 45% restriction in dietary BCAA's have been associated with relieving mitochondrial metabolic overload in skeletal muscle

through preventing the accumulation of short and medium chain acyl CoA's to facilitate the complete oxidation of fatty acids, thus improving efficiency of skeletal muscle β-oxidation (White et al., 2016). This effect was accompanied by improvements in skeletal muscle insulin sensitivity (White et al., 2016). It may be the case, therefore, that lower isoleucine levels observed in the present study result from a favourable adjustment to improve skeletal muscle metabolism, particularly gluco-insular signalling. The aforementioned decreases in plasma glucose would go to support this assumption.

2.6.2 Lipid changes

Assessment of changes in plasma lipid metabolites revealed a significant degree of insight into lipid homeostasis during progressive hypoxic exposure. Increases were observed in the most abundant saturated and unsaturated fatty acids, being palmitic acid in the first instance and linoleic and oleic acids in the second. The change in the unsaturated fatty acids from LDN to EBC demonstrated a negative correlation with the change in body weight, thus indicating a potential link between these two factors. However, whether the increase in circulating unsaturated fatty acids may be a result or cause of decreasing body weight remains to be determined.

This change in circulating fatty acids occurred alongside decreasing levels of the main constituent of body fat, TGs, specifically those containing palmitate and oleate (48:1, 50:1). It is expected that, to retain a balance in circulating TG levels, specific decreases will be accompanied by compensatory increases, as is reported here in TGs 52:3 and 52:4.

TGs containing 48-50 carbons are typically associated with *de novo lipogenesis* (DNL), a process by which excess carbohydrates are converted to fatty acids and subsequently to TGs for storage (Ameer et al., 2014). Decreases in TGs 48:1 and 50:1 with ascent to EBC are therefore indicative of a suppressed DNL, an affect reported previously to be mediated via HIF-1α signalling (Menendez et al., 2007, Suzuki et al., 2014).

Alongside impaired DNL, the results are indicative of increased fat store mobilisation, a process known to be induced via sympathetic nervous system changes, with catecholamine release initiating a cAMP dependent phosphorylation of hormone sensitive lipase. This in turn stimulates TG mobilisation (Kraemer et al., 2002). Insulin acts antagonistically to impair this signalling system, thus inhibiting TG breakdown.

Alterations in both adrenaline/noradrenaline and insulin have been reported in previous investigations of the CXE expedition team. This included CXE investigators (n=24),

whom underwent an identical ascent profile to EBC as that described in the present study, yet remained at EBC for 8 weeks (Siervo et al., 2014). An initial increase in adrenaline and noradrenaline was observed upon ascent to NAM. Theoretically, this sympathetic nervous system activity could induce the fat store mobilisation response observed in the present study.

This initial sympathetic nervous system response observed by Siervo and colleagues was followed by a decrease in adrenaline/noradrenaline and a sharp increase in insulin and C-peptide in response to longer term residence at EBC or above (Siervo et al., 2014). This was thus indicative of an onset of insulin resistance. Increasing circulating levels of free fatty acids (notably palmitic, oleic and linoleic acids) have been shown to induce insulin resistance in several models (Shen et al., 2016, Shi et al., 2006, Benoit et al., 2009), including those of obesity through a mechanism reliant upon c-Jun amino terminal kinases (JNKs) (Hirosumi et al., 2002). It is therefore entirely possible that the increased mobilisation of fat stores reported here, with the resulting increase in circulating fatty acids, is a causative factor for the spike in insulin concentrations observed in response to longer term exposure (Siervo et al., 2014). This may thus suggest that any favourable adjustments in gluco-insular signalling indicated through decreasing isoleucine levels is a short time effect that is followed by the onset of insulin resistance in the long term. However, this conclusion is somewhat speculative and further investigations are required before a firm conclusion can be drawn from possible associations between increasing circulating fatty acids and insulin resistance.

An additional factor that could lead to the build-up of circulating fatty acid levels is impaired β-oxidation capacity. This response is commonly reported amongst high altitude studies (Horscroft et al., 2014). Previous proteomic examination undertaken on CXE expedition subjects revealed decreasing OXPHOS enzyme abundance, which may imply OXPHOS capacity is impaired and so fatty acid metabolism is in turn suppressed (Levett et al., 2015).

Beyond alterations to fat storage and synthesis, lipidomics analysis also revealed changes in key membrane components. This includes the decreases in PC 46:2. PC's are key constituents in the construction of lipoproteins, in particular very low density lipoprotein (VLDL) (Eisenberg, 1984), which is required for lipid transportation from the liver to cells. This observation thus goes to suggest progressive hypoxic exposure may affect lipid transport via VLDL. Disruption to the lipoprotein transport system in hypoxia has been reported previously with regards to the mobilisation of FA's from VLDL via lipoprotein lipase

(LPL). LPL activity was inhibited in adipose tissue and pre-adipocytes exposed to chronic intermittent (Drager et al., 2012) and acute hypoxia (Mahat et al., 2016b), respectively. Further investigation into the lipoprotein transport system in response to hypoxic exposure is thus warranted.

Changes were also observed in the key membrane component, SM. The role of this lipid in hypoxic conditions has not undergone sufficient investigation. However, given the crucial role it plays in membrane of neural tissue, it may be that rising levels are indicative of disruption to membrane composition. This could result from a stress response, both from hypoxia and also the resulting increase in circulating free fatty acids. In particular, saturated fatty acids including palmitic acid have been associated with toxicity, demonstrated through increasing inflammation, generation of ROS and increasing apoptosis (Kennedy et al., 2009, Miao et al., 2015).

There were numerous instances whereby multiple lipid identifications were present. Further investigation to firmly derive exact details may, for instance, involve adoption of a prior chromatography separation step to produce and separate lipid fragments (Dunn et al., 2011a).

2.6.3 Correlation analysis

Correlation analysis revealed a positive correlation with changes in glucose and body weight, yet a negative correlation with changes in unsaturated fatty acids. However, whether the body weight change is a cause of the metabolite alterations or vice versa remains to be determined.

Interestingly, despite the large changes in SpO_2 between LDN to EBC (~20% average decrease), this was not found to correlate with any identified metabolite. This may highlight the importance of other factors aside from the delivery of O_2 to tissues that influences metabolic acclimatisation to hypoxic exposure. This concept has been recognised in the context of VO_2 max, whereby normalisation of arterial O_2 content occurs alongside continued impairment to exercise capacity (Calbet et al., 2003).

2.7 Conclusion

In this study, systemic metabolic responses to progressive high altitude exposure were assessed utilising metabolomics and lipidomic profiling of human plasma. Alterations identified in the aqueous fraction included the novel finding of decreasing isoleucine with

ascent, alongside lactate and glucose changes that were indicative of the well-documented increased reliance upon anaerobic metabolism. Fluctuations in the lipid profile with ascent were suggestive of increased mobilisation of lipid stores and suppressed DNL. This occurred alongside changes to lipids that are essential membrane components, particularly those involved in the lipoprotein transport system. This study has therefore highlighted potential metabolic biomarkers for progressive hypoxic exposure in healthy humans. Further investigation is required to validate these biomarkers with targeted studies and to assess the potential relevance in the context of pathological hypoxia.

3 **Chapter 3 (Study 2):** Antarctica winter expedition pilot study: physiological and metabolic responses to prolonged hypoxia and extreme cold.

3.1 Introduction

Hypoxic exposure, both in healthy humans sojourning to altitudes and resulting from disease states, can be experienced at varying severities and longevities. As already highlighted, much of the discrepancy between previous high altitude studies results from differences in duration and severity of hypoxic exposure (Horscroft et al., 2014). Unravelling the controversy surrounding metabolic remodelling processes therefore needs to encompass this variability. In particular, the responses to chronic hypoxic exposure is a highly understudied area. Indeed, the very definition of 'chronic exposure' is unclear and varies between studies. Some have defined it as ≥42 days (Horscroft et al., 2014), some ≥ 3 months (Woolcott et al., 2015) and others as little as 2 weeks (Siebenmann et al., 2016).

Despite this discrepancy, evidence suggests metabolic responses to chronic hypoxia may differ from those apparent in acute exposure. For instance, reports of decreasing lactate accumulation in response to exercise in chronic compared to short term exposure (the lactate paradox) suggests further shifts in metabolic remodeling processes (Hochachka et al., 2002). This is alongside alterations to the mitochondrial network, with exposure to ≥42 days being associated with decreasing mitochondrial density in skeletal muscle (Horscroft et al., 2014). Interestingly, this trait is present in adapted high altitude native Tibetan populations, whom display a lower skeletal muscle mitochondrial density in comparison to lowlanders (Kayser et al., 1996). Examination of native highland populations at a genetic level reveals the presence of polymorphisms in genes specifically related to metabolic function (Simonson et al., 2012, Simonson, 2015).

Further investigation into chronic exposure is therefore warranted. In the current study, a small cohort of subjects were examined pre and post an attempted winter crossing of Antarctica, which included prolonged exposure to high altitude with 24 weeks at 2,500m. Inevitably, this occurred alongside intermittent exposure to the extreme cold temperatures

of the Antarctic winter that far exceeded the degree of cold exposure experienced by subjects in Chapter 2.

It is generally considered that the decreased P_IO_2 experienced at altitude is the main cause of the observed physiological effects (Woolcott et al., 2015). However, high altitude exposure usually coincides with cold ambient temperatures and the interaction between hypoxia and cold are often overlooked. This is especially pertinent when considering the metabolic effects of cold exposure.

Acclimatisation to extreme cold undoubtedly relies heavily upon behavioural adaptations such as the wearing of warm clothing, but this can be accompanied by significant physiological changes that in turn influence substrate utilisation, specifically increasing reliance upon carbohydrate and fat oxidation (Vallerand et al., 1989).

A fall in body temperature to the lower extreme of thermoneutrality (lower critical temperature) initiates metabolic energy transformation, or thermogenesis (Stocks et al., 2004). In the short term this includes shivering thermogenesis. Despite its reliance upon muscular contraction, substrate utilisation during shivering is not akin to utilisation evoked by exercise as shivering induces larger increases in plasma free fatty acids, β-hydroxybutyrate and insulin compared to exercise (Tipton et al., 1997). This is alongside reports of increasing utilisation of skeletal muscle glycogen stores (Jacobs et al., 1985).

With longer term acclimation to cold, there is also a heavy reliance upon metabolic processes for non-shivering thermogenesis. Of particular relevance are those changes taking place in mitochondria located within adipose tissue. Uncoupling of oxidative phosphorylation here is thought to play an essential role in cold-induced shivering thermogenesis, a response believed to be regulated by the cold-sensing receptor TRPM8 expressed in both white and brown adipose tissue (Frontini et al., 2010, Rossato et al., 2014).

Long term alterations to metabolic processes can also be observed through measurements of basal metabolic rate (BMR) in populations indigenous to extreme cold environments. A strong correlation between BMR and climate has been observed (Roberts, 1952). The BMR of indigenous Siberian populations, for example, was found to be 5% higher than values predicted based on body mass. These elevations appeared to be attributable to environmental stress rather than high dietary protein consumption, as was previously believed (Leonard et al., 2005).

The combination of cold exposure and hypoxia appears to modify responses to both conditions. Whilst cold exposure is reported to increase rate of pulmonary O_2 consumption (VO_2) at rest (Vallerand et al., 1989), this was attenuated at altitude (3,350m and 4,360m), a response reported to be sustained over a 6 week period, only being recovered upon descent (Blatteis et al., 1976). Reliance upon shivering thermogenesis has been reported to increase in hypoxia, both in response to acute (90 mins) cold exposure at 12% O_2 and a longer term (6 week) exposure to both 3,350 and 4,360m (Robinson et al., 1990, Blatteis et al., 1976). Interestingly, the latter study concluded that the combination of suppressed VO_2 alongside increased shivering was indicative of suppression of non-shivering thermogenesis during this prolonged period (Blatteis et al., 1976).

Together, the current literature presents two key points that have been overlooked in high altitude research to date: 1. A lack of understanding regarding the physiological and metabolic responses of healthy humans to chronic hypoxic exposure 2. The combination of hypoxia and cold upon these adaptive responses. Both of these factors are explored in this present thesis chapter.

In this pilot study, a small group (n=5, age 28-54 years) of Trans-Antarctic winter trekkers were assessed pre and post a 40-week expedition, during which 24 weeks were spent above 2,500m. This study is a continuation of the theme explored in Chapter 2, however, the duration of hypoxic exposure, whilst of moderate altitude, far surpasses that of Chapter 2. In addition, given the extreme nature of the Antarctic winter with temperatures on the high plateau regularly falling below -60˚C (British Antarctic Survey https://www.bas.ac.uk/about/antarctica/geography/weather/temperatures/), the degree of cold exposure is way beyond that experienced by subjects in Chapter 2. This pilot study is therefore a unique investigation into, arguably, the most extreme environment on earth.

3.2 Aims and objectives

This applied field study aimed to explore physiological responses of healthy humans exposed to the Antarctic winter for a prolonged period. This encompassed chronic hypoxia and intermittent exposure to extreme cold. The objectives were to gain a broad understanding of physiological changes occurring in response to one of the world's most hostile environments. For the purpose of this thesis, there is a particular focus upon metabolic changes and physiological parameters related to these. For this, serum

metabolomics analysis was undertaken alongside anthropometric and functional physiological measurements to provide a broad characterisation of the response.

This pilot study is the first to provide an in-depth examination of human physiology to prolonged exposure to this extreme environment and so presents as a hypothesis generating study. Whilst changes were expected to occur post expedition compared to pre, the details of expected changes were uncertain.

3.3 Methods

3.3.1 Expedition overview and aims

This expedition was the first ever attempted crossing of the Antarctic in the winter months. The 5 male subjects (aged 28-54 yrs, BMI pre-expedition 26.36 $\pm$ 3.87 kg/m^2) were assessed in the UK prior to and following their 40 week stay in Antarctica, with the attempted winter crossing lasting 33 weeks, including 24 weeks above 2,500m. Due to issues that severely impaired subject safety, the crossing was halted on week 8. Given difficulties in evacuation procedures in the winter months, subjects were subsequently forced to set up winter camp. Living cabins/cabooses were taken along with the expedition on caterpillar trucks. Once winter camp was established, subjects spent the majority of their time residing within the cabins, only being exposed to the outside elements intermittently.

Subjects recorded food diaries and body weight data throughout the expedition. An array of measurements were also taken at King's College London pre and post expedition that included: assessment of metabolic profile, body composition, exercise and lung function testing.

3.3.2 Ethical approval

Prior to participation, written informed consent was obtained from all subjects. All procedures were approved by the National Health Service Wandsworth Research Ethics Committee (reference number: 12/LO/0457) and conformed to the Declaration of Helsinki.

3.3.3 Study design

Pre-testing was conducted at King's College London on 12th December 2012, after which subjects spent a 40-week period in Antarctica, beginning on January 22nd. The attempted winter crossing expedition, outlined in **Figure 3.1**, began with departure from Crown Bay on 21st March and lasted 33 weeks. During this time, subjects spent weeks 5-29

above 2500m and reached the highest altitude of 2,824m on week 8. The crossing was halted on the 9th May and winter camp established on 30th May (week 11) at 2,752m. Subjects remained here until week 28, after which subjects began their descent. The final point near Belgian Princess Elizabeth Station (1,367m) was reached on week 32, being 1st November 2013. Subjects remained here until 23rd November, at which point they flew home. Post testing was conducted at King's on 27th November, 2013.

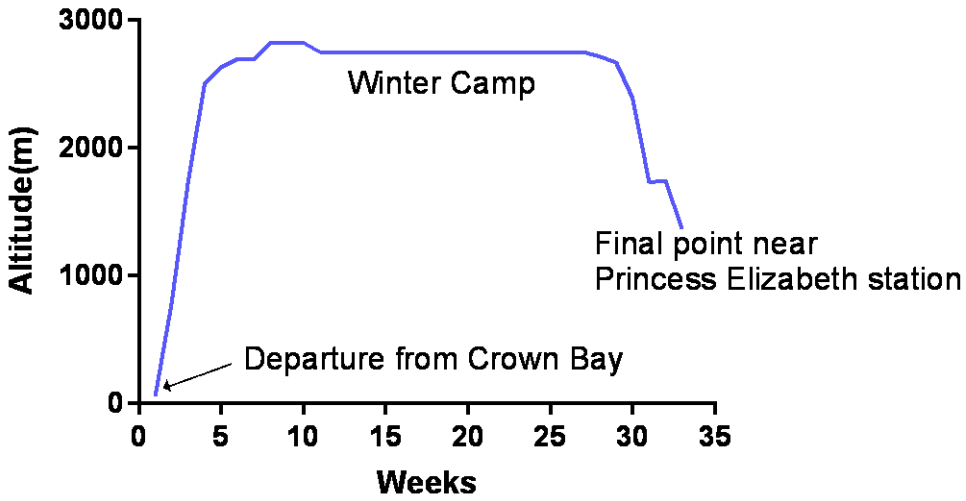

Figure 3.1. A diagrammatic representation of altitude exposure during the attempted Antarctic winter crossing expedition

The 33 week attempted crossing was measured from the point at which subjects departed from Crown Bay.

3.4.4 Measurements taken during the expedition

Dietary intake and activity

Water intake (ml/day) and food intake were recorded, the latter as total energy intake (kcal/day), broken down to: protein, fat and carbohydrate (g/day). These values were obtained through weighed food diaries, taken across a 7-day period at 17 points within the attempted crossing time (33 weeks). Body weights were also recorded at these same periods using digital balance scales (model details not available) following an overnight fast and voiding of urine.

Outside activity data were obtained from diary records taken across a 7 day period at 8 time points within the attempted crossing time. A subjective scale was used to estimate duration of light and heavy work undertaken during these periods. Light work was roughly defined as walking or general camp maintenance and heavy work as, for instance, shoveling snow. Given the degree of subjectivity and lack of accuracy, this measure was merely used as a broad estimation and general overview of subject activity levels.

Both food and activity data are presented as an average over the 7 day periods to present intake or activity on a 'typical' day.

3.3.4 Measurements taken at King's College London

Serum samples

Serum samples were taken from fasted subjects at rest (in the morning, prior to the exercise protocol) pre and post expedition. They were obtained by venesection in serum separating tubes and immediately spun for 10 minutes at 520g at 4°C. The resulting supernatant was pipetted into 2ml polypropylene cryotubes, and immediately frozen at -80°C.

^{1}H-NMR serum metabolomics

For analysis, serum samples were defrosted at room temperature and centrifuged at 16,000g for 10 minutes. The supernatant was aliquoted, leaving the pellet, and the spin repeated. A 300 µl aliquot of the resulting supernatant was then mixed with 300 µl of NMR buffer (250 µl DSS plus phosphate buffered saline (PBS) at a concentration of 5 mM added to 50 µl 99.9% D_2O). The final solution contained 8 % D_2O for the magnetic lock. The

resulting mixture was transferred to 5mm NMR tubes within a 96-tube rack ready for spectral acquisition.

NMR spectral acquisition

The same methodology was adopted as used in Chapter 2 (2.4.3). Given the small number of samples, all were run in the same experiment.

NMR data processing

Data were Fourier transformed using an exponential window function with a line broadening of 0.3Hz in the frequency domain. Spectra were converted from time to frequency domain using serial processing and subsequently phase corrected and aligned, with chemical shifts being manually referenced to DSS (at δ = 0 ppm), in ACD labs (ACD Labs Software.Ink), before being imported into Matlab (Mathworks, Natick, MA) at full resolution. Following this, spectra were normalised using probabilistic-quotient normalisation (Dieterle et al., 2006) and binned using adaptive intelligent binning (De Meyer et al., 2008), both in Matlab.

NMR Data Analysis

Given the hypothesis generating nature of this study, an untargeted approach was adopted to assesssubjects' metabolic profiles, with changes being identified initially through principal components analysis. Principal component 2 (PC2) was shown to capture 30% of variance in the metabolic profiling data. Within this, the peak integrals of glucose and the shoulder of the fatty acid CH_2 resonance underwent a significant decrease post expedition, as tested using a paired Sample T test (see 3.3.10). Identification of the metabolites associated with the peaks undergoing significant changes was undertaken using Chenomx software (Chenomx NMR Suite 7.1).

3.3.5 Cardio pulmonary exercise testing

Maximal oxygen uptake ($\dot{V}O_{2max}$) was determined using a continuous exercise test on a cycle ergometer (Lode Coriva, Lode, Groningen, Netherlands). Breath-by-breath measurements of O_2 and CO_2 concentrations as well as volume of expired air were recorded continually throughout the test (Oxycon Pro; CareFusion, Basingstoke, U.K.). Subjects wore a face mask to which the volume and gas sensors were attached. The O_2 and CO_2 analysers were calibrated with known gases in accordance with the manufacturers'

guidelines. A 3 L syringe was used to calibrate the volume sensor before testing commenced.

Subjects initially cycled at a work rate of 50 W for 3 mins after which the power output continually increased until the subject could no longer continue despite verbal encouragement. The rate of increase of power output (1 – 2W every 3 – 5 s) was estimated for each subject such that maximal effort would be reached within 10 – 12 min. The subjects cycled at constant self-selected rate typically between 75 – 80 rpm. Heart rate was continually monitored throughout the test using a 12 lead ECG. VO_{2max} was determined as the greatest O_2 uptake recorded over a 20s period at the end of the test. To ensure a valid $\dot{V}O_{2max}$ was attained subjects had to meet at least two of these criteria: 1) achievement of maximum heart rate greater than age predicted maximum (220 - Age), 2) a respiratory exchange ratio of >1.15 and 3) a plateau in VO_2 indicated by an increase in VO_2 of no more than 100ml/min in the final two 20 s periods of the test. Ventilatory threshold (VT) was determined using a combination of the v-slope method (the point where a clear steeper increase in $\dot{V}CO_2$ compared to $\dot{V}O_2$ occurs) and the ventilatory equivalent method (the point where $\dot{V}E/\dot{V}O_2$ rises without a concomitant rise in $\dot{V}E/\dot{V}CO_2$). VT was assessed by 2 independent investigators with any differences between the two resolved by a third investigator when necessary (Gaskill et al., 2001).

Respiratory exchange ratio

Calculated from breath by breath measurements of CO_2 and O_2 concentrations taken during the maximal O_2 uptake (VO_2 max) test. To capture changes in RER across each percentile of the VO_2 max test, the area under the curve was assessed for each subject for the full exercise duration.

3.3.6 Body composition

Subject height and mass were determined using a stadiometer and calibrated balance beam scales, respectively. Bone mineral density (BMD) of the whole body, hip and lumbar spine was assessed by dual-energy X-ray absorptiometry (DXA) using a Hologic Discovery A scanner (Hologic, Bedford, MA). Fat mass and fat free mass were also determined from DXA scans.

3.3.7 Resting Cardiovascular Function

Upon arrival at the laboratory resting cardiovascular function was assessed using a Finometer Pro (Finapres Medical Systems, Amsterdam, Netherlands) with a finger cuff attached to the middle finger of the right arm. Systolic (SBP), diastolic (DBP) and mean arterial pressure (MAP) were recorded once every minute for 5 min at the end of a period of 15 min of quiet supine resting, as was resting heart rate. Average values of each variable were calculated.

3.3.8 Lung Function

The greatest peak expiratory flow (PEF), forced vital capacity (FVC), forced expiratory volume in 1s (FEV_1) and FEV_1/FVC% were recorded using an Oxycon Pro (CareFusion, Basingstoke, U.K.) calibrated prior to use. Subjects were instructed to inhale rapidly to total lung capacity and then without pausing exhale as forcefully as possible until no more air can be expired. Subjects were seated and required to maintain an upright posture during all manoeuvres which were performed in accordance with the ATS/ERS Guidelines (Miller et al., 2005).

3.3.9 Maximal voluntary muscle strength

Maximal voluntary strength (MVC) was assessed in the knee extensors of the dominant limb. Subjects were seated upright with their arms folded in a custom-built dynamometer with their knee in 90º of flexion. Their lower leg (~3cm proximal to the ankle) was strapped in a padded steel brace attached by a rigid bar to a strain gauge. Signals from the strain gauge were recorded on Spike 2 software via an analogue-to-digital converter (Cambridge Electronic Design (CED) 1401, U.K.) at a sampling rate of 2 kHz. Percutaneous stimulating electrodes (8 x 12 cm) were strapped around the distal and proximal segments of the quadriceps and attached to a constant current stimulator delivering square wave stimulation (pulse width 0.2 ms at 400 V; Digitimer Stimulator DS7, Digitimer Ltd., U.K.). Waist and shoulder straps were used to minimise any hip or upper body movement. The distance from the centre of rotation of the knee joint to the steel brace was measured to allow torque to be calculated.

The testing procedure began with determination of the maximal twitch response. Current was increased in a stepwise manner until no further increase in torque was

observed. After a brief rest subjects performed 6 MVCs. Subjects were asked to generate maximal force as quickly as possible and hold the contraction for 3-4 s. Strong verbal encouragement and visual feedback from a monitor placed in front of the subject were given. At least 1 min of rest was given between each contraction. During three of the maximal effort contractions a maximal electrical impulse was delivered to the muscle. The greatest MVC was used for analysis.

3.3.10 Statistical analysis

The low subject numbers in this study mean that the emphasis of data interpretation is in the observed trends. However, statistical tests were still performed in order to gauge the degree of change. As this data set contains insufficient numbers for normality testing, a Gaussian distribution was assumed and differences in physiological variables pre to post expedition were identified using a paired Student T test. To display the trends of the data, the individual responses are presented. Correlations between Δ metabolite change and Δ AUC RER were examined using a Pearson correlation coefficient. Statistical analysis and generation of graphs was conducted in Graphpad Prism.

3.4 Results

3.4.1 Food intake, activity and body weight data recorded during the expedition

Dietary intake was recorded throughout the winter expedition through food diaries kept by each subject. This analysis revealed details of nutrient intake on a daily basis, detailed in **Figure 3.2A.** Total protein intake was 108.67 $\pm$ 18.17 g/day ($\pm$ SD), carbohydrate intake 350 $\pm$ 101 g/day and fat intake 122 $\pm$ 25 g/day. Total energy intake was an average (mean) of 2871.8 $\pm$ 543.1 kcal/day (**Figure 3.2B**). Water intake was kept relatively constant (2,167.0 $\pm$ 649.6 ml/day) from weeks 1-20 (**Figure 3.2C**). Following this, from weeks 22-33, water intake increased as did the inter-individual differences, reflected by the increasing SD (3,294.2 $\pm$ 934.0 ml/day).

Exposure to the outside varied throughout the expedition and also significantly between subjects. Total time spent outside averaged 153 $\pm$ 94 mins/day (**Figure 3.3A**). This was divided into a broad estimation of light and heavy work (**Figure 3.3B**), which averaged 128 $\pm$ 80 mins/day and 44 $\pm$ 48 mins/day respectively. A drop in average activity levels can be observed following week 11, which coincides with the point at which winter camp was

established. This then increased once descent from winter camp was underway (week 28). Light work was also performed inside and was sustained at 60mins/day for each subject throughout the duration of the expedition.

Body weight data obtained during the expedition revealed an average decrease of 2.56 ±2.15 kg from week 1 to week 32 **Figure 3.4**. Statistically, this difference was close to significance ($p = 0.063$).

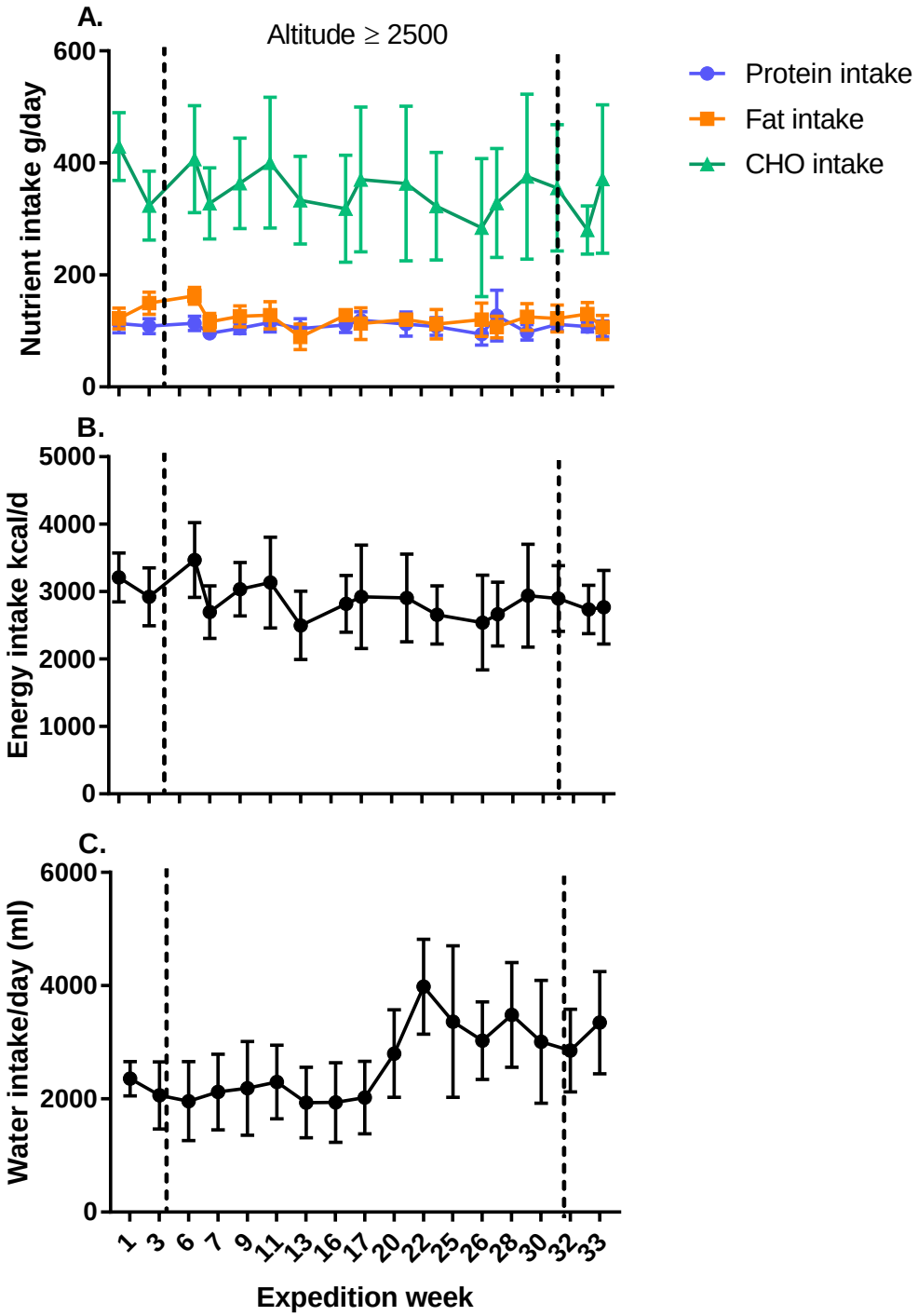

Figure 3.2. Nutrient (A), energy (B) and water (C) intake expressed as daily values throughout the winter expedition duration.

Nutrient intake is broken down into protein, fat and carbohydrate (CHO) intake. Data were collected each day over the 7 day period on the expedition week specified and is expressed as average ± SD, n=5.

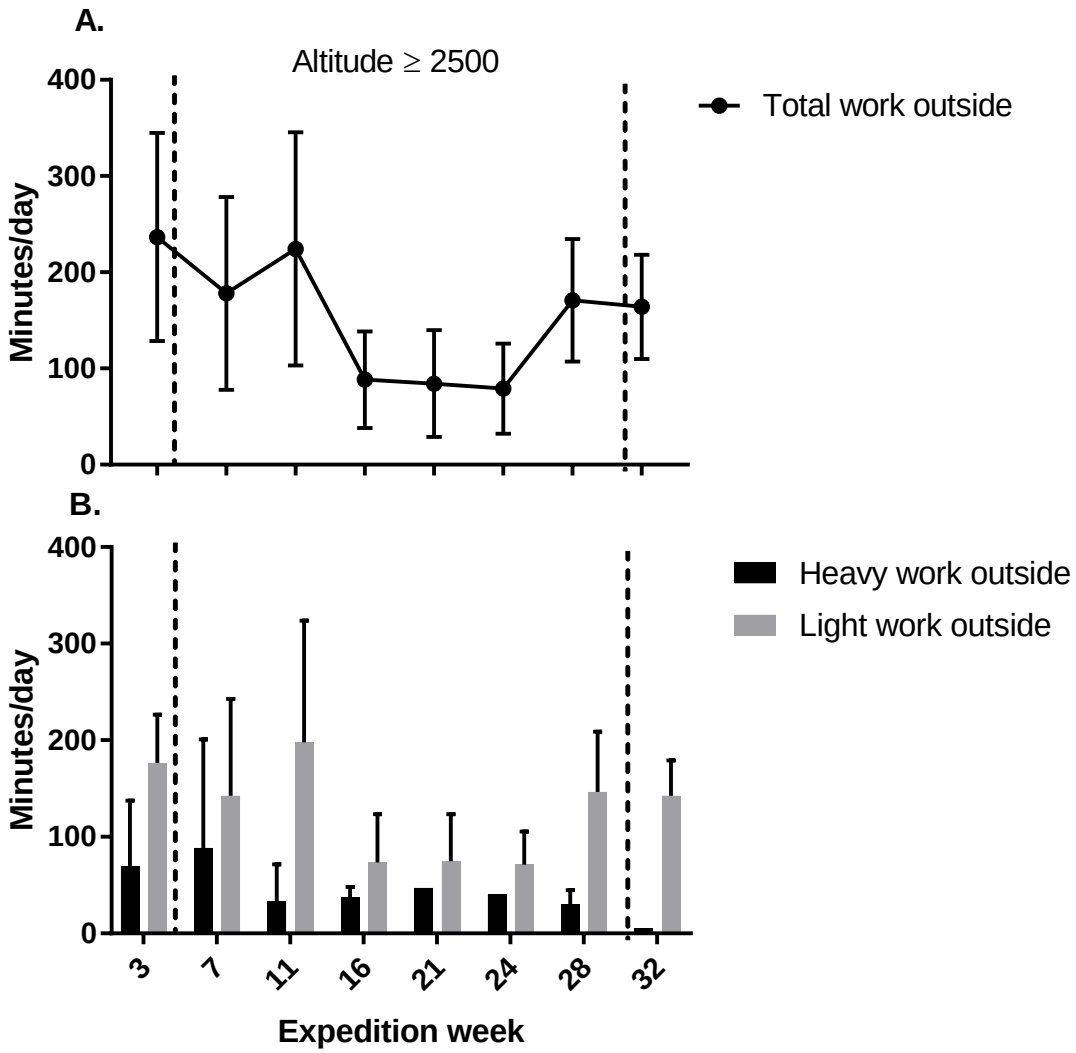

Figure 3.3. Work performed outside throughout the winter expedition duration

*Depicted as total work performed (**A**) and as an estimate of the division between heavy and light work (**B**). Data were collected each day over the 7 day period on the expedition week specified and is expressed as average of this ± SD, n=5.*

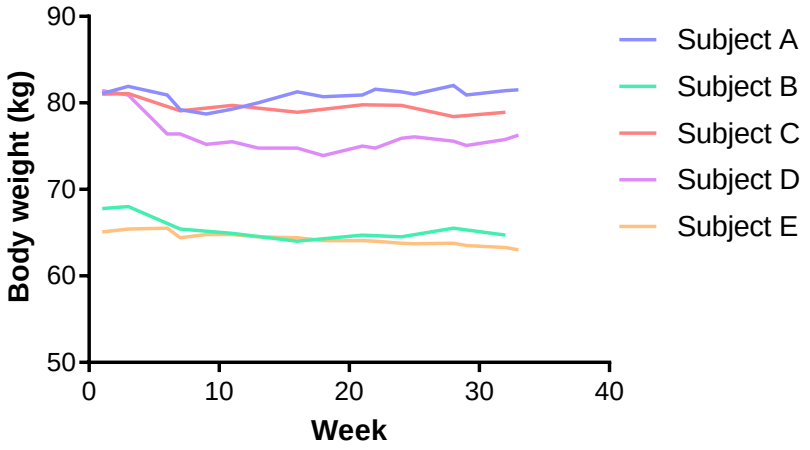

Figure 3.4.Body weight (kg) recorded during the 33 week attempted Antarctica winter crossing.

3.4.2 Pre: post expedition measurements

Metabolic profile changes

The spectra produced from ^{1}H-NMR metabolomics analysis of serum pre and post expedition were overlaid, as shown in **Figure 3.5**. Multivariate statistics revealed a reduction in principal component 2 (PC2) post expedition, which captured 30% of variance in the metabolic profiling data (**Figure 3.6**). The separation of variables by PC2 is demonstrated in **Figure 3.7.** Within PC2, peaks corresponding to glucose and a fatty acid CH_2 resonance underwent significant decreases by 35.9 ($\pm$ 22.9) % and 39.6 ($\pm$ 20.6) % respectively ($p>0.05$) **(Figure 3.8,** detailed in **Table 3.1)**. Unfortunately, it was not possible to identify the subtype of fatty acid from which this resonance was derived.

Anthropometric and functional physiological measurements

The anthropometric and physiological measurements taken pre and post expedition and are summarised in **Table 3.2**. No significant change in body weight was observed post expedition in comparison to pre (**Figure 3.9A**). Equally, no significant change was observed in BMI pre to post expedition (26.4 $\pm$ 3.9 vs. 26.0 $\pm$ 3.5 kg/m^2). However, changes were observed in body composition post expedition, with an increase in % lean and decrease in % fat tissue by 2.1($\pm$ 0.8) % ($p<0.05$), displayed as average values (**Figure 3.9B**) and individual values (Figure 3.9B.C). This change was also reflected in the decrease in body fat by 11 ($\pm$ 5) % ($p<0.05$) (**Figure 3.9E**). In addition, a 1.8 ($\pm$ 0.9) % decrease ($p<0.05$) was observed in spine BMD (**Figure 3.9F**).

Lung function measurements revealed no significant change in either FEV_1 (L) or FVC (L). However, FVC numerically increased in all subjects post expedition, a change that was close to significant ($p=0.06$) and that is reflected in the decrease in the FEV_1/FVC% by 5.8 ($\pm$ 3.3) % post expedition ($p<0.05$) (**Figure 3.9G)**.

Regarding cardiovascular measures, no significant changes were observed in resting blood pressure (sBP, dBP or MAP) or heart rate.

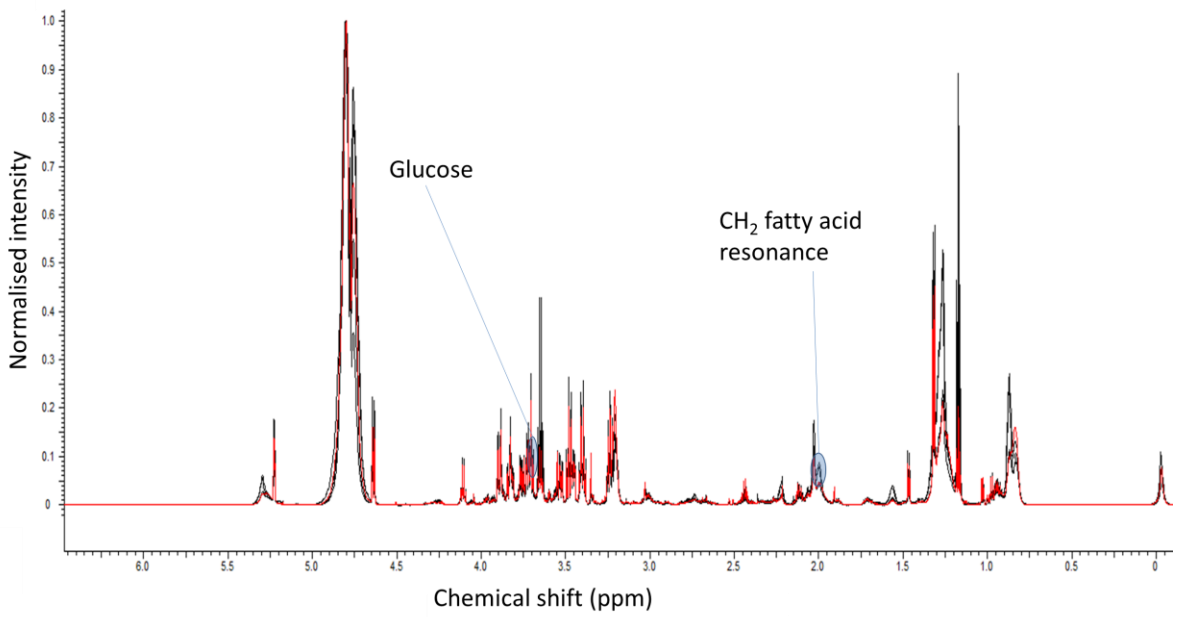

Figure 3.5. An average ^{1}H-NMR spectra taken from all subjects.

Pre expedition (black) overlaid with post expedition (red). Highlighted are the peaks corresponding to glucose and the CH_2 fatty acid resonance.

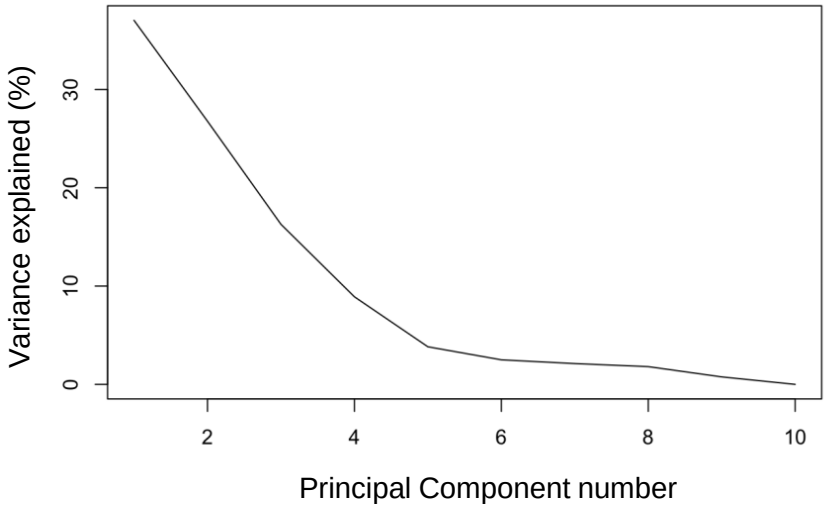

Figure 3.6. Scree plot demonstrating the variance explained by each principal component.

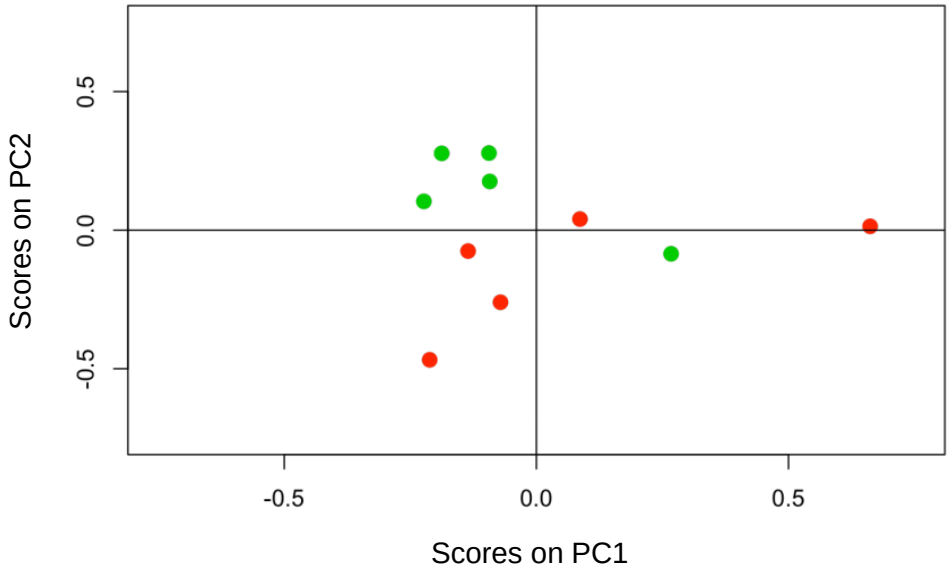

Figure 3.7. Scores plot of principal components 1 and 2.

Green corresponds to pre expedition and red post.

Table 3.1. Serum metabolites undergoing significant changes pre and post expedition.

Variable	Mean Pre (±SD)	Mean Pre (±SD)	Difference (±SD)	P value
Fatty acid CH_2(n) peak	0.05 (0.013)	0.028 (0.010)	-0.018 (0.013)	0.038*
Glucose peak	0.045 (0.012)	0.029 (0.009)	-0.016 (0.016)	0.033*

***Note**: Respective metabolites were identified within principal component 2 following ^{1}H-NMR spectral analysis.*

.

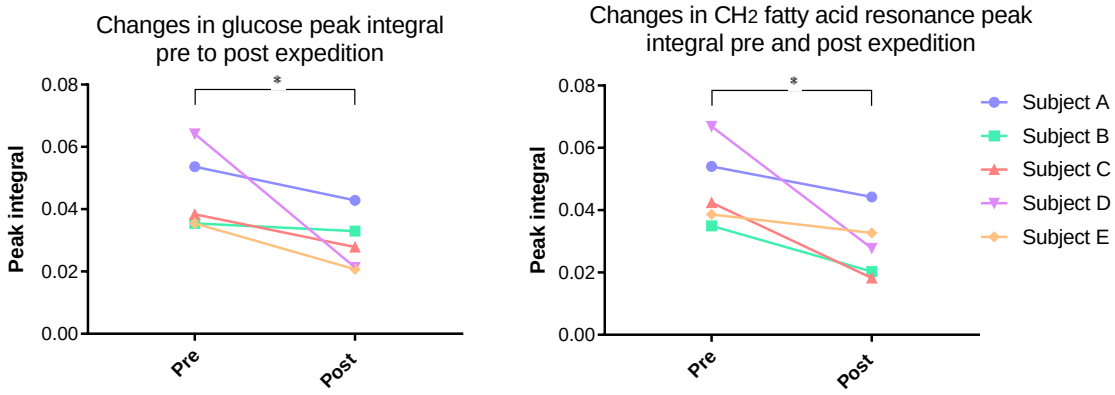

Figure 3.8. Peak integrals undergoing significant decreases within principal component 2.

*This includes the peaks of glucose and the shoulder of the fatty acid CH_2 resonance, *p≤0.05.*

Table 3.2. Summary of changes in anthropometric variables, resting lung function and cardiovascular parameters pre and post expedition.

Variable	Mean Pre (±SD)	Mean Post (±SD)	Difference	P value
% Lean tissue	**79.3 (3.7)**	**81.4 (3.0)**	**2.1 (0.8)**	**0.015***
% Fat tissue	**20.7 (3.7)**	**18.6 (3.0)**	**-2.1 (0.8)**	**0.015***
Body fat (kg)	**16.0 (4.7)**	**14.0 (3.7)**	**-2.0 (1.1)**	**0.034***
Body weight (kg)	77.9 (9.58)	76.9 (9.3)	-1.02 (2.5)	0.41
Spine BMD g/cm^2	**1.2 (0.05)**	**1.13 (0.04)**	**-0.02 (0.01)**	**0.035***
FVC (L)	6.38 (1.29)	7.11 (1.88)	0.72 (0.62)	0.060
FEV1	4.29 (0.65)	4.34 (0.71)	0.05 (0.22)	0.661
FEV_1/FVC%	**68.2 (9.7)**	**62.4 (8.4)**	**-5.8 (3.3)**	**0.016***
Heart rate (bpm)	60 (6)	63 (7)	3 (7)	0.39
sBP	123 (6)	121 (5)	-2 (8)	0.61
dBP	72 (8)	75 (9)	2 (6)	0.37
MAP	93 (9)	93 (7)	-0.04 (5.7)	0.99

Note: *BMD- bone mineral density; FVC - forced vital capacity; FEV_1-forced expiratory volume in 1 second, bpm- beats per minute, sBP – systolic blood pressure, dBP- diastolic blood pressure, MAP – mean arterial blood pressure. n=4-5, values presented as mean ± standard deviation, *denotes significance, p<0.05.*

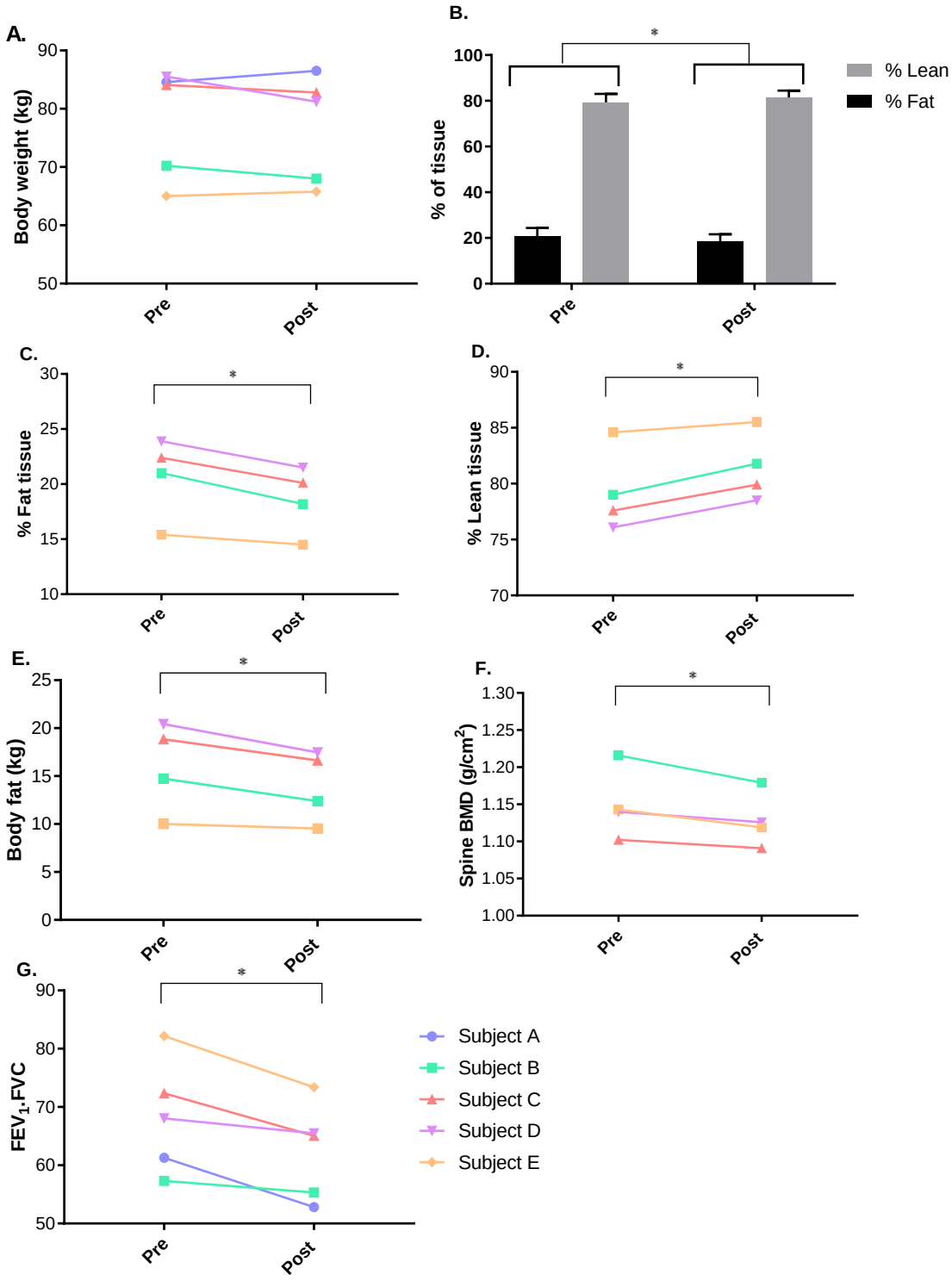

Figure 3.9. Anthropometric and physiological measurements taken pre and post expedition.

Individual body weight (kg) ***B.*** *% lean and fat tissue, presented as mean values (± SD)* ***C.*** *Individual subject values for % fat and* ***D.*** *lean tissue,* ***E.*** *body fat,* ***F.*** *spine BMD (bone mineral density),* ***G.*** *FEV1.FVC% (forced expiratory volume in 1 second: forced vital capacity. *p≤0.05, n=4-5.*

Exercise data

Physiological measures related to exercise are displayed in **Table 3.3**. Examination of maximal muscle strength in the dominant leg revealed an increase in all subjects bar one post expedition (**Figure 3.10**). The trend towards an increase was reflected in the p value that was close to significance (p=0.06).

An 11.6 (±1.9) % increase (p>0.001) was observed in VO_2 max corrected to lean mass post expedition vs. pre (**Figure 3.11A**). Similarly, numerical increases in VO_2 max corrected to total weight were observed in all bar 1 subject post expedition, however, this difference was not significant (**Figure 3.11B**). No difference was observed in maximal heart rate during exercise.

A significant increase was observed in RER. This was recorded at each percentile of the VO_2 max test and the area under the curve (AUC) for each subject was calculated. A 7.8 (± 3.6) % increase (p>0.01) in AUC for RER was observed post expedition compared to pre (p<0.01). The average (mean) response of the group is depicted in **Figure 3.11C**, with individual differences displayed in **Figure 3.11D.**

To examine whether a relationship existed between the identified changes in serum metabolites and the AUC for RER, these variables were correlated. No significant relationship was observed between Δ glucose peak integral (**Figure 3.12A**) or Δ fatty acid peak integral vs. Δ AUC RER (**Figure 3.12B**). However, the relationship displayed in **Figure 3.12B** appears to be indicative of a possible linear association between Δ fatty acid and Δ AUC RER, in spite of the high r^2 and p value (r^2 = 0.62, p=0.11). This would therefore be interesting to investigate further with higher subject numbers.

Table 3.3. Summary of changes in exercise parameters pre and post expedition.

Variable	Mean Pre (±SD)	Mean Post (±SD)	Difference (±SD)	P value
VO2 max (L/min)	3.2 (0.6)	3.5 (0.4)	0.2 (0.3)	0.163
VO_2 max (ml/kg/min)	42.1(4.9)	45.5 (3.8)	3.38 (5.3)	0.187
VO2 max (ml/kg lean tissue)	**50.4 (5.1)**	**56.1 (5.0)**	**5.8 (0.6)**	**0.0003*** **
Max heart rate (bpm)	191.6 (5.6)	189.6 (5.1)	-2.0 (6.8)	0.546
AUC RER	**8.85 (0.30)**	**9.54 (0.26)**	**0.68 (0.31)**	**0.007****
MVC (Nm)	204.5 (16.7)	226.5 (33.9)	22.0 (27.7)	0.062

Note: *VO_2 – pulmonary oxygen uptake; bpm-beats per minute; bpm-beats per minute RER-respiratory exchange ratio; AUC- area under the curve, MVC – maximal voluntary contraction; Nm- Newton meters. n=4-5, values presented as mean ± standard deviation, **denotes significance, p<0.01, ***denotes significance p<0.001.*

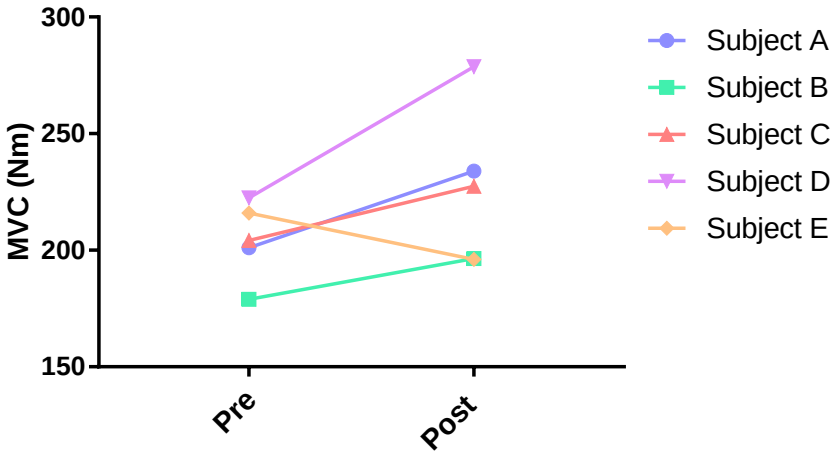

Figure 3.10. Maximal voluntary contraction pre and post expedition

Presented as individual values. No significant difference was observed pre vs post.

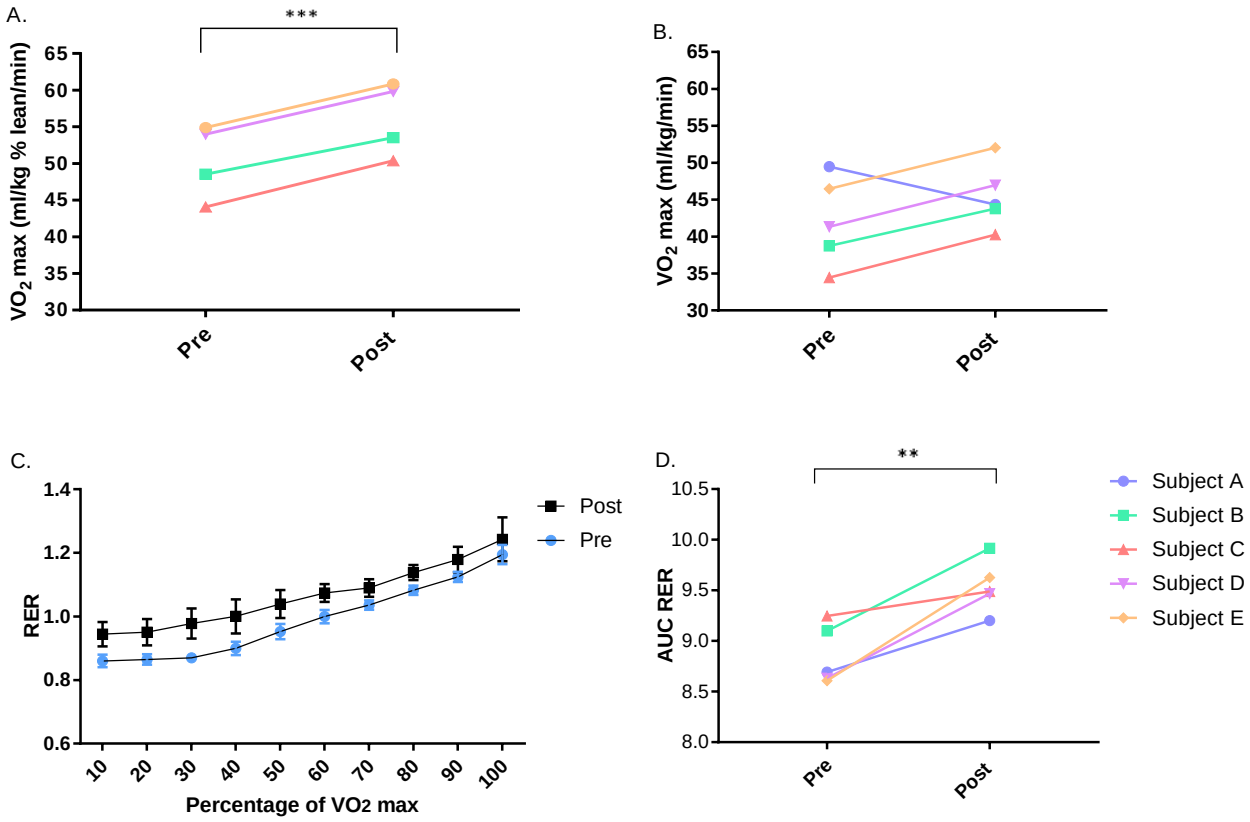

Figure 3.11. Maximal rate of oxygen consumption (VO2 max) and respiratory exchange ratio (RER)

As measured through an incremental exercise test, pre and post expedition, presented as individual values. ***A.*** *VO_2 max corrected to % lean mass* ***B.*** *VO_2 max corrected to total weight.* ***C.*** Average RER (± SD) presented at each 10th percentile of a VO_2 max test, **D.** Area under the curve (AUC) for RER both pre and post expedition values, presented for each subject. *Significance assessed in VO_2 max and RER AUC using a paired t test,* **p<0.01, ****p<0.001, n=4-5.*

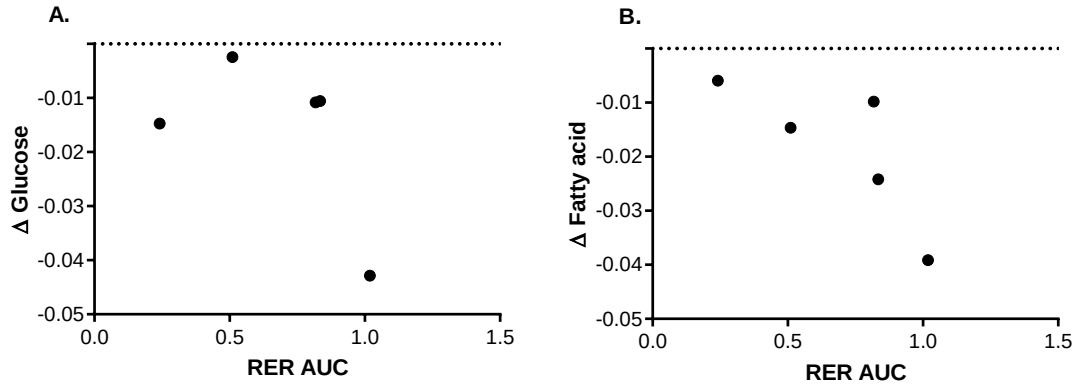

Figure 3.12. Correlation plots for Δ glucose (A) and fatty acid peak integrals (B) (pre: post expedition) vs. respiratory exchange ratio area under the curve (RER AUC).

Examined using Pearson correlation coefficient, n=5.

3.5 Discussion

The Antarctic winter is amongst the most extreme environments on earth and presents significant physiological challenges. Upon the Antarctic plateau, high altitudes (and so hypobaric hypoxia) are combined with monthly mean temperatures falling below -60°C. This pilot study aimed to investigate the effects of prolonged exposure to this environment upon an array of physiological parameters. Measurements obtained from subjects pre and post expedition revealed metabolic profile changes occurring alongside alterations to body composition, exercise capacity (corrected to lean mass) and lung function.

Assessment of serum metabolic profile and RER during incremental exercise pre and post expedition revealed evidence indicative of metabolic remodelling and possible shifts in substrate utilisation. Specifically, metabolomics analysis of serum demonstrated decreases in the peak integrals for glucose and a fatty acid CH_2 resonance. Alongside this is the increase in RER, which is thus suggestive of a shift towards carbohydrate oxidation during exercise.

The exact causes or consequences of these shifts are unclear. Given that dietary intake remained relatively constant throughout the expedition, this suggests that such shifts are provoked by environmental factors as opposed to dietary changes. However, this interpretation is limited as both dietary data and activity data are lacking from the time of pre-expedition, meaning there is no baseline measurement for either. The assumption is therefore made that these subjects sustained similar nutrient take and level of activity prior to the expedition as during.

The observed changes may instead be indicative of hypoxic and/or cold adaptation. Alterations in carbohydrate and fat metabolism have been identified as having a key role both in response to hypoxic (Horscroft et al., 2014) and cold exposure (Vallerand et al., 1989, Stocks et al., 2004). Indeed, results from the previous chapter go to support this, with significant shifts being identified in plasma glucose as well as various lipids in response to short term progressive hypoxic exposure. Given the nature of high altitude environments, this is inextricably linked to a drop in ambient temperatures. Together with the present study, these results therefore suggest changes in carbohydrate and fat metabolism play a key role in shaping the response to a combination of hypoxic and cold exposure.

Specifically relating to cold exposure, increasing RER has been reported in response to acute cold exposure (Vallerand et al., 1989), although this finding is not

consistent (Timmons et al., 1985). Similar disparity is also apparent in hypoxic studies, likely due to differences in duration and severity of hypoxic exposure (McClelland et al., 1998). No prior studies appear to have examined exercise RER measurements in response to such chronic exposure as is presented here.

This shift in metabolic signature may also be reflected through the observed changes in anthropometric measures. This revealed a decrease in % and kg of body fat and an increase in % lean tissue. As dietary intake remained constant, with proportions of fat, carbohydrates and protein as well as overall intake remaining within recommended daily levels (Trumbo et al., 2002), it again suggests such alterations resulted from environmental exposure as opposed to dietary changes. The loss of fat tissue may be indicative of alterations to lipid storage capacity. Indeed, results from Chapter 2 indicate that the processes of *de novo* lipogenesis may be impaired with progressive hypoxic and cold exposure. This concept would align well with the shifts away from fat towards carbohydrate utilisation, as indicated by the RER results of the present study. However, neither the causes nor consequences of these changes in body composition are clear.

Previous high altitude studies reveal mixed results regarding body composition changes, with some reporting an initial loss of fat mass followed by lean and others vice versa (Guilland et al., 1985, Boyer et al., 1984, Rose et al., 1988). Interestingly, these prior studies tend to observe that changes in body composition are accompanied by a loss of body weight, the degree of which increases with increasing altitude severity (Rose et al., 1988, Boyer et al., 1984, Guilland et al., 1985). For instance, Caucasian subjects exposed to 5400m demonstrated a 1.5-1.9kg loss in body weight, which increased to 3.4-4kg at 7100m (Boyer et al., 1984, Guilland et al., 1985). However, weight loss at altitude is not reported across all studies, with subjects being exposed to 3,454m for 28 days reporting no change in either body weight or fat mass (Jacobs et al., 2012). This therefore indicates that maintaining body weight becomes an issue at more extreme altitudes (above ~3500m) and may result from the commonly reported loss of appetite (Vats et al., 2004). The lack of weight change in the subjects of this present study, both during the expedition and measured pre and post, may therefore be due to the altitude exposure being at the lower end of the spectrum (2500m). The consistent nutrient intake reported by the present subjects suggests loss of appetite was not experienced. The lack of body weight change may also be reflective of the prolonged nature of the study, with body weight stabilising over the duration of the

expedition as subjects acclimatised, a trend indicated through body weight changes recorded throughout the expedition.

At a functional level, the apparent shift in metabolic signature and body composition were accompanied by significant improvements in VO_2 max corrected to % lean tissue. Although not significant, trends were also observed for increasing MVC and FVC in most subjects post expedition, the latter contributing to the significant increase in FEV_1/FVC. Together, these changes may indicate a possible training effect. This may be a consequence of increasing physical exertion, however it is not possible to derive such a conclusion in the absence of baseline activity levels and accurate measures of exercise severity. Equally, such measures could reflect potential benefits of hypoxic adaptation upon O_2 delivery, for instance resulting from increasing erythropoiesis and angiogenesis (Rodriguez et al., 1999, Shweiki et al., 1992). However, further investigation is required before a firm conclusion can be derived.

Given previous reports of the effects of extreme environmental exposure upon lung function, it may perhaps appear surprising that FVC tended towards an increase. Cold exposure is known to have a detrimental impact upon lung function (Cotes et al., 2009). In addition, prior altitude studies demonstrated a decrease in resting FVC levels, accompanied by no change in FEV_1 (Welsh et al., 1993, Ziaee et al., 2008). In the instance of the study conducted by Welsh and colleagues, this measure was taken at extreme altitudes (8,848m) and was linked to an increase in chest fluid due to an increase in both pulmonary blood volume and interstitial edema fluid (Welsh et al., 1993). The translation to the current study is therefore limited given the moderate height of altitude and the fact that spirometry measures were conducted at sea level, meaning altitude induced obstruction is not relevant.

Another anthropometric measurement noted to undergo a change that is somewhat set aside from metabolic or performance measures was spine BMD. This underwent a significant decrease post expedition. Although this decrease was slight, such minor changes have been related to increasing fracture risk, so are of high importance (Nguyen et al., 1993). Whilst the causes are not clear, there are numerous possibilities, including effects of hypoxia upon the regulation of bone density (Arnett et al., 2003, Utting et al., 2006) including HIF-1α regulation of osteoclast (Knowles, 2015). Other factors known to impact BMD include decreases in activity levels (Mazzeo et al., 1998, Vuori, 2001), which is not the case here given that subjects maintained a certain degree of activity throughout and in fact displayed an improvement in exercise parameters upon their return. A more plausible possibility is the

effect of dietary changes, particularly changes in Ca^{2+} (Kelly et al., 1990), vitamin C (Aghajanian et al., 2015) and D (Bischoff-Ferrari et al., 2004). Whilst energy intake was reported to remain constant throughout, details on Ca^{2+}, vitamin C and D intake were not recorded, meaning no conclusion can be drawn.

Another factor that may have altered BMD is the altered day-night cycle, with darkness prevailing in the Antarctic winter months. As most humans depend upon sunlight exposure to satisfy their vitamin D requirements (Holick, 2004), it is highly likely that the subjects of this study, with their prolonged lack of sunlight exposure, suffered from insufficient vitamin D levels. This would in turn likely be detrimental to maintenance of BMD.

3.5.1 Study limitations

This study presents a highly unique and novel exploration of the effects of an inhabitable environment upon human physiology. It employs a comprehensive characterisation of physiological changes. However, given that the main aim of the expedition was to cross Antarctica as opposed to conducting a robust scientific experiment, there are numerous limitations in the study design that in turn impact the ability to deduce meaningful conclusions from the data set.

Firstly, the small subject numbers severely limits statistical power, meaning that one outlier in a data set can have a profound effect upon the degree of significance. This was demonstrated in measures of VO_2 max corrected to total body weight and also MVC, whereby the response of 1 subject in the opposite direction to the rest of the group likely impacted the statistical outcome.

Secondly, the means by which physiological measures were taken markedly impacts interpretation. The majority of measures were taken in London pre and post expedition. Measures that are prone to rapid fluxes, including metabolic profile and to a lesser extent body composition and lung function, are thus unlikely to fully reflect the impact of the Antarctic winter environment. This is less of a concern for measures of MVC and perhaps also exercise performance, given that previous studies demonstrating maintenance of muscle energetics in response to altitude exposure were conducted a week after the subjects returned to the UK (Edwards et al., 2010).

The present study is therefore a considerable contrast to that presented in Chapter 2, where measures (including blood samples) were taken at altitude upon a large cohort undergoing a strictly controlled ascent profile.

3.6 Conclusion

This pilot study is the first to provide an in-depth examination of human physiology and metabolism in response to prolonged exposure to high altitude in the coldest environment on Earth. It has highlighted key areas of interest for future investigations into chronic hypoxic and extreme cold exposure. This includes a change in metabolic signature, involving alterations to both glucose and fatty acid homeostasis with a shift towards increased reliance on carbohydrate metabolism during exercise and a reduction in body fat. This was accompanied by an improvement in VO_2 max corrected to % lean mass. In addition, spine BMD and lung function measures were identified as novel parameters of interest.

4 **Chapter 4 (Study 3):** PPARα independent effects of dietary nitrate supplementation on skeletal muscle mitochondrial function in hypoxia.

4.1 Introduction

All oxidative tissues are dependent upon a continuous supply of O_2 to maintain energetic and redox homeostasis. As already discussed, an inadequate supply of O_2, as occurs in response to hypoxic exposure thus requires remodelling of metabolic processes to ensure the demand for ATP is met. Skeletal muscle is particularly interesting in this respect given its high capacity for respiration and for altering metabolic rates. The latter can be adjusted in response to exertion or other features such as mitochondrial density or substrate preference (Murray, 2009, Kiens et al., 2011).

As aforementioned, the metabolic remodelling of skeletal muscle in response to hypoxic exposure remains a debatable topic. To summarise, studies examining the effects of environmental hypoxia in humans and rodents have demonstrated impairment of skeletal muscle mitochondrial function, with an attenuation of oxidative processes including β-oxidation (Viganò et al., 2008, Levett et al., 2012, Roberts et al., 1996, Abdelmalki et al., 1996, Morash et al., 2013, Galbès et al., 2008), TCA cycle activity (Viganò et al., 2008, Green et al., 1989, Abdelmalki et al., 1996, De Palma et al., 2007, Pastoris et al., 1995, Magalhaes et al., 2005) and oxidative phosphorylation (Viganò et al., 2008, Levett et al., 2012, McClelland et al., 2002, De Palma et al., 2007, Pastoris et al., 1995, Jacobs et al., 2013, Magalhaes et al., 2005, Gamboa et al., 2010) (see 1.2.4 for details). The effects upon glycolytic processes are less clear, with some studies demonstrating an increase in glycolytic biomarkers such as lactate dehydrogenase activity, (Green et al., 2000) and some a decrease (Green et al., 1992, Viganò et al., 2008, Green et al., 1989, Levett et al., 2012). This thus throws into doubt the proposal that the downregulation of oxidative processes including fatty acid oxidation is attenuated for by a compensatory shift towards glycolysis, as has been shown in the heart, for instance (Essop, 2007, Cole et al., 2016).

Downregulation of oxidative processes appears to be occurring alongside maintenance of mitochondrial density in the short term (≤14 days). This is altered in response to medium (≤42 days) or long term (42d) exposure, where a significant loss of mitochondrial density has been observed (Horscroft et al., 2014). It has therefore been suggested that hypoxia-induced remodelling of mitochondrial pathways precedes a loss of mitochondrial density (Horscroft et al., 2014).

Developing a means of attenuating the metabolic stress of hypoxia upon mitochondrial functioning would be highly beneficial for aiding human adaptation/survival, either in response to environmental exposure or pathological states. For this, as outlined in section 1.2.7, the potential of dietary nitrate supplementation was investigated. Specifically in this chapter, the focus is upon the effects of nitrate supplementation upon mitochondrial function and potential signalling mechanisms.

Although the potential for dietary nitrate to alleviate hypoxic induced metabolic stress has been recognised, the signalling mechanisms of nitrate action in hypoxia remain unclear. A mechanism outlined previously in skeletal muscle was reliant upon a master regulator of fatty acid oxidation PPARα. Nitrate supplementation was demonstrated to enhance fatty acid oxidation capacity (palmitoyl carnitine stimulated respiration) in rat skeletal muscle through PPARα (Ashmore et al., 2015b). Expression levels of PPARα were shown to increase dose dependently with nitrate supplementation, a response coupled with a rise in PPARα-DNA binding activity and downstream effectors including carnitine palmitoyl transferase 1 (CPT1) (Ashmore et al., 2015b). This mechanism was mediated through NO activation of the sGC-PKG-cGMP secondary messenger signalling system, with inhibition of sGC and the cGMP downstream effector PKG shown to abolish gene expression changes (Ashmore et al., 2015b).

This response is particularly interesting when considering the importance of PPARα signalling upon metabolic control, as discussed in section 1.2.4. A consensus on the role of PPARα in hypoxia is far from being reached. In particular, the role of PPARα in hypoxic skeletal muscle is yet to be sufficiently investigated. Equally, the effects of nitrate supplementation upon PPARα signalling in hypoxia is yet to be explored in depth.

4.2 Aims and objectives

The aims of this study were to investigate potential for dietary nitrate supplementation to preserve skeletal (soleus) muscle mitochondrial function in hypoxia and the involvement of PPARα in this process. For this, a mouse model of PPARα genetic ablation ($PPAR\alpha^{-/-}$) was used. Assessment of mitochondrial function in permeabilised mouse skeletal muscle fibres was performed following four weeks of severe hypoxic (10% O_2) exposure with dietary nitrate supplementation. Alongside this was analysis of numerous proteins related to skeletal muscle metabolic function. Analysis focused on investigating the following objectives:

1. Does nitrate supplementation protect skeletal muscle mitochondria function and aid hypoxic acclimatisation?

2. Is PPARα required for this effect?

An overview of study interventions is outlined in **Figure 4.1**.

4.3 Hypothesis

Dietary nitrate $^{-}$ supplementation would preserve skeletal muscle mitochondrial function in hypoxic conditions and that this process would be reliant upon PPARα.

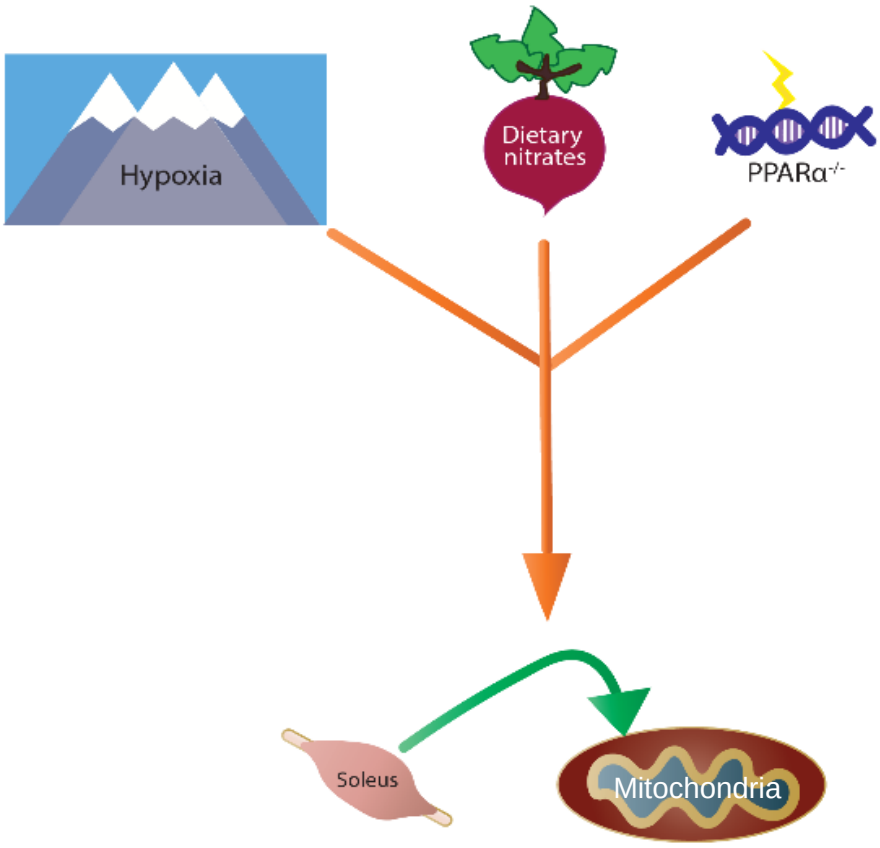

Figure 4.1. Diagrammatic summary of study interventions.

The examination of the interaction between hypoxia, dietary nitrate (NO_3^-*) and PPARα on skeletal muscle metabolism, with a focus upon mitochondrial function in the soleus.*

4.4 Methodology background

Analysis of mitochondrial function is central to the assessment of intracellular energy metabolism (Kuznetsov et al., 2008). Below is given a description of the analysis of mitochondrial function performed in this study. This was assessed *in situ* within selectively permeabilised skeletal muscle fibres using a substrate/inhibitor titration to examine select mitochondrial pathways/complexes. The fundamental principles of this polarographic O_2 sensing technique are outlined below and precede the detailed methodology of this study.

4.4.1 Respirometry

Cellular respiration is an exergonic reaction during which substrates are oxidised and the electron acceptor O_2 is consumed in exchange with the environment (detailed in section 1.2.1). In this study, the consumption of O_2 for mitochondrial respiration was measured in the soleus using respirometry. The soleus was chosen for a number of reasons. Whilst mouse skeletal muscle has a predominating fast twitch fibre type, the soleus does have a relatively higher type 1 fibre make up, in turn leading to a high mitochondrial content (Lin et al., 2002). Additionally, the effects of nitrate supplementation were demonstrated previously in this muscle in rats (Ashmore et al., 2015a) and the assays performed here were shown to work effectively in mouse soleus using Clark type O_2 electrodes (Morash et al., 2013).

Respirometry experiments were performed using a Clark-type electrode (Strathkelvin Instruments, UK), which consists of a probe whose tip is exposed to a cathode and anode. The electrodes are put into electrolyte (10mM KCl). Upon polarisation of the anode and cathode, O_2 reacts with water at the cathode and chloride reacts with silver at the anode simultaneously, as follows:

$$\boldsymbol{O_2 + 2H_20 + 4e^- \rightarrow 4OH^-}$$

Equation 4.1. Reaction at the cathode

$$\boldsymbol{4Ag + 4\text{-}Cl^- \rightarrow 4AgCl + 4e^-}$$

Equation 4.2. Reaction at the anode

The result of these reactions is a current flow. For each O_2 molecule reduced, 4 e^- of current will flow through the circuit. This current varies linearly with O_2 concentration. The system is calibrated with atmospheric O_2 (distilled water added to the chamber and allowed to equilibrate with atmospheric O_2) and in the presence of an O_2 scavenger (sodium

dithionite). Thus, the detected current is converted to an estimation of O_2 concentration within experimental range. As the electrodes are located under an O_2 permeable membrane, this ensures other species do not interfere with the reactions.

Experiments were performed within two water-jacketed chambers in duplicate to control for any differences in electrode performance. Respiratory medium was put into the chambers and the biological sample added to this. The chambers were subsequently capped, meaning the area for gaseous exchange is minimised as the liquid phase meets the gaseous phase within the capillary tube (**Figure 4.2**). Metabolic substrates and inhibitors were added to the chamber in saturating concentrations via the capillary tube, where they subsequently titrate with the medium. The temperature of the chambers was regulated at 37°C via a water bath, via the water-jacketing system, as temperature is known to have a large effect on mass corrected respirometry rates of biological samples (Hughes, 1965).

The cathode consumes O_2 at a rate determined by O_2 in the chamber medium, which is in turn derived from O_2 flux into the sample. Thus, negative changes in O_2 concentration are an indication of O_2 consumption by the tissue and are measured as O_2 flux (JO_2). The majority of this consumption is mitochondrial and so falling levels can be attributed to mitochondrial respiration. The electrical current, therefore O_2 concentration is measured over time and a steady state time derivative of O_2 concentration is determined for each respiratory state.

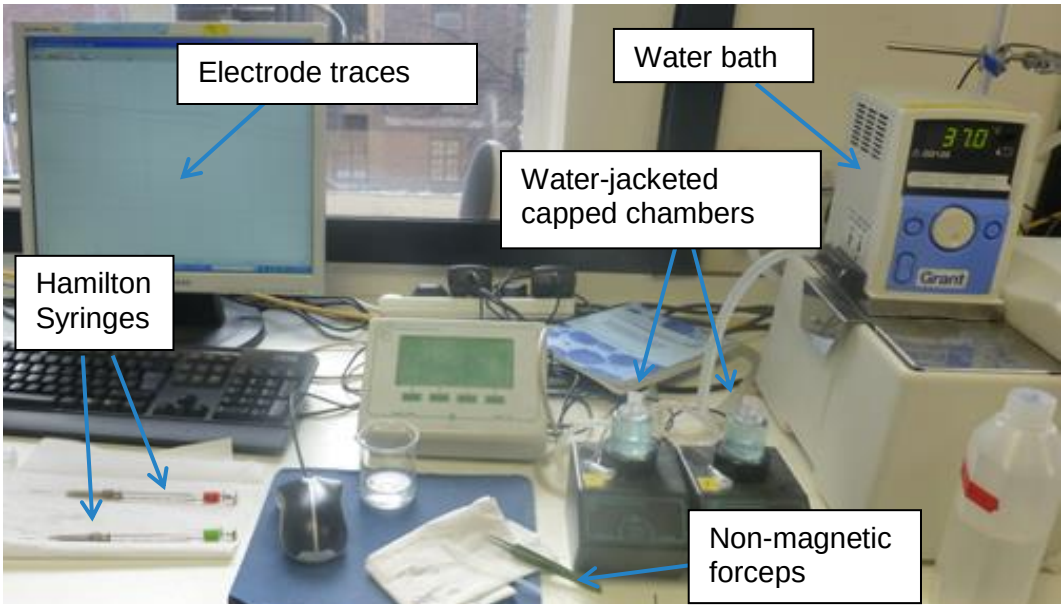

Figure 4.2. The respirometry experimental set up.

Experiments were run simultaneously in the two water-jacketed chambers, with water being heated via the water bath. Fibre bundles were added to the chambers using non-magnetic forceps, to avoid displacing the magnetic stirrer within the chamber. Substrates/inhibitors were added to the chambers using Hamilton syringes (green for substrates, red for inhibitors). The resulting signal detected by the electrodes were depicted on the screen, as shown.

4.4.2 Sample preparation

There are few options for the preparation of biological samples for respirometry. The most physiologically relevant of these methods is the use of intact tissue. This, however, has its limitations in that the main mitochondrial effectors are unable to penetrate the cell membrane (Kuznetsov et al., 2008). The presence of endogenous ATP means that, in the absence of a suitable inhibitor such as oligomycin, ATP synthase is constitutively active. These issues can be avoided by the use of either isolated mitochondria or cell permeabilisation. The latter was used in this study due to ease and speed of sample preparation.

Selective cell membrane permeabilisation was achieved using the detergent saponin. This chemical permeabilisation agent has a hydrophobic steroid core, causing a high affinity for cholesterol. As the plasma membrane contains a greater proportion of

cholesterol per phospholipid in comparison to the mitochondrial outer and inner membranes (0.5 mol vs. 0.07 and 0.01 mol respectively), saponin selectively attacks the plasma membrane, leaving the mitochondrial membranes intact (Kuznetsov et al., 2008). The pores created in the plasma membrane allow for the cytosol and all its solutes, including metabolites and cytosolic enzymes such as lactate dehydrogenase, to be washed out. The composition of the intracellular space becomes equilibrated with incubation medium, meaning functionally intact mitochondria of these permeabilised preparations respond quickly to changes in concentrations of substrates and inhibitors added to the medium (Kuznetsov et al., 2008).

4.4.3 Metabolic substrate/inhibitor assays

The metabolic substrates or inhibitors, added in series, enable the respiratory capacity of different components of the mitochondria to be assessed, including: β-oxidation, TCA cycle and electron transfer chain. In each assay, O_2 consumption/flux (JO_2) was measured in the following states:

1. **Leak state respiration (LEAK)** – JO_2 was first measured in the presence of substrates, but in the absence of adenylates (so no ADP). In this state, protons and electrons are extracted from respiratory substrates during their passage through the TCA cycle and/or β-oxidation. These are accepted by the redox cofactors nicotinamide adenine dinucleotide (NAD) and flavin adenine dinucleotide (FAD) and subsequently donated to the electron transfer chain/system (ETS). Transport of electrons along this chain of complexes generates the energy required to pump protons into the intermembrane space. This results in the generation of a proton motive force ($\Delta\mu H^+$) across the inner mitochondrial membrane, driving protons back into the mitochondrial matrix. Passage of protons back across the inner mitochondrial membrane in this state cannot occur via ATP synthase due to the absence of ATP. It therefore occurs either by proton leak across the membrane itself or proton slip via uncouplers or the mitochondrial complexes. The resulting dissipation of $\Delta\mu H^+$ will drive a low level of flux through the ETS, leading to consumption of the electron acceptor O_2 at complex IV. Thus, $\Delta\mu H^+$ in the LEAK state is not used to drive ATP synthesis. The resulting JO_2 is due to non-phosphorylating electron transfer, so is indicative of maximal $\Delta\mu H^+$ dissipation in the absence of ATP synthesis and is limited by proton leak. This measure may reflect inherent physiological inefficiencies that

are associated with oxidative phosphorylation. However, non-phosphorylating respiration is also thought to have an imperative function in maintaining low ROS production (Nicholls et al., 2013) as well as regulating lipids as fuel substrates (Samec et al., 1998, Rousset et al., 2004) .

2. **Oxidative phosphorylation capacity, (OXPHOS)** – ADP was then added in saturating concentrations, enabling the activity of ATP synthase. Passage of protons via ATP synthase is a path of lower resistance for protons to re-enter the matrix, causing an increased dissipation of $\Delta\mu H^+$ and so in turn a greater JO_2. In this state, JO_2 is limited by either electron donation to the ETS or the OXPHOS capacity of ATP synthase. In this study, ADP was added to differing substrate combinations in assay 1 and 2 to assess the control of various pathways over OXPHOS.

Assay 1

The aim of this assay was to assess the oxidative metabolism of the principle substrates of mitochondrial oxidation: fats and carbohydrates, specifically, long chain fatty acid palmitoyl carnitine and pyruvate respectively.

1. **Malate:** This was added at the start of both assays. Malate is an anion that cannot permeate the lipid bilayer of membranes, therefore is transported into the mitochondria via di or tri-carboxylate carriers or 2-oxoglutarate exchanger. In the matrix, it is converted to oxaloacetate (OAA) and fumarate by the action of malate dehydrogenase and fumarase respectively. In the absence of acetyl CoA, OAA cannot be converted to citrate, therefore accumulates and inhibits succinate dehydrogenase. No further TCA cycle activity can occur and high respiratory capacities are not sustainable.
2. **Palmitoyl carnitine:** Palmitoyl carnitine enters the mitochondrial matrix via carnitine-acylcarntine translocase. Once in the matrix, it is broken down to acetyl CoA via β-oxidation. In this process, protons and electrons will be accepted by NAD^+ to form NADH and FAD to form $FADH_2$. NADH will donate its electrons to complex I and $FADH_2$ to electron transfer flavoprotein (ETF), which lies down stream of complex II. JO_2 here is limited by the flux of electrons from β-oxidation, so is a measure of capacity for β-oxidation, which was investigated in both LEAK (**Figure 4.3A**) and OXPHOS (**Figure 4.3B**) states in this study. Dietary nitrate were shown previously

to enhance the oxidation capacity for this long chain fatty acid in normoxia, a process reliant upon PPARα mediated mechanisms (Ashmore et al., 2015b).

3. **ADP addition**
4. **Pyruvate:** The end product of glycolysis pyruvate, a monocarboxylic acid, passes into the mitochondrial matrix by the pyruvate carrier in exchange for OH^-. Here, it is converted to acetyl CoA by pyruvate dehydrogenase. Electrons and protons released from this process will be accepted by NAD^+ forming NADH, which will pass to complex I. In the presence of OAA, derived from the previous addition of malate, acetyl CoA is then converted to citrate. JO_2 at this stage will be limited by electron supply, which is controlled by the activity of TCA cycle enzymes (**Figure 4.3C**). It is thought that JO_2 recorded following the addition of pyruvate reflects the capacity of TCA cycle flux. However, electron flux will also be influenced in some way by the previous addition of palmitoyl carnitine due to convergence of electron flow at coenzyme Q/ubiquinone.

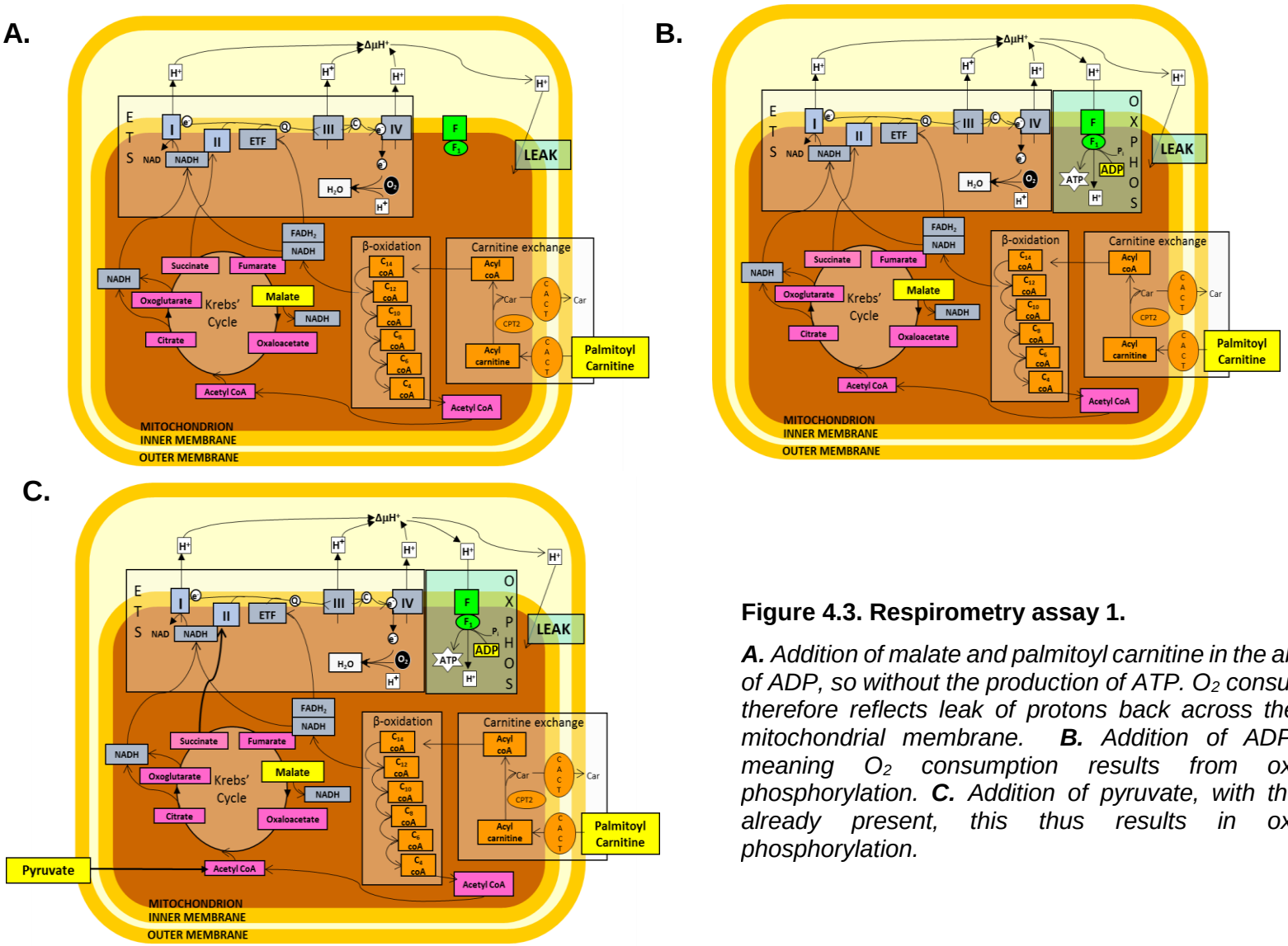

Figure 4.3. Respirometry assay 1.

A. *Addition of malate and palmitoyl carnitine in the absence of ADP, so without the production of ATP. O_2 consumption therefore reflects leak of protons back across the inner mitochondrial membrane.* ***B.*** *Addition of ADP, thus meaning O_2 consumption results from oxidative phosphorylation.* ***C.*** *Addition of pyruvate, with the ADP already present, this thus results in oxidative phosphorylation.*

Assay 2

The aim of this substrate/inhibitor assay was to assess the function of mitochondrial complexes I and II.

1. **Malate:** See above
2. **Glutamate:** Glutamate is transported into the mitochondrial matrix via the glutamate-aspartate carrier. Here, it enters directly into the TCA cycle by combining with OAA to form α-ketoglutarate. NADH formed from this process will donate its electrons to complex I. Oxoglutarate/α-ketoglutarate is subsequently dehydrogenised leading to further NADH production, which will also feed into complex I. Complex II function will be inhibited by the production of fumarate from malate through product inhibition. JO_2 is thus limited by electron flux through complex I, so is indicative of complex I capacity. This was measured both in the LEAK (**Figure 4.4A**) and OXHOS (**Figure 4.4B**) states in this study.
3. **ADP addition**
4. **Rotenone:** Rotenone interferes with the flow of electrons by preventing the transfer of electrons from complex I to ubiquinone.
5. **Succinate:** The addition of saturating concentrations of succinate will drive the succinate fumarate reaction forward, leading to maximal electron donation at succinate dehydrogenase/complex II. JO_2 in this state is limited by complex II activity and so reflects OXPHOS capacity of complex II (**Figure 4.4C**).

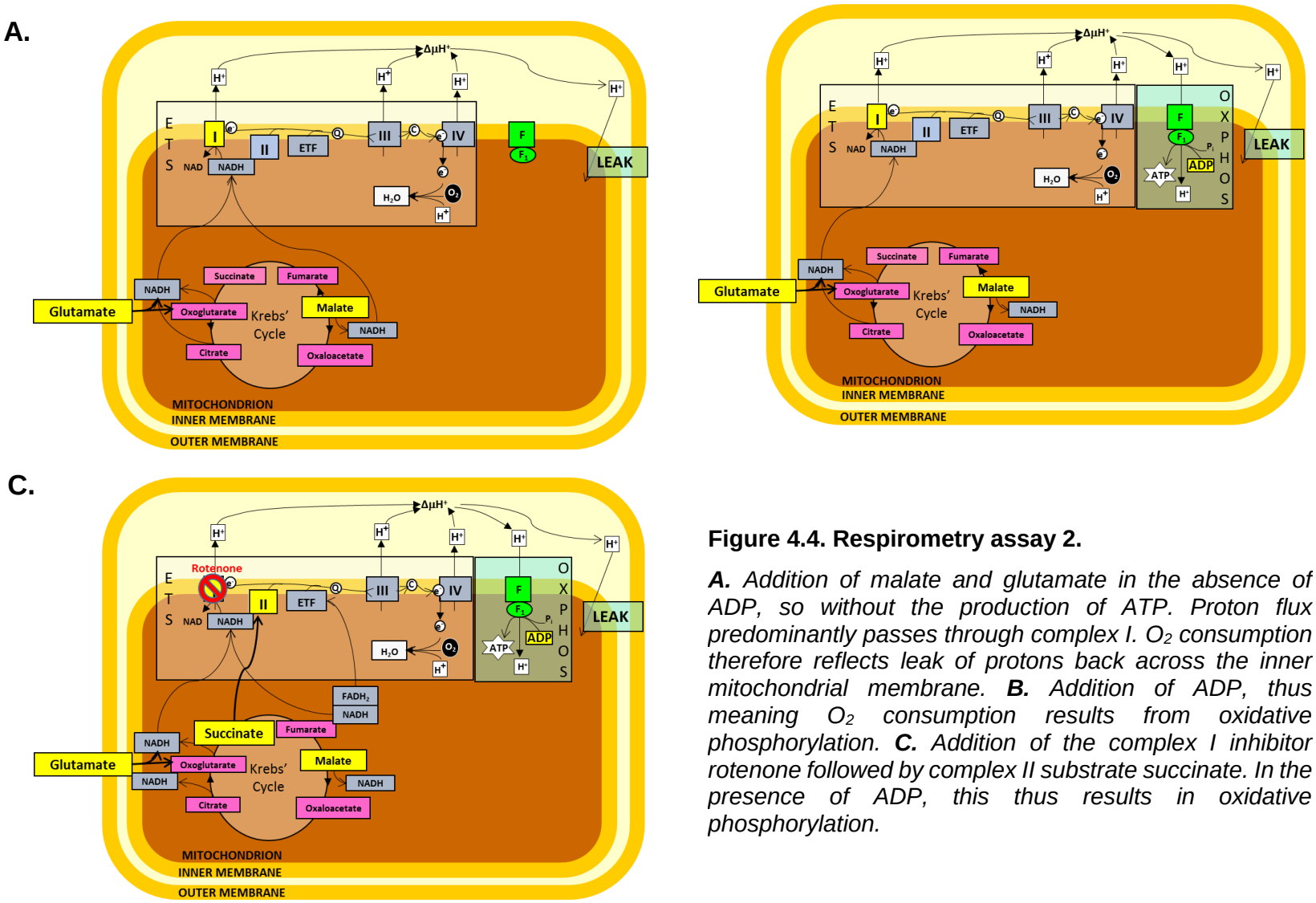

Figure 4.4. Respirometry assay 2.

A. *Addition of malate and glutamate in the absence of ADP, so without the production of ATP. Proton flux predominantly passes through complex I. O_2 consumption therefore reflects leak of protons back across the inner mitochondrial membrane.* ***B.*** *Addition of ADP, thus meaning O_2 consumption results from oxidative phosphorylation.* ***C.*** *Addition of the complex I inhibitor rotenone followed by complex II substrate succinate. In the presence of ADP, this thus results in oxidative phosphorylation.*

Membrane integrity check

At the end of each assay of this study, mitochondrial membrane integrity was assessed following the addition of cytochrome c (Cyt c). Cyt c is a loosely bound peripheral protein of the mitochondrial inner membrane that shuttles electrons from complex III to complex IV. If the inner membrane remains intact, the addition of exogenous cytochrome c will not affect respiration. In the instance of inner membrane damage, however, endogenous cytochrome c is released from the intermembrane space, inhibiting electron transfer to complex IV, thereby inhibiting respiration. The addition of exogenous cytochrome c will thus stimulate respiratory rate and restore maximal ADP stimulated respiration. This thus acts as a control measure as any tissue that consumed O_2 following cytochrome c addition at a rate that exceeds 15% of the rate derived from addition of the previous substrate was discounted. This thus ensured any fibres damaged in the preparation were removed from analysis.

Ratios

From the respirometry data derived from the assays described above, it is possible to calculate oxidative coupling efficiency using the following ratios for each assay.

Assay 1

To measure the efficiency of mitochondrial coupling during oxidation of a long chain fatty acid (palmitoyl carnitine), the following ratio between LEAK and OXPHOS states was calculated:

$$\boldsymbol{OCE1 = 1 - \frac{L_{LCFA}}{P_{LCFA}}}$$

Equation 4.3. Oxidative coupling efficiency, assay 1 (OCE1).

L_{LCFA}= LEAK state for long chain fatty acid oxidation
P_{LCFA}= OXPHOS capacity for long chain fatty acid oxidation

Assay 2

For measuring the coupling efficiency of complex I dependent oxidation, the following ratio between LEAK and OXPHOS states was calculated:

$$\boldsymbol{OCE2 = \frac{L_{Ci}}{P_{Ci}}}$$

Equation 4.4. Oxidative coupling efficiency, assay 2 (OCE2)

L_{Ci} = LEAK state, complex I
P_{Ci} = OXPHOS state, complex I

4.5 Study methodology

All animal work in this study was conducted in accordance with UK Home Office regulations under the Animals in Scientific Procedures Act. Protocols were performed by a personal licence holder under a project licence, and had received prior approval from the University of Cambridge ethical review board.

To investigate the role of PPARα, a PPARα genetic ablated (PPARα$^{-/-}$) mouse strain was utilised. The first PPARα$^{-/-}$ mouse with a 129Ev/Sv genetic background was generated by homologous recombination, whereby exon 8 of the ligand-binding domain was disrupted (Lee et al., 1995). Mice homozygous for this mutation lack the PPARα protein and fail to illicit the peroxisome proliferator pleiotropic response when challenged with the PPARα agonist WY-14,643. They are viable, healthy and fertile suggesting PPARα is not essential for embryonic development. Mice used in this study were kindly donated by Professor Kieran Clarke (Physiology, Anatomy and Genetics, University of Oxford).

For an overview of study design, see

Figure 4.5 below. Male wild-type 129Ev/Sv (n= 42) and PPARα-/- (n=42) were housed in conventional cages from birth in a temperature (23°C) and humidity controlled environment with a 12h/12h light/dark cycle. 21 days (d) after birth, mice were weaned and pair housed. 38 ± 4d after birth, mice were provided with a standard quality-controlled diet RM1 (E) (65.0% carbohydrate, 13.1% crude protein, 3.5% crude fat, 10mg kg-1 NO3-, Special diet services) and distilled water ad libitum.

At 6 weeks of age, mice from both genotypes were randomly assigned to receive drinking water supplemented either with 0.7mM sodium chloride (NaCl, Sigma 38979) or 0.7mM sodium nitrate ($NaNO_3$, Sigma 71752) for the remainder of the study. The former was used as a control to nullify the effects of the sodium intake. A concentration of 0.7mM was chosen as this was the same nitrate concentration shown previously to enhance β-oxidation (Ashmore et al., 2015b) and to effectively increase plasma nitrate concentration in rodent models (Ashmore et al., 2015a, Ashmore et al., 2014, Ashmore et al., 2015b).

One week following the initiation of $NaNO_3$ or NaCl treatment, mice were again randomly assigned either to remain under normoxic conditions (21%O_2) or be housed in hypoxic conditions (10% O_2) in a normobaric hypoxia chamber (PFI Systems Ltd., Milton Keynes, UK). Mice remained in these conditions for four weeks. Nitrate treatment was initiated 7d prior to hypoxic exposure in order to normalise circulating nitrate levels prior to

hypoxic exposure. Body mass, food and water intake were measured upon initiation of treatment, and then weekly henceforth.

Mice were killed 80 ± 4 days after birth by dislocation of the neck, so the use of pharmaceuticals was avoided. From each mouse, one soleus was excised and placed in ice cold biopsy preservation solution (BIOPS) (**Table 4.1**) ready for respirometry experiments. The second soleus was put into a cryovial and snap frozen in liquid nitrogen, ready for western blotting experiments. A drop of blood was taken from the tail vein and loaded into a microcuvette and haemoglobin concentration analysed using a HemoCue Hb 201 Analyzer (Quest Diagnostics, Sweden).

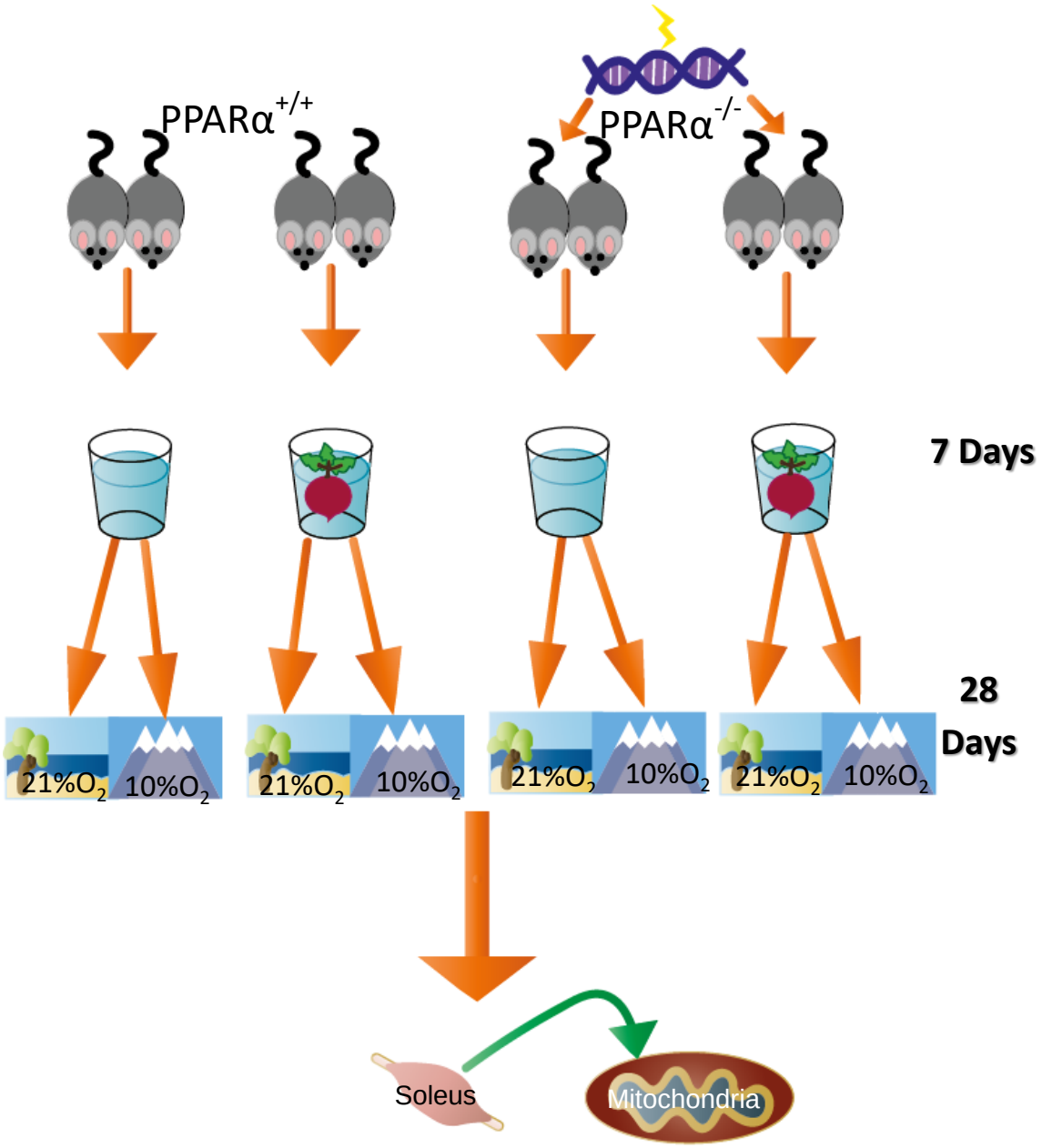

Figure 4.5. A schematic of study design.

At 6 weeks of age, PPARα$^{+/+}$ (n=42) and PPARα$^{-/-}$ (n=42) mice were randomly assigned to receive drinking water supplemented either with 0.7mM sodium chloride (NaCl) or 0.7mM sodium nitrate ($NaNO_3$) for 7 days, given ad libitum. This treatment was continued during 28 days exposure to either normoxic (21%O_2) or hypoxic (10%O_2) conditions. Mice were subsequently sacrificed and the soleus muscle excised for examination.

Table 4.1. Respirometry solutions

Solution	Constituent	Final conc (mM)	Final pH
Biopsy preservation solution (BIOPS)	CaK_2-EGTA	2.77	7.10
	K_2-EGTA	7.23	
	$MgCl_2.6H_20$	6.56	
	Taurine	20	
	Na_2Phosphocreatine	15	
	Imidazole	20	
	Dithiothreitol	0.5	
	MES hydrate	50	
	Na_2ATP *	5.77	
Mitochondrial respiration medium (MiR)	EGTA	0.5	7.4
	$MgCl_2.6H_2O$	3	
	K-lactobionate	60	
	Taurine	20	
	KH_2PO_4	10	
	HEPES	20	
	Sucrose	110	
	Defatted BSA	1g L^{-1}	

Note: *The above constituents were dissolved in distilled water. The pH was altered with drop-wise addition of KOH. Final solutions were filtered, divided into 35ml aliquots and stored at -80°C until use. * Added after thawing.*

4.5.1 Soleus muscle preparation

Fat and connective tissue were removed and the soleus dissected into 4 thin fibre bundle sections in ice cold BIOPS, as shown in **Figure 4.6** below. Care was taken during the dissection not to damage fiber integrity and so avoid disrupting mitochondrial structure.

.

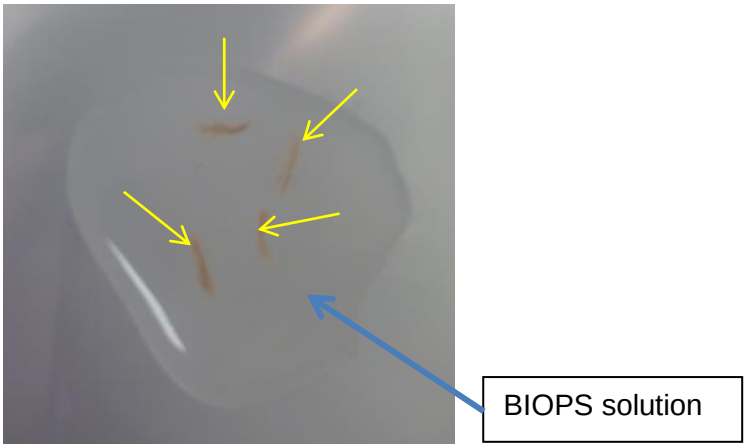

Figure 4.6. A picture of soleus muscle dissection

Dissection was performed in BIOPS solution on a petri dish that was placed on top of ice. Here, the fat and connective tissue have been removed and the muscle dissected into 4 bundles, as indicated by the arrows. Two of these bundles were used for assay 1 and two for assay 2. Following dissection, the fibre bundles were transferred to cryovials for washing in MiR solution.

Fibre bundles were incubated with gentle rocking for 20mins at 4°C in 1.5ml BIOPS supplemented with 15µl of 5mg/L^{-1} saponin (Sigma Aldrich, 47036) to achieve selective cell membrane permeabilisation, leaving the mitochondrial membrane intact (Kuznetsov et al., 2008). Following permeabilisation, the fibres were washed three times with 1ml of fresh respiration medium (MirR, **Table 4.1**) for 5 minutes per wash at 4°C with gentle rocking.

The wet weight of the fibre sample was measured before respirometry analysis. The fibre bundle was first blotted dry on filter paper before being weighed on a microbalance (Mettler Toledo). To ensure consistency, each bundle weighed between 0.5-1.5mg.

4.5.2 Soleus respirometry assays

For respirometry analysis, fibre bundles were added to 500µl atmospheric O_2 equilibrated MiR maintained at 37°C in a water-jacketed Clark-type electrode chamber

(Strathkelvin Instruments, Motherwell, UK). Respiration rates were analysed in two assays by substrate or substrate/inhibitor titrations. Two fibre bundles were used per assay, run simultaneously, 1 per chamber. Measurements taken on the Strathkelvin were normalised to the wet weight of the tissue and volume of fluid in the chamber.

Assay 1

This assay was adapted from that described previously (Heather et al., 2012), with the aim of examining the oxidative metabolism of long chain fatty acids and that of carbohydrates. JO_2 was measured after addition of each of the following substrates once steady state was reached:

- Malate (2mM) and palmitoyl carnitine (40µM) (LEAK)
- Palmitoyl carnitine
- ADP (10mM) was then added to stimulate ATP synthesis (OXPHOS).
- Pyruvate (5mM) (OXPHOS).
- Cytochrome c (10µM) was added in order to assess the integrity of the mitochondrial membrane.

Assay 2

This assay was again adapted from previously described protocols (Pesta et al., 2011, Jacobs et al., 2012), with the aim of assessing complex I and II function. JO_2 was measured in steady state response to the addition of the following:

- Malate (2mM) and glutamate (10mM) (LEAK at complex I)
- ADP (10mM), ATP synthesis stimulated (OXPHOS complex I)
- Rotenone (0.5µM), potent complex I inhibitor
- Succinate (10mM), complex II substrate (OXPHOS, complex II).
- Cytochrome c (10µM)

4.5.3 Tissue homogenates preparation

Once the respirometry assays were complete the contents of the electrode chambers were combined and transferred to a beaker, this included the remaining tissue and the MiR solution. The chambers were then washed in MiR to ensure all the tissue was collected. This was added to the beaker making a total volume of 2ml. 20mg of protease inhibitor (cOmplete Protease Inhibitor Cocktail, Roche) was added to this solution along with 20µl Triton X-100 (1%). This was then homogenised at 25,000rpm for 30s using a Polytron (PT-

10-35 GT Kinematic Inc. Switzerland). 1ml of the resulting homogenate was frozen at -80°C to be used for determination of CS activity and fibre type.

4.5.4 Citrate synthase (CS) activity

CS activity in the tissue remaining from respirometry experiments was measured as described previously (Houle-Leroy et al., 2000, Morash et al., 2013) by using a spectrophotometer and measuring changes in absorbance of light over specific lengths of time.

CS assay

100µl of the homogenised sample recovered from respirometry was added to 825 µl CS assay buffer (20 mM Tris (Fisher BP152-1), 0.1 mM 5,5'-dithiobis-2-nitrobenzoic acid (DTNB, Sigma D8130), pH 8.00) and 25µl of 12 mM Acetyl CoA (Sigma A2056). A magnetic stirrer was added to the cuvette, before warming to reaction temperature (37°C) for 3 minutes in the spectrophotometer (Evolution 220, Thermo Scientific). Baseline measurements were taken for 3 mins before 50µl of 40mM oxaloacetate (40mM oxaloactete, Sigma; 0.5M TEA-HCl buffer*, dH2O) was added. This induced the following reactions:

$$Acetyl\ coA\text{-}SH + Oxaloacetate + H_2O \rightarrow coA\text{-}SH + Citrate$$

Equation 4.5. Citrate synthase assay reaction 1.

$$coA\text{-}SH + DTNB \rightarrow TNB^{2-} + co\text{-}S\text{-}S\text{-}TNB$$

Equation 4.6. Citrate synthase assay reaction 2.

Reaction 1 is catalysed by CS, thus meaning its rate is dependent on CS activity within the sample. This is coupled to reaction 2 as the product coASH reacts with DTNB to produce the absorbing substance TNB^{2-}. This was quantified by measuring the absorbance of light at a wavelength of 412nm for 9 minutes following the addition of oxaloacetate. Recordings were taken once the reaction reached a steady state. The baseline recordings were subtracted from this reaction rate to calculate the enzyme-dependent rate of absorbance change. The following reaction was used to calculate enzyme activity:

$$\boldsymbol{J = \frac{r(A) \times V}{l \times \varepsilon}}$$

Equation 4.7. Calculation of citrate synthase enzyme activity.

J: *Rate of reaction (μmol min^{-1})*

$r(A)$: *Rate of absorbance change (min^{-1})*

V: *Reaction volume (ml)*

l: *Light path length (cm)*

ε: *Extinction coefficient (ml μmol^{-1} cm^{-1})*

The extinction coefficient, ε, was 13.6 and 6.22 ml μmol^{-1} cm^{-1} for DTNB.

2mM acetyl CoA was then added and measurements taken for 6 minutes to confirm the CS reaction had reached saturation. A negative control was performed to ensure the reaction was due to CS activity.

4.5.5 Soleus muscle myosin heavy chain (MyHC) isoform determination

Skeletal muscle is a highly heterogeneous tissue consisting of a variety of slow and fast fibre types. Major differences between fibre types, such as twitch speed and metabolic

substrate utilisation, are closely related to their myosin composition (Schiaffino et al., 2011). Myosin filaments, a key component of the sarcomere, consist of multiple myosin molecules, which in turn comprise of two heavy chains and four light chains. Myosin heavy chain (MyHC) is thus a major component of the contractile apparatus of striated muscle. It is encoded for by a multigene family, the expression of which is dependent upon tissue type and developmental stage, with multiple MyHC genes being expressed in skeletal muscle (Mahdavi et al., 1987). In mouse muscle, the spectrum of pure (non-hybrid) fibre types includes the following: slow type I, fast type IIA, B and X (Schiaffino et al., 2011) . Determining the MyHC composition of skeletal muscle is thus an informative means of distinguishing muscle fibre type, providing useful insight into the contractile properties of the muscle.

Here, assessment of the MyHC isoform proportions of soleus muscle was performed on soleus muscle homogenates (prepared following respirometry experiments) using sodium-dodecyl-sulphate (SDS) polyacrylamide gel electrophoresis (PAGE). This technique separates MyHC isoforms based on molecular weight and has been used to investigate the fibre make up of various muscle types in previous studies. For example, mouse soleus muscle has been shown to constitute of predominantly type I, IIA and IIX fibres, with either minimal or no IIB (Kammoun et al., 2014, Brummer et al., 2013, Blough et al., 1996, Agbulut et al., 2003, Agbulut et al., 1996). This is compared to mouse extensor digitorum longus (EDL) muscle, which has been shown to constitute of predominantly IIX and IIB, with small or negligible amounts of IIA (Agbulut et al., 2003, Agbulut et al., 1996).

There are many variations of the SDS-PAGE protocol in the literature and a significant effort was required to distinguish a protocol that was successful at resolving all myosin isoforms. This included variations in % acrylamide in the stack and separating gels, gel size, current applied, run duration and staining technique. It also involved use of EDL muscle as a control, known to contain IIX and IIB fibres. This was obtained from wild type female mice of PKS genotype, between 9-13 weeks of age, kindly donated by Professor Malcom Logan at King's College London.

Eventually the following protocol was established that resulted in successful separation of type I, IIA, and IIB isoforms in mouse skeletal muscle, confirmed through Western Blotting. Despite attempts through Western Blotting to confirm the presence of a type IIX isoform, this was unsuccessful. It is therefore possible that the type IIA band identified using SDS-PAGE also contains type IIX.

Preparation of muscle samples

The soleus muscle homogenates prepared from the muscle bundles recovered from respirometry experiments (see above) were used for the detection of MyHC isoforms. For the MyHC to be solubilised, it was necessary for the sample to be treated with Laemelli sample buffer (see below) in a concentration that corresponded to the amount of protein in the sample. Thus, an accurate measure of protein content was required.

Protein concentration of soleus muscle homogenates

Protein content of soleus muscle homogenates was assessed using Pierce™ BCA Protein Assay Kit (Thermo Scientific, Prod# 23227, Lot #OL19780), with subsequent detection performed using a Nanodrop™ 2000 spectrophotometer (ThermoFisher Scientific). Briefly, the sample was vortexed and 10µl was added to 10µl working reagent on a 96 well plate and heated at 60°C for 5mins. The plate was left to cool at room temperature, following which 2µl of the resulting solution was added to the Nanodrop and protein concentrations were verified using a standard curve previously established. The standards were prepared using bovine serum albumin (BSA) in concentrations ranging between 0.125-2mg/ml in phosphate buffered saline (PBS) with 3% Triton X, with one standard solution acting as a reference, containing no BSA. Triton was added to the standards to account for that added to the soleus fibre bundle homogenate solution.

The BCA assay relies on two reactions. The first is the temperature dependent reduction of Cu^{2+} ions to Cu^{+} by peptide bonds present in protein, with the degree of reduction relating to the total amount of protein present in solution. Subsequently, two molecules of bicinchoninic acid chelate with each Cu^{+}, forming a purple coloured complex. This strongly absorbs light at a wavelength of 562nm.

The protein concentration of the soleus homogenates ranged between 0.54-1.65mg/ml.

Addition of sample buffer

Samples were spun using a microcentrifuge for 10 minutes at 13,000rpm. The supernatant was tested using SDS-PAGE and found to contain no trace of myosin isoforms so was removed, leaving the pellet. This was re-suspended in laemelli sample buffer (Laemmli, 1970) at a concentration of 40µl/mg protein (or per wet weight of protein in the instance of the soleus muscle). For details of sample buffer constituents, see **Table 4.2** below.

An extra 1µl of bromophenol blue was added to the resulting sample solution to aid visibility when loading into the gel. Following a 2 minute vortex to ensure full mixing of MyHC's with sample buffer, samples were heated at 100°C on a hotplate for 5 minutes. The sample was then centrifuged, again for 10 minutes at 13,000rpm so that any protein artefacts were contained within the pellet and not loaded into the gel. The sample was stored at -80°C until the gel run.

Extensor digitorum longus (EDL) homogenisation

EDL muscle was donated as a gift from Malcolm Logan, dissected from female wild type PKS mice at ~3months of age. Wet weight was obtained and sample buffer added with a minimum of 500µl being required for homogenisation using a gentle MACS dissociator.

4.5.6 SDS-polyacrylamide gel electrophoresis (PAGE)

The gels used for both coomaisse blue stain MyHC band detection and Western Blot analysis were cast in vertical slab mini-gels, 0.75mm. The separating gel, left to set at room temperature overnight, composed of: 30% glycerol, 4% acrylamide-N-N'-methylene-bis-acrylamide (bis) (50:1), 0.2M Tris (pH 8.8), 0.1M Glycine and 0.4% SDS. To prevent the top of the gel from drying out, a thin layer of 10% Sodium Dodecyl Sulphate (SDS) was sprayed and cling film was wrapped around the top of the plates. These protective measures were both removed prior to the addition of the stack gel, which consisted of: 30% glycerol, 4% acrylamide-bis (50:1), 70mM Tris (pH 6.7), 100mM Ethylenediaminetetraacetic acid (EDTA) (pH 7.0), 0.4% SDS. A 0.75mm 10-well spacer was inserted into the stack gel immediately after pouring. This was left to set for 1 hour before the spacer was removed and loading of the samples commenced. The gel constituents were prepared from stock solutions, the details of which are provided below. The pH of the stock solutions for both separating and stack gels was not adjusted after these solutions were mixed. Polymerization of both gels was initiated with 0.05% of NNN'N'-Tetramethylethylenediamine (TEMED) and 0.1% Ammonium persulfate (APS). Details of the stock solutions along with the sources of the chemicals used are given in **Table 4.3**.

A protein marker (Precision Plus Protein™Kaleidoscope™, Bio-rad) was loaded alongside the samples. This enabled visualisation of protein migration during the gel run. It also enabled the molecular weight of the separated bands (~200kDa), and so identification of the MyHC isoforms, to be determined.

The gels were run utilising the Bio-rad Mini-PROTEAN II Cell set up, which allowed for 2 gels to be run together. Upper running buffer, consisting of 50mM Tris, 75mM Glycine and 0.05% SDS was added to the space between the two gels. β-mercaptoethanol was required to aid the clarity of the protein bands following staining (Talmadge et al., 1993). Lower running buffer, containing the same constituents as the upper buffer minus β-mercaptoethanol, was added to the tank. The gel was then run at ~4°C for 24hours at a constant current of 4mA (Bio-rad power supply). The temperature was maintained by placing the gel in an igloo, surrounding the gel set up with ice and covering with aluminium foil.

Coomaisse blue staining

Following completion of the SDS-PAGE run, the stack gel was removed and the separating gel washed in ddH_2O. To visualise and analyse the protein bands, the mini gel was stained with 20ml Coomaisse®G250 stain, SimplyBlue™Safestain, Invitrogen, for one hour on a rocker. It was then washed in 100ml ddH_20 for 1 hour prior to scanning using a HP Scanjet 3500c Series. The bands corresponding to MyHC isoforms, located between 150-250kDa, were analysed by gel densitometry using Fiji (ImageJ). From this, the % of type I and II fibres in each soleus sample were assessed.

Table 4.2. Gel constituents used for SDS-PAGE.

	Stock solution	Working solution	
		Volume (ml) for two gels	% or molarity of constituents
Sample buffer	β-mercaptoethanol Sodium dodecyl sulphate (SDS) 1M Tris (Tris(hydroxymethyl)amino methane) (pH 6.8) Glycerol Bromophenol blue (BPB) dH_2O	0.1 0.4 1.6 2 0.02 5.88 **Total=10**	1% 4% 16% /1M 20% 0.2%
Separating gel (Talmadge et al., 1993)	100% Glycerol 30% Acrylamide-bis (50:1) Tris 1.5M (pH 8.8) 1M Glycine 10% SDS dH_2O Tetramethylethylenediamine (TEMED) 10% Ammonium persulfate(APS)	3 2.667 1.333 1 0.4 1.495 0.005 0.1 **Total=10**	30% 8% 0.2M 0.1M 0.4% 0.05% 0.1%
Stack gel	100% Glycerol 30% Acrylamide-bis (50:1) Tris 0.5M (pH 6.7) 4mM Ethylenediaminetetraacetic acid (EDTA) (pH 7.0) 10% SDS dH_2O TEMED 10% APS	3 1.333 1.4 0.4 0.4 3.362 0.005 0.1 **Total= 10**	30% 4% 70mM 100mM 0.4%
Upper Running buffer		**Total = 150**	50mM Tris 75mM Glycine 0.05% SDS 10% β-mercaptoethanol
Lower running buffer		**Total = 200**	50mM Tris 75mM Glycine 0.05% SDS

Note: *Volumes for separating gel, stack gel, upper and lower running buffer working solutions are correct for 2 gels.*

Table 4.3. Details on chemicals used for SDS-PAGE and Western blotting.

Product/chemical name	Details	Source
Acrylamide		Sigma Life Sciences, A8887.
APS	Ammonium Persulphate	Electran®BDH, Prod 443073E
Blocking grade buffer	Non-fat milk	Biorad, 170-6404
Bisacrylamide	NN'-methylenebisacrylamide, specially purified for electrophoresis	Electran, BDH, Prod 44300
β-Mercaptoethanol	2-mercaptoethanol	Sigma Life Sciences, M3148
Bromophenol blue	Free acid	Sigma B-6896
Coomaisse Blue stain	SimplyBlue™ SafeStain	Invitrogen, LC6060, Lot 1676635
EDTA	Ethlenediaminetetra-acetic acid	GPR™BDH, Prod 2802145
Glycerol		Raymond Lamb, Prod AC006D
Glycine		Sigma Life Science, G8898
Ponceau-S	0.1% Ponceau S in 5% acetic acid	Sigma-Alrdrich Prod.P7170
Protein maker	Precision Plus Protein™Kaleidoscope™	Bio-rad, Cat 161-0375
SDS	Sodium Dodecyl Sulphate	AnalR®BDH, Prod 10807
Sodium Chloride		GPR™ BDH, Prod 301235Q
TEMED	NNN'-Tetramethylethylenediamine	Electran, Prod 443083G
Tris	Tris(hydroxymethyl)methylamine	AnalR®BDH, Prod 103156X
Trizma®Base		Sigma Life Science, T1503
Tween®20		Sigma-Aldrich, P1379

Wet transfer of proteins for Western Blot

Following SDS-PAGE, the gel was washed in ddH_2O and the separated protein was transferred from the gel to a Nitrocellulose membrane (Bio-Rad Trans-Blot® Transfer membrane, pure nitrocellulose membrane 0.2µm, Lot # BR 7257001) using a wet transfer technique as follows. For details on buffer and blocker constituents, see **Table 4.4**. The nitrocellulose membrane was cut to size (maximum 7.5x10.5cm) and soaked in transfer buffer* for 15 minutes. It was then positioned underneath the gel and both were transferred to the cassette (Bio-rad) to form part of the transfer sandwich, which consisted of fibre pads (Bio-Rad) that were wetted and filter paper (Bio-rad, Extra thick blot paper, Mini blot size (7 x8.4 cm, 6sh). For details on the assembly of the transfer sandwich, see **Figure 4.7.**

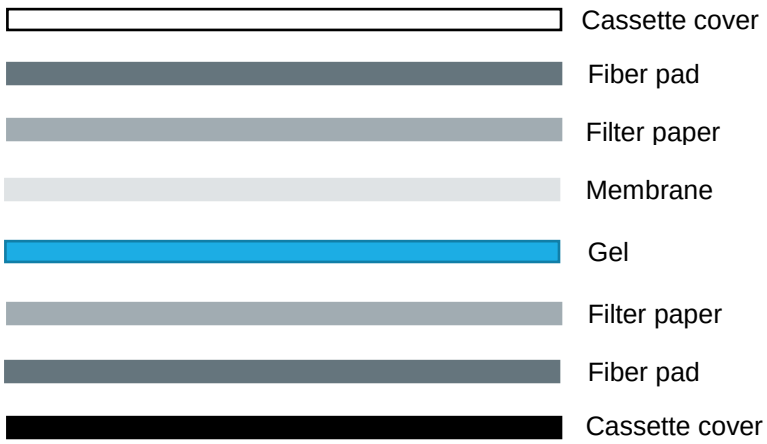

Figure 4.7. A depiction of the transfer sandwich set up used in western blotting procedures.

To remove any bubbles that may have formed during this process, a stripette was rolled along the membrane filter paper prior to closing of the cassette. The cassette was then lowered into the transfer tank, ensuring the black side faced the black side of the tank to enable the transfer of protein from a negative current to positive. A stir bar was placed at the bottom of the tank and a cooling unit added. A litre of transfer buffer was then poured into the tank and the stir bar set near to maximum. The addition of SDS was required in the transfer buffer to aid the transfer of large proteins. The power supply (Bio-rad) was set to 100V/350mA for 1 hour. Two gels, and so two cassette set ups were used per transfer run. Upon completion of the transfer, an initial check of its success was made by carefully peeling off the filter paper and observing if the coloured protein marker had been fully transferred

from the gel to the membrane. To visualise the successful separation of the MyHC bands and transfer to the membrane, a Ponceau stain was used.

Ponceau-S staining

Ponceau-S staining is a rapid, reversible means of visualising proteins transferred onto a nitrocellulose membrane following SDS-PAGE. Ponceau S is a negative stain that binds both to positively charged amino acid groups of the protein and to non-polar regions non-covalently, resulting in reddish-pink protein bands with a clear background. Transferred protein can be detected within the microgram range using this method.

Following wet transfer, the membrane was rinsed in ddH_2O before being immersed in undiluted Ponceau S solution for 5 minutes. The ponceau was drained and retained for future use in a light shielded container and the membrane rinsed with ddH20. If transfer was successful, protein bands were visible as red vertical stripes corresponding to each column loaded with protein sample. To remove the stain, the membrane was rinsed in 0.1M sodium hydroxide solution for ~20 seconds until the bands had fully disappeared. It was then immediately drained off and the membrane rinsed with ddH_2O for 2-3 minutes.

Table 4.4. Buffer and blocking solution details for Western blotting.

Solution	Total volume	Constituents	pH
Transfer buffer	1L	100ml 10xTRIS/Glycine* 200ml methanol 1ml 10%SDS	N/A
***TRIS/glycine**	1L (10x)	Glycine Trizma® base	N/A
Tris Buffer Saline (TBS)	1L (10x)	24.2g Trizma® Base 80g NaCl	7.4
TBS-Tween (TBS-T)	1L	100ml 10x TBS 900ml ddH_20 2ml Tween-20	N/A
Blocking buffer	200ml	10g (5%) Blocking grade buffer (Nonfat milk (NFM), Biorad) 190ml TBS-T	N/A
Blocking buffer for 6H1	100ml	5g (5%) Blocking grade buffer (Biorad) 195ml TBS	N/A

Antibody staining

To detect MyHC type I, IIA and IIB, the following mammalian primary monoclonal antibodies were used respectively: BA-F8 (Immunoglobulin G, IgG), Sc-71 (IgG) and BF-F3 (Immunoglobulin M, IgM). Each were obtained from the developmental studies hybridoma bank, developed by Schiaffino (Schiaffino et al., 1989). The membrane was therefore cut into necessary sections, to enable a separate antibody to be used on each section, and each section transferred to a separate, smaller container.

Initial blocking of the membrane sections was achieved through immersion in 50ml 5% blocking grade buffer (non-fat milk) solution for 1 hour on a shaking table. The membrane was washed for 10 minutes on a shaker in TBS-T four times. The membrane sections were then incubated with the primary antibody diluted in blocking buffer at a concentration of 1:400 in the fridge overnight. The same 4x10minute wash (with TBS-T) was then repeated and

followed by incubation with the secondary antibody for 45 minutes on a shaker at room temperature. In the case of Sc-71 and BA-F8 IgG antibodies, the membrane was incubated with goat anti-mouse IgG-horse radish peroxidase (HRP) (ECL™ Prime Western blotting detection reagent, RPN2232, Lot#9636827 Amersham™) diluted in blocking buffer at a concentration of 1:2000. The same wash steps as stated previously were then repeated. Following this, the membrane was rinsed in dH_2O and incubated with 4ml of ECL Prime Western blotting detection reagent (2ml of both solution A and B) for 5 minutes. For detection, the membrane image was captured using a BioSpectrum® 810 Imaging System, 230V~50Hz UVP Bioimaging systems.

In the case of BF-F3 IgM antibodies, the membrane was incubated with goat anti-mouse IgM-Alkaline phosphatase secondary antibody (A9688, Sigma) diluted in blocking buffer at a concentration of 1:1000 for 45 minutes on a shaker at room temperature. For BF-F3 detection the membrane was then stained with Fast red/Napthol AS-MX tablets (F4648-50SET, Lot# 097K8211, Sigma) diluted in dH_2O (1ml per tablet) targeting Alkaline Phosphatase, until a clear appearance of a detected band, after which it was washed with dH_2O to minimise background.

Attempts were made to detect MyHC IIX using mammalian primary monoclonal antibody 6H1 (IgM). The same secondary antibody incubation (with goat anti-mouse IgM) was used as with BF-F3, only without Tween, given that 6H1 is notoriously delicate. Detection with Fast red/Napthol was attempted, however, no band was resolved. Further attempts were made, with the membrane being incubated with a tertiary reagent, extravadin alkaline phosphatase (Sigma, F4523) diluted in blocking buffer (with TBS) at a concentration of 1:500 for 45 minutes. The wash steps were then repeated, after which the membrane was incubated with diluted Fast red/Napthol. However, again, no band was made apparent.

4.5.7 Western Blot analysis of metabolic proteins

To gain further insight into potential metabolic remodelling processes, Western Blot analysis was performed to detect for changes in levels of specific metabolic enzymes or signalling proteins. This analysis was performed in the laboratory of Dr Andrew Philp at the University of Birmingham.

Muscle preparation

Whole frozen soleus muscle was powdered using a muscle crusher and 100µl lysis buffer (50 mM Tris, pH 7.5, 250 mM sucrose, 1 mM EDTA, 1 mM EGTA, 1% Triton X-100,

1 mM $NaVO_4$, 50 mM NaF, 0.10% DTT, and 0.50% protease inhibitor cocktail) was added. The sample was shaken at 6.0m/sec for 40sec using a FastPrep-24™5G (Millipore, Quickprep setting) and centrifuged at 4°C, 8000G for 10mins. Total protein content of the resulting supernatant was derived from a DC™ Biorad protein assay (Lot# 500-0113) using FLUOstar Omega at absorbance 750nm.

SDS-PAGE gel run

Laemelli sample buffer (250 mM Tris·HCl, pH 6.8, 2% SDS, 10% glycerol, 0.01% bromophenol blue, and 5% β-mercaptoethanol) was added prior to loading equal amounts of sample (19.95µg protein) onto SDS polyacrylamide gels (0.75mm thickness).

For all antibodies excluding OXPHOS (see below), samples were boiled prior to loading. The separating gel constituted 12.5% acrylamide (30% acrylamide/Bis solution, Bio-Rad, 3.3% Cross linker, Electrophoresis purity reagent) and 1.5M Tris-SDS (0.4%) pH 8.8; the stacking gel 5% acrylamide and 1.5M Tris-SDS pH 6.8. Polymerization of both gels was initiated through the addition of 0.1% APS and 0.01% TEMED and was left for 30 minutes. Following the addition of running buffer (0.25mM Tris Base, 2.5mM Glycine, 20% SDS), gels were run at a constant amperage of 23mA/gel for ~45minutes at room temperature.

Protein wet transfer

Following completion of the SDS-PAGE gel run, protein was then transferred to a pure nitrocellulose blotting membrane (PALL®, Pall Corporation, Life Sciences) at 100 V for 1 h, with the addition of transfer buffer (0.4Mm Tris Base, 1.73mM Glycine) and ice. Visualisation of the protein transfer was obtained using Ponceau-S staining.

Antibody staining

After blocking in 3% non-fat milk in Tris-buffered saline with 0.1% Tween 20, the membranes were incubated overnight at 4°C with appropriate primary antibody. The antibodies used were: Total OXPHOS rodent WB antibody cocktail (OXPHOS) (ab110413, Abcam), Anti-citrate synthase (SAB2701077, Sigma), Mitofusin 2 (MFN2) (Cell Signalling 9482), PGC1-α (AB3242, Millipore), carnitine palmitoyltransferase (CPT) 1 (CPT1MIIA, Alpha Diagnostics), long chain acyl co-A dehydrogenase (LCAD, a gift from Prof Jerry Vockley, University of Pittsburgh (Le et al., 2000)), pyruvate dehydrogenase kinase (PDK4, a gift from Prof Grahame Hardie, University of Dundee, (Kiilerich et al., 2010)). All primary antibodies were diluted 1:1000, with the exception of LCAD, which was diluted 1:5000. Further washes in TBS-T were followed by addition of secondary antibodies for 45 mins,

diluted as diluted 1:10,000 as follows: Rabbit anti-mouse IgG (Pierce #31457, lot#OD1691311), rabbit anti-sheep IgG (Pierce #31480, lot#OC16810716), goat anti-rabbit (Pierce #31460 lot#QC214553). Immobilon western chemiluminescent HRP substrate (Merck Millipore) was used to quantify protein content after IgG binding.

Western blot analysis

Blots were visualized on a G: BOX Chemi XT4 imager using GeneSys capture software (Syngene UK, Cambridge, UK). Density of bands corresponding to the target protein were corrected to the loading control (mouse gastrocnemius) for that blot as well as the corresponding actin band.

4.5.8 Statistics

Statistical analyses were performed using R software (The R Foundation for Statistical Computing) and p values ≤0.05 were considered as significant. A three-way ANOVA was performed in order to assess effects of all 3 parameters: hypoxia, nitrate and PPARα. Detection of a significant two or three-way interaction identified by the ANOVA were investigated further using a post hoc Tukey's test. Interpretation of post hoc Tukey's went as follows: a significant three-way interaction was considered the main outcome, any two-way interaction was discounted in this instance. A significant two-way interaction existing without a three-way interaction was considered the main outcome, any significance found in singular parameters by the ANOVA were ignored. In both instances, Tukey's tests on interactions that didn't contain at least one repeated parameter in each of the comparison groups were also discounted.

Exclusion criteria for inclusion of results in statistical analysis were respirometry values that deviated more than 20% from group mean values as well as those fibre bundles responding to the cytochrome c addition. This was employed in an attempt to remove results affected by day to day fluctuations in electrode sensitivity (e.g. one instance of membrane replacement) or by fibre damage. The number therefore varied between 6-10 per group.

Parametric tests, such as ANOVA's, assume a normal, or Gaussian, distribution. The distribution of data can be assessed using normality tests. Whilst ANOVA's have been shown to be robust to normality violation (Maxwell et al., 1990), this effect is likely reduced with smaller sample sizes. Indeed, the small sample size presented in this study significantly reduce the power of normality tests, lowering the ability to detect non-Gaussian distribution. Instead, a test is required to inform whether deviations from the Gaussian distribution are

severe enough to invalidate the statistical methods that assume a Gaussian distribution. Given the exclusion criteria described above, this was expected not to be of concern. A normal distribution was therefore assumed.

Graphs were generated using Graphpad Prism 6 software and follow a specific similar colour/pattern scheme, with white indicating normoxia, blue hypoxia and dashes indicating nitrate treated groups. In addition, the wild type ($PPAR\alpha^{+/+}$) are separated from the knockout ($PPAR\alpha^{-/-}$). The majority of the data set (with the exception of body weight changes) is shown as box and whisker plots, so that the full data spread can be visualised, with significant links between groups depicted. Lines have been drawn to show significant interactions between groups. Black lines are indicative of interactions between genotypes ($PPAR\alpha^{-/-}$ vs. $PPAR\alpha^{+/+}$), blue lines are interactions linked to O_2 state (hypoxia vs. normoxia).

4.6 Results

4.6.1 Effects of hypoxia and PPARα ablation on nitrate intake, body weight and haemoglobin

To investigate the effects of long term, severe hypoxia, mice were exposed to either hypoxic (10% O_2) or normoxic (21%O_2) conditions for four weeks. This was preceded by either one week of sodium nitrate ($NaNO_3$, 0.7mM L^{-1}) or sodium chloride (NaCl, 0.7mM L^{-1}) supplementation via drinking water, which was continued for the study duration. At the end of the study period, the body weight of hypoxic mice was 6.7% lower ($p \leq 0.001\%$) in comparison to normoxic mice and 4.5% lower ($p \leq 0.01$) in PPARα$^{-/-}$ mice in comparison to PPARα$^{+/+}$ at the point of study completion (**Figure 4.8A**). The impact of PPARα genetic ablation upon fat metabolism was also visible with the presence of fat droplets on the liver of PPARα$^{-/-}$ mice, as described previously (Lee et al., 1995).

Over the course of the treatment programme, nitrate intake gained from food and water consumption combined was 7.7 fold ($p \leq 0.001$) higher in nitrate treated mice in comparison to chloride treated mice (**Figure 4.8B**). The severity of the hypoxic exposure was reflected through a two-fold increase in haemoglobin concentration ($p \leq 0.001$, all hypoxic vs. all normoxic) (**Figure 4.8C**).

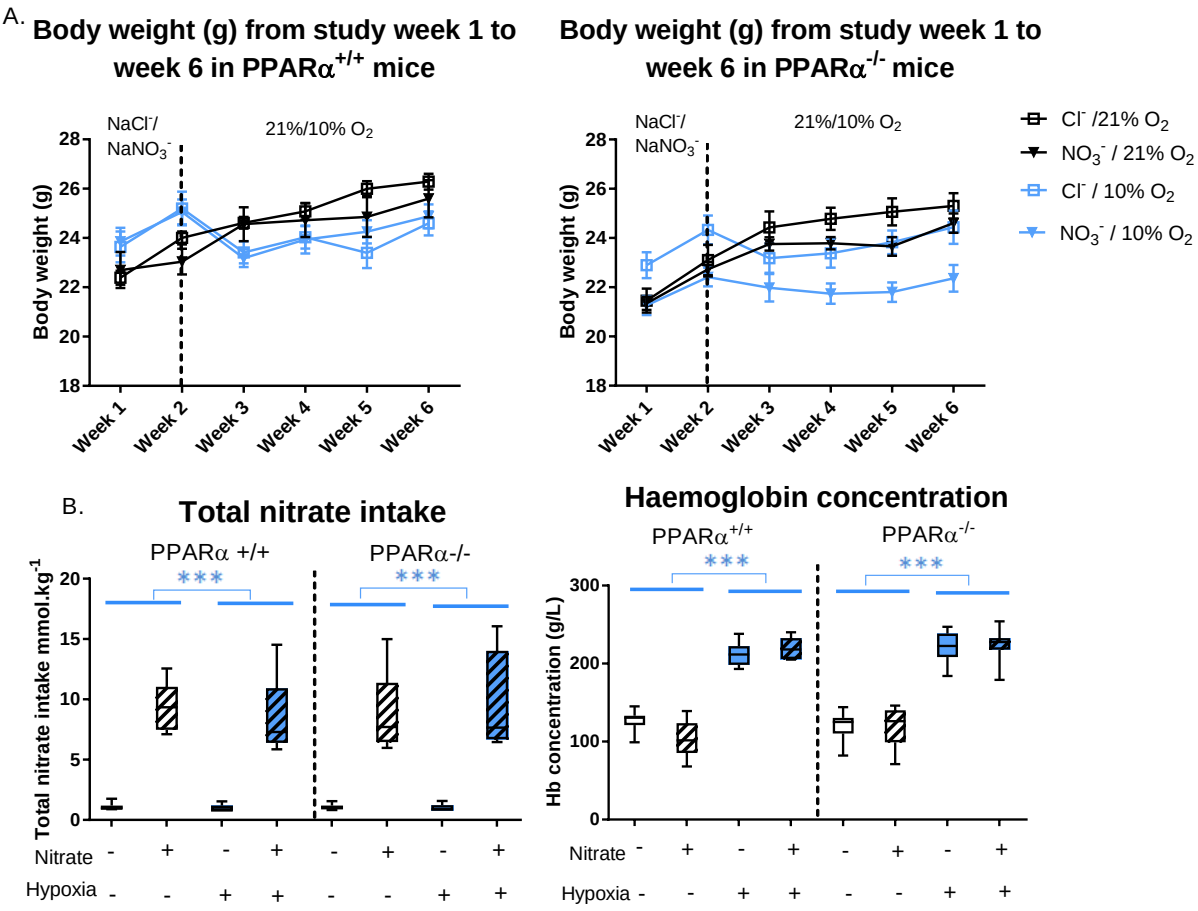

Figure 4.8. Mouse body weight, nitrate (NO_3^-) intake and haemoglobin concentrations.

A. *Average (mean) mouse body weights in each experimental group (n=10-12) in both PPARα$^{+/+}$ and PPARα$^{-/-}$ genotypes measured on the first day of the week indicated, with dietary sodium nitrate ($NaNO_3$) supplementation or sodium chloride ($NaCl^-$) beginning in week 1 and hypoxic treatment beginning at week 2.* ***B.*** *Cumulative* NO_3^- *intake from food and water throughout the study duration.* ***C.*** *Differences in haemoglobin concentration (g/L), derived from HemoCue analysis of a blood droplet taken from the tail vein immediately after sacrifice. A doubling of haemoglobin concentration was observed in the groups exposed to four weeks of hypoxic (10% O_2) treatment. Data for* ***B*** *and* ***C*** *are presented as minimum to maximum box and whisker plots, with the middle line representing the median and the box the interquartile range (25th to 75th percentiles), n=6-12 per experiment group. ***P≤.001.*

4.6.2 Mitochondrial respirometry

PPARα genetic ablation impairs LEAK state respiration

To understand how the interaction between hypoxia, nitrate supplementation and PPARα $^{-/-}$ might affect the oxidation of fat and carbohydrates, respiration rates were measured in permeabilised soleus muscle fibres in response to the addition of a fatty acyl-carnitine substrate (40μM palmitoyl carnitine + 2mM malate) and a product of glycolysis (5mM pyruvate) respectively. In addition, flux through mitochondrial complexes 1 and 2 were assessed through the measurement of respiration rates in response to addition of substrates specific to these complexes (10mM glutamate + 2mM malate and 10mM succinate preceded by 0.5μM of the potent complex I inhibitor rotenone, respectively). PPARα$^{-/-}$ mice exhibited a 9.5% decrease in LEAK state respiration (O_2 consumption in the absence of ADP, so not coupled to ADP phosphorylation) with the addition of the long chain fatty acid, palmitoyl carnitine (**Figure 4.9A**), alongside a 10.8% decrease ($p \leq 0.05$) in LEAK state respiration driven by complex I electron flux (**Figure 4.10A**).

Hypoxia impairs oxidative capacity

The hypoxic insult suppressed a number of measures of soleus muscle mitochondrial function across both genotypes. This was demonstrated through a decrease in respiration rates in response to addition of fatty acid substrate by 26.3% (all normoxic chloride vs. all hypoxic chloride, $p \leq 0.001$) in LEAK state and by 13.9% (all normoxic vs. all hypoxic, $p \leq 0.01$) in OXPHOS state (the latter being O_2 consumption that is coupled to ADP phosphorylation, so in response to the addition of 10mM ADP) (**Figure 4.9A, B**). Pyruvate OXPHOS rates were also suppressed in response to hypoxia, with a 23.1% ($p \leq 0.001$) decrease occurring in chloride treated hypoxic groups in comparison to chloride normoxic groups across both genotypes (**Figure 4.9C**).

Effects of hypoxia upon mitochondrial complex function were apparent through decreases in OXPHOS rate driven by complex II electron flux (**Figure 10C**), an effect again apparent across both genotypes with a 17.6% decrease ($p \leq 0.01$) observed in hypoxic chloride mice in comparison to normoxic chloride across both genotypes. Hypoxia did not affect flux via complex I either in the LEAK or OXPHOS states (**Figure 4.10A, B**).

An insight into coupling efficiency of mitochondrial oxidation, being the proportion of the membrane geared towards ATP synthesis via ATP synthase relative to proton leak across the inner membrane, was gained from calculating oxidative coupling efficiency

(OCE). Calculation of OCE from palmitoyl carnitine oxidation ($\frac{Palmitoyl\ carnitine\ \ LEAK}{Palmiotyl\ carnitine\ OXPHOS}$) revealed an 18.3% decrease ($p \leq 0.01$) in hypoxic PPARα$^{-/-}$ relative to hypoxic PPARα$^{+/+}$ groups (**Figure 4.11A**). OCE for complex I respiration (derived from assay 2) was unaffected by hypoxic exposure **Figure 4.11B**.

Nitrate supplementation recovers aspects of hypoxic induced suppression

The supplementation of drinking water with 0.7mM L^{-1} dietary nitrate $^{-}$ for one week prior to and during hypoxic exposure, was shown to attenuate two measures of hypoxic induced suppression of mitochondrial function, the first of which is the decrease in fatty acid LEAK state. As can be seen in **Figure 4.9A**, the decrease in palmitoyl carnitine LEAK state respiration is only apparent in chloride treated hypoxic mice. No such decreases were observed in the nitrate supplemented experimental groups, indicating a nitrate dependent recovery of mitochondrial function. The same pattern occurs with pyruvate oxidative phosphorylation, as the hypoxic induced suppression is apparent in chloride treated mice, but lost in the nitrate treated groups (**Figure 4.9C**). Other measures of mitochondrial respiration were found to be unaffected by nitrate supplementation.

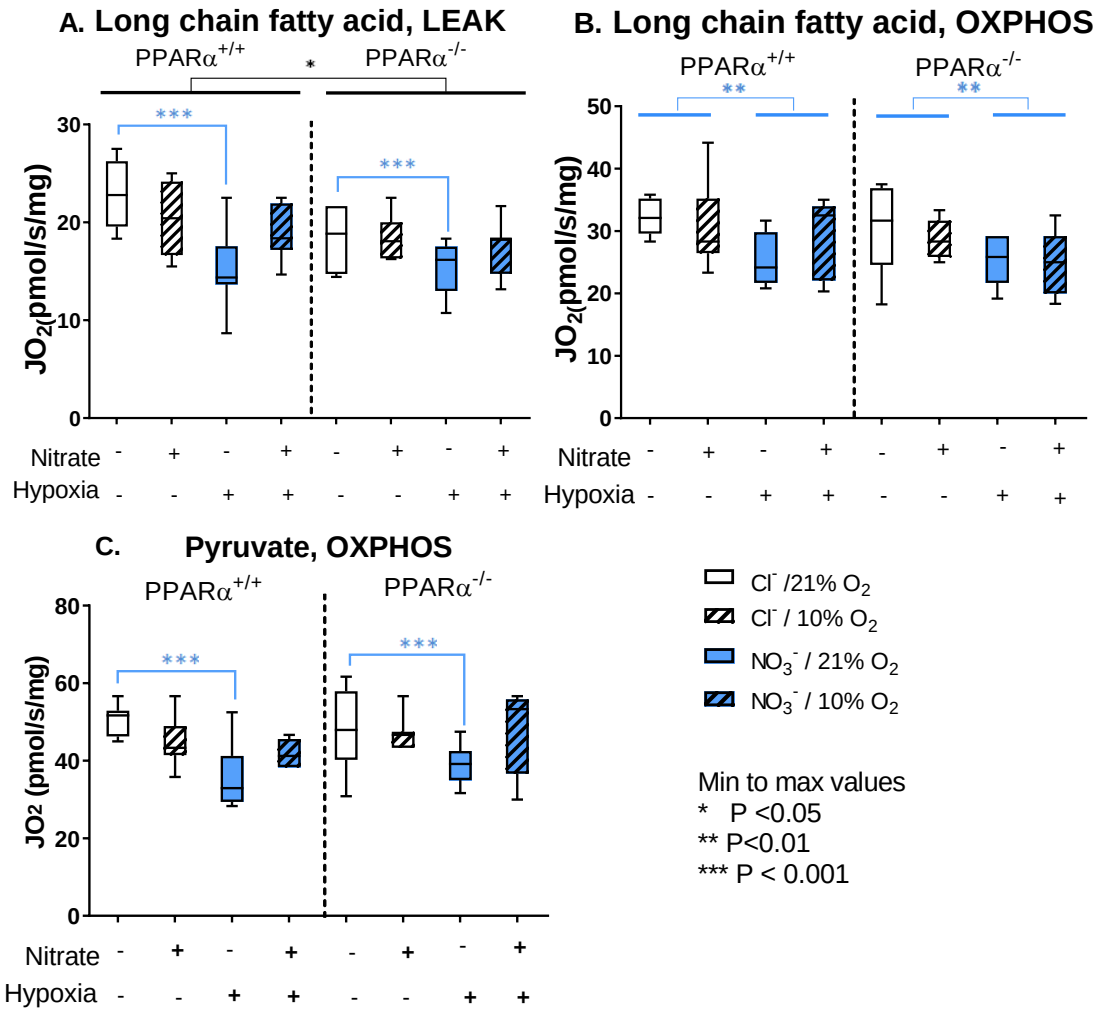

Figure 4.9. Mitochondrial respirometry results from assay 1

Presented as oxygen flux (JO_2) in pmol/second/mg, corrected to wet weight. ***A.*** *Long chain fatty acid (palmitoyl carnitine) stimulated leak state respiration (LEAK), suppressed by PPARα$^{-/-}$ in all conditions and by hypoxia in the chloride treated animals across both genotypes.* ***B.*** *Oxidative phosphorylation (OXPHOS) of long chain fatty acid (palmitoyl carnitine), suppressed by hypoxia in both genotypes and across both chloride (Cl^-) and nitrate (NO_3^-) treated animals.* ***C****. OXPHOS of pyruvate, suppressed by hypoxia in the chloride treated groups only across both genotypes. Data are presented as boxplots, with the box extending from 25th to 75th percentiles and displaying the median line, and whiskers presenting minimum to maximum values, n=6-10 per experiment group. *P≤0.05 ** P≤0.01, ***P≤.001.*

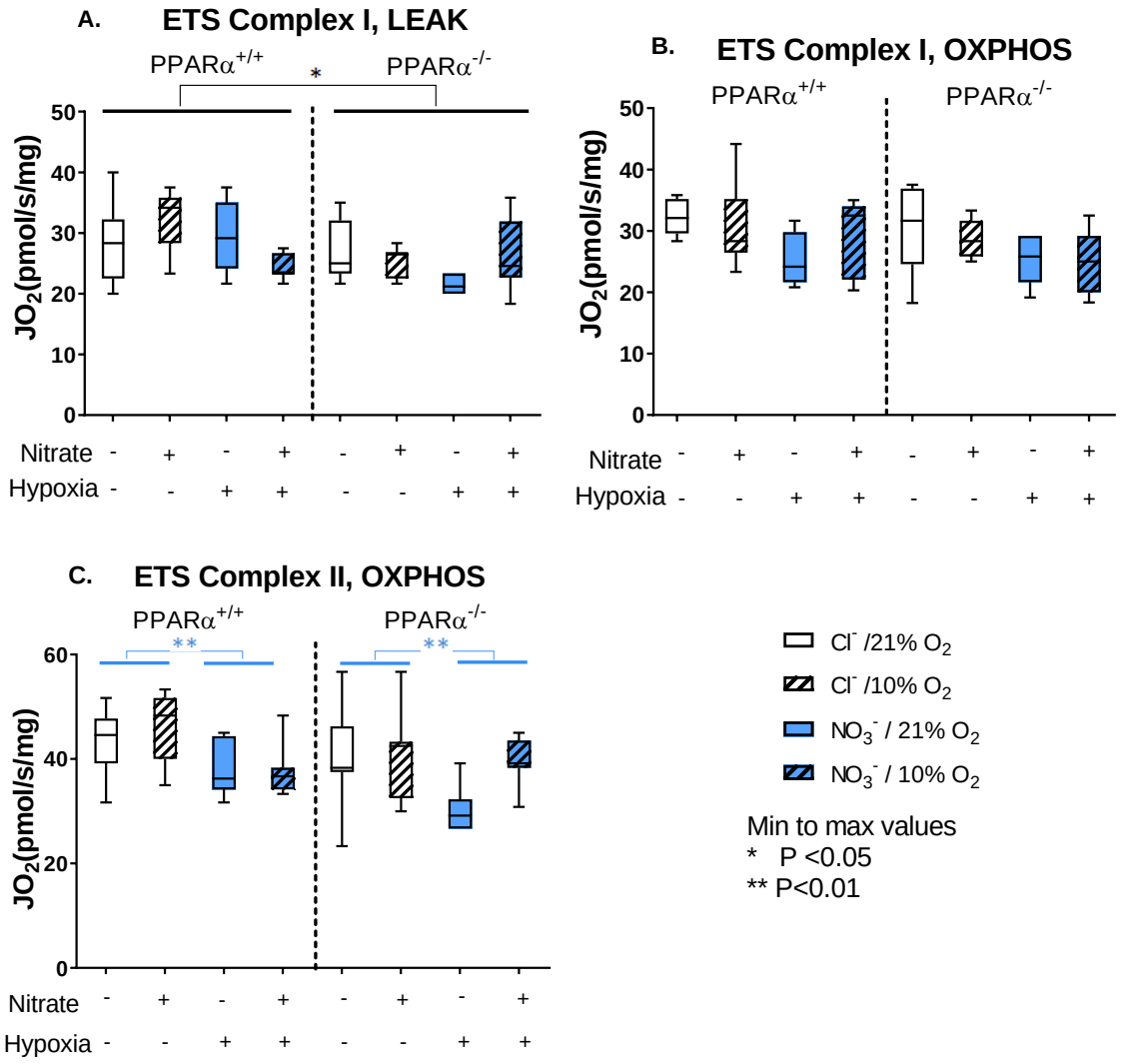

Figure 4.10. Mitochondrial respirometry results from assay 2

Presented as oxygen flux (JO_2) in pmol/second/mg, corrected to wet weight. ***A.*** *Electron transfer chain (ETS) complex I driven leak state respiration, suppressed by PPARα$^{-/-}$ in all conditions.* ***B.*** *ETS complex I driven OXPHOS, no significant difference identified* ***C.*** *ETS complex II driven OXPHOS suppressed by hypoxia in both nitrate (NO_3^-) and chloride (Cl^-) treated conditions and across both genotypes. Data are presented as boxplots extending from 25th to 75th percentiles and displaying the median line, with whiskers presenting minimum to maximum values, n=6-10 per experiment group. *P≤0.05 ** P≤0.01.*

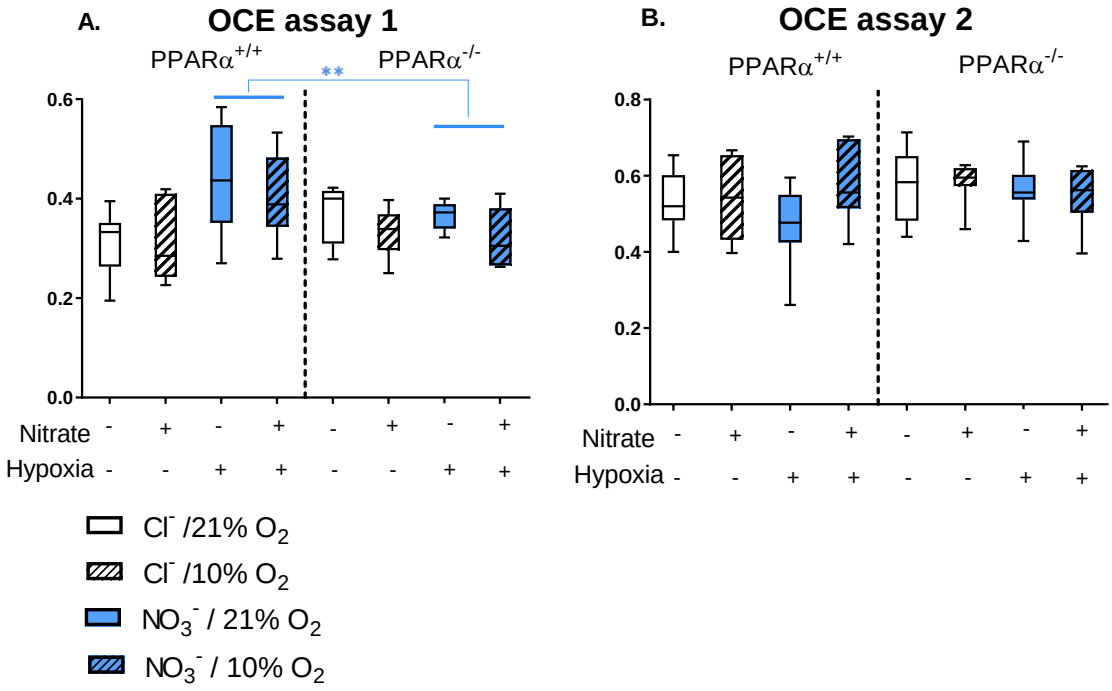

Figure 4.11. Oxidative coupling efficiency (OCE).

A. *OCE for assay 1, decreased in hypoxic PPARα$^{-/-}$ in comparison to PPARα$^{+/+}$ in both nitrate and chloride treated conditions.* ***B.*** *OCE for assay 2, no significant change across any treatment condition. Data are represented as boxplots extending from 25th to 75th percentiles and displaying the median line, with whiskers presenting minimum to maximum values n=5-11 per experiment group. ** P≤0.01.*

$$OCE1 = \frac{Palmitoyl\ carnitine\ LEAK}{Palmitoyl\ carnitine\ OXPHOS}\ OCE2 = \frac{Complex\ 1\ LEAK}{Complex\ 1\ OXPHOS}$$

4.6.3 Metabolic proteins

PPARα genetic ablation and hypoxia affect levels of proteins associated with oxidative metabolism

Assessment of the levels of total protein related to β-oxidation in the soleus revealed decreases in levels of the β-oxidation enzyme long chain acyl co-A dehydrogenase (LCAD) and in the shuttle carnitine palmitoyltransferase 1 (CPT1) by 15.6% and 17.0% respectively ($p \leq 0.05$, $PPAR\alpha^{-/-}$ vs $PPAR\alpha^{+/+}$) (**Figure 4.12A,B**). This is alongside a hypoxic induced decrease in CPT1 protein levels by 17% across both genotypes ($p \leq 0.05$) (**Figure 4.12B**).

The hypoxic induced changes in proteins may thus relate to the decrease in fatty acid oxidation capacity outlined in the respirometry results. This was not the case for carbohydrate oxidation as the hypoxic induced abrogation of pyruvate OXPHOS was not accompanied by changes in protein levels of a key mediator of pyruvate entry into the TCA cycle, pyruvate dehydrogenase kinase 4 (PDK4) (**Figure 4.12C**).

4.6.4 Myosin heavy chain (MyHC) isoforms

Hypoxic exposure induces a shift in myosin heavy chain isoform proportions

Assessment of soleus muscle MyHC isoforms indicated that hypoxia induced a shift in proportions towards a fast type isoform makeup, with a 34% increase in type II isoforms alongside an 11.1% decrease in type I fibres ($p<0.01$) (**Figure 4.13**). Relationships between fibre type proportions and mitochondrial respirometry were investigated. However, no correlation was observed between fibre type and any measured respirometry parameter.

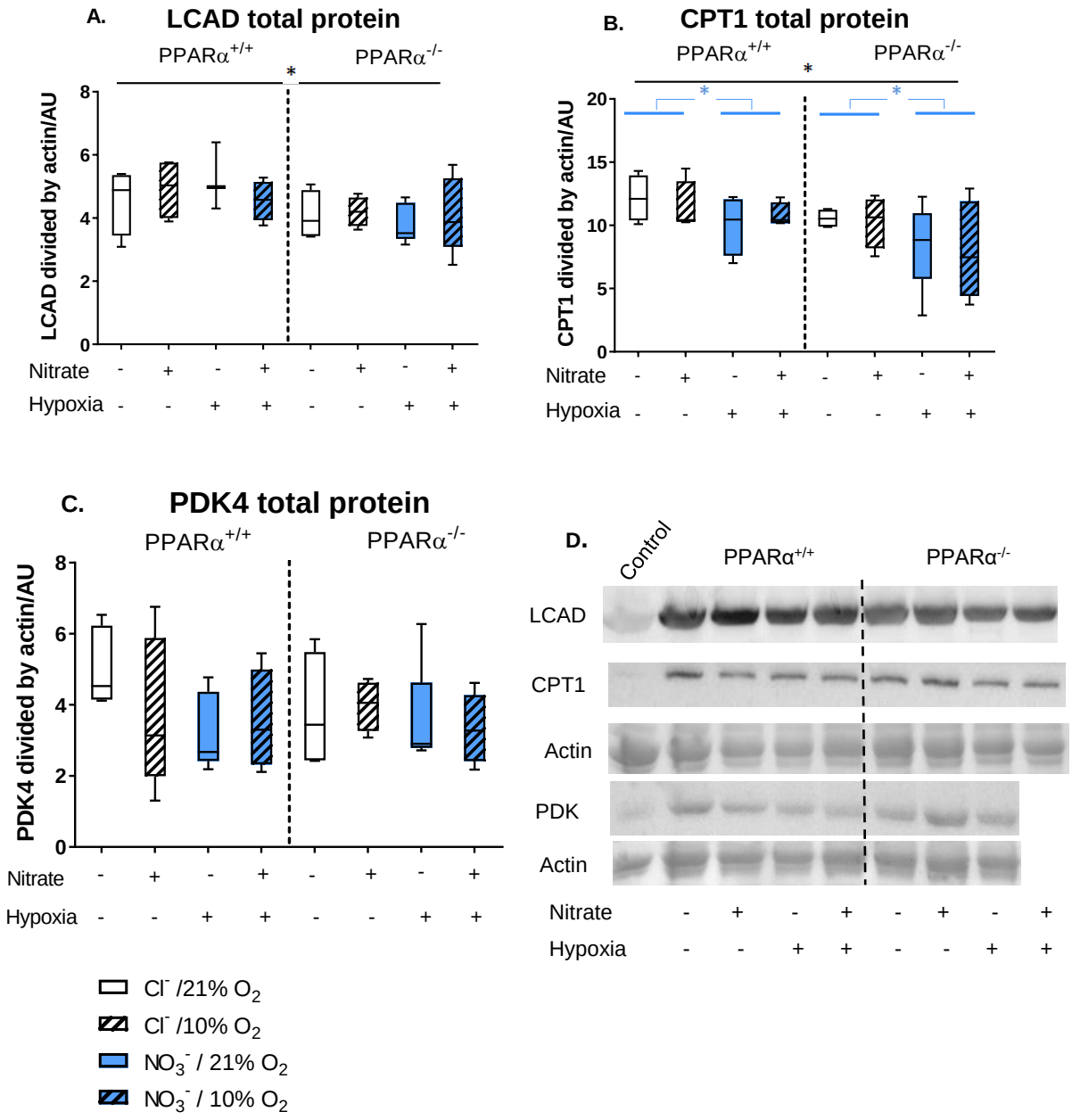

Figure 4.12. Total protein levels assessed by Western Blot.

A. *Levels of long chain 3-hydroxyacyl-coenzyme A dehydrogenase (LCAD)* ***B.*** *Carnitine palmitoyltransferase 1 (CPT1)* ***C.*** *Pyruvate dehydrogenase kinase 4 (PDK4). Data are presented as boxplots extending from 25th to 75th percentiles and displaying the median line, with whiskers representing minimum to maximum values. Values are relative to the actin band and gel loading control, n=3-5 per experiment group. *P≤0.05* ***D.*** *Western blot pictures with corresponding actin band derived from a ponceau stain. Given that LCAD and CPT1 were detected on the same membrane, these are corrected to the same actin bands.*

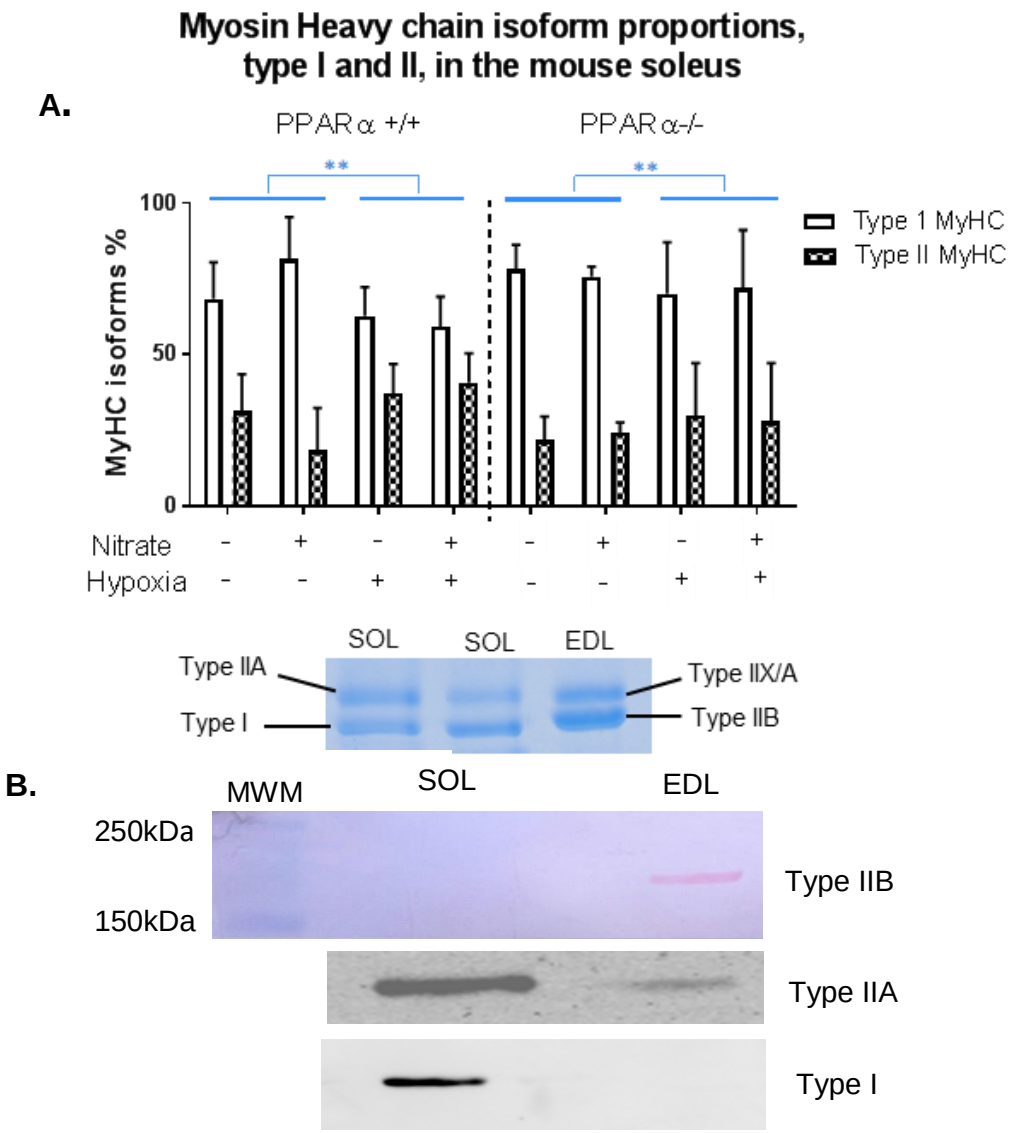

Figure 4.13. Myosin heavy chain isoform type proportions in the soleus.

*These were examined, with separation of fibre type specific bands of the soleus (SOL) shown alongside those of the extensor digitorum longus muscle (EDL) to demonstrate differences in muscle composition. This was quantified using SDS-PAGE **(A)**, with identification of type I, IIA, IIB isoforms confirmed using western blotting **(B).** For graph A, data is presented as mean ±SD, n=3-5 per experiment group. ** P≤0.01.*

4.6.5 Measures of mitochondrial density

PPARα genetic ablation decreases PGC1α

From the aforementioned functional respirometry measurements, it is unclear whether the downregulation of oxidative processes that were observed in both hypoxia and PPARα$^{-/-}$ groups were due to remodelling of mitochondrial pathways or to a loss in mitochondrial density. In other words, was the suppression due to mitochondria functioning less efficiently or because fewer mitochondria were present resulting from alterations in the mitochondrial network? Equally, was nitrate supplementation acting to recover mitochondrial function in hypoxia through changes to the mitochondrial network or through improving the efficiency of oxidative pathways?

This question was investigated further by measuring total protein levels of factors closely related to mitochondrial content and that have been shown previously to be indicative of alterations in mitochondrial networks. One such measure is a key regulator of mitochondrial biogenesis, PGC1α. Whilst no significant changes were observed in PGC1α with nitrate or hypoxic treatments, differences were identified between genotypes, with a 19.8% decrease ($p \leq 0.05$) in PPARα$^{-/-}$ in comparison to PPARα$^{+/+}$ (**Figure 4.14A**). Alongside this was a lack of change in the mediator of fusion between mitochondrial outer membranes, mitofusin 2 (MFN2) (**Figure 4.14B**).

PPARα genetic ablation and hypoxia impair citrate synthase (CS) activity with chloride, but not nitrate, treatment

Another measure closely correlated to mitochondrial density is the activity of the TCA cycle enzyme CS (Larsen et al., 2012). As shown in **Figure 4.14D**, CS activity measured in soleus homogenates was suppressed in the hypoxic chloride treated groups by 23.9% in comparison to normoxic chloride ($p \leq 0.01$). This occurred alongside a 17.5% decrease ($p \leq 0.05$) in CS activity in PPARα$^{-/-}$ chloride in comparison to PPARα$^{+/+}$ chloride groups. No significant decreases were observed in the nitrate treated groups, indicating that this treatment maintained CS activity.

However, the changes in CS total protein were unaffected across all treatment conditions **Figure 4.14C**. Similarly, no change was observed in protein levels of mitochondrial complexes I-V (**Figure 4.15**).

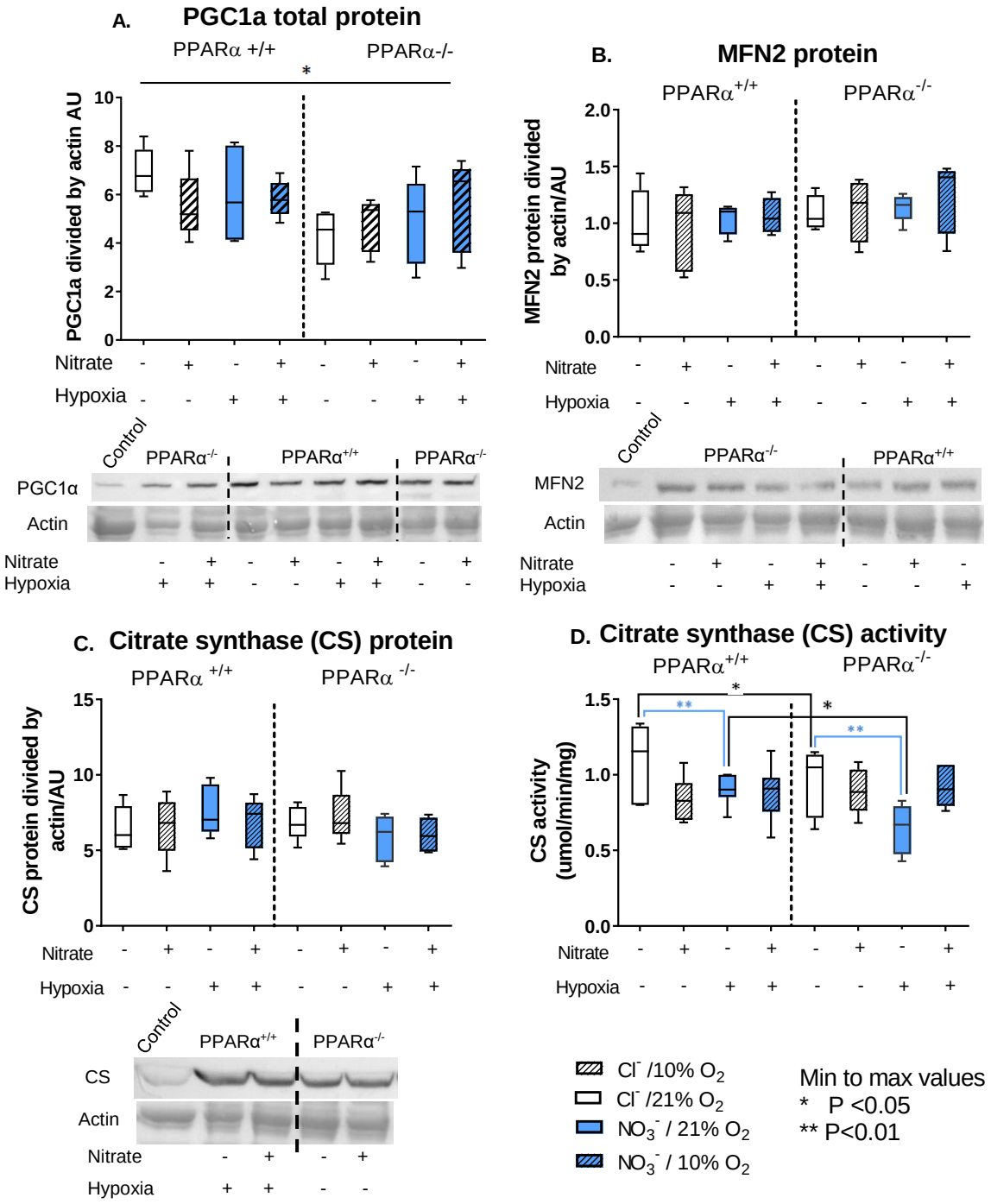

Figure 4.14. Total protein levels of PGC1α (A), MFN2 (B), Citrate synthase (CS) (C) and CS activity (D).

*Data are represented as boxplots extending from 25th to 75th percentiles and displaying the median line, with whiskers presenting minimum to maximum values. Values are relative to the actin band and gel loading control, n=3-5 per experiment group. *P≤0.05 ** P≤0.01.*

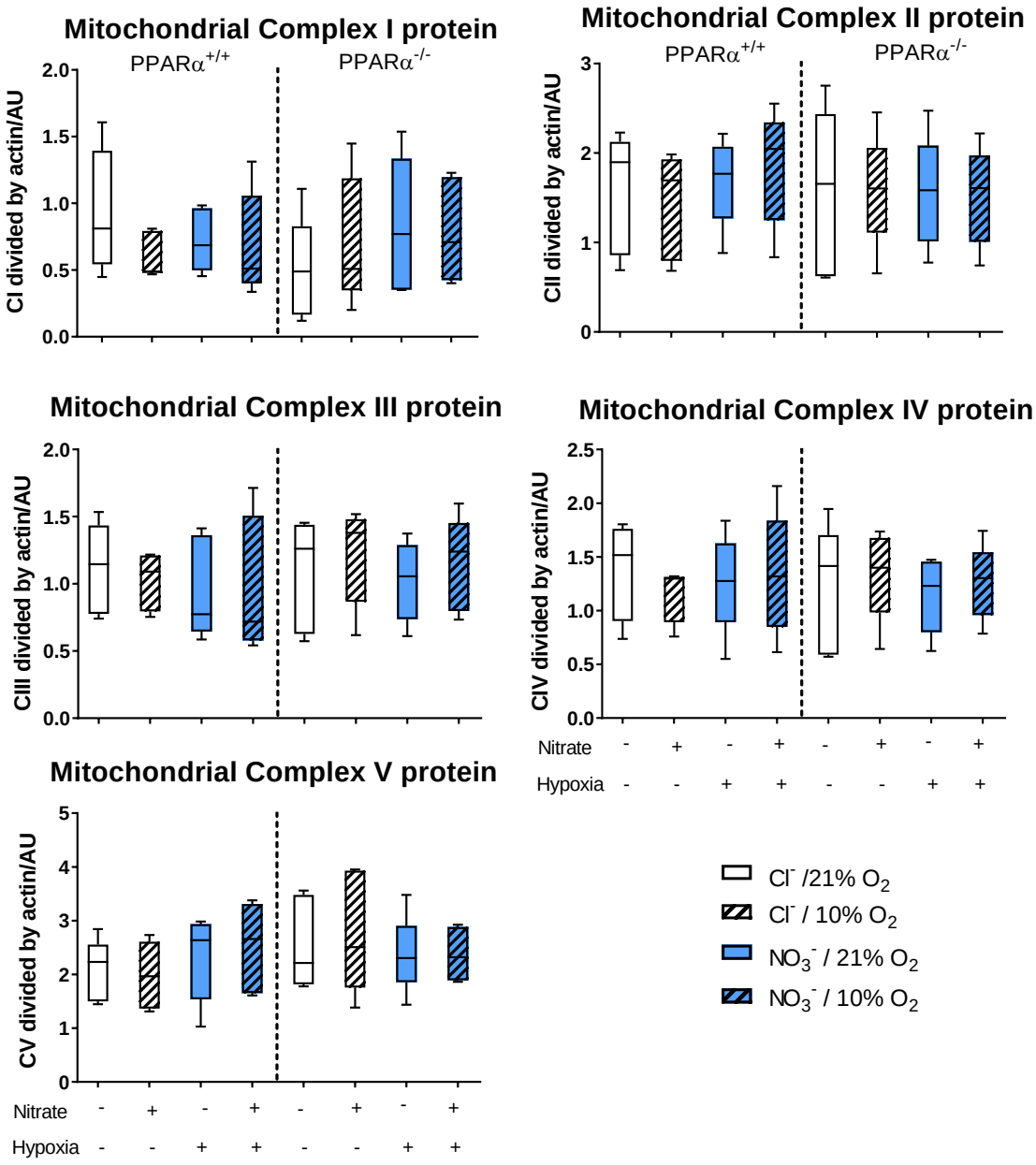

Figure 4.15. Total protein levels of all five mitochondrial complexes, assessed by Western blot.

The corresponding blot picture is presented on the following page. Data presented as boxplots extending from 25th to 75th percentiles and displaying the median line, with whiskers presenting minimum to maximum values. Values are relative to the actin band and gel loading control, n=3-5 per experiment group. No significance was found between any experimental groups.

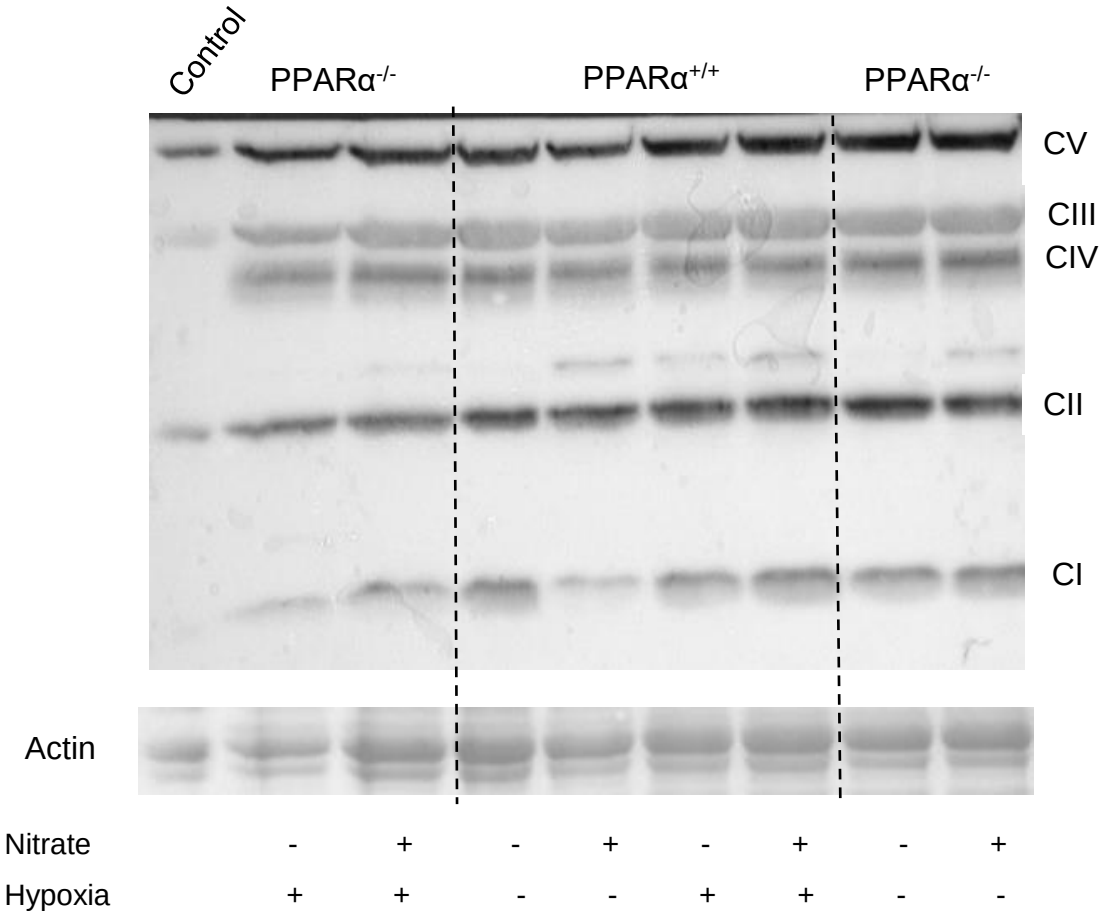
Control
PPARα-/-
PPARα+/+
PPARα-/-
CV
CIII
CIV
CII
CI
Actin
Nitrate - + - + - + - +
Hypoxia + + - - + + - -

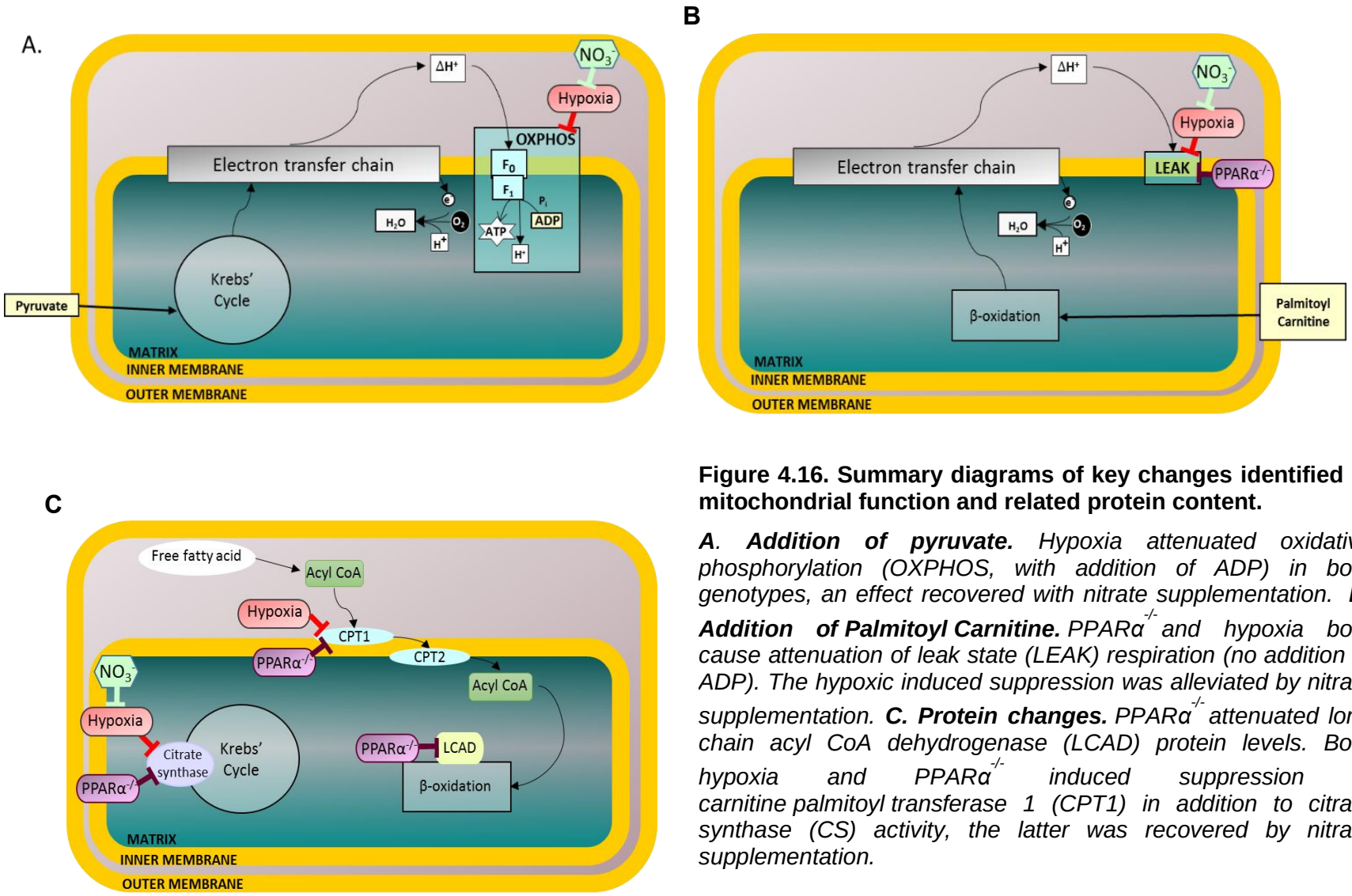

Figure 4.16. Summary diagrams of key changes identified in mitochondrial function and related protein content.

A*. *Addition of pyruvate. *Hypoxia attenuated oxidative phosphorylation (OXPHOS, with addition of ADP) in both genotypes, an effect recovered with nitrate supplementation.* ***B. Addition of Palmitoyl Carnitine.*** *PPARα$^{-/-}$ and hypoxia both cause attenuation of leak state (LEAK) respiration (no addition of ADP). The hypoxic induced suppression was alleviated by nitrate supplementation.* ***C. Protein changes.*** *PPARα$^{-/-}$ attenuated long chain acyl CoA dehydrogenase (LCAD) protein levels. Both hypoxia and PPARα$^{-/-}$ induced suppression of carnitine palmitoyl transferase 1 (CPT1) in addition to citrate synthase (CS) activity, the latter was recovered by nitrate supplementation.*

4.7 Discussion

In this study, four weeks of hypoxic exposure was demonstrated to impair several measures of mass corrected mitochondrial respiration in the mouse soleus muscle. This included a decrease in OXPHOS respiration rates of pyruvate, complex II driven electron flux and long chain fatty acids, with the latter also being impaired in LEAK state. These effects were observed to a similar same degree in both PPARα$^{+/+}$ as well as PPARα$^{-/-}$, thus indicating it is a response elicited independently of PPARα. The impairment of pyruvate OXPHOS and long chain fatty acid LEAK state respiration rates did not occur in mice supplemented with dietary nitrate (**Figure 4.16A and B respectively**). This affect was apparent in both genotypes (PPARα$^{+/+}$ and PPARα$^{-/-}$). This thus suggests nitrate treatment partially recovered the hypoxic induced suppression of skeletal muscle mitochondrial function and that this again occurred via mechanisms independent of PPARα. To the author's knowledge, this is the first time that the interaction between dietary nitrate and PPARα in hypoxia has been explored to this depth in skeletal muscle. The results suggest that nitrate supplementation holds promise as a potential therapy for alleviating hypoxic induced stress in skeletal muscle, which is relevant for various disease states where skeletal muscle impairment is associated with hypoxia (Killian et al., 1992a, Puthucheary et al., 2013), and also in the context of high altitude physiology (Levett et al., 2012).

A key question remaining is the mechanism by which nitrate treatment is acting to recover these specific aspects of mitochondrial function. Given that the biologically active element of dietary nitrate supplementation, NO, is a potent vasodilator, it is possible that the improvements in mouse mitochondrial function reported in this chapter are a result of increased skeletal muscle blood flow, as has been demonstrated in response to acute dietary nitrate supplementation in subjects sojourning to high altitudes (Bakker et al., 2015). As analysis was focused upon *in vitro* measures in this chapter and mouse tissue blood flow was not measured, this cannot be ruled out. However, if this was the case, it would perhaps be expected to be reflected through global improvements in mitochondrial function as opposed to the specific improvements discussed. In addition, enhanced oxidative capacity in response to nitrate treatment has been demonstrated in cultured myocytes (Ashmore et al., 2015b), which is thus an effect occurring independently of an increased O_2 delivery resulting from NO induced vasodilation.

In some respects, it may appear surprising that PPARα genetic ablation had so little effect upon skeletal muscle oxidative metabolic function in hypoxic conditions. This is

especially interesting in light of recent findings on the role of PPARα in the hypoxic adaptation of the heart (Cole et al., 2016). Indeed, Cole and colleagues reported that the changes evoked by PPARα genetic ablation ensured these mice had already undergone the required adaptive cardiac metabolic changes to maintain function in hypoxia. The contradiction between this and the present chapter, which instead suggests a minimal role of PPARα in hypoxia induced skeletal muscle metabolic remodelling, may be due to tissue specific differences. The heart has a higher metabolic rate and mitochondrial density in comparison to skeletal muscle and also relies heavily upon fat oxidation for ATP generation (Neely et al., 1972). Modulation of fat oxidation indeed appears to be a crucial aspect of cardiac hypoxic adaptation (Cole et al., 2016). The dependence upon this adaptation may, at least in part, explain why these apparent discrepancies between the tissue specific responses exist and in turn why a decline in muscle energetics is reported in the heart, but not skeletal muscle. Unlike skeletal muscle, where the PCr half-life is maintained in hypoxic exposure (Edwards et al., 2010), the PCr/ATP ratio is reported to be impaired in the human heart (Holloway et al., 2014, Holloway et al., 2011). It would therefore make sense for skeletal muscle to have other avenues of metabolic adaptation aside from PPARα dependent mechanisms. This would be of interest for future studies to pursue.

Other effects of PPARα ablation upon mouse physiology were largely expected, given previous reports. This included weight loss and the presence of fatty droplets on liver, the latter being an indication of the necessity of PPARα for the regulation of hepatic liver metabolism (Lee et al., 1995), alongside reduced expression of recognised PPARα targets CPT1 and LCAD (**Figure 4.16C**) (Morash et al., 2013, Lee et al., 1995).

PPARα genetic ablation will undoubtedly cause alterations to key positive effectors of inner mitochondrial membrane uncoupling proteins (UCP's): free fatty acids (Woyda-Ploszczyca et al., 2016). This may go to explain the observed decrease in LEAK state in PPARα$^{-/-}$ mice. Moreover, the member of the UCP family, UCP3, has been identified as a PPARα target (Cole et al., 2016). The effects on complex I flux appears to be a novel finding and its relation to the other responses mentioned are not clear.

The severity and longevity of the hypoxic insult in this chapter was reflected through several measures. This included the two-fold difference in the haemoglobin concentrations of those mice exposed to hypoxia in comparison to their normoxic counterparts, a response unaffected by nitrate treatment. This is contrary to previous findings whereby nitrate treatment was shown to decrease haemoglobin concentrations in both hypoxic and

normoxic conditions (Ashmore et al., 2015a), a disparity that may result from the prolonged nitrate treatment duration in this chapter (18 days (Ashmore et al., 2015a) vs. 35 days (present study)).

Hypoxia was also found to alter MyHC isoform proportions, which were indicative of a shift towards a fast type (glycolytic) fibre phenotype. This is in line with previous reports of HIF-1α mediating increases in expression of glycolytic enzymes in response to hypoxic exposure within skeletal muscle (Kim, 2006, Green et al., 1989, Firth et al., 1995). This result is therefore perhaps expected, especially given that the time course of the present chapter is beyond the time frame required to induce fibre type shifts in rodent soleus muscle, which has been reported to occur after as little as 7 days following hind limb suspension (Stevens et al., 1999).

An aspect of metabolic remodelling that has been shown repeatedly in response to environmental hypoxia is a shift away from oxidation of fatty acids (Horscroft et al., 2014). Measures of mitochondrial oxidative respiration presented in this chapter support this concept, as oxidation of long chain fatty acid (palmitoyl carnitine) in both LEAK and OXPHOS states were attenuated by hypoxic exposure. The impact upon β-oxidation is further supported by the suppression of CPT1 protein levels in response to hypoxic exposure (**Figure 4.16C**). This has been reported previously and has been associated with a downregulation of PPARα expression (Morash et al., 2013). Given that this effect occurred in both PPARα$^{+/+}$and PPARα$^{-/-}$ mice, this suggests other signalling mechanisms may play a role in the regulation of CPT1 levels, for instance through PPARβ/δ compensation (Wahli et al., 1995).

The suppression of β-oxidation reported here is thus in accordance with the general consensus that environmental hypoxia induces a shift away from the highly O_2 demanding oxidation of fatty acids (Horscroft et al., 2014). However, the hypoxic induced suppression was not exclusive to β-oxidation as pyruvate oxidation was also shown to be attenuated. The causes of this decline in carbohydrate oxidation are unclear. Previous studies have reported induction of pyruvate dehydrogenase kinase (PDK) isoforms in response to hypoxic exposure, which in turn inhibits pyruvate dehydrogenase thus blocking the conversion of pyruvate to acetyl CoA, causing a shunting of pyruvate from entry into the TCA cycle. The upregulation of PDK1 is HIF-1α mediated in a human B lymphocyte cell line and mouse embryo fibroblasts (Kim, 2006). In cardiac muscle, mediation of a hypoxic induced increase in PDK4 expression has been linked to PPARα (Cole et al., 2016). However, the assessment

of PDK4 protein levels in mouse skeletal muscle revealed no change across the treatment groups, neither in hypoxia or PPARα$^{-/-}$. This discrepancy may again be explained by differences in tissue type, as skeletal muscle may exhibit different mechanisms to concert this suppression of pyruvate oxidation.

The impact of hypoxic exposure upon mitochondrial complex function, as with most other measurements of mitochondrial function mentioned, has shown confusing results in previous studies. For instance, short term exposure (9-11days) to hypobaric hypoxia (4,559m) has been shown to have little effect upon complex I and II function (Jacobs et al., 2013). However, significant suppression of function was demonstrated following a 28 day exposure to 3,454m (Jacobs et al., 2012), and specifically in complex I dependent OXPHOS in rodents (Gamboa et al., 2012). In the present chapter, hypoxia was not reported to affect complex I function, but did induce a decline in complex II dependent OXPHOS. This is in line with previous findings taken from metabolic profiling of human plasma, which revealed a 158% increase in succinic acid concentrations in response to hypoxia (Tissot van Patot et al., 2009). Given that succinic acid (succinate) is the substrate of complex II/succinate dehydrogenase, its accumulation is indicative of a concerted downregulation of complex II function. In cardiac tissue, the accumulation of succinate in response to ischemia is reported to have a toxic effect and has been directly linked to the production of mitochondrial ROS from complex I (Chouchani et al., 2014).

Alongside measurements of mitochondrial respiration were investigations into possible changes occurring to the mitochondrial network. This included the surrogate measure of mitochondrial density, CS activity (Larsen et al., 2012), which was decreased in response to hypoxia and PPARα$^{-/-}$ in chloride treated groups. This thus suggests the hypoxic and PPARα$^{-/-}$ induced suppression of mouse mitochondrial function reported in the respirometry measures may have been linked to a decrease in mitochondrial density as opposed to mass specific changes, as has been reported in previous studies examining long term hypoxic exposure (Horscroft et al., 2014). Given that this affect was restricted to chloride treated animals, this indicates that the potential decrease in mitochondrial density was recovered with nitrate treatment. Indeed, induction of mitochondrial biogenesis triggered by nitrate supplementation has been suggested previously in adipose tissue through increasing levels of a major driver of mitochondrial biogenesis, PGC-1α (Roberts et al., 2015). However, changes in CS activity were not reflected through alterations in the protein levels of CS, which were unaffected across all treatment groups. Equally, no change

was observed in PGC-1α or in mitochondrial complexes I-IV in response to hypoxic exposure. This could suggest either that measures of CS activity are perhaps not as closely related to changes in mitochondrial density as has been recorded previously (Larsen et al., 2012), or that the sensitivity of Western Blotting is not sufficient to detect discrete modifications across treatment conditions. It may also be that alterations in protein levels of these molecules are not apparent at the time point at which these measurements were taken, following 4 weeks of hypoxic exposure. It may be that these changes are occurring at a more acute phase of the hypoxic exposure.

A response that did match was the decline in CS activity observed in chloride treated PPARα$^{-/-}$ mice in comparison to PPARα$^{+/+}$ along with a corresponding fall in PGC-1α total protein in PPARα$^{-/-}$ mice. Both of these results indicate a decline in mitochondrial content and biogenesis, which may also contribute to the decline in LEAK state respiration observed in response to PPARα ablation.

Another indication of possible changes occurring to the mitochondrial network in response to hypoxia is that of fission, a process required to remove damaged mitochondria, which is mediated in part by membrane anchored dynamin family members MFN1 and MFN2 (Youle et al., 2012). A decrease in MFN2 levels have been shown in hypoxic mouse models, whereas inducing MFN2 overexpression has been suggested to attenuate hypoxia-induced apoptosis (Peng et al., 2015). In this chapter, however, protein levels of MFN2 were unchanged across treatment groups.

Nitrate supplementation has recently been demonstrated to induce skeletal muscle fibre type switching towards from fast glycolytic to slow oxidative fibre type (Roberts et al., 2016). However, results of the present chapter do not indicate any effect of nitrate treatment upon MyHC isoform proportions. Although the nitrate dosing used by Roberts and colleagues was the same as used in the present chapter (0.7mM), their treatment was in the absence of a hypoxic insult, which may be severe enough to counteract influences of nitrate treatment upon fibre type.

4.8 Conclusions

This study has confirmed previous reports of hypoxic induced suppression of mitochondrial function in skeletal muscle. Hypoxia impaired numerous measures of mass specific respiration rates in the mouse soleus muscle, including long chain fatty acid LEAK and carbohydrate OXPHOS capacities. These significant decreases were recovered in

nitrate supplemented mice, indicating a nitrate dependent recovery of mitochondrial function. As this nitrate effect was observed in both PPARα$^{+/+}$ and PPARα$^{-/-}$ mice, it suggests the effect is not dependent upon PPARα. In conclusion, results of this study indicate that nitrate can exert effects upon skeletal muscle metabolism in hypoxia independently of PPARα.

5 **Chapter 5 (Study 4):** Effects of acute dietary nitrate supplementation upon metabolism and exercise performance in COPD: a double blind, placebo-controlled, randomised controlled pilot study.

5.1 Introduction

As outlined in the literature review (section 1.2.6), COPD is a highly prevalent disease and exercise limitation is a common symptom amongst patients. Previous findings suggest that tissue O_2 delivery, intramuscular O_2 transport and mitochondrial dysfunction may all contribute to exercise limitation in COPD. Approaches that reduce the O_2 cost of exercise may thus be of therapeutic benefit and current knowledge suggests nitrate supplementation may be beneficial in conditions where O_2 delivery to the muscles is reduced (section 1.2.7).

A number of studies have demonstrated a decrease in the O_2 cost of submaximal exercise in healthy young individuals in response to nitrate supplementation (Larsen et al., 2007, Lansley et al., 2011, Bailey et al., 2009, Vanhatalo et al., 2010), an effect associated with improvements in exercise tolerance and performance (Bailey et al., 2010, Vanhatalo et al., 2010, Murphy et al., 2012). The majority of these studies use beetroot juice as the nitrate source, with the O_2 sparing effect being dependent largely on nitrate itself, as nitrate-depleted beetroot juice fails to illicit the same effect (Lansley et al., 2011). This O_2 sparing effect is also apparent in healthy subjects exposed to conditions where O_2 delivery to the muscle is reduced due to high altitude exposure (5000m) (Masschelein et al., 2012) or a reduced inspired F_IO_2 (14%) administered via a gas mask (Vanhatalo et al., 2011). These studies demonstrated a nitrate dependent improvement in arterial and muscle oxygenation in both rest and exercise (Masschelein et al., 2012); also an improved exercise tolerance (Masschelein et al., 2012, Vanhatalo et al., 2011) occurring alongside a reduction in markers

of muscle fatigue (Vanhatalo et al., 2011). The work presented in the previous chapter on mouse skeletal muscle is in line with these findings by demonstrating the nitrate dependent partial recovery of mitochondrial function in hypoxia.

Prior evidence therefore indicates that nitrate supplementation could potentially have considerable benefits for improving exercise tolerance in chronically hypoxic COPD patients. Whilst this has been investigated in COPD cohorts previously, these studies have produced confounding results likely due to limitations in study design. For instance, although benefits of nitrate supplementation have been demonstrated in COPD patients through increasing exercise time, these studies did not use a robust placebo (Berry et al., 2015, Kerley et al., 2015). Other groups have failed to produce these results when using a robust placebo (Shepherd et al., 2015, Leong et al., 2015), however, in these studies, the nitrate dosing was below that which has been shown to enhance exercise performance in healthy subjects (Wylie et al., 2013). In the case of Leong and colleagues (Leong et al., 2015), testing was performed one hour post dosing, which is prior to the time taken for plasma nitrite levels to peak (Wylie et al., 2013).

In addition to poor study design, an area lacking in these previous studies that could provide significant insight into the effects of nitrate supplementation on this complex disease population is metabolomic analysis. NMR-based metabolomic assessment of plasma in COPD patients has been shown previously to uncover phenotypic information based upon a combination of systemic effects and lung-function parameters (Ubhi et al., 2012b). For instance, it has been used to distinguish between subtypes of COPD patients, with a cohort of 21-38 per patient phenotype. Amongst the distinguishing features were specific changes in amino acid metabolism in those patients additionally suffering from cachexia (Ubhi et al., 2012a). The metabolomics approach thus presents as a means of accounting for the heterogeneity of this complex disease and it has been adopted by numerous studies to further disease characterisation. For example, it has been used to elucidate differences in metabolic profile in COPD patients (n=18) vs. controls (n=12) in response to exercise at 70% maximal work rate, which include differences in the levels of valine, alanine and isoleucine (Rodríguez et al., 2012). Endurance training was demonstrated to have a significant impact upon the metabolic profiles of healthy subjects that were not replicated in COPD patients, in whom the only training-induced effect was a decrease in lactate (Rodríguez et al., 2012). Given these significant advances made through employment of metabolomics techniques,

it thus makes sense to adopt this approach in the examination of nitrate dosing in these patients.

5.2 Aims

In this pilot study, the effects of a higher, acute dosing of dietary nitrate on exercise performance and plasma metabolites in COPD patients were investigated. The latter was achieved through targeted metabolomics using ^{1}H-NMR.

5.3 Hypothesis

Nitrate supplementation would improve exercise performance by increasing endurance time and the effects would be apparent in changing plasma metabolites, providing an insight into the mechanisms of nitrate action.

5.4 Methods

5.4.1 Patient selection

This study was approved by the Bromley Research Ethics Committee (reference 13/LO/0372) and conducted in line with the principles of the Declaration of Helsinki. All participants provided written informed consent prior to enrolment in the study.

COPD patients of GOLD stage II-IV (Rabe et al., 2007) were considered for inclusion in the study and were recruited through outpatient clinics at the Royal Brompton Hospital and through public outreach events such as World COPD day. Recruitment began on 24th June 2013 and was completed on the 28th April 2014, with follow-up completed on 3rd June 2014. This study was registered prospectively on a publicly accessible database (www.iscrn.com/ISRCTN66099139) and all ongoing and related trials for this investigation were also registered.

Detail on the recruitment process is depicted in **Figure 5.1**. Exclusion criteria for the study included patients taking nitrate-based medications or phosphodiesterase V inhibitors, those with other medical conditions likely to benefit from nitrate supplementation (including ischemic heart disease and peripheral vascular disease) and patients on long-term O_2 therapy or antibiotic therapy (whether on an acute of prophylactic basis). Patients considered clinically unstable (defined as being within one month of pulmonary exacerbation), suffering from hypotension or significant renal impairment (eGFR<50ml/min/1.73m^2) were also excluded from the study.

5.4.2 Study design and randomisation

This study was a double-blind, cross-over, placebo-controlled trial. Beverages were allocated using computer-generated randomisation in blocks of 4. This was devised by an independent statistician with consecutive numbers linked to preparations of either placebo or active nitrate treatment. Researchers involved in the enrolment of patients or outcome measurements remained separate from the randomisation process and were blinded throughout the study and data analysis. The principle investigator who was not involved in any patient visits (Dr Hopkinson) held the randomisation list and indicated the order of patient assignment.

Nitrate supplementation was expected to induce a rise in plasma nitrate and nitrite levels, with nitrite being further reduced to NO. Increases in NO were in turn expected to induce vasodilation, to be observed as a decrease in blood pressure. In response to exercise, nitrate supplementation was hypothesised to increase time to exhaustion during symptom-limited cycle ergometry at 70% peak workload as assessed on an incremental, maximal, symptom-limited cardiopulmonary exercise test. Given previous reports of NO decreasing VO_2, it was additionally hypothesised that nitrate supplementation would alter the area under the VO_2 curve. As exercise test duration varied considerably for some subjects between the treatment and placebo exercise tests (irrespective of treatment condition), VO_2 analysis was restricted to the time shared between the two tests. This approach, defined as exercise isotime, ensured discrepancies in exercise test duration did not affect analysis. Changes in exercise performance with nitrate dosing were expected to be reflected through changes in metabolic profile, thus providing an indication of the potential mode of nitrate action.

5.4.3 Intervention

140ml of BEET-IT Sport Stamina Shot (James White Drinks, Ipswich, UK) containing 0.8g nitrate and 140ml of a matched placebo of beetroot juice specifically depleted of nitrate were used as the active and placebo preparations respectively. The placebo preparation was identical in appearance and taste (Lansley et al., 2011), and also produced beeturia. The dose chosen was intended to provide a bolus of nitrate (12.9mmoles) exceeding that necessary to reduce O_2 consumption during submaximal exercise in young healthy subjects (Wylie et al., 2013), and was selected as a convenient dosing method (2x 70ml bottles) which was readily acceptable and easily ingested.

Subjects were requested to avoid foods naturally high in nitrate in the 48hour period prior to the dosing visit and were asked to match food and caffeine consumption on the two days of testing. Subjects were additionally asked to avoid use of mouthwash and chewing gum in the 48hour period prior to testing as this has previously been shown to reduce oral bacterial nitrate reductase activity (Govoni et al., 2008). Subjects were also advised to avoid heavy exercise in the 24 hours prior to each dosing visit.

5.4.4 Study conduct

Following successful screening, the subjects attended the laboratory for measurement of baseline characteristics during which several parameters were recorded including vital signs, anthropometric measures, full pulmonary function testing and an incremental maximal symptom-limited cycle ergometry test was performed.

On the dosing visits, conducted at the Royal Brompton & Harefield NHS Trust, subjects arrived in the morning. Following a 10 minute rest period, blood pressure measurements and baseline plasma samples were obtained, after which the patients were dosed. 3 hours later, both blood pressure measures and blood sampling were repeated prior to endurance cycle ergometry at a constant work rate (70% peak workload achieved on prior maximal incremental testing). The cycle test was conducted at the same time on each occasion. Further blood draws were taken at peak exercise. After a minimum wash-out period of 7 days the protocol was repeated with the crossover beverage. See **Figure 5.1** for an outline of the study design and **Figure 5.2** for details on blood draws.

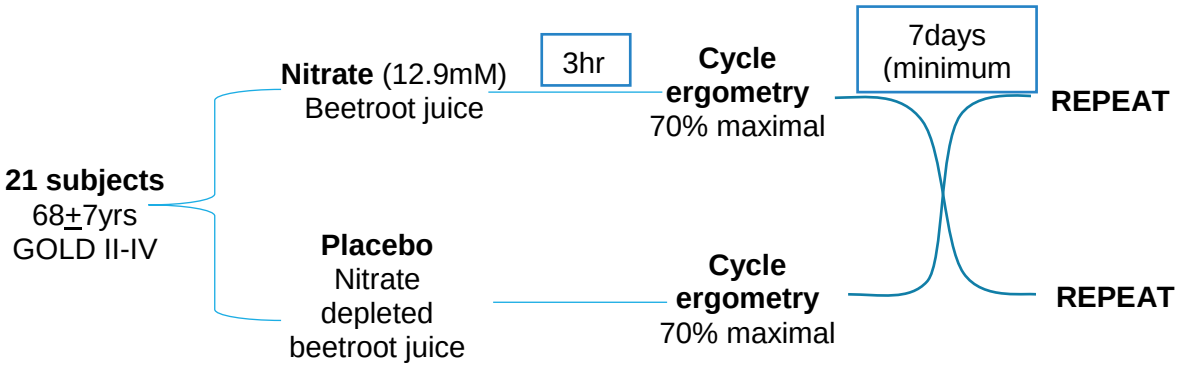

Figure 5.1. Flow diagram of the double-blinded, placebo-controlled, cross-over single dose study design.

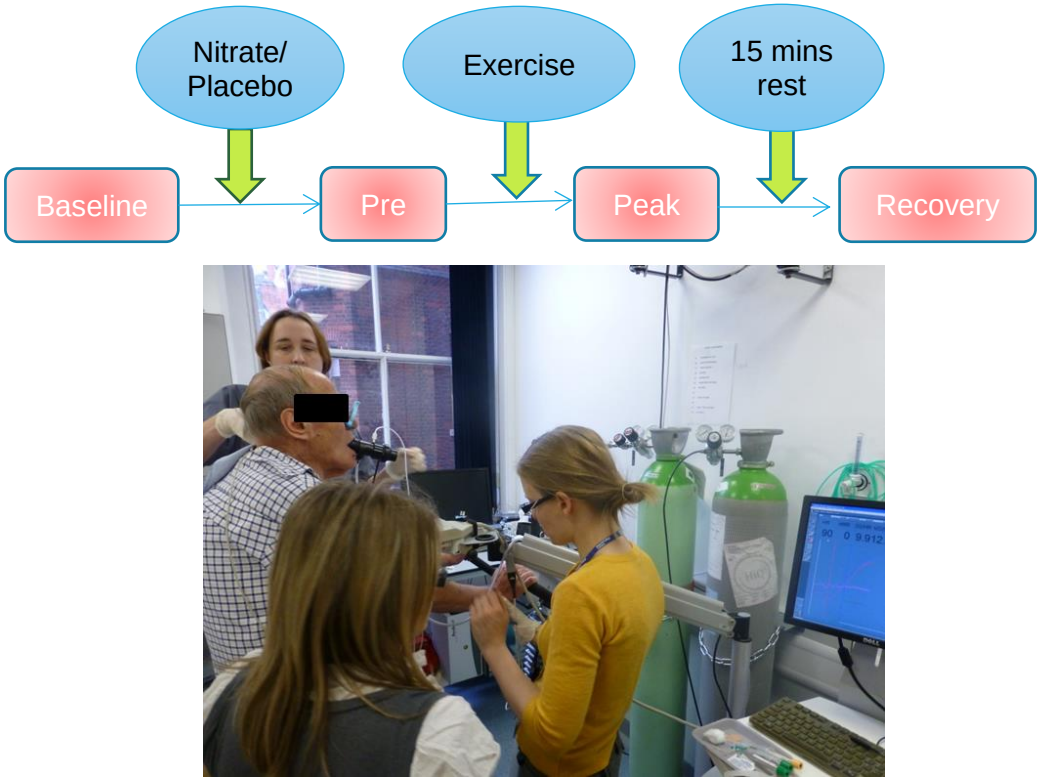

Figure 5.2. Blood samples timeline.

Sampling was conducted at 4 time points throughout the study day. Example of blood sample being taken at peak exercise.

5.4.5 Baseline characteristics

Blood pressure and anthropometrics

Blood pressure was measured using an automated blood pressure monitor (Omron M6, Omron Healthcare Europe, Hoofddorp, Netherlands). Measurement was made in the seated position with the subject's arm supported. A mean of three measurements was recorded. Height (cm) without shoes was measured using a wall mounted measure, and weight (kg) measured using standardised scales.

Pulmonary function testing

Measurements were made in the lung function department of the Royal Brompton Hospital according to international guidelines and with rigorous quality assurance in place with a Jaeger master lab system (CompactLab system, Jaeger, Wurzburg, Germany). Spirometry, gas transfer and plethysmographic lung volumes were also measured in accordance with European Respiratory Society (ERS)/ American Thoracic Society (ATS) guidelines(Miller et al., 2005, Macintyre et al., 2005, Wanger et al., 2005). Standardised lung function testing reference equations were based on the European Coal and Steel Community (ECSC) reference values(Gibson, 1993). Capillary blood gas samples were taken at rest.

5.4.6 Cycle ergometry

A symptom limited incremental exercise test was performed at baseline on a bicycle ergometer (Ergoselect 100, Ergoline, Bitz, Germany) with metabolic measurements collected using a mouthpiece (Masterscreen CPX metabolic cart, CareFusion, Basingstoke, UK) and analysed using JLAB software (JLAB Lab Manager version 5.32, Jaeger, CareFusion, Basingstoke, UK) (See **Figure 5.3**). Following a 2 minute rest period and 2 minute free cycling workload increased by 5 Watts every 30 seconds with subjects being asked to maintain a speed of 60-70 revolutions per minute. Measurements were taken of peak workload, VO_2, VCO_2, minute ventilation, respiratory rate and tidal volume. Peak workload was defined as the greatest workload that the subject could maintain for a 30 second period.

To evaluate the effects of the intervention, endurance cycle ergometry testing was performed 3 hours following dosing at 70% peak workload. This is within the time period at which it has been shown for plasma nitrite levels to peak in plasma following nitrate dosing

(Wylie et al., 2013). The endurance time was calculated as the time from the beginning of loaded cycling to the point of test cessation due to symptom limitation. Breath-by-breath data was obtained and rolling 8-breath averages were used in the isotime analysis. Exercise isotime is defined as the time shared between the treatment and placebo exercise tests for each subject. This ensured discrepancy in the exercise test duration, which were considerable for some subjects, did not affect analysis.

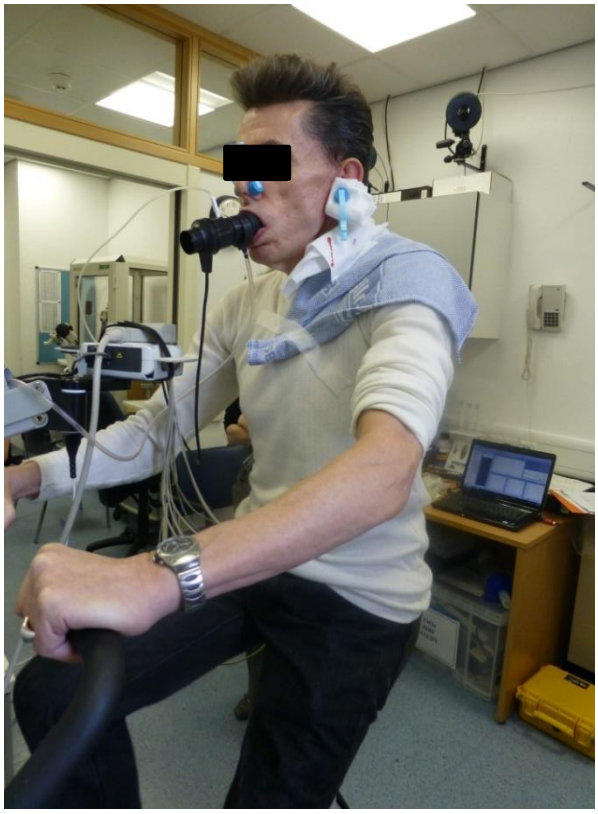

Figure 5.3. A subject undertaking the submaximal cycle ergometry test performed at 70% maximal workload until exhaustion.

Blood gas sampling was taken from the left ear.

5.4.7 Plasma sample processing

All plasma samples (baseline, 3 hours post dosing, peak exercise and recovery) were obtained by venesection in lithium heparin tubes and immediately spun for 10 minutes at 520g at 4°C. The resulting supernatant was pipetted into 2ml polypropylene cryotubes, taking care to avoid any contamination from the buffy coat containing the white cells/ platelets atop the erythrocyte pellet, and immediately frozen at -80°C. These samples were used both for nitrate/nitrite measurements and plasma metabolomics.

Unlike EDTA, the anticoagulant heparin gives only weak and very broad NMR resonances from polysaccharide moieties, thus having a limited effect upon the resulting spectra (Barton et al., 2010).

Plasma nitrate/nitrite measurements

Plasma samples were analysed from the following time points: baseline, post dosing/pre-exercise and peak exercise.

Nitrate and nitrite plasma levels were assessed using a post-column diazo coupling reaction (Griess reaction) in combination with high-performance liquid chromatography (HPLC) (Eicom NOx analyser, ENO-20, San Diego, USA) (Rassaf et al., 2002). Nitrate and nitrite were first separated on the analytical column (**Figure 5.4)**. Nitrite then reacted with the Griess reagent generating diazo compounds, with absorbance measured at 540nm using a spectrophotometric detector. Nitrate passed through the reduction column and was further reduced to nitrite before undergoing the same diazo coupling reaction. The peak areas of absorption of solutions of know standard concentrations were then compared to those produced by the test samples to provide measures of plasma nitrate and nitrite.

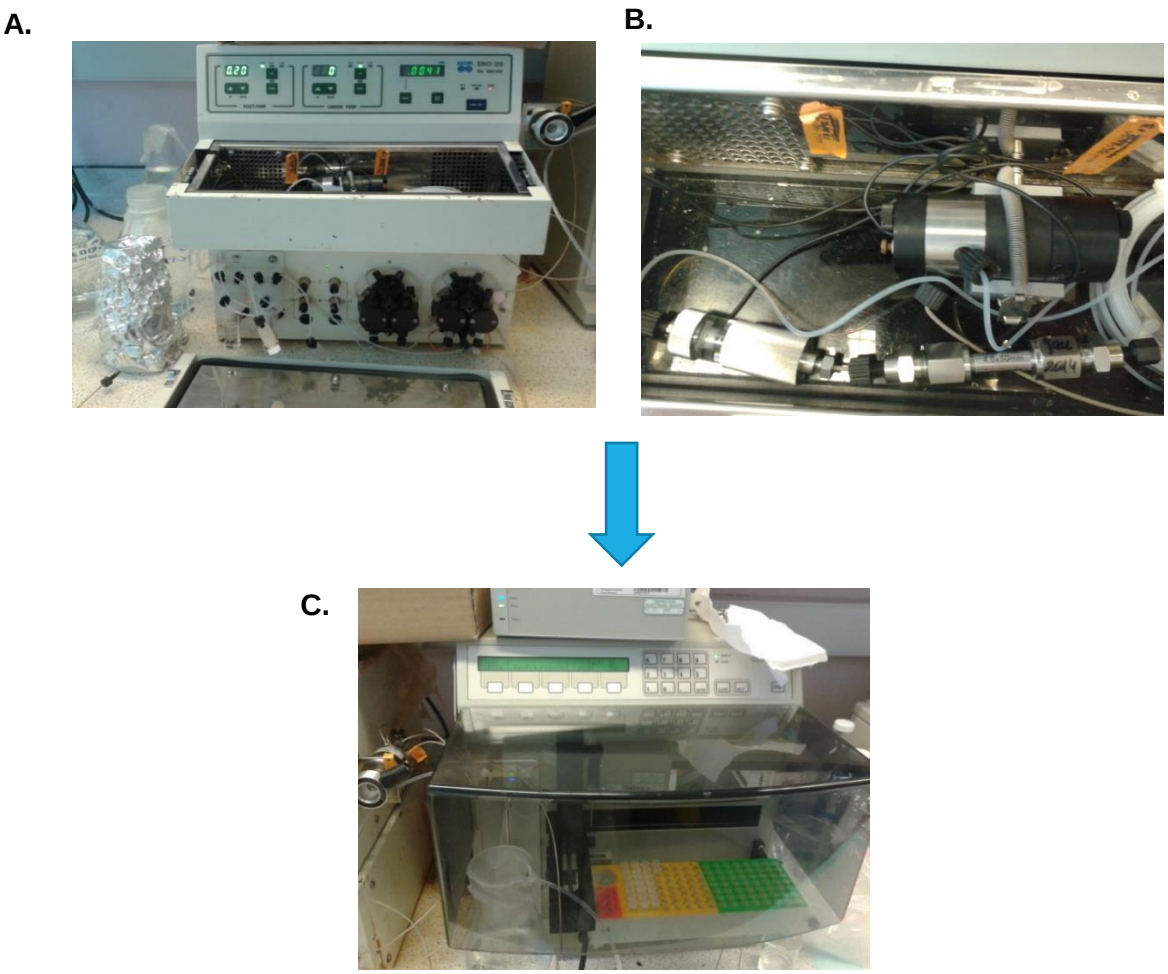

Figure 5.4. Instrumentation used to discern plasma nitrate and nitrite values.

*Nitrate and nitrite were firstly separated using high performance liquid chromatography (analytical column visible in **A** and **B)**. Nitrite, followed by nitrate (which is firstly reduced to nitrite), then reacts with Griess reagent generating a red diazo compound, the absorbance of which was measured at 540nm using a spectrophotometric detector (bottom diagram) **(C)**.*

Plasma metabolomics ^{1}H-NMR

Sample preparation for NMR spectroscopic analysis

Plasma samples were defrosted at room temperature and centrifuged (13,000rpm/16,000g for 10mins). An aliquot of 300µl was then mixed with 300µl of NMR buffer (double distilled water containing 8% D_2O). The resulting mixture was transferred to 5mm NMR tubes within a 96-tube rack.

NMR spectral acquisition

^{1}H-NMR spectra of plasma samples were obtained as described in Chapter 2 (section 2.4.3). As in this section, samples were analysed on a subject by subject basis, meaning plasma taken from the same subject at all 4 time points was defrosted and prepared at the same time and run within the same NMR experiment. This was to ensure any daily differences in experimental procedure were removed from analysis when data between time points were compared.

NMR data processing

Data were Fourier transformed using an exponential window function with a line broadening of 0.3Hz in the frequency domain. Spectra were phased automatically using zero-order phase correction and baselined in Topspin 3.0 (Bruker Biospin, Karlsruhe, Germany) before being imported into Matlab (Mathworks, Natick, MA) at full resolution. All chemical shifts were manually referenced to formate (δ = 8.44 ppm). Following this, spectra were normalised using PQ normalisation (Dieterle et al., 2006) and binned using adaptive intelligent binning (De Meyer et al., 2008), both in Matlab.

NMR Data Analysis

The analysis strategy for this data set was a targeted approach focused upon assessment of specific metabolites that have been previously associated with exercise and with COPD sufferers (Rodríguez et al., 2012, Nobakht M. Gh et al., 2015). This included: lactate, alanine, acetate, glucose, β-hydroxybutyrate, L-arginine, citrate and isoleucine. Lactate, glucose and isoleucine are particularly relevant in this thesis, given their association with progressive hypobaric hypoxic exposure unveiled in chapter 2.

The ppm values for the discernible peaks of these metabolites were identified. The corresponding binned value, and so spectral region containing this peak(s), was taken

forward for analysis. The focus was upon the change in these metabolites between treatment conditions from peak exercise compared to pre (post dosing). The difference between time points was therefore calculated (peak-pre) and a paired students' t-test was subsequently performed to assess differences between the treatment and placebo groups.

The patient cohort included a range of disease severities clearly distinguished by differences in GOLD stage. Previously metabolite changes (specifically perturbations in amino acid metabolism), identified through targeted metabolomics, have been shown to distinguish between sub-categories of COPD patients (Ubhi et al., 2012a). Therefore, analysis was taken further to separate those of GOLD stage I-II from III-IV and distinguish whether metabolite changes between these two sub-categories could be identified.

5.4.8 Data analysis and statistics

A convenience sample of 25 was studied to offer a good chance of identifying a clinically meaningful effect, with 21 of these subjects fully completing the study protocol. Data are presented as mean ± standard deviation and were analysed using GraphPad Prism version 7.0 for Windows (GraphPad Software, San Diego, California, USA).

Repeated measures analysis of variance (ANOVA) was used to compare plasma nitrate metabolites between treatment conditions and at each specific time-point. To compare O_2 consumption between study conditions, individual cardiopulmonary exercise test data periods were expressed as percentiles of isotime (the duration of the shorter of the two tests) and the individual responses grouped to allow analysis of VO_2 against percentage of isotime (plotted at the midpoint of each 10^{th} percentile of isotime). The area under this curve was assessed for each subject and the two conditions then compared using a paired student t-test. Resting and isotime measurements between treatment conditions were compared using paired t-tests, or the appropriate non-parametric test for data that was not normally distributed. In the case of endurance times, which did not fit a normal distribution, a Wilcoxon test was used to compare median values between the two treatment groups. For all results, a p-value of <0.05 was considered to be statistically significant.

Correlations were mapped to assess whether changes in nitrate handling were responsible for changes in physiological parameters induced by nitrate dosing. For this, Δ nitrate and nitrite pre (post dose): peak exercise was correlated with the following: ΔVE, ΔVO_2, Δ power/VO_2. A large degree of variability was also observed in exercise endurance time between subjects, therefore this was also correlated to Δ. To assess whether this

variability was related to changes in nitrate handling, the change in endurance time between treatments was also correlated to plasma nitrate/nitrite changes. Lastly, the subject cohort had a distinct variation in GOLD stage. Therefore, to examine whether the variability in nitrate handling was influenced by disease severity, a measure of airway obstruction, FEV_1, was plotted against plasma nitrate/nitrite changes.

Data that were normally distributed (tested using D'Agostino-Pearson (omnibus K2) normality test) were analysed using Pearson correlation coefficients, with two tailed P values. Otherwise, Spearman Correlation was used for data that was not normally distributed. Again, a p-value <0.05 was considered to be statistically significant. Linear regression was subsequently performed if this was the case.

5.5 Results

5.5.1 Subjects

Of the 25 subjects enrolled in the study, 21 completed the full study protocol **(Figure 5.5**). Recruitment began in June 2013 and the trial was completed by June 2014, by which time the 25 enrolled subjects had either completed or been withdrawn from the study. Baseline characteristics that are relevant for the purposes of this thesis are presented in **Table 5.1**. All patients were 100% compliant with the dosing protocol and no adverse effects were reported other than beeturia.

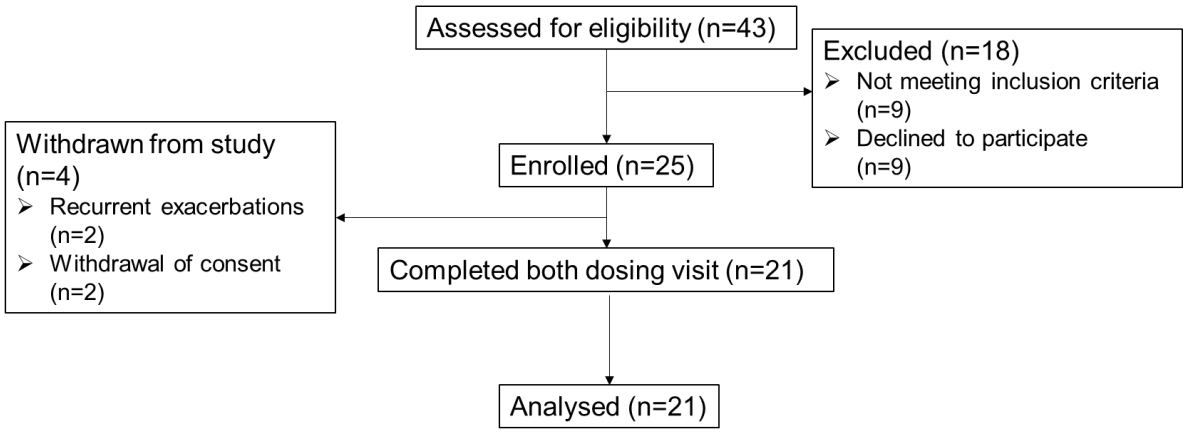

Figure 5.5. CONSORT recruitment diagram for enrolment and study recruitment.

Table 5.1. Baseline clinical characteristics of the subjects

Measurement	Mean	SD (+)
Sex (male:female)	16:5	
Age (years)	68	7
Systolic BP (mmHg)	137	19
Diastolic BP (mmHg)	79	7
BMI (kg/m^2)	25.2	5.5
FEV_1(L)	1.33	0.58
FEV_1 % predicted	50.1	21.6
RV % predicted	167	53
TLC % predicted	119	14
RV/TLC ratio (%)	52.3	8.7
PaO_2 (kPa)	10.7	1.2
Peak power on cycle (Watts)	71.9	30.8
Peak VO_2 (ml/min/kg)	18.0	5.9
GOLD I/II:III/IV	12:9	

Note: *(n=21), presented as mean +/-SD. BP-blood pressure; BMI-body mass index; FEV_1-forced expiratory volume in 1 second; RV- residual volume; TLC-total lung capacity, PaO_2 – partial pressure of arterial O_2; VO_2 – pulmonary oxygen uptake, GOLD – Global initiative for chronic obstructive lung disease.*

5.5.2 Venous nitrate and nitrite measures

Alterations in plasma nitrate at each time point are presented in **Figure 5.6**. As expected, significant increases in plasma nitrate levels were observed post dosing with nitrate-rich beetroot juice (37.0 ± 16.4μM baseline vs. 820.2 ± 187.7μM post dosing, $p<0.0001$). Levels remained elevated at peak exercise, although a greater variability was observed between subjects (917.1 ± 291.6 μM) (Individual values plotted in **Figure 5.7A**). No significant changes were observed in plasma nitrate with placebo treatment (45.7± 15.8μM baseline vs. 45.3μM ± 16.5μM post dosing).

For changes in plasma nitrite, levels at baseline for all bar 3 subjects were below the quantifiable limit (0.2μM) to be detected. The representation of changes from baseline to pre and post exercise levels are therefore only presented for plasma nitrate. Plasma nitrite levels remained at this level for the placebo treatment, but underwent a significant increase following nitrate supplementation to 1.57 ± 0.98μM. Despite the slight decrease in value, this level was retained at peak exercise (1.37± 0.65μM) (**Figure 5.7B**).

These results thus demonstrate that the nitrate dosing altered plasma levels of nitrate metabolites (nitrate and nitrite), but that there was a large degree of variability between subjects. Baseline measurements of plasma nitrate ranged from 16-70μM. Changes in nitrate levels from baseline to post dosing ranged from 483.7-1217.4μM and post dosing plasma nitrite levels ranged from 0.5-4.0μM. To investigate whether a relationship existed between the individual degree of change in nitrate and nitrite following nitrate dosing, these two variables were correlated (**Figure 5.8**). However, no significant correlation was revealed.

Further investigation into possible inter-individual differences in nitrate handling are presented below.

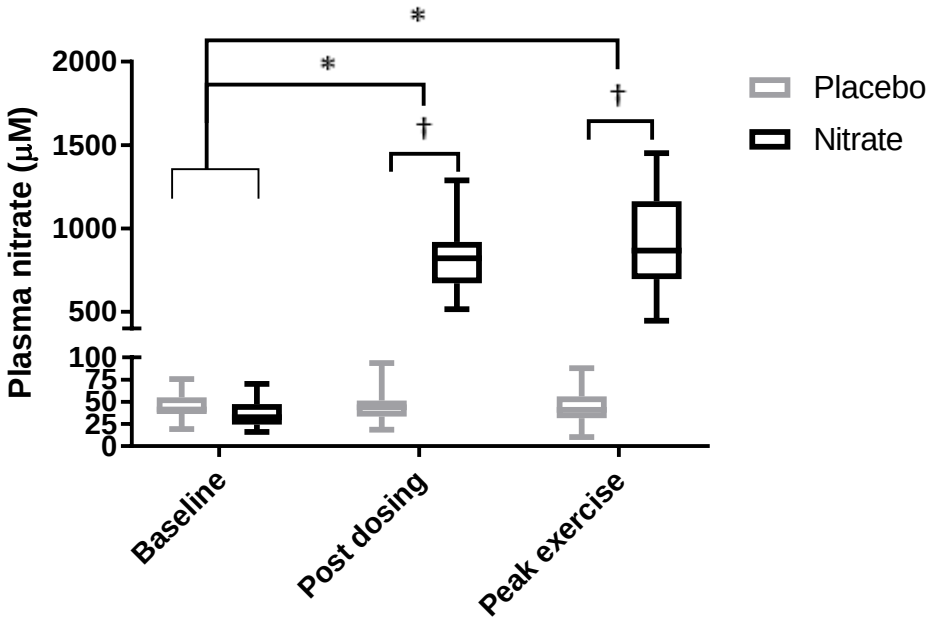

Figure 5.6. Alterations in plasma nitrate following dosing.

*Plasma nitrate concentrations assessed prior to dosing at baseline, post dosing (pre exercise) and at peak exercise. This includes the initial post dosing/pre-exercise time point, taken 3 hours following placebo/nitrate beverage consumption, and peak exercise, taken at the point of exhaustion following submaximal endurance cycle ergometry testing. *Significantly different from baseline †significantly different from placebo P<0.0001, ± SD.*

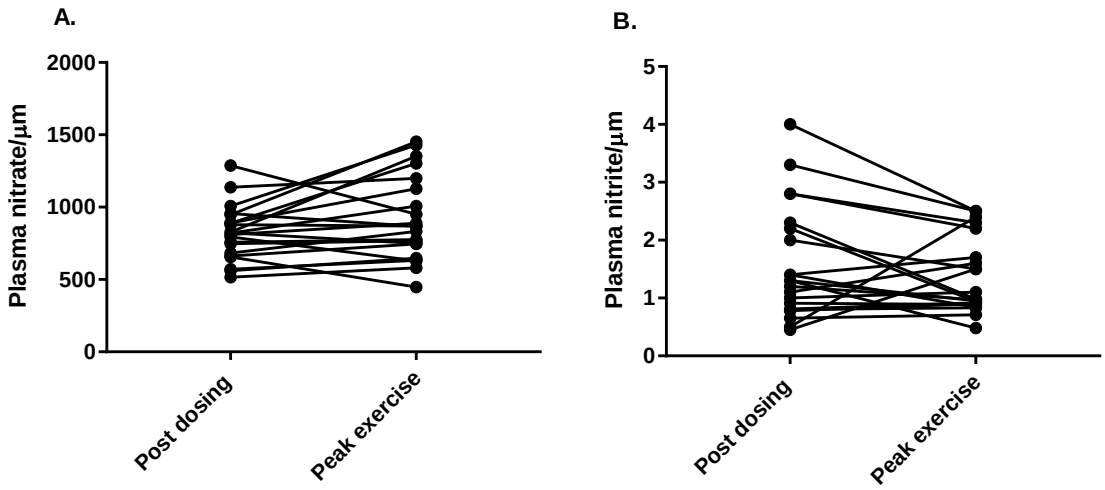

Figure 5.7. Plasma nitrate (A) and nitrite (B) levels post dosing (pre-exercise) and at peak exercise represented as individual values.

No significant difference was found between conditions, n=21.

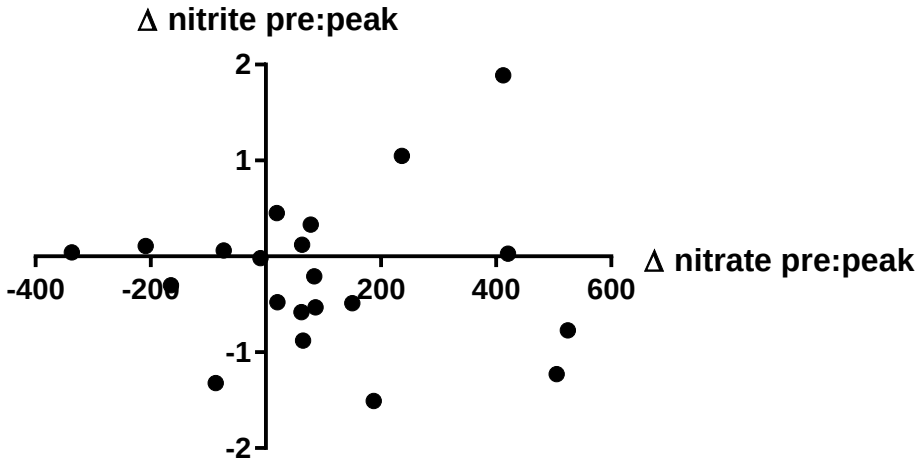

Figure 5.8. Correlation of the Δ nitrate pre (post dosing): peak exercise against Δ nitrite.

Values are taken from the nitrate dosing condition. No significant correlation between both parameters, n=21.

5.5.3 Blood pressure

Changes to systolic, diastolic and mean arterial blood pressures at 3 hours post dosing in comparison to baseline measurements are presented in **Figure 5.9**. Diastolic blood pressure underwent a significant decrease with nitrate dosing, with the nitrate treated group undergoing a 7 ± 8 mmHg reduction from baseline ($p = 0.008$) in comparison to a 1 ± 8mmHg reduction with placebo treatment. Neither systolic nor mean arterial pressures (MAP) underwent any significant alterations with nitrate treatment, however, MAP did display a numerical decrease although this was not statistically significant (7 ± 8 nitrate vs. 3 ± 8mmHg placebo, $p=0.07$).

5.5.4 Endurance exercise time during 70% max workload

Individual cycle ergometry endurance exercise times at 70% max workloads are presented for both treatments in **Figure 5.10**. No significant difference was found in median endurance time between the treatment groups (5.65 (3.90-10.40) nitrate vs. 6.40 (4.01-9.67) minutes placebo, $p=0.50$). A treatment order effect was tested for, but again, no significant difference was observed between the Δ endurance time if the placebo was administered first compared to nitrate supplementation (2.30 ± 4.64 mins vs.1.92 ± 4.16, $p=0.13$).

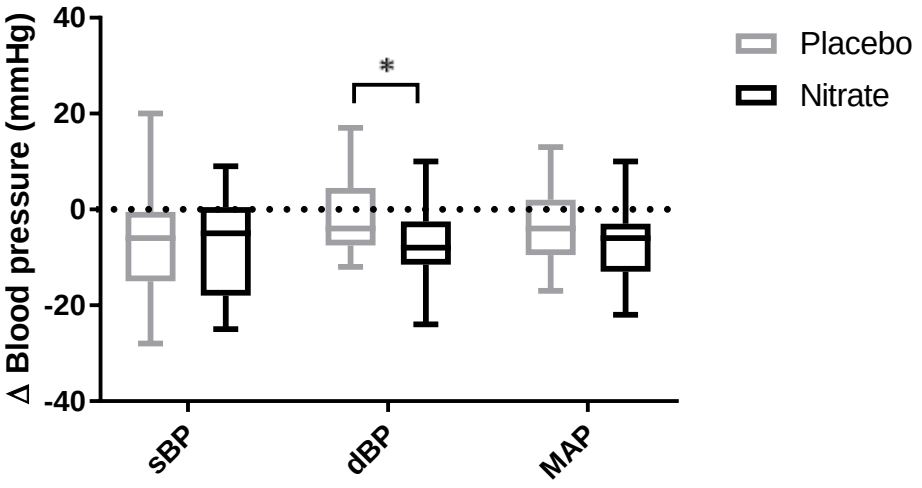

Figure 5.9. Blood pressure changes following nitrate dosing.

*Blood pressure parameters including systolic blood pressure (sBP), diastolic blood pressure (dBP) and mean arterial blood pressure (MAP)) are presented as 3hr post dose (pre-exercise) values relative to baseline. *Significantly different from placebo, P<0.01, ± SD, n=21.*

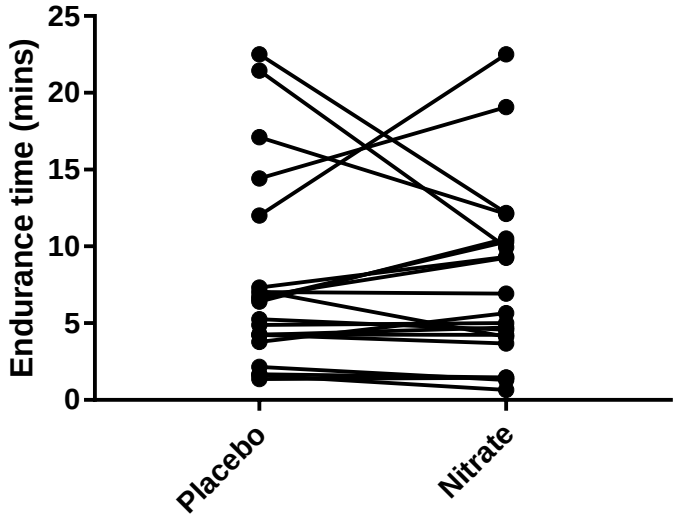

Figure 5.10. Endurance time during cycle ergometry.

This was performed at 70% maximal workload assessed in both placebo and nitrate dosing conditions. No significant difference in endurance time was found between the two conditions, n=21.

5.5.5 Rest and isotime analysis of cardiopulmonary exercise test parameters

Mean values for all cardiopulmonary parameters at both rest and isotime (being the longest time of equivalent exercise completed under either study condition) are presented in **Table 5.2**. At isotime, significant decreases were observed in minute ventilation (V_E) (4.5 (±10.6) %, p=0.029), pulmonary O_2 uptake (VO_2) (3.3% (±9.1) %, p=0.043) and relative O_2 pulse (2.3 (± 11.9) %, p=0.043) (**Figure 5.11 A-C**). A numerical improvement was observed in the power/VO_2 relationship with a 4.3 (± 9.7) % increase, which was close to significance (p=0.053) (**Figure 5.11D**)**.** No significant changes were observed in any other parameter presented in table 2 at either rest or isotime, including: heart rate, breathing frequency, tidal volume, exhaled carbon dioxide production and peripheral arterial O_2 saturation. In addition, no alteration was reported in the rating of perceived exertion with exercise, as the average Borg scale values for dyspnea at peak exercise were 5 (± 3) and for legs 3 (± 2) across both treatment conditions.

Table 5.2. Cardiopulmonary exercise testing presented as rest and isotime

Parameter	Time point	Placebo (±SD)	Nitrate (±SD)	Difference (±SD)	P value
HR (bpm)	Rest	85 (11)	87 (11)	2 (7)	0.063
HR (bpm)	Isotime	122 (17)	121 (20)	-1 (10)	0.30
BF (breaths/min)	Rest	16 (4)	17 (4)	1 (3)	0.095
BF (breaths/min)	Isotime	32 (8)	32 (5)	0 (7)	0.48
VT (L)	Rest	0.93 (0.43)	0.87 (0.25)	-0.06 (0.26)	0.33
VT (L)	Isotime	1.44 (0.39)	1.40 (0.47)	-0.04 (0.18)	0.12
V_E (L/min)	Rest	13.27 (3.90)	13.37 (3.95)	0.10 (2.29)	0.34
V_E (L/min)	**Isotime**	**43.85 (13.94)**	**41.88 (14.85)**	**-1.97 (4.52)**	**0.029***
VO_2 (ml/min/kg)	Rest	4.5 (1.2)	4.4 (1.3)	-0.1 (0.9)	0.32
VO_2 (ml/min/kg)	**Isotime**	**17.2 (6.0)**	**16.6 (6.0)**	**-0.6 (1.48)**	**0.043***
VCO_2 (ml/min/kg)	Rest	4.2 (1.2)	4.2 (1.3)	0.0 (0.82)	0.49
VCO_2 (ml/min/kg)	Isotime	17.1 (6.0)	16.7 (6.3)	-0.4 (1.74)	0.14
SpO_2 (%)	Rest	95 (2)	96 (2)	0 (2)	0.26
SpO_2 (%)	Isotime	92 (4)	93 (4)	1 (2)	0.15
Relative oxygen pulse (ml/beat/kg)	Rest	0.053 (0.0138)	0.051 (0.014)	-0.002 (0.010)	0.15
Relative oxygen pulse(ml/beat/kg)	**Isotime**	**0.143 (0.039)**	**0.138 (0.036)**	**-0.0005 (0.014)**	**0.043***
Power/VO_2 ratio	Isotime	2.92 (0.73)	3.03 (0.73)	0.11 (0.29)	0.053

***Note**: Data are presented as mean (SD). *p<0.05. Abbreviations: HR – heart rate, BF – breath frequency, VT – tidal volume, V_E – minute ventilation, VO_2 – pulmonary oxygen uptake, VCO_2 – exhaled carbon dioxide production, SpO_2 – peripheral oxygen saturation.*

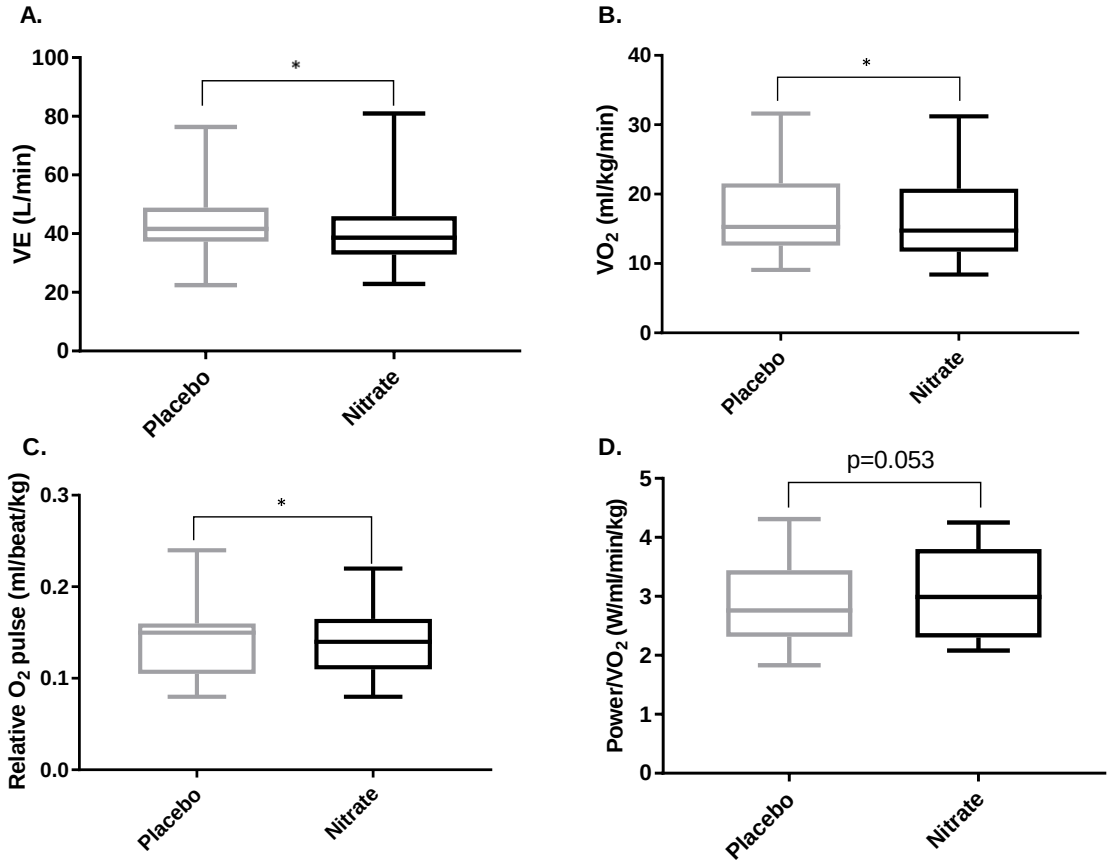

Figure 5.11. Cardiopulmonary isotime exercise test parameters presented in the placebo and nitrate treated conditions

A. *Minute ventilation (VE),* ***B.*** *Pulmonary O_2 uptake (VO_2),* ***C.*** *Relative O_2 pulse,* ***D.*** *Power/VO_2 relationship. Calculated by dividing the power output (W) at 70% VO_2 max by the isotime VO_2 (ml/min/kg). *Nitrate significantly lower than placebo, p<0.05, n=21.*

VO_2 curves to isotime

The average VO_2 curve to isotime is presented in **Figure 5.12.** A separation is visible between the two treatment conditions. This is reflected in the 7.3 (±0.8) % drop (p=0.027) in the amplitude of area under the curve (AUC) with nitrate treatment, which is displayed in **Figure 5.13**.

5.5.6 Plasma metabolomics using ^{1}H-NMR

Analysis of select plasma metabolites, assessed using ^{1}H-NMR, presented in **Figure 5.14**, revealed no significant difference in abundance between pre-exercise (post dosing) to peak exercise between the two treatment conditions. Separation of the patient cohort by GOLD stage also did not reveal any significant differences.

5.5.7 Correlation analysis

As presented above, a large inter-individual variability in both plasma nitrate and nitrite levels were observed in the response to exercise following nitrate dosing. To investigate the presence of subgroups in response to nitrate dosing (i.e. responders vs. non-responders), the difference in plasma nitrate and nitrite from pre-exercise (post dosing) to peak exercise were correlated with the following exercise parameters: ΔVE, Δ VO_2, Δ AUC VO_2 Δ power output/VO_2 and Δ endurance time. No significance was observed in the correlations with Δ plasma nitrate (**Figure 5.15)** or Δ plasma nitrite (**Figure 4.16**). The large spread of data that can be observed in these correlation plots highlights the complexity of this patient cohort. To investigate the effects of a measure of disease severity upon plasma nitrate/nitrite changes, Δ plasma nitrate/nitrite was correlated with FEV_1 (**Figure 5.17**). Whilst no correlation was observed with Δ plasma nitrate, significance was observed with Δ plasma nitrite (**Figure 5.17B**). This is despite a weak r^2 displayed from linear regression analysis ($p = 0.0486$, $r^2 = 0.189$).

It has been demonstrated previously that resting plasma nitrate levels in healthy subjects correlate with maximal power output (W) (Jungersten et al., 1997). This association between physical fitness and nitrate metabolism was investigated in this cohort (**Figure 5.18**), but no correlation was found.

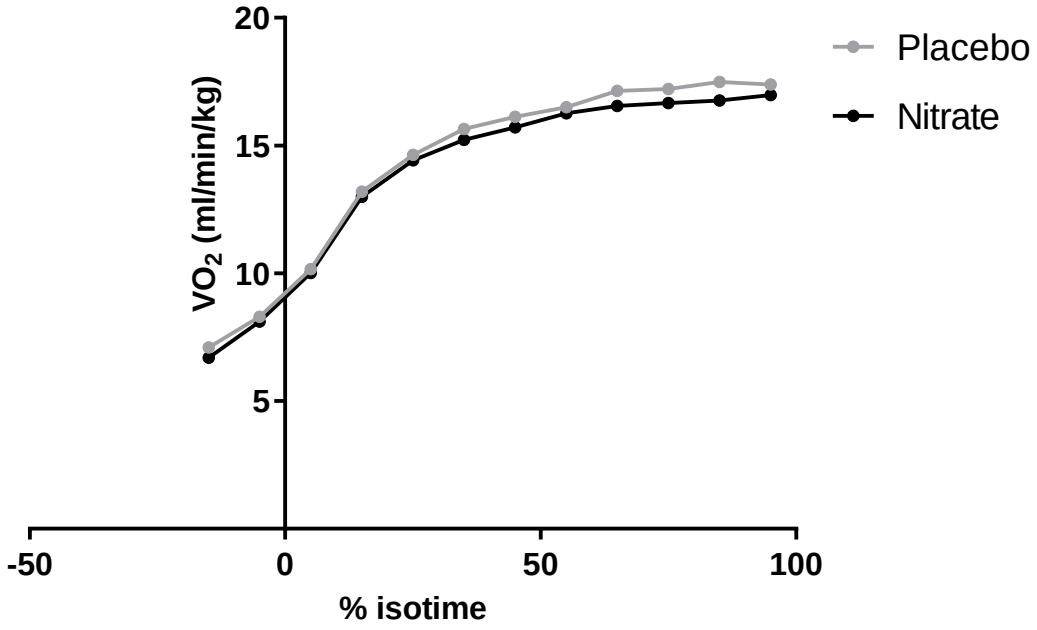

Figure 5.12. Average isotime VO_2 analysis.

VO_2 is presented at each 10th percentile of isotime (n=21). 0% represents the initiation of loaded cycling at 70% maximal workload (as assessed by incremental cycle ergometry). For reasons of visibility, error bars are not included.

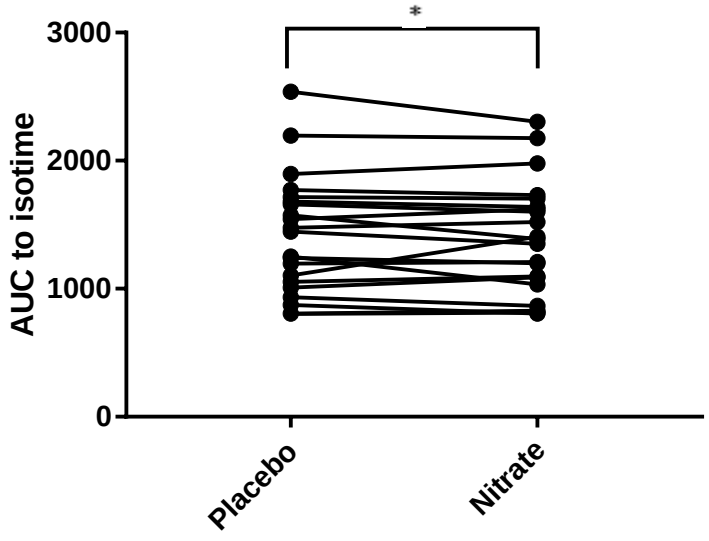

Figure 5.13. Area under the curve to VO_2 isotime (AUC) presented as individual responses to placebo and nitrate treatments.

*A significant decrease occurred between placebo and nitrate treated groups *p=0.027, as assessed using a Paired T test. n=21.*

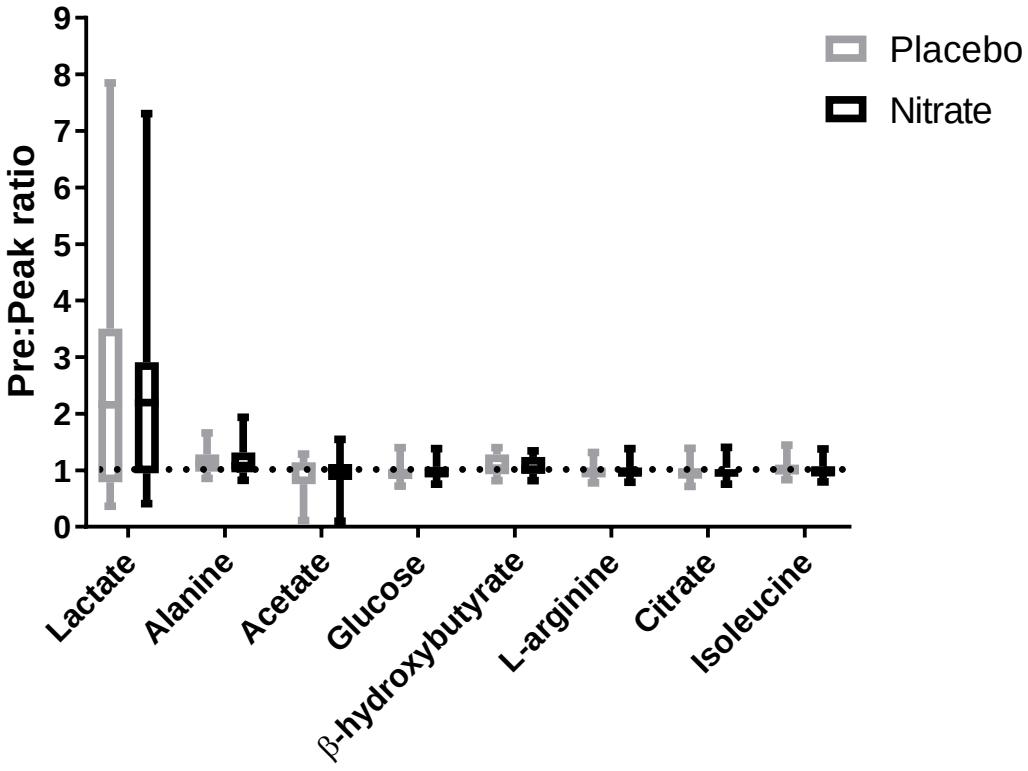

Figure 5.14. Plasma metabolite changes in placebo and nitrate conditions

Metabolites expressed as pre (post dosing): peak exercise ratio, with a value of 1 indicative of no change. Paired t-tests were utilised to compare metabolite levels between treatment conditions, with no significant changes observed in any metabolite (n=20).

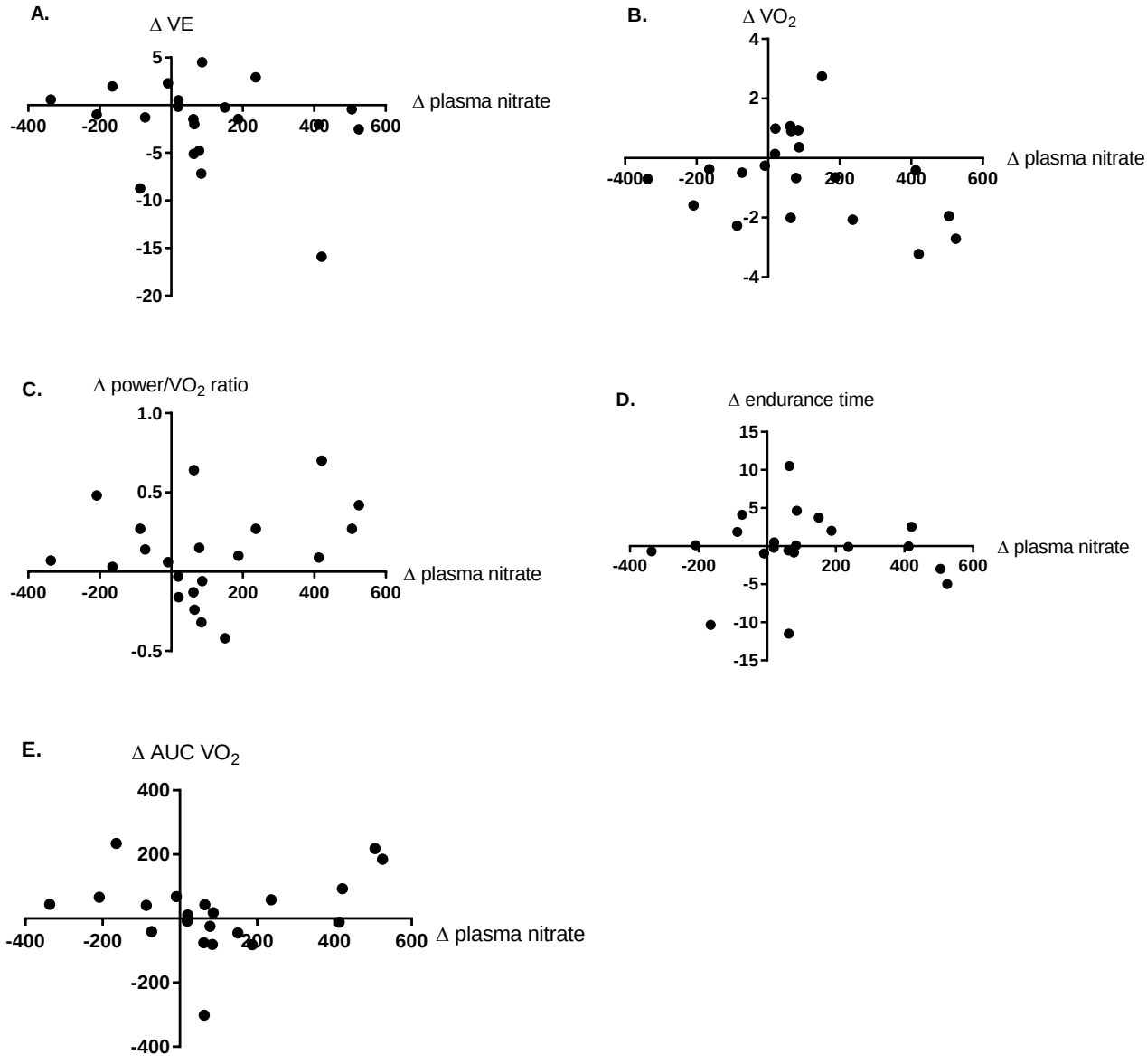

Figure 5.15. Correlations between changes in plasma nitrate (pre (post dosing) to peak exercise) and changes in exercise parameters to placebo and nitrate treatment.

*This includes: **A**. Minute ventilation (VE), **B.** Pulmonary O_2 uptake (VO_2), **C.** the power/VO_2 ratio and **D.** Endurance time, **E.** Area under the curve (AUC) VO_2. n=21. No significant correlation was identified.*

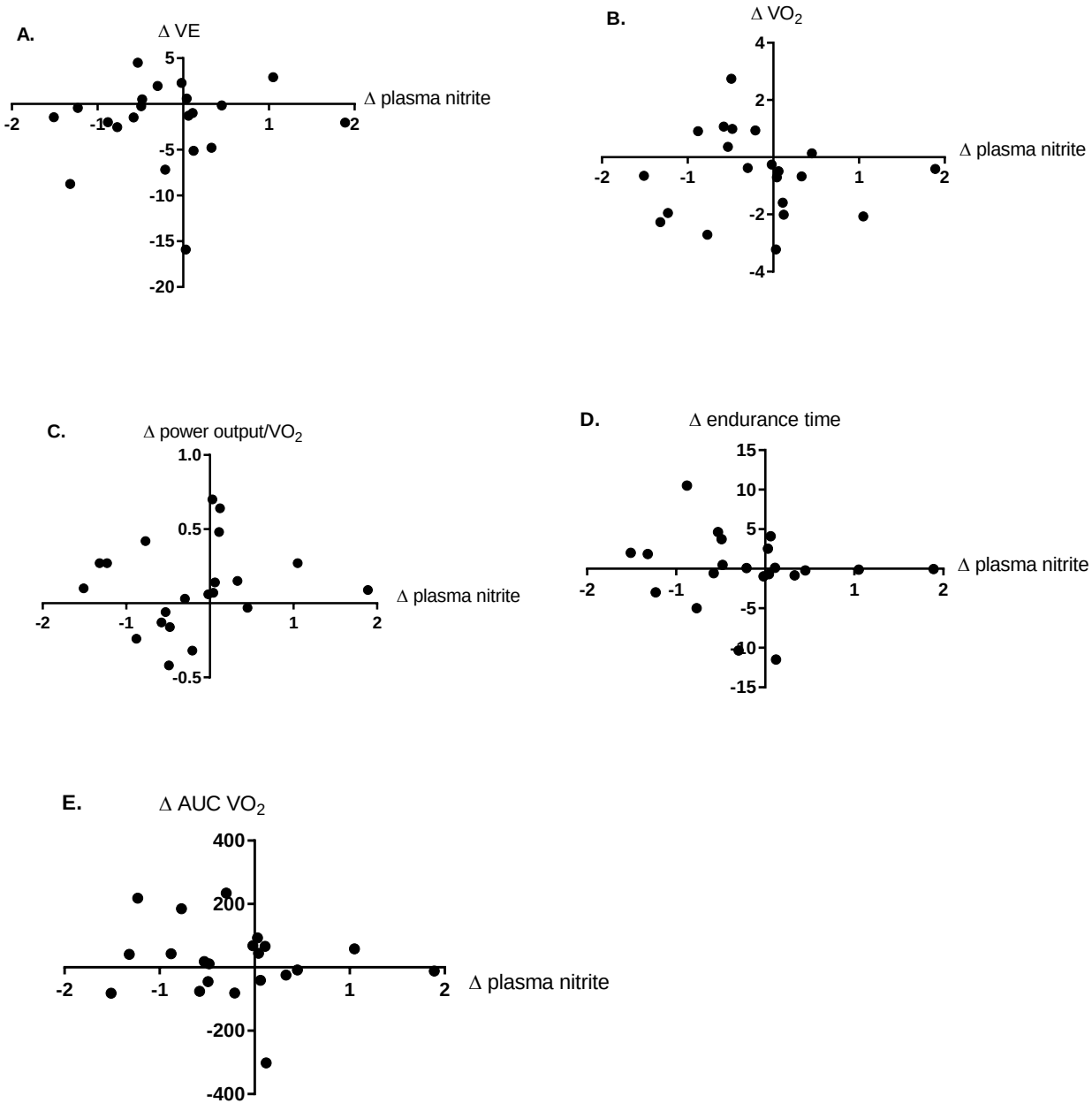

Figure 5.16. Correlations between changes in plasma nitrite (pre (post dosing) to peak exercise) and changes in exercise parameters between placebo and nitrate treatment.

*This includes: **A**. Minute ventilation (VE), **B.** Pulmonary O_2 uptake (VO_2), **C.** the power/VO_2 ratio and **D.** endurance time, **E.** Area under the curve (AUC) VO_2. n=21. No significant correlation was identified.*

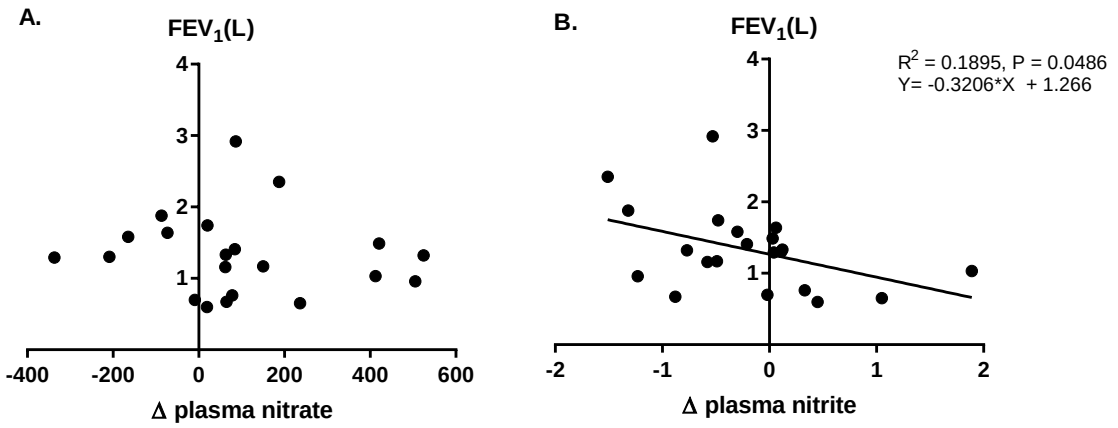

Figure 5.17. Correlations between changes in plasma nitrate and nitrite at pre (post dosing) and peak exercise and forced expired volume in 1 second (FEV_1).

A significant negative correlation was observed using Pearson correlation coefficient) in Δ plasma nitrite vs. FEV_1, (P=0.0486), n=21

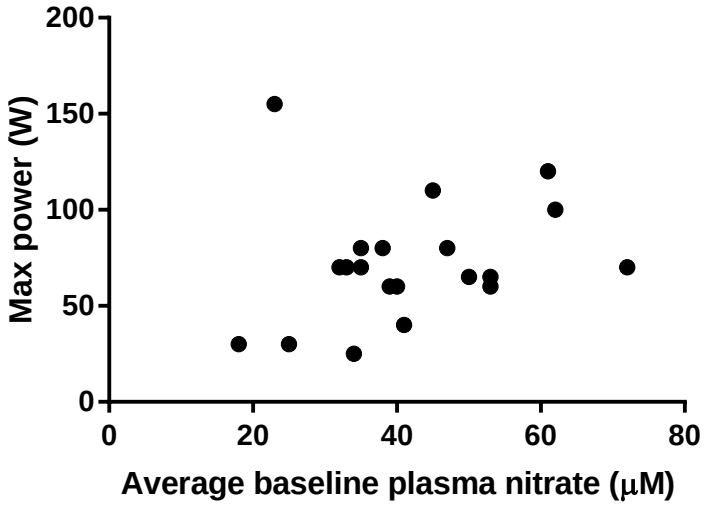

Figure 5.18. Correlation between baseline plasma nitrate (taken as an average across both study arms) and maximal power (W).

No significant correlation was identified. n=21

5.6 Discussion

In this chapter, the effects of acute nitrate supplementation (12mM nitrate vs. placebo ingested 3hours pre-exercise) upon endurance exercise time and related metabolite changes were investigated in COPD patients (n=21, age 68±7 years, GOLD I-IV). The nitrate-rich beetroot juice dose had the expected response of increasing circulating plasma nitrate within 3 hours of dosing, occurring alongside increases nitrite formed via reduction. The biological activity of this nitrate dose, thought to be mediated via NO, was reflected through changes in diastolic blood pressure at rest. In addition, decreases were observed in both oxygen consumption (VO_2), minute ventilation (V_E) and relative O_2 pulse at exercise isotime with nitrate treatment. However, no effect was observed upon endurance time and so exercise performance, between the two treatments. In addition, no changes were observed in plasma levels of metabolites associated with exercise and COPD pathophysiology.

5.6.1 Effective dosing with nitrate-rich beetroot juice shown through plasma nitrate/nitrite levels

Inherent variabilities have been reported in previous studies to nitrate treatment, with even elite athlete populations displaying subgroups of 'responders' and 'non-responders' that are suggested to be linked to inter-individual differences in oral nitrate reductase activity (Hultström et al., 2015). The combined effects of advanced age along with the complex pathophysiology of COPD upon digestion, enterosalivary circulation and activity of oral commensal bacterial upon dietary nitrate intake are unknown. Consequently, the capacity of subjects to respond to nitrate treatment was also uncertain. This is on the background of a lack of consensus amongst previous studies examining the effects of nitrate supplementation upon COPD patients, with some showing no beneficial effects (Shepherd et al., 2015, Leong et al., 2015). A key concern with the current chapter therefore was that nitrate metabolism may be impacted in this population and that the nitrate dose administered would not translate to a subsequent increase in biologically active NO.

Baseline recordings of plasma nitrate, and so endogenous levels, were within the range (16.0-70.2uM) of those reported in healthy subjects with varying physical capacities (Jungersten et al., 1997). Endogenous plasma nitrate levels are thought to be the major inactive pool of NO, resulting from a reaction with Hb to form NOHb, followed by subsequent conversion to nitrite and finally nitrate (Yoshida et al., 1980). Whilst this measure does not

give insight into the degree of NO stored within S-nitrosylated proteins or the tissue localisation of NO production, it does give an indication of endogenous NO production and so suggests that this is within normal range. A further assessment of endogenous NO activity can be gained through correlation between plasma nitrate levels and maximal power output, as in healthy cohorts, increasing resting plasma nitrate levels are shown to correlate with increasing maximal power output (Jungersten et al., 1997). However, this relationship was not apparent in the data, which may indicate that the association between physical fitness and NO production reported in healthy subjects may be affected in this disease population.

In response to dosing, plasma nitrate levels achieved with dosing (22-fold increase) exceeded those produced by administration of a higher dose of nitrate in healthy young individuals (Wylie et al., 2013). A concomitant rise in plasma nitrite was accompanied by decreasing dBP, a parameter mediated via NO action. This observation is in line with previous studies on healthy subjects (Larsen et al., 2006, Webb et al., 2008) and COPD patients (Berry et al., 2015, Kerley et al., 2015). Interestingly, the range of plasma nitrate concentrations was greater at peak exercise compared to pre-exercise, with the average concentration being numerically (although not significantly) higher. This may be explained by the conversion of biologically active NO to the nitrate storage pool.

Whilst these results go to suggest that the reduction of dietary nitrate in the patient cohort was unaffected in comparison to healthy subjects (Larsen et al., 2006, Carlstrom et al., 2010), correlation analysis demonstrated that an increase in airway obstruction (FEV_1) may be associated with lower plasma nitrite levels. This may suggest that nitrate reduction could be implicated in more severe cases of COPD.

It can therefore be concluded that this patient cohort displayed similarities in nitrate metabolism with healthy populations and were responsive to nitrate dosing. However, certain aspects of the response to nitrate dosing may be affected and are worthy of note for future investigations in this complex disease population.

Of potential concern relating to the plasma analysis were baseline levels of nitrite, which fell below the quantifiable limit in the vast majority of subjects. There are two explanations for this, one being the presence of a small interfering peak thought to originate from beetroot juice. The second is that samples were not treated with thiol-blocking agent prior to centrifugation. This treatment prevents flux of nitrite across blood cell membranes, which may act to lower plasma concentration. Although we were unable to observe baseline

nitrite production, high levels of plasma nitrites were readily measured following nitrate dosing.

In this chapter, nitrate dosing occurred in the absence of any adverse side effects, aside from beeturia. A singular, higher dose of nitrate is therefore both safe and biologically active in the COPD patient population. The unchanging nitrate levels in the placebo treatment from baseline also confirmed that the placebo was robust.

5.6.2 Effects of nitrate dosing upon exercise physiology

Contrary to the study hypothesis, nitrate dosing did not improve endurance exercise performance, as no significant difference in endurance time was observed between conditions. This occurred along with unchanged levels of perceived exertion, either in the legs or in the level of dyspnoea. These results thus indicate exercise tolerance was unaffected with nitrate treatment. This is in spite of a reduced O_2 requirement of exercise, shown through a decrease in pulmonary O_2 uptake by 3.3%, which is a similar magnitude to that recorded in healthy individuals in response to nitrate treatment (Wylie et al., 2013). Alongside this was a fall in minute ventilation and a numerical (close to significant) increase in the power/VO_2 relationship. Correlation analysis did not reveal any significant trends between these exercise parameters and the change in plasma nitrate/nitrite during exercise, indicating that inter-individual variation in nitrate metabolism did not affect the degree of physiological change observed. Indeed, the spread of data in these plots demonstrate the heterogeneity of this population.

Decreasing O_2 uptake during exercise occurred in the absence of impairment in power output, which is a well-recognised response to nitrate supplementation in healthy humans (Larsen et al., 2011, Larsen et al., 2007, Bailey et al., 2009, Vanhatalo et al., 2010, Lansley et al., 2011), but has not been reported previously for COPD patients. The mechanisms behind this response are not clear, but may involve a combination of enhancing the following: changes in blood flow to working muscles (Cosby et al., 2003, Bentley et al., 2014), effects upon energy consuming processes required for skeletal muscle contraction (Evangelista et al., 2010, Ishii et al., 1998) and improved efficiency of mitochondrial oxidative phosphorylation. The latter may be best explained through the action of NO at the respiratory chain, as it has been demonstrated to be an inhibitor of complex IV activity, which is the site of O_2 consumption (Brudvig et al., 1980, Brown et al., 1994). However, unlike the outcome measures from prior studies involving healthy human studies (Bailey et al., 2009,

Cermak et al., 2012, Wylie et al., 2013), the drop in VO_2 was not accompanied by improvements in submaximal exercise performance.

There are a number of possible explanations for failing to see any change in submaximal endurance time, a key factor being the large degree of variability in exercise time. This is somewhat expected, given the day-to-day symptom variability in COPD (Kessler et al., 2011). But the extent of variability was surprising as it was beyond what has been observed in previous endurance cycle ergometry tests at 75% peak workload in a similar population (O'Donnell et al., 2011). It is possible that familiarising subjects to the endurance test through a trial run could improve consistency. However, this is improbable given that no order affect was identified. It is also possible that incorporating a larger sample size may have given a positive result through improving statistical power, however, this is unlikely given that exercise time was numerically shorter in the nitrate treated group. The desired effect of improving endurance capacity in these subjects would not likely be achieved through an increase in nitrate dosing, although this may further alter plasma NO_2^- and the O_2 cost of moderate intensity exercise (Wylie et al., 2013).

It may simply be that the small improvements in the O_2 cost of exercise observed with nitrate treatment do not affect the rate limiting parameters of exercise in ventilatory limited patients. It may also be the case that effects upon exercise performance with nitrate dosing become more apparent in patients who are more severely affected by COPD, in which case this chapter focused upon the wrong patient group as patients on O_2 supplementation were not included. It may be possible that a reduction in the O_2 cost of exercise offers the greatest benefit in this patient phenotype.

Lastly, it has been shown that the effects of dietary nitrate upon skeletal muscle contractile processes, including increasing contractile force and intracellular [Ca_2^+], is most prominent in fast twitch type II fibres (Hernández et al., 2012). Beneficial effects of nitrate supplementation may therefore become more apparent in response to short duration, high intensity exercise requiring recruitment of this fibre type.

5.6.3 Unchanging metabolite levels indicate no compensatory increase in anaerobic glycolysis

The analytical strategy adopted towards plasma metabolite analysis was for a targeted approach of select metabolites, either those known to be affected by exercise or those previously reported through metabolomics approaches to be affected in this disease

population (Rodríguez et al., 2012, Nobakht M. Gh et al., 2015). Whilst no significant changes were observed in any of the targeted metabolites between treatments, these results do still provide an interesting insight. The lack of change in plasma lactate as well as glucose is an indication of no alteration in anaerobic metabolism, given that glucose is the substrate and lactate the metabolic end-product of anaerobic glycolysis. This is in line with previous reports that demonstrate decreasing VO_2 induced via nitrate supplementation is not compensated for by an increase in anaerobic means of ATP generation (Bailey et al., 2009, Larsen et al., 2007).

Equally, the lack of change in other metabolites assessed indicate that the nitrate effects happen independently of associated pathways. This includes: TCA cycle activity indicated by the key components/intermediates acetate (from which acetyl CoA is derived) and citrate; ketone body metabolism indicated by β-hydroxybutyrate; as well as amino acid metabolism demonstrated by alanine, L-arginine and isoleucine.

5.7 Conclusion

Acute oral administration of nitrate did not alter median endurance time nor targeted metabolomic analysis in COPD patients. However, the nitrate dose was associated with a decrease in VO_2 and V_E with submaximal exercise. This was not accompanied by increasing plasma lactate or decreases in plasma glucose, indicating these effects occurred in the absence of a compensatory rise in anaerobic glycolysis. Further investigation into the potential of nitrate supplementation as an ergogenic aid for COPD sufferers should encompass different durations of supplementation and exercise intensities and should perhaps focus upon sufferers of severe COPD (GOLD III-IV), being the more hypoxic phenotype.

6 **Chapter 6:** General Discussion

6.1 Summary of findings

The work presented in this thesis encompassed two overarching themes:

1. To further understanding of metabolic acclimatisation in healthy humans in the face of environmental hypoxia
2. To elucidate the potential for dietary nitrate supplementation to alleviate hypoxic induced metabolic stress.

This first theme was approached through examination of plasma and serum metabolic (and lipidomic) profiles obtained from healthy humans exposed to high altitude of differing durations and severity. In Chapter 2 (study 1), plasma metabolic and lipid profiles were assessed in a large subject cohort exposed to progressive hypoxia through a strictly controlled ascent to EBC. The results were indicative of a shift towards anaerobic glycolysis, mobilisation of fat stores and impairment of *de novo* lipogenesis with ascent. This was alongside an indication of changes to lipoprotein transportation. In Chapter 3 (study 2), plasma metabolic profiles were assessed alongside various physiological measures in a small number of subjects exposed to chronic hypoxia and extreme cold during a 33-week attempted crossing of Antarctica in winter time. Results revealed a shift in metabolic profile, with an increased reliance upon carbohydrates during exercise post expedition. This was alongside alterations to body composition, with loss of fat tissue, and a decline in spine BMD.

The second overarching theme of this thesis was approached firstly at the mechanistic level in Chapter 4 (study 3), through use of a mouse model in which a master regulator of β-oxidation, PPAR-α, was genetically ablated. Here, prolonged dietary nitrate supplementation recovered decreases in pyruvate OXPHOS and long chain fatty acid LEAK state respiration induced by 4 weeks severe hypoxic exposure (10% O_2). However, mechanisms of nitrate action remain unclear, although they do appear to be induced independently of PPARα. The potential for nitrate supplementation to aid hypoxic acclimation was further examined in a clinical (COPD) population in Chapter 5 (study 4). The desired result of increasing performance through improvements in endurance time were not observed. However, VO_2 decreased in the absence of a compensatory increase in markers of anaerobic glycolysis. A summary of the findings of the thesis is outlined in **Figure 6.1**.

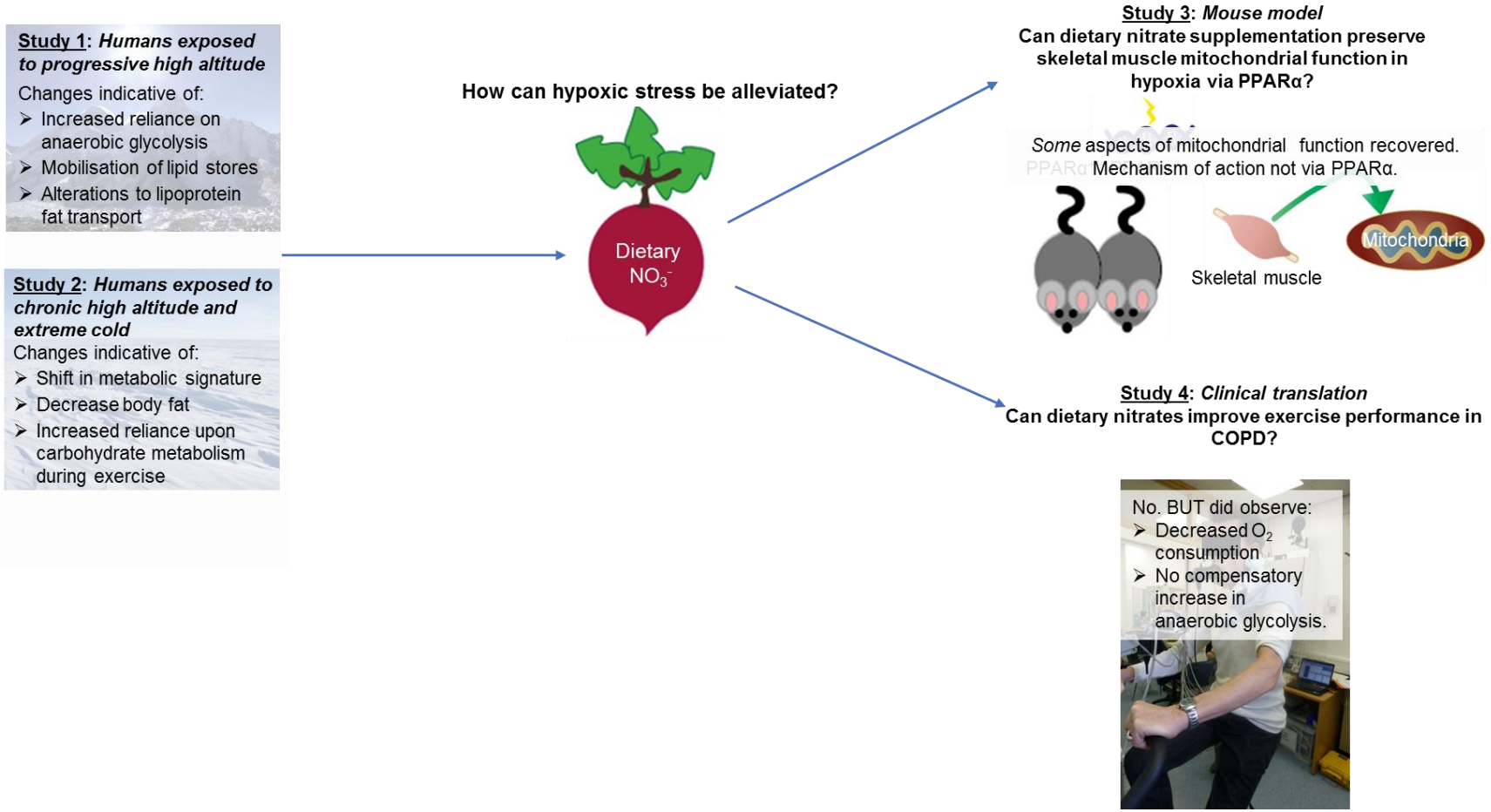

Figure 6.1. Summary of thesis study findings.

6.2 Metabolic remodeling induced by environmental hypoxia

As already outlined in depth, the controversy surrounding metabolic remodelling in response to hypoxic exposure calls for more stringent investigation. The work in this thesis highlighted several metabolic pathways and potential biomarkers of interest in healthy humans affected by environmental hypoxia.

The work presented in Chapters 2 and 3 identified clear alterations to carbohydrate metabolism. In response to acute, progressive hypoxia experienced in Chapter 2, the increased circulating lactate along with decreased glucose were indicative of an increased reliance upon anaerobic glycolysis for ATP generation. The fall in plasma glucose was also associated with a decrease in body weight. The role of carbohydrate metabolism appeared equally important in long term exposure, as demonstrated in Chapter 3, whereby decreases in plasma glucose were accompanied by increases in RER during exercise. These responses align with previous reports of either maintenance or enhancement of glycolytic capacity in the face of hypoxic exposure (Horscroft et al., 2014, Cole et al., 2016). Whilst the results in this thesis do not provide detailed insight into glycolytic pathway changes with regards to transporter protein or enzyme activity changes, they did confirm the importance of carbohydrate metabolism in response to both acute progressive and chronic hypoxic exposure.

Alongside increasing reliance upon carbohydrate oxidation, a body of evidence goes to suggest that this is accompanied by a shift away from O_2 costly fatty acid metabolism (Horscroft et al., 2014). Examination of lipid metabolism is therefore of utmost importance when considering high altitude adaptation. This was addressed in most depth in Chapter 2, whereby lipidomic analysis of plasma revealed substantial alterations to TG storage and mobilisation, with accompanying increases in free fatty acids, alongside changes to lipids that are crucial to membrane composition with ascent. The rise in unsaturated fatty acids was associated with the loss in body weight. To the author's knowledge, this was the first time plasma lipid profile changes have been examined in such a large study cohort undergoing altitude ascent. Comparison to prior altitude studies is therefore limited and consideration of potential causes of these changes, for instance through the sympathetic nervous system responses, was largely speculative. However, it did highlight that the dynamics of adipose tissue and the transportation of fat are crucial in hypoxic induced

metabolic remodeling. The results also highlighted the importance of lipids acting as indicators of membrane structural changes. The body composition changes outlined in response to prolonged hypoxic exposure experienced in Chapter 3, with body fat decreasing post expedition, suggest changes in lipid metabolism may be sustained over longer periods.

An aspect of metabolism often overlooked in high altitude investigation is that of amino acids. The substantial decrease in isoleucine levels with ascent observed in Chapter 2 was thus a novel finding. The role of BCAA's in metabolism is gaining increasing interest, with a growing body of evidence supporting their role as metabolic regulators in protein, lipid and glucose metabolism (Zhang et al., 2017). Plasma isoleucine levels may therefore present as an important biomarker for induction of metabolic remodeling in hypoxia, particularly hypoxic scenarios whereby nutrient uptake and preservation of muscle mass are severely compromised, for instance in critical care patients (Ackland et al., 2000, Puthucheary et al., 2013).

Interestingly, measures of SpO_2 reported in Chapter 2 did not correlate with changes in any of the identified metabolites/lipids. This thus suggested that inter-individual differences in the degree of O_2 delivery to the tissues may not directly impact the metabolic acclimatisation processes.

6.3 Dietary nitrate as a potential alleviator of hypoxic induced metabolic stress

Much debate surrounds the field of nitrate supplementation. The reported actions upon O_2 delivery and consumption at the level of the mitochondria make nitrate supplementation appear an ideal candidate for aiding metabolic acclimatisation to hypoxic exposure. The investigation into the mechanisms of nitrate action in hypoxia and the effects of nitrate supplementation on performance as was conducted in this thesis was therefore warranted.

In Chapter 4, nitrate supplementation was found to enhance very specific aspects of skeletal muscle mitochondrial function. In spite of previous reports of the dependence of NO action upon PPARα signaling (Ashmore et al., 2015a), these affects were found to occur independently of PPARα, as demonstrated through the use of PPARα genetic ablation. It may be that mechanisms alter depending on the degree and duration of hypoxic exposure, with the prolonged period examined in Chapter 4 allowing sufficient time for compensatory mechanisms to be initiated. For instance, the role of PPARδ in this model required more in-

depth investigation. In addition, comparison to the responses of other tissues would be beneficial to determine whether the observations are specific to skeletal muscle. It would also be beneficial to investigate the possible translation of these effects at a whole-organism level and in response to an exercise challenge.

In Chapter 5, a decreased VO_2 during submaximal exercise was reported with nitrate, yet endurance time did not undergo a significant change. The implications of a fall in O_2 requirement were thus unclear. The absence of a rise in plasma lactate was indicative of an absent compensatory increase in anaerobic glycolysis, as has been reported previously (Bailey et al., 2009, Larsen et al., 2007). However, neither the consequences upon the O_2 cost of ATP production (so mitochondrial P/O ratio) (Larsen et al., 2011) nor the ATP cost of force production (Bailey et al., 2010) can be determined. Further investigation is therefore required to outline any potential benefits of such dietary intervention upon the exercise capacity of this hypoxic patient cohort.

There are a number of factors that could be included into the study design of future work into dietary nitrate supplementation in the COPD patient cohort. This includes the choice of exercise intervention, for instance a lower % of peak may prove to be more tolerable for this patient group. Another possibility is altering the focus away from endurance towards recruitment of type II fibres through short exercise bursts at a higher intensity. In addition, the dosing regimen could be extended to examine effects beyond an acute bolus dose. Finally, focusing on a specific subtype of this patient population, for instance upon GOLD I/II or GOLD III/IV rather than including both within the same study may help to improve homogeneity of responses between subjects.

6.4 Critique of methodology

6.4.1 Critique of metabolomics/lipidomics

Both metabolomics and lipidomics have the capacity to provide a highly sensitive measure of biological phenotype and to unveil potential biomarkers related to perturbations such as environmental hypoxia. Employment of these techniques can thus present as a powerful analytical tool, particularly when used in conjunction. For the purposes of this thesis, the adoption of these techniques was aimed at identifying potential biomarkers that could be examined in more detail in future investigations. The lack of consensus surrounding metabolic remodelling in hypoxia means that further investigation into this field lends itself

to untargeted and hypothesis generating approaches, as was adopted with the metabolomics experiments performed in this thesis.

The profiling approach does have limitations, however, particularly when examining a small diverse cohort. In the instance of Chapter 5, a small cohort with a large range of pathological complications were examined. A targeted approach to metabolomic analysis was therefore adopted. This analysis had limitations given that key patterns of change in metabolic profile are omitted. Despite the low subject numbers, patterns related to the experimental intervention were identified in the metabolic profile of subjects in Chapter 3. The importance of this observation was realised when relating it to other physiological parameters along with dietary recordings. Together this highlighted that some caution is required when adopting such -omics approaches to pilot studies and that maximal interpretation can be gained when combining this with other functional measures.

The processing, analysis and interpretation of -omics data presents as a significant challenge. In spite of attempts made to standardise such procedures (Sumner et al., 2007), much discordance exists amongst previous studies. Whilst there are clear precautions to consider, there is no set 'right' way to proceed. The approaches adopted in this thesis attempted to adapt accordingly both to the nature of the data set produced and the initial experiment aims.

One clear limitation that remained with the interpretation of metabolomics/lipidomics data set regardless of the choice of analysis method was the inability to define for certain whether changes in a metabolite are a result of changes in production/supply or consumption. In essence, this technique provides a highly sensitive insight into a snapshot in time. Even when associated with other metabolite changes, in addition to other physiological measures, a degree of speculation is required. A way to confirm the impacts and relevance of the findings highlighted in this thesis would be through metabolic flux analysis, for instance through ^{13}C flux (Wiechert, 2001). This has the potential to provide far greater insight into the remodelling of relevant pathways highlighted in this thesis.

6.4.2 Critique of field work approach

A key component of Chapters 2 and 3 of this thesis was field work, in both instances occurring in extreme environmental conditions. This work therefore extended beyond the standardised, controlled laboratory environment, as was utilised in Chapters 4 and 5. Whilst considerable effort was made to ensure accuracy and subjectivity did not impair measures

taken, the limitations in equipment and resources undoubtedly made this difficult. Measures, such as body weight data or the diary analysis presented in Chapter 3 thus need to be interpreted with a degree of caution.

Another factor lacking with this approach is the inclusion of a control group. In order to isolate the effects of hypoxia, this would require exposure to the same external factors minus hypoxia. Indeed, a key issue with high altitude investigation is in attributing the effects of high altitude exposure solely to hypoxia. Whilst hypoxia has been recognised to be the major contributor to the physiological responses observed at altitudes (Woolcott et al., 2015), there are undoubtedly influences from other factors. For instance, when investigating metabolic alterations, dietary changes were an important consideration and were lacking in Chapter 2. The analysis approach attempted to address this concern. By looking at extreme changes occurring with ascent across the 5 altitude locations, this directed focus upon the altitude effect. However, this stringent approach did limit metabolite/lipid identification. This was particularly apparent in the metabolomic results whereby only 3 metabolites were taken forward for Bayesian modelling. Such a compromise was considered worthwhile to ensure confidence in the results.

For future investigations into progressive acute or chronic hypoxic exposure, numerous measures could be adopted to minimise the influence of external factors. This would include the use of a hypobaric chamber, more frequent blood withdrawals as well as accurate recordings of daily dietary intake.

6.5 Concluding remarks

The work presented in this thesis outlines metabolic remodelling processes occurring in response to environmental hypoxia. The results confirm those of prior studies and unveil novel findings. The specific metabolites identified may be viewed as biomarkers for such exposure and highlight potential metabolic pathways to be examined in future studies. In addition, the work delved into the mechanisms of nitrate action and its potential as a therapy for sufferers of disease where hypoxia is a known comorbidity. Whilst mechanisms remain unclear, *in vitro* results indicate dietary nitrate supplementation may act as an aid to metabolic acclimatisation in hypoxia. However, the effectiveness of nitrate supplementation on alleviating hypoxic stress *in vivo*, and so its use as a potential therapy in a clinical context, requires further investigation.

References

ABDELMALKI, A., FIMBEL, S., MAYET-SORNAY, M., SEMPORE, B. & FAVIER, R. 1996. Aerobic capacity and skeletal muscle properties of normoxic and hypoxic rats in response to training. *Pflügers Archiv,* 431**,** 671-679.

ACKLAND, G., GROCOTT, M. P. & MYTHEN, M. G. 2000. Understanding gastrointestinal perfusion in critical care: so near, and yet so far. *Critical Care,* 4**,** 269.

AGBULUT, O., LI, Z., MOULY, V. & BUTLER-BROWNE, G. S. 1996. Analysis of skeletal and cardiac muscle from desmin knock-out and normal mice by high resolution separation of myosin heavy-chain isoforms. *Biology of the Cell,* 88**,** 131-135.

AGBULUT, O., NOIREZ, P., BEAUMONT, F. & BUTLER-BROWNE, G. 2003. Myosin heavy chain isoforms in postnatal muscle development of mice. *Biology of the Cell,* 95**,** 399-406.

AGHAJANIAN, P., HALL, S., WONGWORAWAT, M. D. & MOHAN, S. 2015. The roles and mechanisms of actions of vitamin C in bone: new developments. *Journal of Bone and Mineral Research,* 30**,** 1945-1955.

AMEER, F., SCANDIUZZI, L., HASNAIN, S., KALBACHER, H. & ZAIDI, N. 2014. De novo lipogenesis in health and disease. *Metabolism,* 63**,** 895-902.

ARAGONÉS, J., SCHNEIDER, M., VAN GEYTE, K., FRAISL, P., DRESSELAERS, T., MAZZONE, M., DIRKX, R., ZACCHIGNA, S., LEMIEUX, H. & JEOUNG, N. H. 2008. Deficiency or inhibition of oxygen sensor Phd1 induces hypoxia tolerance by reprogramming basal metabolism. *Nature genetics,* 40**,** 170-180.

ARNETT, T. R., GIBBONS, D. C., UTTING, J. C., ORRISS, I. R., HOEBERTZ, A., ROSENDAAL, M. & MEGHJI, S. 2003. Hypoxia is a major stimulator of osteoclast formation and bone resorption. *Journal of cellular physiology,* 196**,** 2-8.

ASHMORE, T., FERNANDEZ, B. O., BRANCO-PRICE, C., WEST, J. A., COWBURN, A. S. & HEATHER, L. C. 2014. Dietary nitrate increases arginine availability and protects mitochondrial complex I and energetics in the hypoxic rat heart. *J Physiol,* 592.

ASHMORE, T., FERNANDEZ, B. O., EVANS, C. E., HUANG, Y., BRANCO-PRICE, C., GRIFFIN, J. L., JOHNSON, R. S., FEELISCH, M. & MURRAY, A. J. 2015a. Suppression of erythropoiesis by dietary nitrate. *The FASEB Journal,* 29**,** 1102-1112.

ASHMORE, T., ROBERTS, L. D., MORASH, A. J., KOTWICA, A. O., FINNERTY, J., WEST, J. A., MURFITT, S. A., FERNANDEZ, B. O., BRANCO, C., COWBURN, A. S., CLARKE, K., JOHNSON, R. S., FEELISCH, M., GRIFFIN, J. L. & MURRAY, A. J. 2015b. Nitrate enhances skeletal muscle fatty acid oxidation via a nitric oxide-cGMP-PPAR-mediated mechanism. *BMC Biology,* 13**,** 110.

ATHERTON, H. J., BAILEY, N. J., ZHANG, W., TAYLOR, J., MAJOR, H., SHOCKCOR, J., CLARKE, K. & GRIFFIN, J. L. 2006. A combined 1H-NMR spectroscopy-and mass spectrometry-based metabolomic study of the PPAR-α null mutant mouse defines profound systemic changes in metabolism linked to the metabolic syndrome. *Physiological genomics,* 27**,** 178-186.

AUCOUTURIER, J., BOISSIÈRE, J., PAWLAK-CHAOUCH, M., CUVELIER, G. & GAMELIN, F.-X. 2015. Effect of dietary nitrate supplementation on tolerance to supramaximal intensity intermittent exercise. *Nitric Oxide,* 49**,** 16-25.

BAILEY, D. P., SMITH, L. R., CHRISMAS, B. C., TAYLOR, L., STENSEL, D. J., DEIGHTON, K., DOUGLAS, J. A. & KERR, C. J. 2015. Appetite and gut hormone responses to moderate-intensity continuous exercise versus high-intensity interval exercise, in normoxic and hypoxic conditions. *Appetite,* 89**,** 237-245.

BAILEY, S. J., FULFORD, J., VANHATALO, A., WINYARD, P. G., BLACKWELL, J. R., DIMENNA, F. J., WILKERSON, D. P., BENJAMIN, N. & JONES, A. M. 2010. *Dietary nitrate supplementation enhances muscle contractile efficiency during knee-extensor exercise in humans*.

BAILEY, S. J., WINYARD, P., VANHATALO, A., BLACKWELL, J. R., DIMENNA, F. J., WILKERSON, D. P., TARR, J., BENJAMIN, N. & JONES, A. M. 2009. Dietary nitrate supplementation reduces the O2 cost of low-intensity exercise and enhances tolerance to high-intensity exercise in humans. *Journal of Applied Physiology,* 107**,** 1144-1155.

BAKKER, E., ENGAN, H., PATRICIAN, A., SCHAGATAY, E., KARLSEN, T., WISLØFF, U. & GAUSTAD, S. E. 2015. Acute dietary nitrate supplementation improves arterial endothelial function at high altitude: A double-blinded randomized controlled cross over study. *Nitric Oxide,* 50**,** 58-64.

BALDI, P. & LONG, A. D. 2001. A Bayesian framework for the analysis of microarray expression data: regularized t-test and statistical inferences of gene changes. *Bioinformatics,* 17**,** 509-519.

BALL, K. A., NELSON, A. W., FOSTER, D. G. & POYTON, R. O. 2012. Nitric oxide produced by cytochrome c oxidase helps stabilize HIF-1α in hypoxic mammalian cells. *Biochemical and biophysical research communications,* 420**,** 727-732.

BARBIER, O., TORRA, I. P., DUGUAY, Y., BLANQUART, C., FRUCHART, J.-C., GLINEUR, C. & STAELS, B. 2002. Pleiotropic actions of peroxisome proliferator–activated receptors in lipid metabolism and atherosclerosis. *Arteriosclerosis, Thrombosis, and Vascular Biology,* 22**,** 717-726.

BARTON, R. H., WATERMAN, D., BONNER, F. W., HOLMES, E., CLARKE, R., NICHOLSON, J. K., LINDON, J. C. & CONSORTIUM, P. 2010. The influence of EDTA and citrate anticoagulant addition to human plasma on information recovery from NMR-based metabolic profiling studies. *Molecular BioSystems,* 6**,** 215-224.

BASSETT, D. R. & HOWLEY, E. T. 2000. Limiting factors for maximum oxygen uptake and determinants of endurance performance. *Medicine and science in sports and exercise,* 32**,** 70-84.

BECKONERT, O., KEUN, H. C., EBBELS, T. M., BUNDY, J., HOLMES, E., LINDON, J. C. & NICHOLSON, J. K. 2007. Metabolic profiling, metabolomic and metabonomic procedures for NMR spectroscopy of urine, plasma, serum and tissue extracts. *Nature protocols,* 2**,** 2692-2703.

BEHROOZ, A. & ISMAIL-BEIGI, F. 1999. Stimulation of glucose transport by hypoxia: signals and mechanisms. *Physiology,* 14**,** 105-110.

BENJAMIN, N., O'DRISCOLL, F., DOUGALL, H., DUNCAN, C., SMITH, L., GOLDEN, M. & MCKENZIE, H. 1994. Stomach NO synthesis.

BENOIT, S. C., KEMP, C. J., ELIAS, C. F., ABPLANALP, W., HERMAN, J. P., MIGRENNE, S., LEFEVRE, A.-L., CRUCIANI-GUGLIELMACCI, C., MAGNAN, C. & YU, F. 2009. Palmitic acid mediates hypothalamic insulin resistance by altering PKC-θ subcellular localization in rodents. *The Journal of clinical investigation,* 119**,** 2577-2589.

BENTLEY, R., GRAY, S. R., SCHWARZBAUER, C., DAWSON, D., FRENNEAUX, M. & HE, J. 2014. Dietary nitrate reduces skeletal muscle oxygenation response to physical exercise: a quantitative muscle functional MRI study. *Physiological reports,* 2**,** e12089.

BERARDI, M. J. & CHOU, J. J. 2014. Fatty acid flippase activity of UCP2 is essential for its proton transport in mitochondria. *Cell metabolism,* 20**,** 541-552.

BERRY, M. J., JUSTUS, N. W., HAUSER, J. I., CASE, A. H., HELMS, C. C., BASU, S., ROGERS, Z., LEWIS, M. T. & MILLER, G. D. 2015. Dietary nitrate supplementation improves exercise performance and decreases blood pressure in COPD patients. *Nitric Oxide,* 48**,** 22-30.

BISCHOFF-FERRARI, H. A., DIETRICH, T., ORAV, E. J. & DAWSON-HUGHES, B. 2004. Positive association between 25-hydroxy vitamin D levels and bone mineral density: a population-based study of younger and older adults. *The American journal of medicine,* 116**,** 634-639.

BLATTEIS, C. & LUTHERER, L. 1976. Effect of altitude exposure on thermoregulatory response of man to cold. *Journal of applied physiology,* 41**,** 848-858.

BLOUGH, E. R., RENNIE, E. R., ZHANG, F. & REISER, P. J. 1996. Enhanced electrophoretic separation and resolution of myosin heavy chains in mammalian and avian skeletal muscles. *Analytical biochemistry,* 233**,** 31-35.

BOTHWELL, J. H. F. & GRIFFIN, J. L. 2011. An introduction to biological nuclear magnetic resonance spectroscopy. *Biological Reviews,* 86**,** 493-510.

BOX, G. E. & TIAO, G. C. 2011. *Bayesian inference in statistical analysis*, John Wiley & Sons.

BOYER, S. J. & BLUME, F. D. 1984. Weight loss and changes in body composition at high altitude. *Journal of Applied Physiology,* 57**,** 1580-1585.

BRADLEY, P. H., BRAUER, M. J., RABINOWITZ, J. D. & TROYANSKAYA, O. G. 2009. Coordinated concentration changes of transcripts and metabolites in Saccharomyces cerevisiae. *PLoS Comput Biol,* 5**,** e1000270.

BRANDT, J. M., DJOUADI, F. & KELLY, D. P. 1998. Fatty Acids Activate Transcription of the Muscle Carnitine Palmitoyltransferase I Gene in Cardiac Myocytes via the Peroxisome Proliferator-activated Receptor α. *Journal of Biological Chemistry,* 273**,** 23786-23792.

BREDT, D. S. 1999. Endogenous nitric oxide synthesis: biological functions and pathophysiology. *Free radical research,* 31**,** 577-596.

BROADHURST, D. I. & KELL, D. B. 2006. Statistical strategies for avoiding false discoveries in metabolomics and related experiments. *Metabolomics,* 2**,** 171-196.

BROWN, G. C. & COOPER, C. E. 1994. Nanomolar concentrations of nitric oxide reversibly inhibit synaptosomal respiration by competing with oxygen at cytochrome oxidase. *FEBS letters,* 356**,** 295-298.

BRUDVIG, G. W., STEVENS, T. H. & CHAN, S. I. 1980. Reactions of nitric oxide with cytochrome c oxidase. *Biochemistry,* 19**,** 5275-5285.

BRUMMER, H., ZHANG, M. Y., PIDDOUBNY, M. & MEDLER, S. 2013. Hybrid Fibers Transform into Distinct Fiber Types in Maturing Mouse Muscles. *Cells Tissues Organs,* 198**,** 227-236.

BUIST, A. S., MCBURNIE, M. A., VOLLMER, W. M., GILLESPIE, S., BURNEY, P., MANNINO, D. M., MENEZES, A. M., SULLIVAN, S. D., LEE, T. A. & WEISS, K. B. 2007. International variation in the prevalence of COPD (the BOLD Study): a population-based prevalence study. *The Lancet,* 370**,** 741-750.

CALBET, J. A. L., BOUSHEL, R., RÅDEGRAN, G., SØNDERGAARD, H., WAGNER, P. D. & SALTIN, B. 2003. Why is V˙o 2 max after altitude acclimatization still reduced despite normalization of arterial O2 content? *American Journal of Physiology - Regulatory, Integrative and Comparative Physiology,* 284**,** R304-R316.

CARLSTROM, M., LARSEN, F. J., NYSTROM, T., HEZEL, M., BORNIQUEL, S. & WEITZBERG, E. 2010. Dietary inorganic nitrate reverses features of metabolic syndrome in endothelial nitric oxide synthase-deficient mice. *Proc Natl Acad Sci U S A,* 107.

CARVAJAL, J. A., GERMAIN, A. M., HUIDOBRO-TORO, J. P. & WEINER, C. P. 2000. Molecular mechanism of cGMP-mediated smooth muscle relaxation. *Journal of cellular physiology,* 184**,** 409-420.

CASTELLO, P. R., DAVID, P. S., MCCLURE, T., CROOK, Z. & POYTON, R. O. 2006. Mitochondrial cytochrome oxidase produces nitric oxide under hypoxic conditions: Implications for oxygen sensing and hypoxic signaling in eukaryotes. *Cell Metabolism,* 3**,** 277-287.

CASTELLO, P. R., WOO, D. K., BALL, K., WOJCIK, J., LIU, L. & POYTON, R. O. 2008. Oxygen-regulated isoforms of cytochrome c oxidase have differential effects on its nitric oxide production and on hypoxic signaling. *Proceedings of the National Academy of Sciences,* 105**,** 8203-8208.

CASTRESANA, J., LÜBBEN, M., SARASTE, M. & HIGGINS, D. 1994. Evolution of cytochrome oxidase, an enzyme older than atmospheric oxygen. *The EMBO journal,* 13**,** 2516.

CERMAK, N. M., GIBALA, M. J. & VAN LOON, L. J. 2012. Nitrate supplementation's improvement of 10-km time-trial performance in trained cyclists. *International Journal of Sport Nutrition andExercise Metabolism,* 22**,** 64.

CERRETELLI, P. 1976. Limiting factors to oxygen transport on Mount Everest. *Journal of applied physiology,* 40**,** 658-667.

CHOUCHANI, E. T., METHNER, C., NADTOCHIY, S. M., LOGAN, A., PELL, V. R., DING, S., JAMES, A. M., COCHEME, H. M., REINHOLD, J., LILLEY, K. S., PARTRIDGE, L., FEARNLEY, I. M., ROBINSON, A. J., HARTLEY, R. C., SMITH, R. A. J., KRIEG, T., BROOKES, P. S. & MURPHY, M. P. 2013. Cardioprotection by S-nitrosation of a cysteine switch on mitochondrial complex I. *Nat Med,* 19**,** 753-759.

CHOUCHANI, E. T., PELL, V. R., GAUDE, E., AKSENTIJEVIĆ, D., SUNDIER, S. Y., ROBB, E. L., LOGAN, A., NADTOCHIY, S. M., ORD, E. N. & SMITH, A. C. 2014. Ischaemic accumulation of succinate controls reperfusion injury through mitochondrial ROS. *Nature,* 515**,** 431-435.

CLEMENTI, E., BROWN, G. C., FEELISCH, M. & MONCADA, S. 1998. Persistent inhibition of cell respiration by nitric oxide: crucial role of S-nitrosylation of mitochondrial complex I and protective action of glutathione. *Proceedings of the National Academy of Sciences,* 95**,** 7631-7636.

CLERC, P., RIGOULET, M., LEVERVE, X. & FONTAINE, E. 2007. Nitric oxide increases oxidative phosphorylation efficiency. *Journal of bioenergetics and biomembranes,* 39**,** 158-166.

COLE, M. A., JAMIL, A. H. A., HEATHER, L. C., MURRAY, A. J., SUTTON, E. R., SLINGO, M., SEBAG-MONTEFIORE, L., TAN, S. C., AKSENTIJEVIĆ, D. & GILDEA, O. S. 2016. On the pivotal role of PPARα in adaptation of the heart to hypoxia and why fat in the diet increases hypoxic injury. *The FASEB Journal***,** fj. 201500094R.

CORNFIELD, J. 1966. Sequential trials, sequential analysis and the likelihood principle. *The American Statistician,* 20**,** 18-23.

CORREIA-MELO, C., MARQUES, F. D., ANDERSON, R., HEWITT, G., HEWITT, R., COLE, J., CARROLL, B. M., MIWA, S., BIRCH, J., MERZ, A., RUSHTON, M. D., CHARLES, M., JURK, D., TAIT, S. W., CZAPIEWSKI, R., GREAVES, L., NELSON, G., BOHLOOLY-Y, M., RODRIGUEZ-CUENCA, S., VIDAL-PUIG, A., MANN, D., SARETZKI, G., QUARATO, G., GREEN, D. R., ADAMS, P. D., VON ZGLINICKI, T., KOROLCHUK, V. I. & PASSOS, J. F. 2016. Mitochondria are required for pro-ageing features of the senescent phenotype. *The EMBO Journal*.

COSBY, K., PARTOVI, K. S., CRAWFORD, J. H., PATEL, R. P., REITER, C. D., MARTYR, S., YANG, B. K., WACLAWIW, M. A., ZALOS, G. & XU, X. 2003. Nitrite reduction to nitric oxide by deoxyhemoglobin vasodilates the human circulation. *Nature medicine,* 9**,** 1498-1505.

COTES, J. E., CHINN, D. J. & MILLER, M. R. 2009. *Lung function: physiology, measurement and application in medicine*, John Wiley & Sons.

CREEK, D. J., DUNN, W. B., FIEHN, O., GRIFFIN, J. L., HALL, R. D., LEI, Z., MISTRIK, R., NEUMANN, S., SCHYMANSKI, E. L., SUMNER, L. W., TRENGOVE, R. & WOLFENDER, J.-L. 2014. Metabolite identification: are you sure? And how do your peers gauge your confidence? *Metabolomics,* 10**,** 0.

CUNNINGHAM, J. T., RODGERS, J. T., ARLOW, D. H., VAZQUEZ, F., MOOTHA, V. K. & PUIGSERVER, P. 2007. mTOR controls mitochondrial oxidative function through a YY1–PGC-1&agr; transcriptional complex. *nature,* 450**,** 736-740.

DANESHRAD, Z., GARCIA-RIERA, M., VERDYS, M. & ROSSI, A. 2000. Differential responses to chronic hypoxia and dietary restriction of aerobic capacity and enzyme levels in the rat myocardium. *Molecular and Cellular Biochemistry,* 210**,** 159-166.

DANHIER, P., BAŃSKI, P., PAYEN, V. L., GRASSO, D., IPPOLITO, L., SONVEAUX, P. & PORPORATO, P. E. 2017. Cancer metabolism in space and time: beyond the Warburg effect. *Biochimica et Biophysica Acta (BBA) - Bioenergetics*.

DE MEYER, T., SINNAEVE, D., VAN GASSE, B., RIETZSCHEL, E.-R., DE BUYZERE, M. L., LANGLOIS, M. R., BEKAERT, S., MARTINS, J. C. & VAN CRIEKINGE, W. 2010. Evaluation of standard and advanced preprocessing methods for the univariate analysis of blood serum 1H-NMR spectra. *Analytical and bioanalytical chemistry,* 398**,** 1781-1790.

DE MEYER, T., SINNAEVE, D., VAN GASSE, B., TSIPORKOVA, E., RIETZSCHEL, E. R., DE BUYZERE, M. L., GILLEBERT, T. C., BEKAERT, S., MARTINS, J. C. & VAN CRIEKINGE, W. 2008. NMR-based characterization of metabolic alterations in hypertension using an adaptive, intelligent binning algorithm. *Analytical Chemistry,* 80**,** 3783-3790.

DE PALMA, S., RIPAMONTI, M., VIGANÒ, A., MORIGGI, M., CAPITANIO, D., SAMAJA, M., MILANO, G., CERRETELLI, P., WAIT, R. & GELFI, C. 2007. Metabolic Modulation Induced by Chronic Hypoxia in Rats Using a Comparative Proteomic Analysis of Skeletal Muscle Tissue. *Journal of Proteome Research,* 6**,** 1974-1984.

DIETERLE, F., ROSS, A., SCHLOTTERBECK, G. & SENN, H. 2006. Probabilistic quotient normalization as robust method to account for dilution of complex biological mixtures. Application in 1H NMR metabonomics. *Analytical chemistry,* 78**,** 4281-4290.

DRAGER, L. F., LI, J., SHIN, M.-K., REINKE, C., AGGARWAL, N. R. & JUN, J. C. 2012. Intermittent hypoxia inhibits clearance of triglyceride-rich lipoproteins and inactivates adipose lipoprotein lipase in a mouse model of sleep apnoea. *Eur Heart J,* 33.

DUAN, C. 2016. Hypoxia-inducible factor 3 biology: complexities and emerging themes. *American Journal of Physiology - Cell Physiology,* 310**,** C260-C269.

DUAN, Y., DUAN, Y., LI, F., LI, Y., GUO, Q., JI, Y., TAN, B., LI, T. & YIN, Y. 2016a. Effects of supplementation with branched-chain amino acids to low-protein diets on expression of genes related to lipid metabolism in skeletal muscle of growing pigs. *Amino acids,* 48**,** 2131-2144.

DUAN, Y., GUO, Q., WEN, C., WANG, W., LI, Y., TAN, B., LI, F. & YIN, Y. 2016b. Free Amino Acid Profile and Expression of Genes Implicated in Protein Metabolism in Skeletal Muscle of Growing Pigs Fed Low-Protein Diets Supplemented with Branched-Chain Amino Acids. *Journal of Agricultural and Food Chemistry,* 64**,** 9390-9400.

DUNCAN, C., DOUGALL, H., JOHNSTON, P., GREEN, S., BROGAN, R., LEIFERT, C., SMITH, L., GOLDEN, M. & BENJAMIN, N. 1995. Chemical generation of nitric oxide in the mouth from the enterosalivary circulation of dietary nitrate. *Nature medicine,* 1**,** 546-551.

DUNN, W. B., BAILEY, N. J. & JOHNSON, H. E. 2005. Measuring the metabolome: current analytical technologies. *Analyst,* 130**,** 606-625.

DUNN, W. B., BROADHURST, D., BEGLEY, P., ZELENA, E., FRANCIS-MCINTYRE, S., ANDERSON, N., BROWN, M., KNOWLES, J. D., HALSALL, A. & HASELDEN, J. N. 2011a. Procedures for large-scale metabolic profiling of serum and plasma using gas chromatography and liquid chromatography coupled to mass spectrometry. *Nature protocols,* 6**,** 1060-1083.

DUNN, W. B., BROADHURST, D. I., ATHERTON, H. J., GOODACRE, R. & GRIFFIN, J. L. 2011b. Systems level studies of mammalian metabolomes: the roles of mass spectrometry and nuclear magnetic resonance spectroscopy. *Chemical Society Reviews,* 40**,** 387-426.

EDWARDS, L. M., MURRAY, A. J., TYLER, D. J., KEMP, G. J., HOLLOWAY, C. J., ROBBINS, P. A., NEUBAUER, S., LEVETT, D., MONTGOMERY, H. E. & GROCOTT, M. P. 2010. The effect of high-altitude on human skeletal muscle energetics: 31P-MRS results from the Caudwell Xtreme Everest expedition. *PloS one,* 5**,** e10681.

EDWARDS, L. M. & THIELE, I. 2013. Applying systems biology methods to the study of human physiology in extreme environments. *Extreme Physiol Med,* 2.

EISENBERG, S. 1984. High density lipoprotein metabolism. *Journal of lipid research,* 25**,** 1017-1058.

ERZURUM, S., GHOSH, S., JANOCHA, A., XU, W., BAUER, S., BRYAN, N., TEJERO, J., HEMANN, C., HILLE, R. & STUEHR, D. 2007. Higher blood flow and circulating NO products offset high-altitude hypoxia among Tibetans. *Proceedings of the National Academy of Sciences,* 104**,** 17593-17598.

ESSÉN, B. 1978. Glycogen depletion of different fibre types in human skeletal muscle during intermittent and continuous exercise. *Acta Physiologica Scandinavica,* 103**,** 446-455.

ESSOP, M. F. 2007. Cardiac metabolic adaptations in response to chronic hypoxia. *The Journal of Physiology,* 584**,** 715-726.

EVANGELISTA, A. M., RAO, V. S., FILO, A. R., MAROZKINA, N. V., DOCTOR, A., JONES, D. R., GASTON, B. & GUILFORD, W. H. 2010. Direct regulation of striated muscle myosins by nitric oxide and endogenous nitrosothiols. *PLoS One,* 5**,** e11209.

FAHY, E., SUBRAMANIAM, S., MURPHY, R. C., NISHIJIMA, M., RAETZ, C. R., SHIMIZU, T., SPENER, F., VAN MEER, G., WAKELAM, M. J. & DENNIS, E. A. 2009. Update of the LIPID MAPS comprehensive classification system for lipids. *Journal of lipid research,* 50**,** S9-S14.

FAISS, R., GIRARD, O. & MILLET, G. P. 2013. Advancing hypoxic training in team sports: from intermittent hypoxic training to repeated sprint training in hypoxia. *British journal of sports medicine,* 47**,** i45-i50.

FERGUSON, S. K., HOLDSWORTH, C. T., WRIGHT, J. L., FEES, A. J., ALLEN, J. D., JONES, A. M., MUSCH, T. I. & POOLE, D. C. 2015. Microvascular oxygen pressures in muscles comprised of different fiber types: Impact of dietary nitrate supplementation. *Nitric Oxide,* 48**,** 38-43.

FINCK, B. N., LEHMAN, J. J., LEONE, T. C., WELCH, M. J., BENNETT, M. J., KOVACS, A., HAN, X., GROSS, R. W., KOZAK, R. & LOPASCHUK, G. D. 2002. The cardiac phenotype induced by PPARα overexpression mimics that caused by diabetes mellitus. *The Journal of clinical investigation,* 109**,** 121-130.

FIRTH, J. D., EBERT, B. L. & RATCLIFFE, P. J. 1995. Hypoxic regulation of lactate dehydrogenase A Interaction between hypoxia-inducible factor 1 and cAMP response elements. *Journal of Biological Chemistry,* 270**,** 21021-21027.

FONTANA, L., CUMMINGS, NICOLE E., ARRIOLA APELO, SEBASTIAN I., NEUMAN, JOSHUA C., KASZA, I., SCHMIDT, BRIAN A., CAVA, E., SPELTA, F., TOSTI, V., SYED, FAIZAN A., BAAR, EMMA L., VERONESE, N., COTTRELL, SARA E., FENSKE, RACHEL J., BERTOZZI, B., BRAR, HARPREET K., PIETKA, T., BULLOCK, ARNOLD D., FIGENSHAU, ROBERT S., ANDRIOLE, GERALD L., MERRINS, MATTHEW J., ALEXANDER, CAROLINE M., KIMPLE, MICHELLE E. & LAMMING, DUDLEY W. 2016. Decreased Consumption of Branched-Chain Amino Acids Improves Metabolic Health. *Cell Reports,* 16**,** 520-530.

FORRISTAL, C. E. & LEVESQUE, J.-P. 2013. Targeting the Hypoxia-Sensing Pathway in Clinical Hematology. *Stem Cells,* 2014**,** 135-140.

FORSYTHE, J. A., JIANG, B.-H., IYER, N. V., AGANI, F., LEUNG, S. W., KOOS, R. D. & SEMENZA, G. L. 1996. Activation of vascular endothelial growth factor gene transcription by hypoxia-inducible factor 1. *Molecular and cellular biology,* 16**,** 4604-4613.

FRONTINI, A. & CINTI, S. 2010. Distribution and development of brown adipocytes in the murine and human adipose organ. *Cell metabolism,* 11**,** 253-256.

FUKUDA, R., ZHANG, H., KIM, J.-W., SHIMODA, L., DANG, C. V. & SEMENZA, GREGG L. 2007. HIF-1 Regulates Cytochrome Oxidase Subunits to Optimize Efficiency of Respiration in Hypoxic Cells. *Cell,* 129**,** 111-122.

FULFORD, J., WINYARD, P. G., VANHATALO, A., BAILEY, S. J., BLACKWELL, J. R. & JONES, A. M. 2013. Influence of dietary nitrate supplementation on human skeletal muscle metabolism and force production during maximum voluntary contractions. *Pflügers Archiv-European Journal of Physiology,* 465**,** 517-528.

FURUTA, E., PAI, S. K., ZHAN, R., BANDYOPADHYAY, S., WATABE, M., MO, Y.-Y., HIROTA, S., HOSOBE, S., TSUKADA, T. & MIURA, K. 2008. Fatty acid synthase gene is up-regulated by hypoxia via activation of Akt and sterol regulatory element binding protein-1. *Cancer research,* 68**,** 1003-1011.

GALBÈS, O., GORET, L., CAILLAUD, C., MERCIER, J., OBERT, P., CANDAU, R. & PY, G. 2008. Combined effects of hypoxia and endurance training on lipid metabolism in rat skeletal muscle. *Acta Physiologica,* 193**,** 163-173.

GAMBOA, J. L. & ANDRADE, F. H. 2010. Mitochondrial content and distribution changes specific to mouse diaphragm after chronic normobaric hypoxia. *American Journal of Physiology-Regulatory, Integrative and Comparative Physiology,* 298**,** R575-R583.

GAMBOA, J. L. & ANDRADE, F. H. 2012. Muscle endurance and mitochondrial function after chronic normobaric hypoxia: contrast of respiratory and limb muscles. *Pflügers Archiv-European Journal of Physiology,* 463**,** 327-338.

GAO, S., CHEN, J., BRODSKY, S. V., HUANG, H., ADLER, S., LEE, J. H., DHADWAL, N., COHEN-GOULD, L., GROSS, S. S. & GOLIGORSKY, M. S. 2004. Docking of Endothelial Nitric Oxide Synthase (eNOS) to the Mitochondrial Outer Membrane A PENTABASIC AMINO ACID SEQUENCE IN THE AUTOINHIBITORY DOMAIN OF eNOS TARGETS A PROTEINASE K-CLEAVABLE PEPTIDE ON THE CYTOPLASMIC FACE OF MITOCHONDRIA. *Journal of Biological Chemistry,* 279**,** 15968-15974.

GARLID, K. D., JABŮREK, M. & JEŽEK, P. 1998. The mechanism of proton transport mediated by mitochondrial uncoupling proteins. *FEBS letters,* 438**,** 10-14.

GASKILL, S. E., RUBY, B. C., WALKER, A. J., SANCHEZ, O. A., SERFASS, R. C. & LEON, A. S. 2001. Validity and reliability of combining three methods to determine ventilatory threshold. *Medicine and science in sports and exercise,* 33**,** 1841-1848.

GEARING, K., GÖTTLICHER, M., TEBOUL, M., WIDMARK, E. & GUSTAFSSON, J.-Å. 1993. Interaction of the peroxisome-proliferator-activated receptor and retinoid X receptor. *Proceedings of the National Academy of Sciences,* 90**,** 1440-1444.

GIBSON, G. J. 1993. Standardised lung function testing. *Eur Respir J,* 6**,** 155-7.

GIORDANO, F. J. 2005. Oxygen, oxidative stress, hypoxia, and heart failure. *The Journal of clinical investigation,* 115**,** 500-508.

GORE, C. J., HAHN, A. G., SCROOP, G. C., WATSON, D., NORTON, K. I., WOOD, R., CAMPBELL, D. & EMONSON, D. 1996. Increased arterial desaturation in trained cyclists during maximal exercise at 580 m altitude. *Journal of applied physiology,* 80**,** 2204-2210.

GOSKER, H. R., ENGELEN, M. P., VAN MAMEREN, H., VAN DIJK, P. J., VAN DER VUSSE, G. J., WOUTERS, E. F. & SCHOLS, A. M. 2002. Muscle fiber type IIX atrophy is involved in the loss of fat-free mass in chronic obstructive pulmonary disease. *The American journal of clinical nutrition,* 76**,** 113-119.

GOTTLIEB, H. E., KOTLYAR, V. & NUDELMAN, A. 1997. NMR Chemical Shifts of Common Laboratory Solvents as Trace Impurities. *The Journal of Organic Chemistry,* 62**,** 7512-7515.

GOVONI, M., JANSSON, E. A., WEITZBERG, E. & LUNDBERG, J. O. 2008. The increase in plasma nitrite after a dietary nitrate load is markedly attenuated by an antibacterial mouthwash. *Nitric Oxide,* 19**,** 333-7.

GREEN, H., ROY, B., GRANT, S., OTTO, C., PIPE, A., MCKENZIE, D. & JOHNSON, M. 2000. Human skeletal muscle exercise metabolism following an expedition to Mount Denali. *American*

Journal of Physiology - Regulatory, Integrative and Comparative Physiology, 279**,** R1872-R1879.

GREEN, H., SUTTON, J., CYMERMAN, A., YOUNG, P. & HOUSTON, C. 1989. Operation Everest II: adaptations in human skeletal muscle. *Journal of Applied Physiology,* 66**,** 2454-2461.

GREEN, H., SUTTON, J., WOLFEL, E., REEVES, J., BUTTERFIELD, G. & BROOKS, G. 1992. Altitude acclimatization and energy metabolic adaptations in skeletal muscle during exercise. *Journal of Applied Physiology,* 73**,** 2701-2708.

GRIFFIN, J. L. 2006. The Cinderella story of metabolic profiling: does metabolomics get to go to the functional genomics ball? *Philosophical Transactions of the Royal Society B: Biological Sciences,* 361**,** 147-161.

GROCOTT, M., MONTGOMERY, H. & VERCUEIL, A. 2007a. High-altitude physiology and pathophysiology: implications and relevance for intensive care medicine. *Critical Care,* 11**,** 203.

GROCOTT, M., RICHARDSON, A., MONTGOMERY, H. & MYTHEN, M. 2007b. Caudwell Xtreme Everest: a field study of human adaptation to hypoxia. *Critical Care,* 11**,** 151.

GROVER, R. F., WEIL, J. V. & REEVES, J. T. 1985. Cardiovascular adaptation to exercise at high altitude. *Exercise and sport sciences reviews,* 14**,** 269-302.

GUILLAND, J. & KLEPPING, J. 1985. Nutritional alterations at high altitude in man. *European journal of applied physiology and occupational physiology,* 54**,** 517-523.

GULICK, T., CRESCI, S., CAIRA, T., MOORE, D. D. & KELLY, D. P. 1994. The peroxisome proliferator-activated receptor regulates mitochondrial fatty acid oxidative enzyme gene expression. *Proceedings of the National Academy of Sciences,* 91**,** 11012-11016.

GULSTON, M. K., RUBTSOV, D. V., ATHERTON, H. J., CLARKE, K., DAVIES, K. E., LILLEY, K. S. & GRIFFIN, J. L. 2008. A combined metabolomic and proteomic investigation of the effects of a failure to express dystrophin in the mouse heart. *Journal of proteome research,* 7**,** 2069-2077.

GUZY, R. D., HOYOS, B., ROBIN, E., CHEN, H., LIU, L., MANSFIELD, K. D., SIMON, M. C., HAMMERLING, U. & SCHUMACKER, P. T. 2005. Mitochondrial complex III is required for hypoxia-induced ROS production and cellular oxygen sensing. *Cell metabolism,* 1**,** 401-408.

HACKETT, P., RENNIE, D. & LEVINE, H. 1976. The incidence, importance, and prophylaxis of acute mountain sickness. *The Lancet,* 308**,** 1149-1155.

HAGEN, T., TAYLOR, C. T., LAM, F. & MONCADA, S. 2003. Redistribution of intracellular oxygen in hypoxia by nitric oxide: effect on HIF1α. *Science,* 302**,** 1975-1978.

HARPER, M.-E., DENT, R., MONEMDJOU, S., BÉZAIRE, V., VAN WYCK, L., WELLS, G., KAVASLAR, G. N., GAUTHIER, A., TESSON, F. & MCPHERSON, R. 2002. Decreased mitochondrial proton leak and reduced expression of uncoupling protein 3 in skeletal muscle of obese diet-resistant women. *Diabetes,* 51**,** 2459-2466.

HEATHER, L., COLE, M., TAN, J.-J., AMBROSE, L. A., POPE, S., ABD-JAMIL, A., CARTER, E., DODD, M., YEOH, K., SCHOFIELD, C. & CLARKE, K. 2012. Metabolic adaptation to chronic hypoxia in cardiac mitochondria. *Basic Research in Cardiology,* 107**,** 1-12.

HERNÁNDEZ, A., SCHIFFER, T. A., IVARSSON, N., CHENG, A. J., BRUTON, J. D., LUNDBERG, J. O., WEITZBERG, E. & WESTERBLAD, H. 2012. Dietary nitrate increases tetanic [Ca2+] i and contractile force in mouse fast-twitch muscle. *The Journal of physiology,* 590**,** 3575-3583.

HESS, D., CHISHOLM, J. W. & IGAL, R. A. 2010. Inhibition of StearoylCoA Desaturase Activity Blocks Cell Cycle Progression and Induces Programmed Cell Death in Lung Cancer Cells. *PLoS One,* 5.

HIROSUMI, J., TUNCMAN, G., CHANG, L., GORGUN, C. Z., UYSAL, K. T., MAEDA, K., KARIN, M. & HOTAMISLIGIL, G. S. 2002. A central role for JNK in obesity and insulin resistance. *Nature,* 420**,** 333-336.

HOBBS, D. A., KAFFA, N., GEORGE, T. W., METHVEN, L. & LOVEGROVE, J. A. 2012. Blood pressure-lowering effects of beetroot juice and novel beetroot-enriched bread products in normotensive male subjects. *British Journal of Nutrition,* 108**,** 2066-2074.

HOCHACHKA, P. & LUTZ, P. 2001. Mechanism, origin, and evolution of anoxia tolerance in animals. *Comparative Biochemistry and Physiology Part B: Biochemistry and Molecular Biology,* 130**,** 435-459.

HOCHACHKA, P. W., BEATTY, C. L., BURELLE, Y., TRUMP, M. E., MCKENZIE, D. C. & MATHESON, G. O. 2002. The Lactate Paradox in Human High-Altitude Physiological Performance. *Physiology,* 17**,** 122-126.

HOCHACHKA, P. W., CLARK, C. M., HOLDEN, J. E., STANLEY, C., UGURBIL, K. & MENON, R. S. 1996. 31P magnetic resonance spectroscopy of the Sherpa heart: a phosphocreatine/adenosine triphosphate signature of metabolic defense against hypobaric hypoxia. *Proceedings of the National Academy of Sciences,* 93**,** 1215-1220.

HOLICK, M. F. 2004. Sunlight and vitamin D for bone health and prevention of autoimmune diseases, cancers, and cardiovascular disease. *The American journal of clinical nutrition,* 80**,** 1678S-1688S.

HOLLOWAY, C. J., MONTGOMERY, H. E., MURRAY, A. J., COCHLIN, L. E., CODREANU, I., HOPWOOD, N., JOHNSON, A. W., RIDER, O. J., LEVETT, D. Z. & TYLER, D. J. 2011. Cardiac response to hypobaric hypoxia: persistent changes in cardiac mass, function, and energy metabolism after a trek to Mt. Everest Base Camp. *The FASEB Journal,* 25**,** 792-796.

HOLLOWAY, C. J., MURRAY, A. J., MITCHELL, K., MARTIN, D. S., JOHNSON, A. W., COCHLIN, L. E., CODREANU, I., DHILLON, S., RODWAY, G. W. & ASHMORE, T. 2014. Oral Coenzyme Q10 Supplementation Does Not Prevent Cardiac Alterations During a High Altitude Trek to Everest Base Camp. *High altitude medicine & biology,* 15**,** 459-467.

HOPPELER, H. & VOGT, M. 2001. Muscle tissue adaptations to hypoxia. *Journal of experimental biology,* 204**,** 3133-3139.

HOPPELER, H., VOGT, M. 2001. Muscle tissue adaptations to hypoxia. *Journal of experimental biology,* 204**,** 3133-3139.

HORD, N. G., TANG, Y. & BRYAN, N. S. 2009. Food sources of nitrates and nitrites: the physiologic context for potential health benefits. *The American journal of clinical nutrition,* 90**,** 1-10.

HORSCROFT, J. A. & MURRAY, A. J. 2014. Skeletal muscle energy metabolism in environmental hypoxia: climbing towards consensus. *Extreme Physiol Med,* 3.

HOSOGAI, N., FUKUHARA, A., OSHIMA, K., MIYATA, Y., TANAKA, S., SEGAWA, K., FURUKAWA, S., TOCHINO, Y., KOMURO, R. & MATSUDA, M. 2007. Adipose tissue hypoxia in obesity and its impact on adipocytokine dysregulation. *Diabetes,* 56**,** 901-911.

HOULE-LEROY, P., GARLAND, T., SWALLOW, J. G. & GUDERLEY, H. 2000. Effects of voluntary activity and genetic selection on muscle metabolic capacities in house mice Mus domesticus. *Journal of Applied Physiology,* 89**,** 1608-1616.

HUGHES, A. P. 1965. Plant growth and the aerial environment. *New Phytologist,* 64**,** 323-329.

HULTSTRÖM, M., AMORIM DE PAULA, C., PORCELLI, S., FERGUSON, S. K., BOURDILLON, N., HOON, M. W., MICHIELLI, D. W., FAISS, R., CORONA, B. T., DA SILVEIRA, A. L. B., SINDLER, A. L., JOHNSON, B. D., BESCOS, R., CODY, L. C., WANNER, S. P., REHMAN, S., ANTÔNIO PELIKY FONTES, M., BELLISTRI, G., PUGLIESE, L., RASICA, L., MARZORATI, M., PAVEI, G., HOLDSWORTH, C. T., MUSCH, T. I., POOLE, D. C., BURKE, L. M., MILLET, G. P., GREEN, M. S., CASEY, D. P., WHEATLEY, C. M., CARLSON-PHILLIPS, A., KUNCES, L. J., MARTENS, C. R., JUSTICE, J. N., BALLAK, S. B. & BALLAK, D. B. 2015. Commentaries on Viewpoint: Can elite athletes benefit from dietary nitrate supplementation?Commentaries on Viewpoint: Can

elite athletes benefit from dietary nitrate supplementation?Commentaries on Viewpoint: Can elite athletes benefit from dietary nitra…. *Journal of Applied Physiology,* 119**,** 762-769.

HUSS, J. M., LEVY, F. H. & KELLY, D. P. 2001. Hypoxia Inhibits the Peroxisome Proliferator-activated Receptor α/Retinoid X Receptor Gene Regulatory Pathway in Cardiac Myocytes a mechanism for O2-dependent modulation of mitochondrial fatty acid oxidation *Journal of biological chemistry,* 276**,** 27605-27612.

ISHII, T., SUNAMI, O., SAITOH, N., NISHIO, H., TAKEUCHI, T. & HATA, F. 1998. Inhibition of skeletal muscle sarcoplasmic reticulum Ca 2+-ATPase by nitric oxide. *FEBS letters,* 440**,** 218-222.

ISSEMANN, I. & GREEN, S. 1990. Activation of a member of the steroid hormone receptor superfamily by peroxisome proliferators. *Nature,* 347**,** 645-650.

ITO, K., ITO, M., ELLIOTT, W. M., COSIO, B., CARAMORI, G., KON, O. M., BARCZYK, A., HAYASHI, S., ADCOCK, I. M. & HOGG, J. C. 2005. Decreased histone deacetylase activity in chronic obstructive pulmonary disease. *New England Journal of Medicine,* 352**,** 1967-1976.

IVAN, M., KONDO, K., YANG, H., KIM, W., VALIANDO, J., OHH, M., SALIC, A., ASARA, J. M., LANE, W. S. & KAELIN JR, W. G. 2001. HIFα targeted for VHL-mediated destruction by proline hydroxylation: implications for O2 sensing. *Science,* 292**,** 464-468.

JACOBS, I., ROMET, T. T. & KERRIGAN-BROWN, D. 1985. Muscle glycogen depletion during exercise at 9‡ C and 21‡ C. *European Journal of Applied Physiology and Occupational Physiology,* 54**,** 35-39.

JACOBS, R. A., BOUSHEL, R., WRIGHT-PARADIS, C., CALBET, J. A., ROBACH, P. & GNAIGER, E. 2013. Mitochondrial function in human skeletal muscle following high-altitude exposure. *Exp Physiol,* 98.

JACOBS, R. A., SIEBENMANN, C., HUG, M., TOIGO, M., MEINILD, A.-K. & LUNDBY, C. 2012. Twenty-eight days at 3454-m altitude diminishes respiratory capacity but enhances efficiency in human skeletal muscle mitochondria. *The FASEB Journal,* 26**,** 5192-5200.

JAKOBSSON, P., JORFELDT, L. & BRUNDIN, A. 1990. Skeletal muscle metabolites and fibre types in patients with advanced chronic obstructive pulmonary disease (COPD), with and without chronic respiratory failure. *European Respiratory Journal,* 3**,** 192-196.

JIANG, C., KIM, J.-H., LI, F., QU, A., GAVRILOVA, O., SHAH, Y. M. & GONZALEZ, F. J. 2013. Hypoxia-inducible factor 1α regulates a SOCS3-STAT3-adiponectin signal transduction pathway in adipocytes. *Journal of Biological Chemistry,* 288**,** 3844-3857.

JIANG, C., QU, A., MATSUBARA, T., CHANTURIYA, T., JOU, W., GAVRILOVA, O., SHAH, Y. M. & GONZALEZ, F. J. 2011. Disruption of hypoxia-inducible factor 1 in adipocytes improves insulin sensitivity and decreases adiposity in high-fat diet–fed mice. *Diabetes,* 60**,** 2484-2495.

JOBIN, J., MALTAIS, F., DOYON, J.-F., LEBLANC, P., SIMARD, P.-M., SIMARD, A.-A. & SIMARD, C. 1998. Chronic obstructive pulmonary disease: capillarity and fiber-type characteristics of skeletal muscle. *Journal of Cardiopulmonary Rehabilitation and Prevention,* 18**,** 432-437.

JOHNSON, B. G., WRIGHT, A. D., BEAZLEY, M. F., HARVEY, T. C., HILLENBRAND, P. & IMRAY, C. H. 2005. The sharpened Romberg test for assessing ataxia in mild acute mountain sickness. *Wilderness & environmental medicine,* 16**,** 62-66.

JONES, A. M. 2014. Dietary nitrate supplementation and exercise performance. *Sports Medicine,* 44**,** 35-45.

JONVIK, K. L., NYAKAYIRU, J., VAN LOON, L. J. & VERDIJK, L. B. 2015. Can elite athletes benefit from dietary nitrate supplementation? *Journal of Applied Physiology***,** jap. 00232.2015.

JUNGERSTEN, L., AMBRING, A., WALL, B. & WENNMALM, Å. 1997. Both physical fitness and acute exercise regulate nitric oxide formation in healthy humans. *Journal of applied physiology,* 82**,** 760-764.

KAELIN, W. G. & RATCLIFFE, P. J. 2008. Oxygen sensing by metazoans: the central role of the HIF hydroxylase pathway. *Molecular cell,* 30**,** 393-402.

KAMMOUN, M., CASSAR-MALEK, I., MEUNIER, B. & PICARD, B. 2014. A simplified immunohistochemical classification of skeletal muscle fibres in mouse. *European Journal of Histochemistry,* 58.

KAMPHORST, J. J., CROSS, J. R., FAN, J., DE STANCHINA, E., MATHEW, R., WHITE, E. P., THOMPSON, C. B. & RABINOWITZ, J. D. 2013. Hypoxic and Ras-transformed cells support growth by scavenging unsaturated fatty acids from lysophospholipids. *Proceedings of the National Academy of Sciences,* 110**,** 8882-8887.

KAPIL, V., WEITZBERG, E., LUNDBERG, J. & AHLUWALIA, A. 2014. Clinical evidence demonstrating the utility of inorganic nitrate in cardiovascular health. *Nitric Oxide,* 38**,** 45-57.

KARPIEVITCH, Y. V., DABNEY, A. R. & SMITH, R. D. 2012. Normalization and missing value imputation for label-free LC-MS analysis. *BMC bioinformatics,* 13**,** S5.

KARPIEVITCH, Y. V., NIKOLIC, S. B., WILSON, R., SHARMAN, J. E. & EDWARDS, L. M. 2014. Metabolomics Data Normalization with EigenMS. *PloS one,* 9**,** e116221.

KATAJAMAA, M. & OREŠIČ, M. 2007. Data processing for mass spectrometry-based metabolomics. *Journal of chromatography A,* 1158**,** 318-328.

KAYSER, B., HOPPELER, H., DESPLANCHES, D., MARCONI, C., BROERS, B. & CERRETELLI, P. 1996. Muscle ultrastructure and biochemistry of lowland Tibetans. *Journal of Applied Physiology,* 81**,** 419-425.

KELLY, J., VANHATALO, A., BAILEY, S. J., WYLIE, L. J., TUCKER, C., LIST, S., WINYARD, P. G. & JONES, A. M. 2014. Dietary nitrate supplementation: effects on plasma nitrite and pulmonary O2 uptake dynamics during exercise in hypoxia and normoxia. *American Journal of Physiology-Regulatory, Integrative and Comparative Physiology,* 307**,** R920-R930.

KELLY, P. J., POCOCK, N. A., SAMBROOK, P. N. & EISMAN, J. A. 1990. Dietary calcium, sex hormones, and bone mineral density in men. *British Medical Journal,* 300**,** 1361-1364.

KENNEDY, A., MARTINEZ, K., CHUANG, C.-C., LAPOINT, K. & MCINTOSH, M. 2009. Saturated fatty acid-mediated inflammation and insulin resistance in adipose tissue: mechanisms of action and implications. *The Journal of nutrition,* 139**,** 1-4.

KERLEY, C. P., CAHILL, K., BOLGER, K., MCGOWAN, A., BURKE, C., FAUL, J. & CORMICAN, L. 2015. Dietary nitrate supplementation in COPD: An acute, double-blind, randomized, placebo-controlled, crossover trial☆. *Nitric Oxide,* 44**,** 105-111.

KERSTEN, S., DESVERGNE, B. & WAHLI, W. 2000. Roles of PPARs in health and disease. *Nature,* 405**,** 421-424.

KESSLER, R., PARTRIDGE, M. R., MIRAVITLLES, M., CAZZOLA, M., VOGELMEIER, C., LEYNAUD, D. & OSTINELLI, J. 2011. Symptom variability in patients with severe COPD: a pan-European cross-sectional study. *European Respiratory Journal,* 37**,** 264-272.

KEUN, H. C., EBBELS, T. M. D., ANTTI, H., BOLLARD, M. E., BECKONERT, O., HOLMES, E., LINDON, J. C. & NICHOLSON, J. K. 2003. Improved analysis of multivariate data by variable stability scaling: application to NMR-based metabolic profiling. *Analytica Chimica Acta,* 490**,** 265-276.

KIENS, B., ALSTED, T. J. & JEPPESEN, J. 2011. Factors regulating fat oxidation in human skeletal muscle. *Obes Rev,* 12.

KIILERICH, K., ADSER, H., JAKOBSEN, A. H., PEDERSEN, P. A., HARDIE, D. G., WOJTASZEWSKI, J. F. P. & PILEGAARD, H. 2010. PGC-1α increases PDH content but does not change acute PDH regulation in mouse skeletal muscle. *American Journal of Physiology - Regulatory, Integrative and Comparative Physiology,* 299**,** R1350-R1359.

KILLIAN, K. J., LEBLANC, P., MARTIN, D. H., SUMMERS, E., JONES, N. L. & CAMPBELL, E. J. M. 1992a. Exercise Capacity and Ventilatory, Circulatory, and Symptom Limitation in Patients with Chronic Airflow Limitation. *American Review of Respiratory Disease,* 146**,** 935-940.

KILLIAN, K. J., LEBLANC, P., MARTIN, D. H., SUMMERS, E., JONES, N. L. & CAMPBELL, E. M. 1992b. Exercise capacity and ventilatory, circulatory, and symptom limitation in patients with chronic airflow limitation. *American review of respiratory disease,* 146**,** 935-940.

KIM, J.-W., TCHERNYSHYOV, I., SEMENZA, G. L. & DANG, C. V. 2006. HIF-1-mediated expression of pyruvate dehydrogenase kinase: a metabolic switch required for cellular adaptation to hypoxia. *Cell metabolism,* 3**,** 177-185.

KIM, J., TCHERNYSHYOV, I., SEMENZA, GL., DANG, CV 2006. HIF-1-mediated expression of pyruvate dehydrogenase kinase: a metabolic switch required for cellular adaptation to hypoxia. *Cell metabolism,* 3**,** 177-185.

KIRWAN, J. A., WEBER, R. J., BROADHURST, D. I. & VIANT, M. R. 2014. Direct infusion mass spectrometry metabolomics dataset: a benchmark for data processing and quality control. *Scientific data,* 1.

KNOWLES, H. J. 2015. Hypoxic regulation of osteoclast differentiation and bone resorption activity. *Hypoxia,* 3**,** 73.

KOCH, L. G. & BRITTON, S. L. 2008. Aerobic metabolism underlies complexity and capacity. *The Journal of physiology,* 586**,** 83-95.

KOECHLIN, C., MALTAIS, F., SAEY, D., MICHAUD, A., LEBLANC, P., HAYOT, M. & PRÉFAUT, C. 2005. Hypoxaemia enhances peripheral muscle oxidative stress in chronic obstructive pulmonary disease. *Thorax,* 60**,** 834-841.

KOTA, B. P., HUANG, T. H.-W. & ROUFOGALIS, B. D. 2005. An overview on biological mechanisms of PPARs. *Pharmacological Research,* 51**,** 85-94.

KOULMAN, A., PRENTICE, P., WONG, M. C. Y., MATTHEWS, L., BOND, N. J., EIDEN, M., GRIFFIN, J. L. & DUNGER, D. B. 2014. The development and validation of a fast and robust dried blood spot based lipid profiling method to study infant metabolism. *Metabolomics,* 10**,** 0.

KRAEGEN, E., COONEY, G., YE, J.-M., THOMPSON, A. & FURLER, S. 2001. The role of lipids in the pathogenesis of muscle insulin resistance and beta cell failure in type II diabetes and obesity. *Experimental and Clinical Endocrinology & Diabetes,* 109**,** S189-S201.

KRAEMER, F. B. & SHEN, W.-J. 2002. Hormone-sensitive lipase control of intracellular tri-(di-) acylglycerol and cholesteryl ester hydrolysis. *Journal of lipid research,* 43**,** 1585-1594.

KRIAT, M., CONFORT-GOUNY, S., VION-DURY, J., SCIAKY, M., VIOUT, P. & COZZONE, P. J. 1992. Quantitation of metabolites in human blood serum by proton magnetic resonance spectroscopy. A comparative study of the use of formate and TSP as concentration standards. *NMR in Biomedicine,* 5**,** 179-184.

KRUSCHKE, J. K. 2010. What to believe: Bayesian methods for data analysis. *Trends in cognitive sciences,* 14**,** 293-300.

KRUSCHKE, J. K. & VANPAEMEL, W. 2015. Bayesian estimation in hierarchical models. *The Oxford Handbook of Computational and Mathematical Psychology.* Oxford University Press, USA.

KUME, S., YAMATO, M., TAMURA, Y., JIN, G., NAKANO, M., MIYASHIGE, Y., EGUCHI, A., OGATA, Y., GODA, N. & IWAI, K. 2015. Potential biomarkers of fatigue identified by plasma metabolome analysis in rats. *PloS one,* 10**,** e0120106.

KUZNETSOV, A. V., VEKSLER, V., GELLERICH, F. N., SAKS, V., MARGREITER, R. & KUNZ, W. S. 2008. Analysis of mitochondrial function in situ in permeabilized muscle fibers, tissues and cells. *Nat. Protocols,* 3**,** 965-976.

LAEMMLI, U. K. 1970. Cleavage of structural proteins during the assembly of the head of bacteriophage T4. *nature,* 227**,** 680-685.

LAMBERT, A. J. & BRAND, M. D. 2004. Inhibitors of the quinone-binding site allow rapid superoxide production from mitochondrial NADH: ubiquinone oxidoreductase (complex I). *Journal of Biological Chemistry,* 279**,** 39414-39420.

LANSLEY, K. E., WINYARD, P. G., FULFORD, J., VANHATALO, A., BAILEY, S. J., BLACKWELL, J. R., DIMENNA, F. J., GILCHRIST, M., BENJAMIN, N. & JONES, A. M. 2011. Dietary nitrate supplementation reduces the O2 cost of walking and running: a placebo-controlled study. *Journal of Applied Physiology,* 110**,** 591-600.

LARSEN, F., WEITZBERG, E., LUNDBERG, J. & EKBLOM, B. 2007. Effects of dietary nitrate on oxygen cost during exercise. *Acta physiologica,* 191**,** 59-66.

LARSEN, F. J., EKBLOM, B., SAHLIN, K., LUNDBERG, J. O. & WEITZBERG, E. 2006. Effects of dietary nitrate on blood pressure in healthy volunteers. *New England Journal of Medicine,* 355**,** 2792-2793.

LARSEN, F. J., SCHIFFER, T. A., BORNIQUEL, S., SAHLIN, K., EKBLOM, B., LUNDBERG, J. O. & WEITZBERG, E. 2011. Dietary inorganic nitrate improves mitochondrial efficiency in humans. *Cell metabolism,* 13**,** 149-159.

LARSEN, F. J., WEITZBERG, E., LUNDBERG, J. O. & EKBLOM, B. 2010. Dietary nitrate reduces maximal oxygen consumption while maintaining work performance in maximal exercise. *Free Radical Biology and Medicine,* 48**,** 342-347.

LARSEN, S., NIELSEN, J., HANSEN, C. N., NIELSEN, L. B., WIBRAND, F., STRIDE, N., SCHRODER, H. D., BOUSHEL, R., HELGE, J. W. & DELA, F. 2012. Biomarkers of mitochondrial content in skeletal muscle of healthy young human subjects. *The Journal of physiology,* 590**,** 3349-3360.

LE, W., ABBAS, A. S., SPRECHER, H., VOCKLEY, J. & SCHULZ, H. 2000. Long-chain acyl-CoA dehydrogenase is a key enzyme in the mitochondrial β-oxidation of unsaturated fatty acids. *Biochimica et Biophysica Acta (BBA) - Molecular and Cell Biology of Lipids,* 1485**,** 121-128.

LEE, S., PINEAU, T., DRAGO, J., LEE, E. J., OWENS, J. W., KROETZ, D. L., FERNANDEZ-SALGUERO, P. M., WESTPHAL, H. & GONZALEZ, F. J. 1995. Targeted disruption of the alpha isoform of the peroxisome proliferator-activated receptor gene in mice results in abolishment of the pleiotropic effects of peroxisome proliferators. *Molecular and cellular biology,* 15**,** 3012-3022.

LEONARD, W. R., SNODGRASS, J. J. & SORENSEN, M. V. 2005. Metabolic adaptation in indigenous Siberian populations. *Annu. Rev. Anthropol.,* 34**,** 451-471.

LEONG, P., BASHAM, J. E., YONG, T., CHAZAN, A., FINLAY, P., BARNES, S., BARDIN, P. G. & CAMPBELL, D. 2015. A double blind randomized placebo control crossover trial on the effect of dietary nitrate supplementation on exercise tolerance in stable moderate chronic obstructive pulmonary disease. *BMC pulmonary medicine,* 15**,** 1.

LESNEFSKY, E. J., MOGHADDAS, S., TANDLER, B., KERNER, J. & HOPPEL, C. L. 2001. Mitochondrial dysfunction in cardiac disease: ischemia–reperfusion, aging, and heart failure. *Journal of molecular and cellular cardiology,* 33**,** 1065-1089.

LEVETT, D. Z., FERNANDEZ, B. O., RILEY, H. L., MARTIN, D. S., MITCHELL, K., LECKSTROM, C. A., INCE, C., WHIPP, B. J., MYTHEN, M. G. & MONTGOMERY, H. E. 2011. The role of nitrogen oxides in human adaptation to hypoxia. *Scientific reports,* 1.

LEVETT, D. Z., MARTIN, D. S., WILSON, M. H., MITCHELL, K., DHILLON, S., RIGAT, F., MONTGOMERY, H. E., MYTHEN, M. G. & GROCOTT, M. P. 2010. Design and conduct of Caudwell Xtreme Everest: an observational cohort study of variation in human adaptation to progressive environmental hypoxia. *BMC medical research methodology,* 10**,** 98.

LEVETT, D. Z., RADFORD, E. J., MENASSA, D. A., GRABER, E. F., MORASH, A. J., HOPPELER, H., CLARKE, K., MARTIN, D. S., FERGUSON-SMITH, A. C. & MONTGOMERY, H. E. 2012. Acclimatization of

skeletal muscle mitochondria to high-altitude hypoxia during an ascent of Everest. *The FASEB journal,* 26**,** 1431-1441.

LEVETT, D. Z., VIGANÒ, A., CAPITANIO, D., VASSO, M., DE PALMA, S., MORIGGI, M., MARTIN, D. S., MURRAY, A. J., CERRETELLI, P. & GROCOTT, M. P. 2015. Changes in muscle proteomics in the course of the Caudwell Research Expedition to Mt. Everest. *Proteomics,* 15**,** 160-171.

LIN, J., WU, H., TARR, P. T., ZHANG, C.-Y., WU, Z., BOSS, O., MICHAEL, L. F., PUIGSERVER, P., ISOTANI, E., OLSON, E. N., LOWELL, B. B., BASSEL-DUBY, R. & SPIEGELMAN, B. M. 2002. Transcriptional co-activator PGC-1[alpha] drives the formation of slow-twitch muscle fibres. *Nature,* 418**,** 797-801.

LIN, L., YU, Q., YAN, X., HANG, W., ZHENG, J., XING, J. & HUANG, B. 2010. Direct infusion mass spectrometry or liquid chromatography mass spectrometry for human metabonomics? A serum metabonomic study of kidney cancer. *Analyst,* 135**,** 2970-2978.

LÓPEZ-BARNEO, J., PARDAL, R. & ORTEGA-SÁENZ, P. 2001. Cellular mechanism of oxygen sensing. *Annual Review of Physiology,* 63**,** 259-287.

LOZANO, R., NAGHAVI, M., FOREMAN, K., LIM, S., SHIBUYA, K., ABOYANS, V., ABRAHAM, J., ADAIR, T., AGGARWAL, R. & AHN, S. Y. 2013. Global and regional mortality from 235 causes of death for 20 age groups in 1990 and 2010: a systematic analysis for the Global Burden of Disease Study 2010. *The Lancet,* 380**,** 2095-2128.

LUNDBERG, J. O. & GOVONI, M. 2004. Inorganic nitrate is a possible source for systemic generation of nitric oxide. *Free Radical Biology and Medicine,* 37**,** 395-400.

LUNDBY, C., PILEGAARD, H., VAN HALL, G., SANDER, M., CALBET, J., LOFT, S. & MØLLER, P. 2003. Oxidative DNA damage and repair in skeletal muscle of humans exposed to high-altitude hypoxia. *Toxicology,* 192**,** 229-236.

MACINTYRE, N., CRAPO, R. O., VIEGI, G., JOHNSON, D. C., VAN DER GRINTEN, C. P., BRUSASCO, V., BURGOS, F., CASABURI, R., COATES, A., ENRIGHT, P., GUSTAFSSON, P., HANKINSON, J., JENSEN, R., MCKAY, R., MILLER, M. R., NAVAJAS, D., PEDERSEN, O. F., PELLEGRINO, R. & WANGER, J. 2005. Standardisation of the single-breath determination of carbon monoxide uptake in the lung. *Eur Respir J,* 26**,** 720-35.

MAGALHAES, J., ASCENSAO, A., SOARES, J. M., FERREIRA, R., NEUPARTH, M. J., MARQUES, F. & DUARTE, J. A. 2005. Acute and severe hypobaric hypoxia increases oxidative stress and impairs mitochondrial function in mouse skeletal muscle. *Journal of applied physiology,* 99**,** 1247-1253.

MAHAT, B., CHASSÉ, É., MAUGER, J.-F. & IMBEAULT, P. 2016a. Effects of Acute Hypoxia on Human Adipose Tissue Lipoprotein Lipase Activity and Lipolysis. *The FASEB Journal,* 30**,** 758.6-758.6.

MAHAT, B., CHASSÉ, É., MAUGER, J.-F. & IMBEAULT, P. 2016b. Effects of acute hypoxia on human adipose tissue lipoprotein lipase activity and lipolysis. *Journal of Translational Medicine,* 14**,** 212.

MAHDAVI, V., IZUMO, S. & NADAL-GINARD, B. 1987. Developmental and hormonal regulation of sarcomeric myosin heavy chain gene family. *Circulation Research,* 60**,** 804-14.

MARTIN, D. S., LEVETT, D. Z., GROCOTT, M. P. & MONTGOMERY, H. E. 2010. Variation in human performance in the hypoxic mountain environment. *Experimental Physiology,* 95**,** 463-470.

MARTIN, K., SMEE, D., THOMPSON, K. G. & RATTRAY, B. 2014. No improvement of repeated-sprint performance with dietary nitrate. *International Journal of Sports Physiology & Performance,* 9.

MARTINELLI, M., WINTERHALDER, R., CERRETELLI, P., HOWALD, H. & HOPPELER, H. 1990. Muscle lipofuscin content and satellite cell volume is increased after high altitude exposure in humans. *Experientia,* 46**,** 672-676.

MASSCHELEIN, E., VAN THIENEN, R., WANG, X., VAN SCHEPDAEL, A., THOMIS, M. & HESPEL, P. 2012. Dietary nitrate improves muscle but not cerebral oxygenation status during exercise in hypoxia. *Journal of Applied Physiology,* 113**,** 736-745.

MATHESON, G. O., ALLEN, P. S., ELLINGER, D. C., HANSTOCK, C. C., GHEORGHIU, D., MCKENZIE, D. C., STANLEY, C., PARKHOUSE, W. S. & HOCHACHKA, P. W. 1991. Skeletal muscle metabolism and work capacity: a 31P-NMR study of Andean natives and lowlanders. *Journal of Applied Physiology,* 70**,** 1963-1976.

MATSCHKE, J., WIEBECK, E., HURST, S., RUDNER, J. & JENDROSSEK, V. 2016. Role of SGK1 for fatty acid uptake, cell survival and radioresistance of NCI-H460 lung cancer cells exposed to acute or chronic cycling severe hypoxia. *Radiation Oncology,* 11**,** 75.

MAXWELL, S. E. & DELANEY, H. D. 1990. Designing experiments and analyzing data: A model comparison approach. *Belmont, CA: Wadsworth*.

MAYER, C. M. & BELSHAM, D. D. 2010. Palmitate attenuates insulin signaling and induces endoplasmic reticulum stress and apoptosis in hypothalamic neurons: rescue of resistance and apoptosis through adenosine 5′ monophosphate-activated protein kinase activation. *Endocrinology,* 151**,** 576-585.

MAZZEO, R. S., CAVANAGH, P., EVANS, W. J., FIATARONE, M., HAGBERG, J., MCAULEY, E. & STARTZELL, J. 1998. Exercise and physical activity for older adults. *Medicine and science in sports and exercise,* 30**,** 992-1008.

MCCLELLAND, G. B. & BROOKS, G. A. 2002. Changes in MCT 1, MCT 4, and LDH expression are tissue specific in rats after long-term hypobaric hypoxia. *Journal of Applied Physiology,* 92**,** 1573-1584.

MCCLELLAND, G. B., HOCHACHKA, P. W. & WEBER, J.-M. 1998. Carbohydrate utilization during exercise after high-altitude acclimation: a new perspective. *Proceedings of the National Academy of Sciences,* 95**,** 10288-10293.

MCDONAGH, S. T., VANHATALO, A., FULFORD, J., WYLIE, L. J., BAILEY, S. J. & JONES, A. M. 2016. Dietary nitrate supplementation attenuates the reduction in exercise tolerance following blood donation. *American Journal of Physiology-Heart and Circulatory Physiology,* 311**,** H1520-H1529.

MCDONALD, L. J. & MURAD, F. 1996. Nitric oxide and cyclic GMP signaling. *Experimental Biology and Medicine,* 211**,** 1-6.

MENENDEZ, J. A. & LUPU, R. 2007. Fatty acid synthase and the lipogenic phenotype in cancer pathogenesis. *Nature Reviews Cancer,* 7**,** 763-777.

MIAO, H., CHEN, L., HAO, L., ZHANG, X., CHEN, Y., RUAN, Z. & LIANG, H. 2015. Stearic acid induces proinflammatory cytokine production partly through activation of lactate-HIF1α pathway in chondrocytes. *Scientific reports,* 5**,** 13092.

MILLAR, T. M., STEVENS, C. R., BENJAMIN, N., EISENTHAL, R., HARRISON, R. & BLAKE, D. R. 1998. Xanthine oxidoreductase catalyses the reduction of nitrates and nitrite to nitric oxide under hypoxic conditions. *FEBS letters,* 427**,** 225-228.

MILLER, M. R., HANKINSON, J., BRUSASCO, V., BURGOS, F., CASABURI, R., COATES, A., CRAPO, R., ENRIGHT, P., VAN DER GRINTEN, C. P., GUSTAFSSON, P., JENSEN, R., JOHNSON, D. C., MACINTYRE, N., MCKAY, R., NAVAJAS, D., PEDERSEN, O. F., PELLEGRINO, R., VIEGI, G., WANGER, J. & FORCE, A. E. T. 2005. Standardisation of spirometry. *Eur Respir J,* 26**,** 319-38.

MITCHELL, P. 1961. Coupling of phosphorylation to electron and hydrogen transfer by a chemi-osmotic type of mechanism. *Nature,* 191**,** 144-148.

MODIN, A., BJÖRNE, H., HERULF, M., ALVING, K., WEITZBERG, E. & LUNDBERG, J. O. N. 2001. Nitrite-derived nitric oxide: a possible mediator of 'acidic–metabolic' vasodilation. *Acta Physiologica Scandinavica,* 171**,** 9-16.

MORASH, A. J., KOTWICA, A. O. & MURRAY, A. J. 2013. Tissue-specific changes in fatty acid oxidation in hypoxic heart and skeletal muscle. *American Journal of Physiology-Regulatory, Integrative and Comparative Physiology,* 305**,** R534-R541.

MUKHERJEE, K., EDGETT, B. A., BURROWS, H. W., CASTRO, C., GRIFFIN, J. L., SCHWERTANI, A. G., GURD, B. J. & FUNK, C. D. 2014. Whole blood transcriptomics and urinary metabolomics to define adaptive biochemical pathways of high-intensity exercise in 50-60 year old masters athletes. *PloS one,* 9**,** e92031.

MURATSUBAKI, H. & YAMAKI, A. 2011. Profile of Plasma Amino Acid Levels in Rats Exposed to Acute Hypoxic Hypoxia. *Indian Journal of Clinical Biochemistry,* 26**,** 416-419.

MURPHY, M., ELIOT, K., HEUERTZ, R. M. & WEISS, E. 2012. Whole beetroot consumption acutely improves running performance. *Journal of the Academy of Nutrition and Dietetics,* 112**,** 548-552.

MURRAY, A. J. 2009. Metabolic adaptation of skeletal muscle to high altitude hypoxia: how new technologies could resolve the controversies. *Genome Med,* 1**,** 117-117.

NEELY, J. R., ROVETTO, M. J. & ORAM, J. F. 1972. Myocardial utilization of carbohydrate and lipids. *Progress in Cardiovascular Diseases,* 15**,** 289-329.

NGUYEN, T., SAMBROOK, P., KELLY, P., JONES, G., LORD, S., FREUND, J. & EISMAN, J. 1993. Prediction of osteoporotic fractures by postural instability and bone density. *Bmj,* 307**,** 1111-1115.

NICHOLLS, D. G. & FERGUSON, S. 2013. *Bioenergetics*, Academic Press.

NICHOLSON, J. K., BUCKINGHAM, M. J. & SADLER, P. J. 1983. High resolution 1H nmr studies of vertebrate blood and plasma. *Biochemical Journal,* 211**,** 605-615.

NICHOLSON, J. K. & LINDON, J. C. 2008. Systems biology: metabonomics. *Nature,* 455**,** 1054-1056.

NICHOLSON, J. K. & WILSON, I. D. 1989. High resolution proton magnetic resonance spectroscopy of biological fluids. *Progress in Nuclear Magnetic Resonance Spectroscopy,* 21**,** 449-501.

NIEMELÄ, P. S., OLLILA, S., HYVÖNEN, M. T., KARTTUNEN, M. & VATTULAINEN, I. 2007. Assessing the nature of lipid raft membranes. *PLoS Comput Biol,* 3**,** e34.

NISOLI, E., TONELLO, C., CARDILE, A., COZZI, V., BRACALE, R., TEDESCO, L., FALCONE, S., VALERIO, A., CANTONI, O. & CLEMENTI, E. 2005. Calorie restriction promotes mitochondrial biogenesis by inducing the expression of eNOS. *Science,* 310**,** 314-317.

NOBAKHT M. GH, B. F., ALIANNEJAD, R., REZAEI-TAVIRANI, M., TAHERI, S. & OSKOUIE, A. A. 2015. The metabolomics of airway diseases, including COPD, asthma and cystic fibrosis. *Biomarkers,* 20**,** 5-16.

O'DONNELL, D. E., CASABURI, R., VINCKEN, W., PUENTE-MAESTU, L., SWALES, J., LAWRENCE, D., KRAMER, B. & GROUP, I. S. 2011. Effect of indacaterol on exercise endurance and lung hyperinflation in COPD. *Respiratory medicine,* 105**,** 1030-1036.

ONG, S.-B., SUBRAYAN, S., LIM, S. Y., YELLON, D. M., DAVIDSON, S. M. & HAUSENLOY, D. J. 2010. Inhibiting mitochondrial fission protects the heart against ischemia/reperfusion injury. *Circulation,* 121**,** 2012-2022.

OPIE, L. H. 2004. *Heart Physiology From Cell to Circulation*, Lippincott Williams and Wilkins.

ORMEROD, J. O. M., EVANS, J. D. W., CONTRACTOR, H., BERETTA, M., ARIF, S., FERNANDEZ, B. O., FEELISCH, M., MAYER, B., KHARBANDA, R. K., FRENNEAUX, M. P. & ASHRAFIAN, H. 2017. Human Second Window Pre-Conditioning and Post-Conditioning by Nitrite Is Influenced by a Common Polymorphism in Mitochondrial Aldehyde Dehydrogenase. *JACC: Basic to Translational Science*.

OU, L. & LEITER, J. 2004. Effects of exposure to a simulated altitude of 5500 m on energy metabolic pathways in rats. *Respiratory physiology & neurobiology,* 141**,** 59-71.

PALMER, R. M., FERRIGE, A. & MONCADA, S. 1987. Nitric oxide release accounts for the biological activity of endothelium-derived relaxing factor.

PASTORIS, O., FOPPA, P., CATAPANO, M. & DOSSENA, M. 1995. Effects of hypoxia on enzyme activities in skeletal muscle of rats of different ages. An attempt at pharmacological treatment. *Pharmacological research,* 32**,** 375-381.

PAUWELS, R. A., BUIST, A. S., CALVERLEY, P. M., JENKINS, C. R. & HURD, S. S. 2012. Global strategy for the diagnosis, management, and prevention of chronic obstructive pulmonary disease. *American journal of respiratory and critical care medicine*.

PE'ER, J., SHWEIKI, D., ITIN, A., HEMO, I., GNESSIN, H. & KESHET, E. 1995. Hypoxia-induced expression of vascular endothelial growth factor by retinal cells is a common factor in neovascularizing ocular diseases. *Laboratory investigation; a journal of technical methods and pathology,* 72**,** 638-645.

PENG, C., RAO, W., ZHANG, L., WANG, K., HUI, H., WANG, L., SU, N., LUO, P., HAO, Y.-L., TU, Y., ZHANG, S. & FEI, Z. 2015. Mitofusin 2 ameliorates hypoxia-induced apoptosis via mitochondrial function and signaling pathways. *The International Journal of Biochemistry & Cell Biology,* 69**,** 29-40.

PESTA, D., HOPPEL, F., MACEK, C., MESSNER, H., FAULHABER, M., KOBEL, C., PARSON, W., BURTSCHER, M., SCHOCKE, M. & GNAIGER, E. 2011. Similar qualitative and quantitative changes of mitochondrial respiration following strength and endurance training in normoxia and hypoxia in sedentary humans. *American Journal of Physiology-Regulatory, Integrative and Comparative Physiology,* 301**,** R1078-R1087.

POLLARD, A., MASON, N., BARRY, P., POLLARD, R., COLLIER, D., FRASER, R., MILLER, M. & MILLEDGE, J. 1996. Effect of altitude on spirometric parameters and the performance of peak flow meters. *Thorax,* 51**,** 175-178.

POLLARD, A. J., BARRY, P. W., MASON, N. P., COLLIER, D. J., POLLARD, R. C., POLLARD, P. F., MARTIN, I., FRASER, R. S., MILLER, M. R. & MILLEDGE, J. S. 1997. Hypoxia, hypocapnia and spirometry at altitude. *Clinical Science,* 92**,** 593-598.

PORCELLI, S., RAMAGLIA, M., BELLISTRI, G., PAVEI, G., PUGLIESE, L., MONTORSI, M., RASICA, L. & MARZORATI, M. 2014. Aerobic Fitness Affects the Exercise Performance Responses to Nitrate Supplementation. *Medicine and science in sports and exercise*.

PSYCHOGIOS, N., HAU, D. D., PENG, J., GUO, A. C., MANDAL, R., BOUATRA, S., SINELNIKOV, I., KRISHNAMURTHY, R., EISNER, R. & GAUTAM, B. 2011. The human serum metabolome. *PloS one,* 6**,** e16957.

PUGH, L. 1964. Cardiac output in muscular exercise at 5,800 m (19,000 ft). *Journal of applied physiology,* 19**,** 441-447.

PUGH, L., GILL, M., LAHIRI, S., MILLEDGE, J., WARD, M. & WEST, J. 1964. Muscular exercise at great altitudes. *Journal of Applied Physiology,* 19**,** 431-440.

PUTHUCHEARY, Z. A., RAWAL, J., MCPHAIL, M., CONNOLLY, B., RATNAYAKE, G., CHAN, P., HOPKINSON, N. S., PADHKE, R., DEW, T. & SIDHU, P. S. 2013. Acute skeletal muscle wasting in critical illness. *Jama,* 310**,** 1591-1600.

RABE, K. F., HURD, S., ANZUETO, A., BARNES, P. J., BUIST, S. A., CALVERLEY, P., FUKUCHI, Y., JENKINS, C., RODRIGUEZ-ROISIN, R., VAN WEEL, C., ZIELINSKI, J. & GLOBAL INITIATIVE FOR CHRONIC OBSTRUCTIVE LUNG, D. 2007. Global strategy for the diagnosis, management, and prevention of chronic obstructive pulmonary disease: GOLD executive summary. *Am J Respir Crit Care Med,* 176**,** 532-55.

RABINOVICH, R. A., BASTOS, R., ARDITE, E., LLINÀS, L., OROZCO-LEVI, M., GEA, J., VILARÓ, J., BARBERÀ, J. A., RODRÍGUEZ-ROISIN, R., FERNÁNDEZ-CHECA, J. C. & ROCA, J. 2007. Mitochondrial dysfunction in COPD patients with low body mass index. *European Respiratory Journal,* 29**,** 643-650.

RAGUSO, C. A., GUINOT, S. L., JANSSENS, J.-P., KAYSER, B. & PICHARD, C. 2004. Chronic hypoxia: common traits between chronic obstructive pulmonary disease and altitude. *Current Opinion in Clinical Nutrition & Metabolic Care,* 7**,** 411-417.

RAINFORD & GRADWELL 2006. *Ernsting's Aviation Medicine*, Hodder Arnold.

RAINFORD, D. J., GRADWELL, D.P 2006. *Ernsting's Aviation Medicine* Hodder Arnold

RANKIN, E. B., RHA, J., SELAK, M. A., UNGER, T. L., KEITH, B., LIU, Q. & HAASE, V. H. 2009. Hypoxia-inducible factor 2 regulates hepatic lipid metabolism. *Molecular and cellular biology,* 29**,** 4527-4538.

RASSAF, T., BRYAN, N. S., KELM, M. & FEELISCH, M. 2002. Concomitant presence of N-nitroso and S-nitroso proteins in human plasma. *Free Radic Biol Med,* 33**,** 1590-6.

RATCLIFFE, P. J., O'ROURKE, J. F., MAXWELL, P. H. & PUGH, C. W. 1998. Oxygen sensing, hypoxia-inducible factor-1 and the regulation of mammalian gene expression. *Journal of experimental biology,* 201**,** 1153-1162.

RATTLE, H. 1995. *An NMR Primer for Life Sciences*, Partnership Press.

REGULA, K. M., ENS, K. & KIRSHENBAUM, L. A. 2002. Inducible expression of BNIP3 provokes mitochondrial defects and hypoxia-mediated cell death of ventricular myocytes. *Circulation research,* 91**,** 226-231.

RINGNÉR, M. 2008. What is principal component analysis? *Nature biotechnology,* 26**,** 303.

ROBERTS, A., REEVES, J., BUTTERFIELD, G., MAZZEO, R., SUTTON, J., WOLFEL, E. & BROOKS, G. 1996. Altitude and beta-blockade augment glucose utilization during submaximal exercise. *Journal of Applied Physiology,* 80**,** 605-615.

ROBERTS, D. F. 1952. Basal metabolism, race and climate. *Journal of the Anthropological Institute of Great Britain and Ireland***,** 169-183.

ROBERTS, L. D., ASHMORE, T., KOTWICA, A. O., MURFITT, S. A., FERNANDEZ, B. O. & FEELISCH, M. 2015. Inorganic nitrate promotes the browning of white adipose tissue through the nitrate-nitrite-nitric oxide pathway. *Diabetes,* 64.

ROBERTS, L. D., ASHMORE, T., MCNALLY, B. D., MURFITT, S. A., FERNANDEZ, B. O., FEELISCH, M., LINDSAY, R., SIERVO, M., WILLIAMS, E. A. & MURRAY, A. J. 2016. Inorganic Nitrate Mimics Exercise-Stimulated Muscular Fiber-type Switching and Myokine and GABA Release. *Diabetes***,** db160843.

ROBERTS, L. D. & GERSZTEN, R. E. 2013. Toward new biomarkers of cardiometabolic diseases. *Cell metabolism,* 18**,** 43-50.

ROBERTS, L. D., MCCOMBIE, G., TITMAN, C. M. & GRIFFIN, J. L. 2008. A matter of fat: an introduction to lipidomic profiling methods. *Journal of Chromatography B,* 871**,** 174-181.

ROBINSON, K. A. & HAYMES, E. M. 1990. Metabolic effects of exposure to hypoxia plus cold at rest and during exercise in humans. *Journal of applied physiology,* 68**,** 720-725.

RODRÍGUEZ, D. A., ALCARRAZ-VIZÁN, G., DÍAZ-MORALLI, S., REED, M., GÓMEZ, F. P., FALCIANI, F., GÜNTHER, U., ROCA, J. & CASCANTE, M. 2012. Plasma metabolic profile in COPD patients: effects of exercise and endurance training. *Metabolomics,* 8**,** 508-516.

RODRIGUEZ, F. A., CASAS, H., CASAS, M., PAGÉS, T., RAMA, R., RICART, A., VENTURA, J. L., IBDA EZ, J. & VISCOR, G. 1999. Intermittent hypobaric hypoxia stimulates erythropoiesis and improves aerobic capacity. *Medicine and Science in Sports and Exercise,* 31**,** 264-268.

ROSE, M. S., HOUSTON, C. S., FULCO, C. S., COATES, G., SUTTON, J. R. & CYMERMAN, A. 1988. Operation Everest. II: Nutrition and body composition. *Journal of Applied Physiology,* 65**,** 2545-2551.

ROSSATO, M., GRANZOTTO, M., MACCHI, V., PORZIONATO, A., PETRELLI, L., CALCAGNO, A., VENCATO, J., DE STEFANI, D., SILVESTRIN, V. & RIZZUTO, R. 2014. Human white adipocytes

express the cold receptor TRPM8 which activation induces UCP1 expression, mitochondrial activation and heat production. *Molecular and cellular endocrinology,* 383**,** 137-146.

ROUSSET, S., ALVES-GUERRA, M.-C., MOZO, J., MIROUX, B., CASSARD-DOULCIER, A.-M., BOUILLAUD, F. & RICQUIER, D. 2004. The biology of mitochondrial uncoupling proteins. *Diabetes,* 53**,** S130-S135.

SACCENTI, E., HOEFSLOOT, H. C., SMILDE, A. K., WESTERHUIS, J. A. & HENDRIKS, M. M. 2014. Reflections on univariate and multivariate analysis of metabolomics data. *Metabolomics,* 10**,** 0.

SALEK, R. M., STEINBECK, C., VIANT, M. R., GOODACRE, R. & DUNN, W. B. 2013. The role of reporting standards for metabolite annotation and identification in metabolomic studies. *GigaScience,* 2**,** 13.

SALLOUM, F. N., CHAU, V. Q., HOKE, N. N., ABBATE, A., VARMA, A., OCKAILI, R. A., TOLDO, S. & KUKREJA, R. C. 2009. Phosphodiesterase-5 inhibitor, tadalafil, protects against myocardial ischemia/reperfusion through protein-kinase G–dependent generation of hydrogen sulfide. *Circulation,* 120**,** S31-S36.

SALLOUM, F. N., STURZ, G. R., YIN, C., REHMAN, S., HOKE, N. N., KUKREJA, R. C. & XI, L. 2015. Beetroot juice reduces infarct size and improves cardiac function following ischemia–reperfusion injury: Possible involvement of endogenous H2S. *Experimental Biology and Medicine,* 240**,** 669-681.

SAMEC, S., SEYDOUX, J. & DULLOO, A. G. 1998. Role of UCP homologues in skeletal muscles and brown adipose tissue: mediators of thermogenesis or regulators of lipids as fuel substrate? *The FASEB Journal,* 12**,** 715-724.

SARASTE, M. 1994. Structure and evolution of cytochrome oxidase. *Antonie Van Leeuwenhoek,* 65**,** 285-287.

SAUER, U., HEINEMANN, M. & ZAMBONI, N. 2007. Getting closer to the whole picture. *Science(Washington),* 316**,** 550-551.

SAVORANI, F., TOMASI, G. & ENGELSEN, S. B. 2010. icoshift: A versatile tool for the rapid alignment of 1D NMR spectra. *Journal of Magnetic Resonance,* 202**,** 190-202.

SCHIAFFINO, S., GORZA, L., SARTORE, S., SAGGIN, L., AUSONI, S., VIANELLO, M., GUNDERSEN, K. & LØMO, T. 1989. Three myosin heavy chain isoforms in type 2 skeletal muscle fibres. *Journal of Muscle Research & Cell Motility,* 10**,** 197-205.

SCHIAFFINO, S. & REGGIANI, C. 2011. Fiber types in mammalian skeletal muscles. *Physiological reviews,* 91**,** 1447-1531.

SCHILD, L., REINHECKEL, T., REISER, M., HORN, T. F., WOLF, G. & AUGUSTIN, W. 2003. Nitric oxide produced in rat liver mitochondria causes oxidative stress and impairment of respiration after transient hypoxia. *The FASEB journal,* 17**,** 2194-2201.

SCHRAUWEN, P., HESSELINK, M. K., VAARTJES, I., KORNIPS, E., SARIS, W. H., GIACOBINO, J.-P. & RUSSELL, A. 2002. Effect of acute exercise on uncoupling protein 3 is a fat metabolism-mediated effect. *American Journal of Physiology-Endocrinology And Metabolism,* 282**,** E11-E17.

SEMENZA, G. L. 1999. Regulation of mammalian O2 homeostasis by hypoxia-inducible factor 1. *Annual review of cell and developmental biology,* 15**,** 551-578.

SEMENZA, G. L. 2001. Hypoxia-inducible factor 1: oxygen homeostasis and disease pathophysiology. *Trends in molecular medicine,* 7**,** 345-350.

SEMENZA, G. L., ROTH, P. H., FANG, H.-M. & WANG, G. L. 1994. Transcriptional regulation of genes encoding glycolytic enzymes by hypoxia-inducible factor 1. *Journal of biological chemistry,* 269**,** 23757-23763.

SEMENZA, G. L. & WANG, G. L. 1992. A nuclear factor induced by hypoxia via de novo protein synthesis binds to the human erythropoietin gene enhancer at a site required for transcriptional activation. *Molecular and cellular biology,* 12**,** 5447-5454.

SHEN, W. & MCINTOSH, M. K. 2016. Nutrient Regulation: Conjugated Linoleic Acid's Inflammatory and Browning Properties in Adipose Tissue. *In:* STOVER, P. J. (ed.) *Annual Review of Nutrition, Vol 36.*

SHEPHERD, A. I., WILKERSON, D. P., DOBSON, L., KELLY, J., WINYARD, P. G., JONES, A. M., BENJAMIN, N., SHORE, A. C. & GILCHRIST, M. 2015. The effect of dietary nitrate supplementation on the oxygen cost of cycling, walking performance and resting blood pressure in individuals with chronic obstructive pulmonary disease: A double blind placebo controlled, randomised control trial. *Nitric Oxide,* 48**,** 31-37.

SHI, H., KOKOEVA, M. V., INOUYE, K., TZAMELI, I., YIN, H. & FLIER, J. S. 2006. TLR4 links innate immunity and fatty acid–induced insulin resistance. *The Journal of clinical investigation,* 116**,** 3015-3025.

SHIELDS, G. S., COISSI, G. S., JIMENEZ-ROYO, P., GAMBAROTA, G., DIMBER, R., HOPKINSON, N. S., MATTHEWS, P. M., BROWN, A. P. & POLKEY, M. I. 2015. Bioenergetics and intermuscular fat in chronic obstructive pulmonary disease-associated quadriceps weakness. *Muscle & nerve,* 51**,** 214-221.

SHIVA, S., SACK, M. N., GREER, J. J., DURANSKI, M., RINGWOOD, L. A., BURWELL, L., WANG, X., MACARTHUR, P. H., SHOJA, A., RAGHAVACHARI, N., CALVERT, J. W., BROOKES, P. S., LEFER, D. J. & GLADWIN, M. T. 2007. Nitrite augments tolerance to ischemia/reperfusion injury via the modulation of mitochondrial electron transfer. *The Journal of Experimental Medicine,* 204**,** 2089-2102.

SHUKLA, V., SINGH, S. N., VATS, P., SINGH, V. K., SINGH, S. B. & BANERJEE, P. 2005. Ghrelin and leptin levels of sojourners and acclimatized lowlanders at high altitude. *Nutritional neuroscience,* 8**,** 161-165.

SHWEIKI, D., ITIN, A., SOFFER, D. & KESHET, E. 1992. Vascular endothelial growth factor induced by hypoxia may mediate hypoxia-initiated angiogenesis. *Nature,* 359**,** 843.

SIEBENMANN, C., RASMUSSEN, P., HUG, M., KEISER, S., FLÜCK, D., FISHER, J. P., HILTY, M. P., MAGGIORINI, M. & LUNDBY, C. 2016. Parasympathetic withdrawal increases heart rate after two weeks at 3,454 m altitude. *The Journal of Physiology*.

SIERVO, M., RILEY, H. L., FERNANDEZ, B. O., LECKSTROM, C. A., MARTIN, D. S., MITCHELL, K., LEVETT, D. Z., MONTGOMERY, H. E., MYTHEN, M. G. & GROCOTT, M. P. 2014. Effects of prolonged exposure to hypobaric hypoxia on oxidative stress, inflammation and gluco-insular regulation: the not-so-sweet price for good regulation. *PLoS One,* 9**,** e94915.

SIMONSON, T. S. 2015. Altitude adaptation: a glimpse through various lenses. *High altitude medicine & biology,* 16**,** 125-137.

SIMONSON, T. S., MCCLAIN, D. A., JORDE, L. B. & PRCHAL, J. T. 2012. Genetic determinants of Tibetan high-altitude adaptation. *Human genetics,* 131**,** 527-533.

SIMONSON, T. S., YANG, Y., HUFF, C. D., YUN, H., QIN, G., WITHERSPOON, D. J., BAI, Z., LORENZO, F. R., XING, J. & JORDE, L. B. 2010. Genetic evidence for high-altitude adaptation in Tibet. *Science,* 329**,** 72-75.

SPIEGELHALDER, B., EISENBRAND, G. & PREUSSMANN, R. 1976. Influence of dietary nitrate on nitrite content of human saliva: Possible relevance to in vivo formation of N-nitroso compounds. *Food and Cosmetics Toxicology,* 14**,** 545-548.

SREEKUMAR, A., POISSON, L. M., RAJENDIRAN, T. M., KHAN, A. P., CAO, Q., YU, J., LAXMAN, B., MEHRA, R., LONIGRO, R. J., LI, Y., NYATI, M. K., AHSAN, A., KALYANA-SUNDARAM, S., HAN, B., CAO, X., BYUN, J., OMENN, G. S., GHOSH, D., PENNATHUR, S., ALEXANDER, D. C., BERGER,

A., SHUSTER, J. R., WEI, J. T., VARAMBALLY, S., BEECHER, C. & CHINNAIYAN, A. M. 2009. Metabolomic profiles delineate potential role for sarcosine in prostate cancer progression. *Nature,* 457**,** 910-914.

STAMLER, J. S. & MEISSNER, G. 2001. Physiology of Nitric Oxide in Skeletal Muscle. *Physiological Reviews,* 81**,** 209-237.

STERNE, G. D., COULTON, G. R., BROWN, R. A., GREEN, C. J. & TERENGHI, G. 1997. Neurotrophin-3–enhanced Nerve Regeneration Selectively Improves Recovery of Muscle Fibers Expressing Myosin Heavy Chains 2b. *The Journal of Cell Biology,* 139**,** 709-715.

STEVENS, L., GOHLSCH, B., MOUNIER, Y. & PETTE, D. 1999. Changes in myosin heavy chain mRNA and protein isoforms in single fibers of unloaded rat soleus muscle. *FEBS letters,* 463**,** 15-18.

STOCK, D., GIBBONS, C., ARECHAGA, I., LESLIE, A. G. W. & WALKER, J. E. 2000. The rotary mechanism of ATP synthase. *Current Opinion in Structural Biology,* 10**,** 672-679.

STOCKS, J. M., TAYLOR, N. A., TIPTON, M. J. & GREENLEAF, J. E. 2004. Human physiological responses to cold exposure. *Aviation, space, and environmental medicine,* 75**,** 444-457.

SUMNER, L. W., AMBERG, A., BARRETT, D., BEALE, M. H., BEGER, R., DAYKIN, C. A., FAN, T. W., FIEHN, O., GOODACRE, R. & GRIFFIN, J. L. 2007. Proposed minimum reporting standards for chemical analysis. *Metabolomics,* 3.

SUN, K., HALBERG, N., KHAN, M., MAGALANG, U. J. & SCHERER, P. E. 2013. Selective inhibition of hypoxia-inducible factor 1α ameliorates adipose tissue dysfunction. *Molecular and cellular biology,* 33**,** 904-917.

SURKS, H. K. 2007. cGMP-Dependent Protein Kinase I and Smooth Muscle Relaxation: A Tale of Two Isoforms. *Circulation Research,* 101**,** 1078-1080.

SUTTON, J. R., REEVES, J. T., WAGNER, P. D., GROVES, B. M., CYMERMAN, A., MALCONIAN, M. K., ROCK, P. B., YOUNG, P. M., WALTER, S. D. & HOUSTON, C. S. 1988. Operation Everest II: oxygen transport during exercise at extreme simulated altitude. *Journal of applied physiology,* 64**,** 1309-1321.

SUVITAIVAL, T., ROGERS, S. & KASKI, S. 2014a. Stronger findings for metabolomics through Bayesian modeling of multiple peaks and compound correlations. *Bioinformatics,* 30**,** i461-i467.

SUVITAIVAL, T., ROGERS, S. & KASKI, S. 2014b. Stronger findings from mass spectral data through multi-peak modeling. *BMC bioinformatics,* 15**,** 208.

SUZUKI, K., KIZAKI, T., HITOMI, Y., NUKITA, M., KIMOTO, K., MIYAZAWA, N., KOBAYASHI, K., OHNUKI, Y. & OHNO, H. 2003. Genetic variation in hypoxia-inducible factor 1α and its possible association with high altitude adaptation in Sherpas. *Medical hypotheses,* 61**,** 385-389.

SUZUKI, T., SHINJO, S., ARAI, T., KANAI, M. & GODA, N. 2014. Hypoxia and fatty liver. *World Journal of Gastroenterology: WJG,* 20**,** 15087.

SWALLOW, E. B., GOSKER, H. R., WARD, K. A., MOORE, A. J., DAYER, M. J., HOPKINSON, N. S., SCHOLS, A. M., MOXHAM, J. & POLKEY, M. I. 2007. A novel technique for nonvolitional assessment of quadriceps muscle endurance in humans. *Journal of Applied Physiology,* 103**,** 739-746.

TALMADGE, R. J. & ROY, R. R. 1993. Electrophoretic separation of rat skeletal muscle myosin heavy-chain isoforms. *Journal of Applied Physiology,* 75**,** 2337-2340.

TAYLOR, D. A., BOWMAN, B. & STULL, J. 1989. Cytoplasmic Ca2+ is a primary determinant for myosin phosphorylation in smooth muscle cells. *Journal of Biological Chemistry,* 264**,** 6207-6213.

THIELE, I., SWAINSTON, N., FLEMING, R. M., HOPPE, A., SAHOO, S., AURICH, M. K., HARALDSDOTTIR, H., MO, M. L., ROLFSSON, O. & STOBBE, M. D. 2013. A community-driven global reconstruction of human metabolism. *Nature biotechnology,* 31**,** 419-425.

THOMAS, D. D., LIU, X., KANTROW, S. P. & LANCASTER, J. R. 2001. The biological lifetime of nitric oxide: Implications for the perivascular dynamics of NO and O2. *Proceedings of the National Academy of Sciences,* 98**,** 355-360.

THOMPSON, C., WYLIE, L. J., FULFORD, J., KELLY, J., BLACK, M. I., MCDONAGH, S. T., JEUKENDRUP, A. E., VANHATALO, A. & JONES, A. M. 2015. Dietary nitrate improves sprint performance and cognitive function during prolonged intermittent exercise. *European journal of applied physiology,* 115**,** 1825-1834.

THOMPSON, J., RAITT, J., HUTCHINGS, L., DRENOS, F., BJARGO, E., LOSET, A., GROCOTT, M. & MONTGOMERY, H. 2007. Angiotensin-converting enzyme genotype and successful ascent to extreme high altitude. *High altitude medicine & biology,* 8**,** 278-285.

TIMMONS, B. A., ARAUJO, J. & THOMAS, T. R. 1985. Fat utilization enhanced by exercise in a cold environment. *Medicine and science in sports and exercise,* 17**,** 673-678.

TIPTON, M., FRANKS, G., MENEILLY, G. & MEKJAVIC, I. 1997. Substrate utilisation during exercise and shivering. *European journal of applied physiology and occupational physiology,* 76**,** 103-108.

TISSOT VAN PATOT, M. C., SERKOVA, N. J., HASCHKE, M., KOMINSKY, D. J., ROACH, R. C., CHRISTIANS, U., HENTHORN, T. K. & HONIGMAN, B. 2009. Enhanced leukocyte HIF-1α and HIF-1 DNA binding in humans after rapid ascent to 4300 m. *Free Radical Biology and Medicine,* 46**,** 1551-1557.

TO, M., YAMAMURA, S., AKASHI, K., CHARRON, C. E., BARNES, P. J. & ITO, K. 2012. Defect of Adaptation to Hypoxia in Patients With COPD Due to Reduction of Histone Deacetylase 7Poor Adaptation to Hypoxia in COPD. *CHEST Journal,* 141**,** 1233-1242.

TROY, H., CHUNG, Y.-L., MAYR, M., LY, L., WILLIAMS, K., STRATFORD, I., HARRIS, A., GRIFFITHS, J. & STUBBS, M. 2005. Metabolic profiling of hypoxia-inducible factor-1β-deficient and wild type Hepa-1 cells: effects of hypoxia measured by 1H magnetic resonance spectroscopy. *Metabolomics,* 1**,** 293-303.

TRUMBO, P., SCHLICKER, S., YATES, A. A. & POOS, M. 2002. Dietary Reference Intakes for Energy, Carbohydrate, Fiber, Fat, Fatty Acids, Cholesterol, Protein and Amino Acids. *Journal of the American Dietetic Association,* 102**,** 1621-1630.

TSAI, T.-H., TADESSE, M. G., DI POTO, C., PANNELL, L. K., MECHREF, Y., WANG, Y. & RESSOM, H. W. 2013. Multi-profile Bayesian alignment model for LC-MS data analysis with integration of internal standards. *Bioinformatics,* 29**,** 2774-2780.

TUDER, R., YUN, J., BHUNIA, A. & FIJALKOWSKA, I. 2007. Hypoxia and chronic lung disease. *Journal of Molecular Medicine,* 85**,** 1317-1324.

UBHI, B. K., CHENG, K. K., DONG, J., JANOWITZ, T., JODRELL, D., TAL-SINGER, R., MACNEE, W., LOMAS, D. A., RILEY, J. H. & GRIFFIN, J. L. 2012a. Targeted metabolomics identifies perturbations in amino acid metabolism that sub-classify patients with COPD. *Molecular BioSystems,* 8**,** 3125-3133.

UBHI, B. K., RILEY, J. H., SHAW, P. A., LOMAS, D. A., TAL-SINGER, R., MACNEE, W., GRIFFIN, J. L. & CONNOR, S. C. 2012b. Metabolic profiling detects biomarkers of protein degradation in COPD patients. *European Respiratory Journal,* 40**,** 345-355.

UNDERBAKKE, E. S., IAVARONE, A. T., CHALMERS, M. J., PASCAL, B. D., NOVICK, S., GRIFFIN, P. R. & MARLETTA, M. A. 2014. Nitric oxide-induced conformational changes in soluble guanylate cyclase. *Structure,* 22**,** 602-611.

UTTING, J., ROBINS, S., BRANDAO-BURCH, A., ORRISS, I., BEHAR, J. & ARNETT, T. 2006. Hypoxia inhibits the growth, differentiation and bone-forming capacity of rat osteoblasts. *Experimental cell research,* 312**,** 1693-1702.

VALDEZ, L. B., ZAOBORNYJ, T., ALVAREZ, S., BUSTAMANTE, J., COSTA, L. E. & BOVERIS, A. 2004. Heart mitochondrial nitric oxide synthase. Effects of hypoxia and aging. *Molecular aspects of medicine,* 25**,** 49-59.

VALLERAND, A. L. & JACOBS, I. 1989. Rates of energy substrates utilization during human cold exposure. *European Journal of Applied Physiology and Occupational Physiology,* 58**,** 873-878.

VAN PATOT, M. C. T., MURRAY, A. J., BECKEY, V., CINDROVA-DAVIES, T., JOHNS, J., ZWERDLINGER, L., JAUNIAUX, E., BURTON, G. J. & SERKOVA, N. J. 2010. Human placental metabolic adaptation to chronic hypoxia, high altitude: hypoxic preconditioning. *American Journal of Physiology-Regulatory, Integrative and Comparative Physiology,* 298**,** R166-R172.

VANDER HEIDEN, M. G., CANTLEY, L. C. & THOMPSON, C. B. 2009. Understanding the Warburg Effect: The Metabolic Requirements of Cell Proliferation. *Science,* 324**,** 1029-1033.

VANHATALO, A., BAILEY, S. J., BLACKWELL, J. R., DIMENNA, F. J., PAVEY, T. G., WILKERSON, D. P., BENJAMIN, N., WINYARD, P. G. & JONES, A. M. 2010. Acute and chronic effects of dietary nitrate supplementation on blood pressure and the physiological responses to moderate-intensity and incremental exercise. *American Journal of Physiology-Regulatory, Integrative and Comparative Physiology,* 299**,** R1121-R1131.

VANHATALO, A., FULFORD, J., BAILEY, S. J., BLACKWELL, J. R., WINYARD, P. G. & JONES, A. M. 2011. Dietary nitrate reduces muscle metabolic perturbation and improves exercise tolerance in hypoxia. *The Journal of physiology,* 589**,** 5517-5528.

VATS, P., SINGH, S. N., SHYAM, R., SINGH, V. K., SINGH, S. B., BANERJEE, P. K. & SELVAMURTHY, W. 2004. Leptin may not be responsible for high altitude anorexia. *High altitude medicine & biology,* 5**,** 90-92.

VAZQUEZ-JIMENEZ, J. G., CHAVEZ-REYES, J., ROMERO-GARCIA, T., ZARAIN-HERZBERG, A., VALDES-FLORES, J., GALINDO-ROSALES, J. M., RUEDA, A., GUERRERO-HERNANDEZ, A. & OLIVARES-REYES, J. A. 2016. Palmitic acid but not palmitoleic acid induces insulin resistance in a human endothelial cell line by decreasing SERCA pump expression. *Cellular signalling,* 28**,** 53-59.

VICTOR, V. M., NUÑEZ, C., D'OCÓN, P., TAYLOR, C. T., ESPLUGUES, J. V. & MONCADA, S. 2009. Regulation of oxygen distribution in tissues by endothelial nitric oxide. *Circulation research,* 104**,** 1178-1183.

VIGANÒ, A., RIPAMONTI, M., DE PALMA, S., CAPITANIO, D., VASSO, M., WAIT, R., LUNDBY, C., CERRETELLI, P. & GELFI, C. 2008. Proteins modulation in human skeletal muscle in the early phase of adaptation to hypobaric hypoxia. *Proteomics,* 8**,** 4668-4679.

VUORI, I. M. 2001. Dose-response of physical activity and low back pain, osteoarthritis, and osteoporosis. *Medicine and science in sports and exercise,* 33**,** S551-86; discussion 609-10.

WAGNER, P. D. 2000. Reduced maximal cardiac output at altitude—mechanisms and significance. *Respiration physiology,* 120**,** 1-11.

WAGNER, P. D. 2010. Operation Everest II. *High altitude medicine & biology,* 11**,** 111-119.

WAHLI, W., BRAISSANT, O. & DESVERGNE, B. 1995. Peroxisome proliferator activated receptors: transcriptional regulators of adipogenesis, lipid metabolism and more…. *Chemistry & biology,* 2**,** 261-266.

WANG, G. L., JIANG, B.-H., RUE, E. A. & SEMENZA, G. L. 1995. Hypoxia-inducible factor 1 is a basic-helix-loop-helix-PAS heterodimer regulated by cellular O2 tension. *Proceedings of the National Academy of Sciences,* 92**,** 5510-5514.

WANGER, J., CLAUSEN, J. L., COATES, A., PEDERSEN, O. F., BRUSASCO, V., BURGOS, F., CASABURI, R., CRAPO, R., ENRIGHT, P., VAN DER GRINTEN, C. P., GUSTAFSSON, P., HANKINSON, J., JENSEN, R., JOHNSON, D., MACINTYRE, N., MCKAY, R., MILLER, M. R., NAVAJAS, D., PELLEGRINO, R. & VIEGI, G. 2005. Standardisation of the measurement of lung volumes. *Eur Respir J,* 26**,** 511-22.

WARD, J. P. 2008. Oxygen sensors in context. *Biochimica et Biophysica Acta (BBA)-Bioenergetics,* 1777**,** 1-14.

WASSE, L. K., SUNDERLAND, C., KING, J. A., BATTERHAM, R. L. & STENSEL, D. J. 2012. Influence of rest and exercise at a simulated altitude of 4,000 m on appetite, energy intake, and plasma concentrations of acylated ghrelin and peptide YY. *Journal of Applied Physiology,* 112**,** 552-559.

WATERMAN, C. L., CURRIE, R. A., COTTRELL, L. A., DOW, J., WRIGHT, J., WATERFIELD, C. J. & GRIFFIN, J. L. 2010. An integrated functional genomic study of acute phenobarbital exposure in the rat. *BMC genomics,* 11**,** 9.

WEBB, A. J., PATEL, N., LOUKOGEORGAKIS, S., OKORIE, M., ABOUD, Z., MISRA, S., RASHID, R., MIALL, P., DEANFIELD, J. & BENJAMIN, N. 2008. Acute blood pressure lowering, vasoprotective, and antiplatelet properties of dietary nitrate via bioconversion to nitrite. *Hypertension,* 51**,** 784-790.

WEE, J. & CLIMSTEIN, M. 2015. Hypoxic training: Clinical benefits on cardiometabolic risk factors. *Journal of Science and Medicine in Sport,* 18**,** 56-61.

WEIBEL, E. R. 1984. *The pathway for oxygen. Structure and function in the mammalian respiratory system* Cambridge, Massachusetts, Harvard University Press

WELSH, C. H., WAGNER, P. D., REEVES, J. T., LYNCH, D., CINK, T. M., ARMSTRONG, J., MALCONIAN, M. K., ROCK, P. B. & HOUSTON, C. S. 1993. Operation Everest II: spirometric and radiographic changes in acclimatized humans at simulated high altitudes. *American Review of Respiratory Disease,* 147**,** 1239-1239.

WEST, J. Lactate during exercise at extreme altitude. Federation proceedings, 1986. 2953-2957.

WEST, J. B., BOYER, S., GRABER, D., HACKETT, P., MARET, K., MILLEDGE, J., PETERS, R., PIZZO, C., SAMAJA, M. & SARNQUIST, F. 1983. Maximal exercise at extreme altitudes on Mount Everest. *Journal of applied physiology,* 55**,** 688-698.

WHITE, P. J., LAPWORTH, A. L., AN, J., WANG, L., MCGARRAH, R. W., STEVENS, R. D., ILKAYEVA, O., GEORGE, T., MUEHLBAUER, M. J., BAIN, J. R., TRIMMER, J. K., BROSNAN, M. J., ROLPH, T. P. & NEWGARD, C. B. 2016. Branched-chain amino acid restriction in Zucker-fatty rats improves muscle insulin sensitivity by enhancing efficiency of fatty acid oxidation and acyl-glycine export. *Molecular Metabolism,* 5**,** 538-551.

WHO 2003. Nitrate and nitrite in drinking-water: Background document for development of WHO Guidelines for Drinking-water Quality.

WIECHERT, W. 2001. 13C metabolic flux analysis. *Metabolic engineering,* 3**,** 195-206.

WILLSON, T. M., BROWN, P. J., STERNBACH, D. D. & HENKE, B. R. 2000. The PPARs: from orphan receptors to drug discovery. *Journal of medicinal chemistry,* 43**,** 527-550.

WISHART, D. S. 2011. Advances in metabolite identification. *Bioanalysis,* 3**,** 1769-1782.

WISHART, D. S., JEWISON, T., GUO, A. C., WILSON, M., KNOX, C., LIU, Y., DJOUMBOU, Y., MANDAL, R., AZIAT, F. & DONG, E. 2012. HMDB 3.0—the human metabolome database in 2013. *Nucleic acids research***,** gks1065.

WISHART, D. S., TZUR, D., KNOX, C., EISNER, R., GUO, A. C., YOUNG, N., CHENG, D., JEWELL, K., ARNDT, D. & SAWHNEY, S. 2007. HMDB: the human metabolome database. *Nucleic acids research,* 35**,** D521-D526.

WOOD, I. S., STEZHKA, T. & TRAYHURN, P. 2011. Modulation of adipokine production, glucose uptake and lactate release in human adipocytes by small changes in oxygen tension. *Pflügers Archiv-European Journal of Physiology,* 462**,** 469-477.

WOOD, I. S. & TRAYHURN, P. 2003. Glucose transporters (GLUT and SGLT): expanded families of sugar transport proteins. *British Journal of Nutrition,* 89**,** 3-9.

WOODS, D. R., POLLARD, A. J., COLLIER, D. J., JAMSHIDI, Y., VASSILIOU, V., HAWE, E., HUMPHRIES, S. E. & MONTGOMERY, H. E. 2002. Insertion/deletion polymorphism of the angiotensin I-

converting enzyme gene and arterial oxygen saturation at high altitude. *American journal of respiratory and critical care medicine,* 166**,** 362-366.

WOOLCOTT, O. O., ADER, M. & BERGMAN, R. N. 2015. Glucose homeostasis during short-term and prolonged exposure to high altitudes. *Endocrine reviews,* 36**,** 149-173.

WOYDA-PLOSZCZYCA, A. M. & JARMUSZKIEWICZ, W. 2016. The conserved regulation of mitochondrial uncoupling proteins: from unicellular eukaryotes to mammals. *Biochimica et Biophysica Acta (BBA)-Bioenergetics*.

WULLSCHLEGER, S., LOEWITH, R. & HALL, M. N. TOR Signaling in Growth and Metabolism. *Cell,* 124**,** 471-484.

WULLSCHLEGER, S., LOEWITH, R. & HALL, M. N. 2006. TOR signaling in growth and metabolism. *Cell,* 124**,** 471-484.

WYLIE, L. J., BAILEY, S. J., KELLY, J., BLACKWELL, J. R., VANHATALO, A. & JONES, A. M. 2016. Influence of beetroot juice supplementation on intermittent exercise performance. *European journal of applied physiology,* 116**,** 415-425.

WYLIE, L. J., KELLY, J., BAILEY, S. J., BLACKWELL, J. R., SKIBA, P. F., WINYARD, P. G., JEUKENDRUP, A. E., VANHATALO, A. & JONES, A. M. 2013. Beetroot juice and exercise: pharmacodynamic and dose-response relationships. *Journal of applied Physiology,* 115**,** 325-336.

XIA, Y., WARSHAW, J. B. & HADDAD, G. G. 1997. Effect of chronic hypoxia on glucose transporters in heart and skeletal muscle of immature and adult rats. *American Journal of Physiology-Regulatory, Integrative and Comparative Physiology,* 273**,** R1734-R1741.

YETUKURI, L., EKROOS, K., VIDAL-PUIG, A. & OREŠIČ, M. 2008. Informatics and computational strategies for the study of lipids. *Molecular BioSystems,* 4**,** 121-127.

YOSHIDA, K., KASAMA, K., KITABATAKE, M., OKUDA, M. & IMAI, M. 1980. Metabolic fate of nitric oxide. *International archives of occupational and environmental health,* 46**,** 71-77.

YOULE, R. J. & VAN DER BLIEK, A. M. 2012. Mitochondrial fission, fusion, and stress. *Science,* 337**,** 1062-1065.

YOUNG, A. J., EVANS, W. J., FISHER, E. C., SHARP, R. L., COSTILL, D. L. & MAHER, J. T. 1984. Skeletal muscle metabolism of sea-level natives following short-term high-altitude residence. *European Journal of Applied Physiology and Occupational Physiology,* 52**,** 463-466.

YOUNG, P. M., ROSE, M. S., SUTTON, J. R., GREEN, H. J., CYMERMAN, A. & HOUSTON, C. S. 1989. Operation Everest II: plasma lipid and hormonal responses during a simulated ascent of Mt. Everest. *Journal of Applied Physiology,* 66**,** 1430-1435.

YSART, G., MILLER, P., BARRETT, G., FARRINGTON, D., LAWRANCE, P. & HARRISON, N. 1999. Dietary exposures to nitrate in the UK. *Food Additives & Contaminants,* 16**,** 521-532.

ZHANG, C.-Y., BAFFY, G., PERRET, P., KRAUSS, S., PERONI, O., GRUJIC, D., HAGEN, T., VIDAL-PUIG, A. J., BOSS, O. & KIM, Y.-B. 2001. Uncoupling protein-2 negatively regulates insulin secretion and is a major link between obesity, β cell dysfunction, and type 2 diabetes. *Cell,* 105**,** 745-755.

ZHANG, H., BOSCH-MARCE, M., SHIMODA, L. A., TAN, Y. S., BAEK, J. H., WESLEY, J. B., GONZALEZ, F. J. & SEMENZA, G. L. 2008. Mitochondrial autophagy is an HIF-1-dependent adaptive metabolic response to hypoxia. *Journal of Biological Chemistry,* 283**,** 10892-10903.

ZHANG, S., ZENG, X., REN, M., MAO, X. & QIAO, S. 2017. Novel metabolic and physiological functions of branched chain amino acids: a review. *Journal of Animal Science and Biotechnology,* 8**,** 10.

ZIAEE, V., ALIZADEH, R. & MOVAFEGH, A. 2008. Pulmonary function parameters changes at different altitudes in healthy athletes. *Iranian Journal of Allergy, Asthma and Immunology,* 7**,** 79-84.